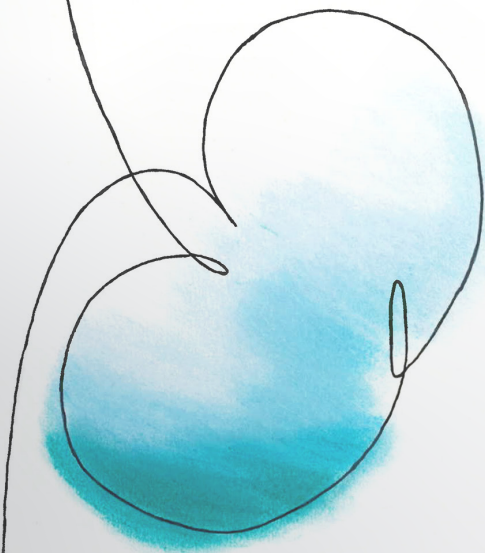


Connecting vascular inflammation
and endothelial dysfunction
in the cardio-renal axis

Marian Wesseling



Connecting vascular inflammation and
endothelial dysfunction in the cardio-renal axis

Marian Wesseling

Connecting vascular inflammation and endothelial dysfunction in the cardio-renal axis

© Marian Wesseling, 2020

ISBN: 978-90-393-7260-9

Lay out: Wendy Schoneveld, www.wenziD.nl

Printed by: ProefschriftMaken | Proefschriftmaken.nl

The research described in this thesis was supported by a grant of the Dutch Heart Foundation (CVON 2014 RECONNECT).

Financial support by the Dutch Heart Foundation for the publication of this thesis is gratefully acknowledged.

The printing of this thesis was financially supported by Fujifilm VisualSonics Inc.

Connecting vascular inflammation and endothelial dysfunction in the cardio-renal axis

Het verband tussen vasculaire ontsteking en
disfunctioneel endotheel in de cardio-renale as
(met een samenvatting in het Nederlands)

Proefschrift

ter verkrijging van de graad van doctor aan de
Universiteit Utrecht
op gezag van de
rector magnificus, prof.dr. H.R.B.M. Kummeling,
ingevolge het besluit van het college voor promoties
in het openbaar te verdedigen op

dinsdag 20 oktober 2020 des ochtends te 11.00 uur

door

Marian Wesseling

geboren op 16 mei 1991
te Wageningen

Promotoren

Prof. dr. G. Pasterkamp

Prof. dr. M.J.T.H. Goumans

Copromotoren

Dr. S.C.A. de Jager

Dr. G. Sanchez

TABLE OF CONTENTS

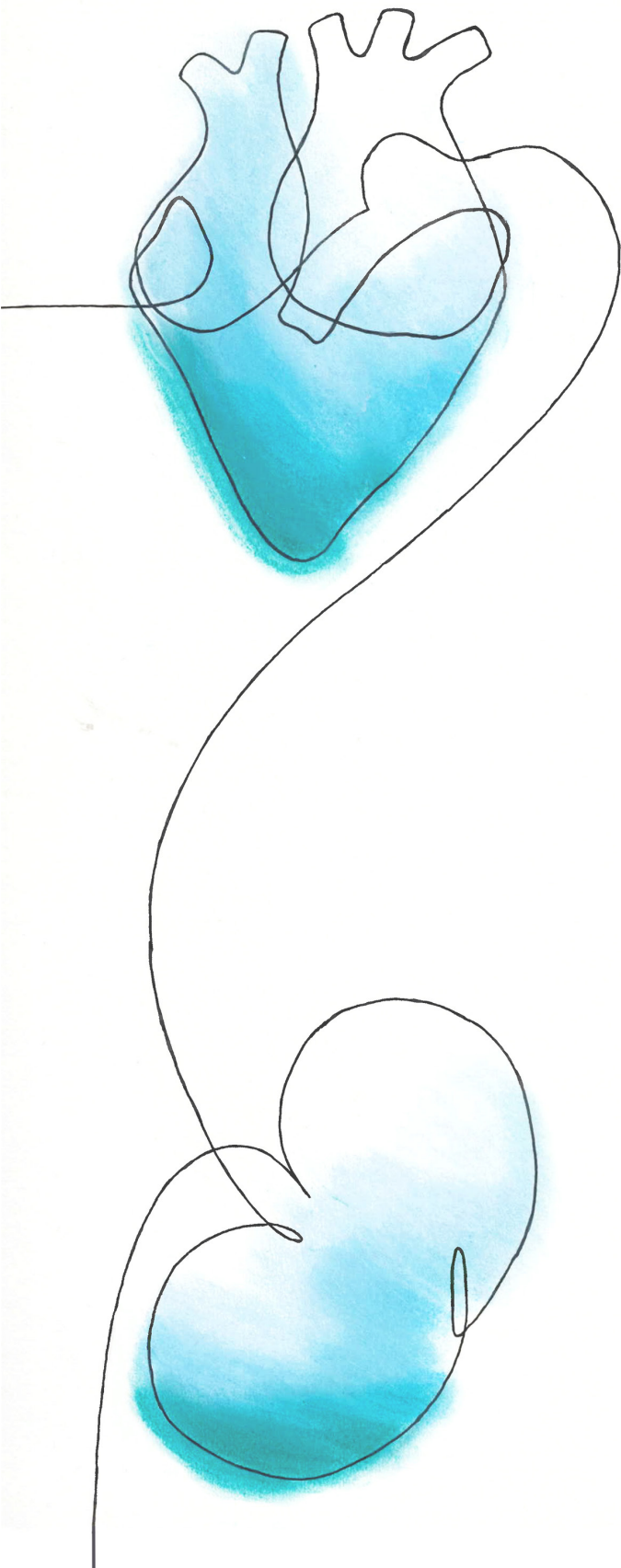
Chapter 1	General introduction and thesis outline	9
Part I Vascular inflammation and renal dysfunction in atherosclerosis		
Chapter 2	The morphological and molecular mechanism of epithelial/endothelial-to-mesenchymal transition and its involvement in atherosclerosis	23
Chapter 3	Impaired kidney function is associated with intraplaque hemorrhage in Patients undergoing carotid endarterectomy	41
Part II The underlying pathophysiology of cardiac remodeling		
Chapter 4	High renin expression in the absence of kidney injury in the murine trans aortic constriction model	67
Chapter 5	Sex specific cardiac remodeling in mice undergoing transverse aortic constriction	83
Part III GDF15 as biomarker and target		
Chapter 6	GDF15 in adverse cardiac remodeling: from biomarker to causal player	111
Chapter 7	GDF15 as a marker and mediator of vascular dysfunction in heart failure of non-ischemic origin	129

Part IV Summary and general discussion

Chapter 8	Summary and general discussion	163
-----------	--------------------------------	-----

Appendix

Nederlandse samenvatting	178
Dankwoord	183
List of publications	189
Curriculum Vitae	191



1

General introduction and thesis outline

Cardiovascular disease

Cardiovascular disease (CVD) is the leading cause of death globally with more than 17.3 million deaths annually and accounting for more than 31% of total mortality¹. Especially in Western countries, increased prevalence of major CVD risk factors such as diabetes, hypertension and obesity enhanced the CVD incidence in the general aging population^{2,3}. CVD covers many vascular and cardiac pathologies, from coronary artery disease to heart failure and stroke⁴. A common cause for CVD, including myocardial infarction (MI) and subsequent heart failure, is atherosclerosis⁵. Atherosclerosis is a slow but progressive lipid-driven inflammatory disease, causing narrowing of the arterial lumen via lesion development in the vascular wall⁶. Risk factors such as high blood pressure, smoking, high cholesterol or inflammation activate the endothelial cells, which increase the expression of adhesion molecules (thereby actively recruiting inflammatory cells like monocytes and T-cells) and the uptake of lipid particles⁷⁻⁹. The sub-endothelial lipid accumulation triggers an inflammatory response, which results in fatty streak formation and an inflammatory culprit lesion⁶. During disease progression, the local monocytic cells laden with lipids (foam cells) progressively die, thereby contributing to the formation of a hypoxic necrotic core which triggers neovascularisation^{6,10,11}. Unlike mature vessels, the newly formed neovessels are prone to leakage, thereby favoring unstable lesions. The formation of luminal thrombus in patients with severe coronary atherosclerosis may lead to complete vessel occlusion and lack of oxygen supply to the heart, also known as a MI^{6,12}.

Patients with advanced lesions and a severe narrowed coronary lumen suffer from local ischemia (unstable angina), whereas patients with complete coronary occlusion suffer from an acute MI¹³. The treatment for both types of patients with unstable angina or MI consists of a catheterization procedure to re-open the occluded artery to restore blood flow and oxygen supply¹³. After ischemic injury, cardiac remodeling is induced to maintain its functions. However ventricular remodeling can result in adverse cardiac remodeling and eventually chronic heart failure^{14,15}. Chronic heart failure concerns all patients with reduced cardiac output and/or elevated intracardiac pressure caused by structural and/or functional cardiac abnormalities^{16,17}. The clinical symptoms for chronic heart failure are shortness of breath and fatigue during stress and rest¹⁸. Historically, heart failure classification was based on symptoms, whereas currently the left ventricular ejection fraction (LVEF) is mostly used to diagnose heart failure¹⁸. Heart failure patients with a normal LVEF ($\geq 50\%$) are classified as heart failure with preserved ejection fraction (HFpEF), whereas patients with a reduced LVEF ($< 40\%$) are classified as heart failure with reduced ejection fraction (HFrEF) and the patients with an intermediated LVEF (40-49%) were recently classified as heart failure with mid-range ejection fraction (HFmrEF)¹⁸. Changes in lifestyle (healthy living) such as quit smoking and reducing salt intake in combination with pharmaceutical interventions including lipid lowering drugs, has resulted in a decline of the number of acute cardiovascular death¹⁹. Drugs for chronic heart failure management are for example, beta blockers and angiotensin converting enzyme (ACE)-inhibitors and

prescription of diuretics for symptomatic relief^{15,20,21}. Most of the prescribed medications have been clinically proven beneficial for heart failure management in HFrEF patients^{18,22}, while they are not effective in HFpEF patients, suggesting a different pathophysiology between HFpEF and HFrEF. Overall, current heart failure treatment is based on relieving the heart as a curative treatment is not yet found. Further investigation is needed to understand the pathophysiological mechanisms for HFpEF, in order to provide beneficial therapeutic interventions and novel disease biomarkers²³. Despite pharmacological and interventional therapies many patients are left with suboptimal treatment, as patients with comorbidities have long been excluded from clinical trials.

HFpEF and HFrEF patients have different clinical characteristics. Unlike the large amount of epidemiological or clinical studies for HFrEF, information is sparse for patients with HFpEF, as they remain asymptomatic for a longer period of time while developing heart failure²⁴. HFpEF appears as a heterogeneous disorder associated with non-cardiovascular comorbidities that relate to adverse outcome of HFpEF²⁴. Oxidative stress and endothelial dysfunction are prominent features of non-cardiovascular comorbidities, characterized by the presence of systemic inflammation, which seem to be more apparent with HFpEF severity^{23,25}. Furthermore, a systemic inflammatory state promotes myocardial and microvascular dysfunction, leading to concentric remodeling, LV diastolic dysfunction and a higher prevalence of adverse clinical outcomes and mortality^{23,24,26,27}.

Non-cardiac comorbidities in cardiovascular disease

A recent study with patient data from the *Get With The Guidelines–Heart Failure* registry (running from 2005 to 2014) showed that 82% of all patients with heart failure suffered from at least 1 non-cardiovascular comorbidity and 25% of all patients suffered from ≥ 3 non-cardiovascular comorbidities²⁸. The most common non-cardiovascular comorbidities in heart failure patients are diabetes mellitus, anemia, pulmonary disease and renal dysfunction²⁹. Especially in the HFpEF population, a higher frequency of non-cardiovascular comorbidities is observed^{24,30,31}. Patients with HFpEF have diastolic dysfunction, concentric LV remodeling or hypertrophy and is more common in a younger population with multiple comorbidities compared to HFrEF^{32,33}. The combination of non-cardiovascular comorbidities and heart failure compromises the general health of the patient, leading to increased risk for hospitalization and mortality²⁸. In 2016, the European society of cardiology (ESC) has updated their clinical practice guidelines for heart failure patient classification, including several extra-cardiac co-morbidities like diabetes, hypertension and kidney function¹⁸. The combination of vascular dysfunction and heart failure with co-morbidities makes disease management a challenge as current therapy is merely based on symptomatic treatment of heart failure and may interfere with each other³⁴. For HFpEF patients, management of co-morbidities as key component in holistic patient care would be beneficial, and one should therefore treat heart failure as a syndrome rather than a disease^{18,23}.

Cardio-renal syndrome

Multiple studies have shown that over 50% of all heart failure patients have renal dysfunction (eGFR <60 ml/min/1.73m² and/or albuminuria >30 albumin/1 g of urine creatinine) which is associated with increased mortality rates^{29,35}. Especially non-ischemic heart failure patients without coronary artery disease suffer from chronic kidney disease (CKD)^{16,29}, defined as abnormalities of the kidney structure or function, present for more than 3 months³⁶. The presence of CKD based on eGFR is similar between HFrEF and HFpEF patients³⁷, although the presence of urinary markers, like urinary albumin excretion shows a stronger association with HFpEF than HFrEF³⁸. The clinical characterization of patients with both heart and kidney failure is described as cardio-renal syndrome (CRS). Within CRS, 5 types of disease have been classified, according to the first failing organ in combination with an acute or chronic disease phenotype (Table 1). For example, CRS type 2 describes the contribution of heart failure to CKD progression, whereas CRS type 4 describes the effects of CKD on the onset and progression of chronic heart failure³⁹⁻⁴¹ (Table 1). The key cardio-renal parameters suggested to drive CRS are hemodynamic interactions (i.e., organ congestion and salt retention), (neuro) hormonal mechanisms (i.e., RAAS activation) and cardiovascular disease-associated mechanisms (i.e., anaemia and cachexia)^{16,42,43}.

Table 1. Five subtypes of cardio-renal syndromes.

Type 1	Type 2	Type 3	Type 4	Type 5
Acute cardio-renal syndrome	Chronic cardio-renal syndrome	Acute reno-cardiac syndrome	Chronic reno-cardiac syndrome	Secondary cardio-renal syndrome
Acute HF	Chronic HF	AKI	CKD	Systemic insult (e.g. severe sepsis)
↓	↓	↓	↓	↓
AKI	Progressive and permanent CKD	Acute HF	Chronic and progressive HF	Simultaneous organ injury

The five subtypes are defined on the direction of effect and the acute or chronic stage of organ inflammation. AKI; acute kidney injury, CKD; chronic kidney disease, HF; heart failure.

As patients with renal dysfunction are often excluded from clinical trials and patient cohort studies, a substantial amount of relevant information of these patients may be missing¹⁸. In this sense, patients primary seen by the nephrologist will not visit the cardiologist until disease develops into severe stages where cardiac dysfunction is revealed. However, even in mild stages of organ dysfunction, the systemic effects of impaired kidney function have large consequences on cardiac function due to inflammation, increased sodium retention, RAAS activation and uremic toxins levels^{16,44-46}. The presence of comorbidities in HFpEF, including renal dysfunction, favors systemic chronic inflammation, consisting in an increased production of pro inflammatory cytokines, oxidative stress and acidosis

as source of microinflammation^{30,47}. Induced by renal tissue inflammation, the pro-inflammatory cytokines are produced by circulating monocytes and endothelial cells⁴⁷. In CRS patients, systemic inflammatory activation as consequence of renal dysfunction is associated with disease progression and worse outcome of heart failure⁴⁸.

Inflammation as a key driver in heart failure and cardio-renal syndrome

Although elevated serum levels of pro-inflammatory cytokines are common to HFpEF and HFrEF, their contributions to both disease pathogenesis differs^{27,49}. In HFrEF, the complex inflammatory response initially needed for appropriate tissue repair of the injured myocardium after an MI, eventually will promote adverse cardiac remodeling^{25,27}. Recently, a novel paradigm was postulated for HFpEF, suggesting that chronic low grade systemic inflammation induced by the presence of comorbidities, contribute to the onset and progression of heart failure through coronary microvascular endothelial inflammation^{25,27,50} (Figure 1). A systemic pro-inflammatory state initiates the production of reactive oxygen species (ROS) in coronary microvascular endothelial cells^{25,50,51}. The production of ROS limits the endothelial nitric oxide (NO) bioavailability for the adjacent cardiomyocytes, thereby decrease protein kinase G (PKG) activity and inducing cardiomyocyte hypertrophy and cellular stiffening⁵⁰. Cardiac stiffening is enhanced by an increase in interstitial and perivascular fibrosis, as coronary microvascular dysfunction upregulates pro-fibrotic cytokines like transforming growth factor (TGF)- β ^{52,53}. TGF- β produced by cardiomyocytes or inflammatory cells can increase collagen production in cardiac myofibroblasts resulting in interstitial fibrosis. While circulating TGF- β is also able to induce endothelial-to-mesenchymal cell transition (EndMT) in endothelial cells^{54,55}. With the transition to a mesenchymal phenotype the endothelial cell loses its primary function as semi-selective barrier and will primarily start to produce collagens, thereby inducing perivascular fibrosis^{56,57}. EndMT has been shown to impair the healthy vascular function and contribute to both cardiac and vascular fibrosis^{49,57}. Therefore, both cardiomyocyte hypertrophy and perivascular and myocardial fibrosis trigger HFpEF-specific concentric cardiac remodeling and stiffening of the cardiovascular wall^{25,52}.

Another factor that contributes to microvascular dysfunction is the production of ROS, since ROS can induce endothelial cell apoptosis and thereby loss of vascular integrity⁵⁸. Upon loss of endothelial cells, the subendothelial extracellular matrix (ECM) becomes exposed to the blood within the vessel, thereby initiating platelet accumulation and clot formation⁵⁹. During cardiac microvascular endothelial dysfunction fibrinolysis is inhibited²⁵, which hampers clot degradation^{60,61}. Persistence of suppressed fibrinolysis may cause microvascular thrombi contributing to an impaired microcirculatory function. Impaired microcirculatory flow can also arise as a direct consequence of coronary endothelial dysfunction. Dysfunctional microvessels endothelial cells exhibit impaired vascular relaxation in response to vasodilators like Bradykinin. This is due to impaired regulation of blood vessel tone via effects on endothelial NO production and calcium handling in smooth muscle cells^{25,62-64}. Impaired vascular relaxation can result in vascular spasms with subsequent reduced coronary flow⁶⁵, and local hypoxia⁶⁶.

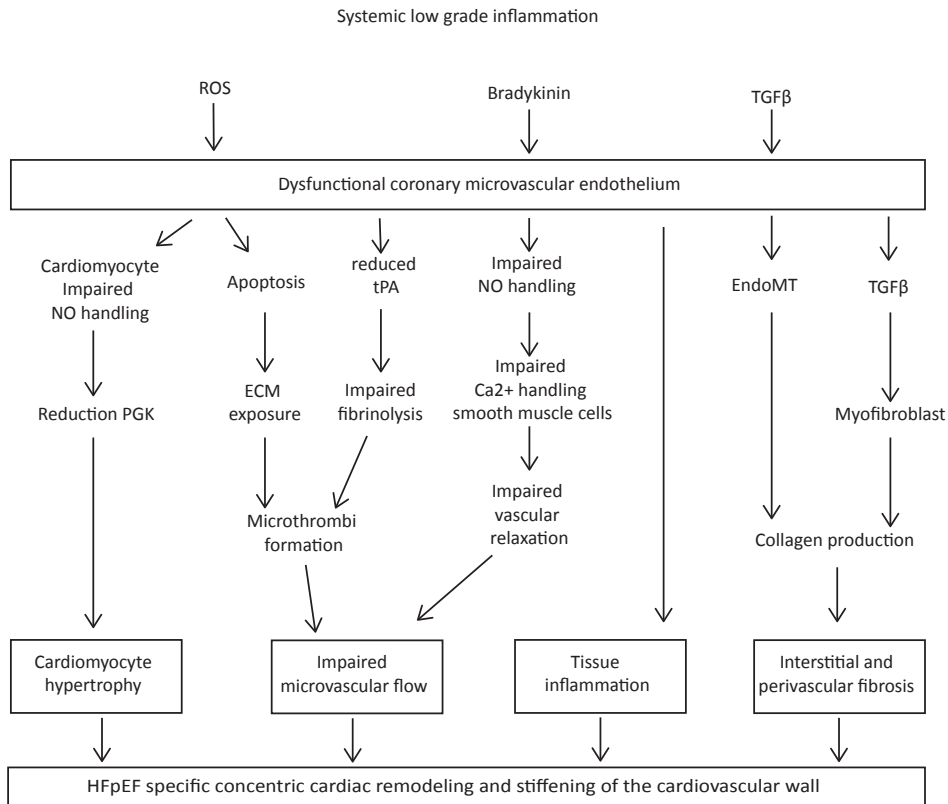


Figure 1. Chronic low grade systemic inflammation contributing to heart failure via coronary microvascular endothelial inflammation.

As a consequence of systemic low grade inflammation, expression of ROS, Bradykinin and TGF- β , endothelial dysfunction is induced. Consequently affecting several endothelial responses, including apoptosis, tPA expression and NO handling and resulting in impaired vascular flow and enhanced tissue inflammation. TGF- β will induce collagen production and fibrosis via the induction of EndoMT in endothelial cells and in the recruitment of myofibroblasts. In addition, impaired NO handling will result in cardiomyocyte hypertrophy. Combined, this will result in a HFpEF specific concentric cardiac remodeling and stiffening of the cardiovascular wall. ROS; Reactive oxygen species, TGF- β ; transforming growth factor beta, NO; nitric oxide, ECM; extracellular matrix, PGK; protein kinase G, tPA; tissue plasminogen activator, HFpEF; heart failure with preserved ejection fraction.

Furthermore, decreased Bradykinin sensitivity and systemic inflammation induces adhesion molecules expression on cardiac endothelial cells, promoting trans endothelial migration of immune cells⁵¹, and expedite the onset or progression of subendothelial tissue inflammation increasing the levels of TGF- β .

Inflammation as a potential target for heart failure therapy

The last decade, inflammation is more recognized for its prominent role in the pathogenesis of both HFrEF and HFpEF, and consequently investigated as possible target for heart failure treatment^{49,67}. Thus far disappointing results have been obtained within

several inflammation targeted strategies in (pre-) clinical trials^{67,68} for heart failure. This might be due to the fact that inflammation is a very complex process irrespective of its trigger, and HFpEF patients comprises a very heterogeneous population. For example, clinical trials targeting Tumor Necrosis Factor (TNF)- α using Infliximab (TNF neutralizing antibodies) or Etanercept (soluble TNF receptor) showed no beneficial effects on cardiac function without major safety issues in chronic heart failure patients^{69,70}. Recently, the IL-1 β inhibitor Canakinumab gained a lot of attention, as the results of the CANTOS trial showed that this drug was able to reduce the risk for recurrent cardiovascular events compared to the placebo group of ischemic heart failure patients⁷¹. Further insights into the diversity and complexity of inflammation specifically in cardiac disorders are required to be able to design cardiac-specific therapies. For example, specific mediators for cardiac tissue inflammation could be promising therapeutic targets, but discovering these specific mediators is needed in future research⁷². Especially HFpEF patients with current insufficient disease management and vascular low grade inflammation would highly benefit from new therapeutic options.

Thesis outline

There is an urgent need for improved diagnostics and prognostic biomarkers for the classification of chronic non-ischemic heart failure patients, as the presence of multiple co-morbidities interfere with current standard disease management. Any improvement is only possible after thorough understanding of the underlying pathophysiological mechanism. With this thesis we highlight the effects of renal dysfunction and vascular inflammation on the development and progression of heart failure. This thesis will address possible mechanisms involved with vascular inflammation in heart failure and suggest GDF15 as potential new therapeutic target.

In **chapter 2** we provide a review on the molecular and morphological mechanisms essential in Endothelial-to-Mesenchymal Transition (EndMT) during cardiovascular development or pathological remodeling during disease. We focus on the role of EndMT in progression and destabilization of atherosclerosis plaques and the potential for future target studies. In **chapter 3** we investigated the influence of kidney dysfunction and inflammation on plaque stability in human carotid plaques obtained by carotid endarterectomy. We observed an association between decreased kidney function and intraplaque hemorrhage, which is strongly associated to plaque vulnerability and poor outcome in patients. As chronic heart failure is associated with an increased risk of chronic kidney disease, in **chapter 4** we evaluate if kidney function decreased upon heart failure progression in a murine pressure overload model. We report that with heart failure progression, elevated levels of renin are present which indicate RAS activation in response to a reduced renal blood flow. Despite severe heart failure we did not find any functional or structural abnormality in the kidneys indicative for kidney dysfunction. Besides risk factors such as kidney dysfunction we know that sex is a major

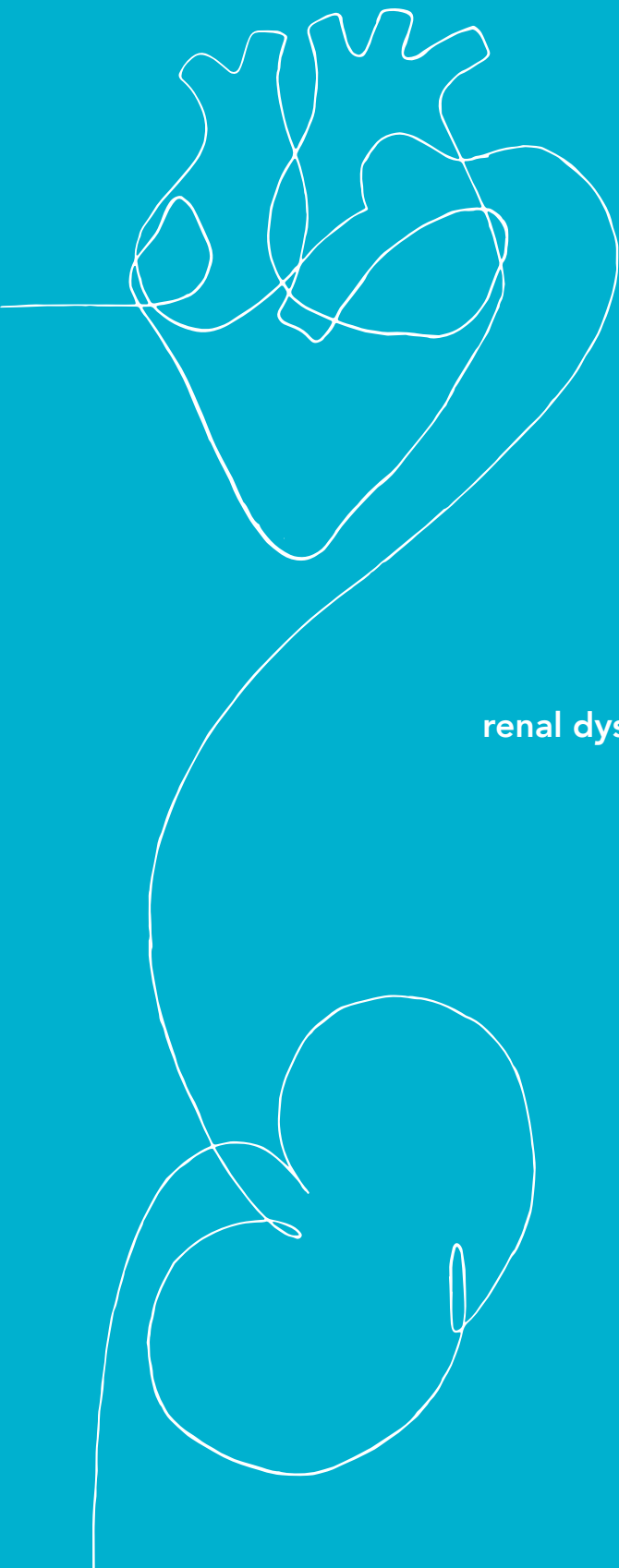
determinant in cardiovascular disease. From the clinic we know sex plays a role in cardiac remodeling, however the underlying pathophysiological mechanisms driving these differences are unknown. Therefore, in **chapter 5** we investigated the biological sex differences in cardiac remodeling after induction of pressure overloaded heart failure in mice. Although both male and female mice show a deteriorated cardiac function by an increased end systolic and end diastolic volume, we observed eccentric cardiac remodeling in male and concentric cardiac remodeling in female mice. When looking at the underlying sex differences in pathophysiological mechanisms, we found new potential sex specific pathways possibly involved in the alternate cardiac remodeling. In **chapter 6** we introduce growth differentiation factor 15 (GDF15) as a causal player and possible therapeutic target in adverse cardiac remodeling. Although GDF15 is a proven valuable biomarker and high levels are a strong prognostic marker for worse outcome in heart failure, we address crucial points when considering GDF15 as standard care biomarker or therapeutic target. In **chapter 7** we focus on the causal role of GDF15 in severe heart failure. We show that increased GDF15 levels associate with worse outcome in 2 independent cohorts of non-ischemic heart failure patients and GDF15 expression is increased upon cardiac pressure overload in mice. As such we set out to establish if GDF15 is causally involved in adverse remodeling. We used a GDF15 knock-out mouse which show extreme adverse cardiac remodeling upon pressure overload (by transverse aortic constriction) compared to wildtype mice. When assessing the myocardial tissue on a microscopic levels we observed that perivascular fibrosis and EndMT was significantly increased in hearts of GDF15 knock-out mice. We therefore decided to address the possible role of GDF15 on EndMT and vascular dysfunction underlying the adverse cardiac remodeling. Finally in **chapter 8**, we discuss the most important findings of this thesis and provide critical directions for future research and highlight opportunities for improved patient care, i.e. targeting disease mediating tissue inflammation.

References

1. Cardiovascular diseases (CVDs). [https://www.who.int/en/news-room/fact-sheets/detail/cardiovascular-diseases-\(cvds\)](https://www.who.int/en/news-room/fact-sheets/detail/cardiovascular-diseases-(cvds)).
2. Dimmeler, S. Cardiovascular disease review series. *EMBO Mol. Med.* 3, 697 (2011).
3. Tran, J. *et al.* Patterns and temporal trends of comorbidity among adult patients with incident cardiovascular disease in the UK between 2000 and 2014: A population-based cohort study. *PLOS Med.* 15, e1002513 (2018).
4. Stewart, J., Manmathan, G. & Wilkinson, P. Primary prevention of cardiovascular disease: A review of contemporary guidance and literature. *JRSM Cardiovasc. Dis.* 6, 1–9 (2017).
5. Frostegård, J. Immunity, atherosclerosis and cardiovascular disease. *BMC Med.* 11, 1–13 (2013).
6. Libby, P., Ridker, P. M. & Maseri, A. Inflammation and atherosclerosis. *Circulation* 105, 1135–1143 (2002).
7. Tabas, I., Williams, K. J. & Boren, J. Subendothelial lipoprotein retention as the initiating process in atherosclerosis: update and therapeutic implications. *Circulation* 116, 1832–1844 (2007).
8. Zhang, C. The role of inflammatory cytokines in endothelial dysfunction. *Basic Res. Cardiol.* 103, 398–406 (2008).
9. Lovren, F., Teoh, H. & Verma, S. Obesity and Atherosclerosis: Mechanistic Insights. *Can. J. Cardiol.* 31, 177–183 (2015).
10. Stary, H. C. *et al.* A definition of advanced types of atherosclerotic lesions and a histological classification of atherosclerosis: A report from the Committee on Vascular Lesions of the council on arteriosclerosis, American heart association. *Circulation* 92, 1355–1374 (1995).
11. Pelisek, J. *et al.* Impact of chronic kidney disease on carotid plaque vulnerability. *J. Vasc. Surg.* 54, 1643–1649 (2011).
12. Lüscher, A. J. Atherosclerosis. *Nature* 407, 233–241 (2000).
13. Deckers, J. W. Classification of myocardial infarction and unstable angina: a re-assessment. *Int. J. Cardiol.* 167, 2387–2390 (2013).
14. Minicucci, M. F., Azevedo, P. S., Polegato, B. F., Paiva, S. A. R. & Zornoff, L. A. M. Heart failure after myocardial infarction: clinical implications and treatment. *Clin. Cardiol.* 34, 410–414 (2011).
15. Bahit, M. C., Kochar, A. & Granger, C. B. Post-Myocardial Infarction Heart Failure. *JACC. Heart Fail.* 6, 179–186 (2018).
16. Schefold, J. C., Filippatos, G., Hasenfuss, G., Anker, S. D. & Von Haehling, S. Heart failure and kidney dysfunction: Epidemiology, mechanisms and management. *Nat. Rev. Nephrol.* 12, 610–623 (2016).
17. Ponikowski, P. *et al.* Heart failure: preventing disease and death worldwide. *ESC Hear. Fail.* 1, 4–25 (2014).
18. Ponikowski, P. *et al.* 2016 ESC Guidelines for the Diagnosis and Treatment of Acute and Chronic Heart Failure. *Rev. Española Cardiol.* 69, 1167 (2016).
19. Herrington, W., Lacey, B., Sherliker, P., Armitage, J. & Lewington, S. Epidemiology of Atherosclerosis and the Potential to Reduce the Global Burden of Atherothrombotic Disease. *Circ. Res.* 118, 535–546 (2016).
20. Stough, W. G. & Patterson, J. H. Role and Value of Clinical Pharmacy in Heart Failure Management. *Clin. Pharmacol. Ther.* 102, 209–212 (2017).
21. Alghamdi, F. & Chan, M. Management of heart failure in the elderly. *Curr. Opin. Cardiol.* 32, 217–223 (2017).
22. Voors, A. A. *et al.* A systems BIOlogy Study to TAilored Treatment in Chronic Heart Failure: rationale, design, and baseline characteristics of BIOSTAT-CHF. *Eur. J. Heart Fail.* 18, 716–726 (2016).
23. Tibrewala, A. & Yancy, C. W. Heart Failure with Preserved Ejection Fraction in Women. *Heart Fail. Clin.* 15, 9–18 (2019).
24. Liu, M., Fang, F. & Yu, C. M. Noncardiac comorbidities in heart failure with preserved ejection fraction – A Commonly ignored fact. *Circ. J.* 79, 954–959 (2015).
25. Paulus, W. J. & Tschöpe, C. A novel paradigm for heart failure with preserved ejection fraction: comorbidities drive myocardial dysfunction and remodeling through coronary microvascular endothelial inflammation. *J. Am. Coll. Cardiol.* 62, 263–71 (2013).
26. Sorop, O. *et al.* Multiple common comorbidities produce left ventricular diastolic dysfunction associated with coronary microvascular dysfunction, oxidative stress, and myocardial stiffening. *Cardiovasc. Res.* 114, 954–964 (2018).
27. Da Silva, D. M., Langer, H. & Graf, T. Inflammatory and molecular pathways in heart failure-ischemia, HFpEF and transthyretin cardiac amyloidosis. *Int. J. Mol. Sci.* 20, 1–28 (2019).
28. Sharma, A. *et al.* Trends in Noncardiovascular Comorbidities Among Patients Hospitalized for Heart Failure: Insights From the Get With The Guidelines-Heart Failure Registry. *Circ. Heart Fail.* 11, e004646 (2018).
29. van Deursen, V. M. *et al.* Co-morbidities in patients with heart failure: an analysis of the European Heart Failure Pilot Survey. *Eur. J. Heart Fail.* 16, 103–111 (2014).
30. Gombert-Maitland, M., Shah, S. J. & Guazzi, M. Inflammation in Heart Failure With Preserved Ejection Fraction Time to Put Out the Fire. *JACC Hear. Fail.* 4, 325–328 (2016).

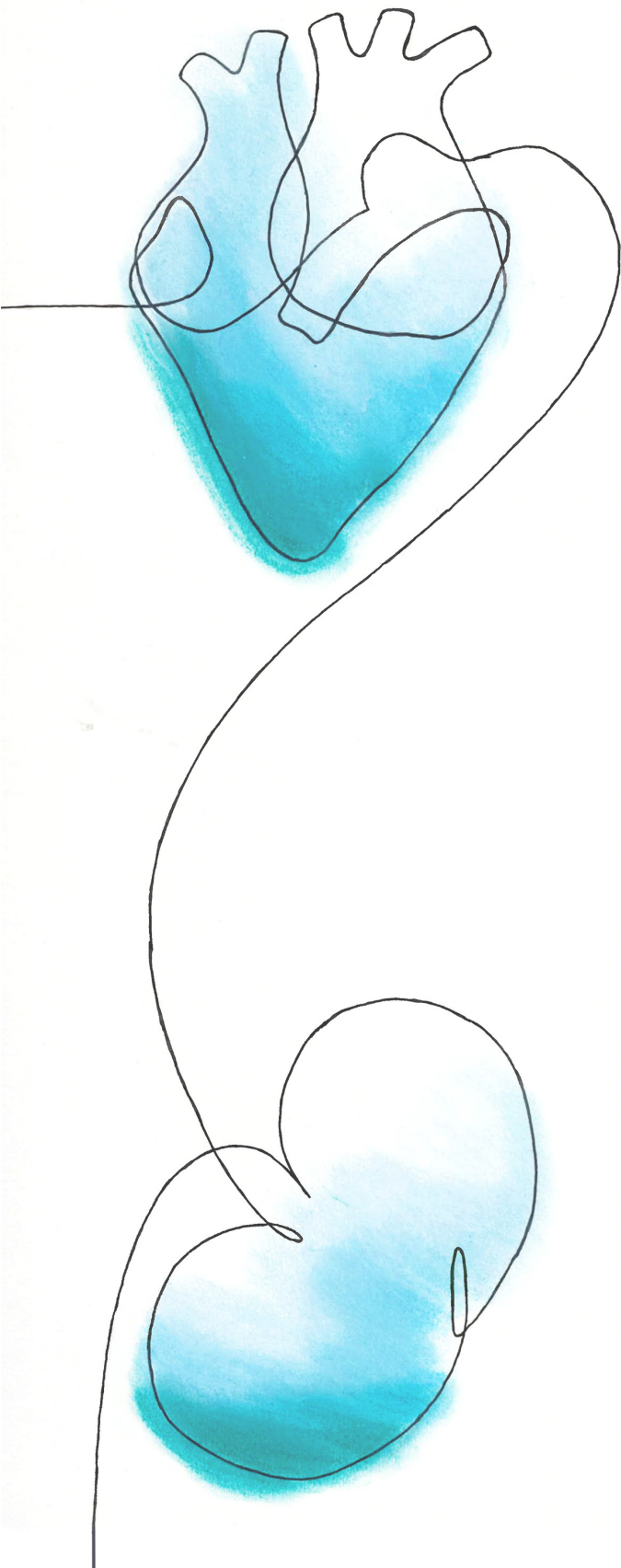
31. Ather, S. *et al.* Impact of noncardiac comorbidities on morbidity and mortality in a predominantly male population with heart failure and preserved versus reduced ejection fraction. *J. Am. Coll. Cardiol.* 59, 998–1005 (2012).
32. Zacharias, M. *et al.* Clinical epidemiology of heart failure with preserved ejection fraction (HFpEF) in comparatively young hospitalized patients. *Int. J. Cardiol.* 202, 918–921 (2016).
33. Lekavich, C. L., Barksdale, D. J., Neelon, V. & Wu, J.-R. Heart failure preserved ejection fraction (HFpEF): an integrated and strategic review. *Heart Fail. Rev.* 20, 643–653 (2015).
34. Lyle, M. A. & Brozovich, F. V. HFpEF, a Disease of the Vasculature: A Closer Look at the Other Half. *Mayo Clin. Proc.* 93, 1305–1314 (2018).
35. Hillege, H. L. *et al.* Renal function as a predictor of outcome in a broad spectrum of patients with heart failure. *Circulation* 113, 671–678 (2006).
36. Ketteler, M. *et al.* Executive summary of the 2017 KDIGO Chronic Kidney Disease–Mineral and Bone Disorder (CKD-MBD) Guideline Update: what's changed and why it matters. *Kidney Int.* 92, 26–36 (2017).
37. Yancy, C. W., Lopatin, M., Stevenson, L. W., De Marco, T. & Fonarow, G. C. Clinical presentation, management, and in-hospital outcomes of patients admitted with acute decompensated heart failure with preserved systolic function: A report from the Acute Decompensated Heart Failure National Registry (ADHERE) database. *J. Am. Coll. Cardiol.* 47, 76–84 (2006).
38. Brouwers, F. P. *et al.* Incidence and epidemiology of new onset heart failure with preserved vs. reduced ejection fraction in a community-based cohort: 11-year follow-up of PREVEND. *Eur. Heart J.* 34, 1424–1431 (2013).
39. Zannad, F. & Rossignol, P. Cardiorenal Syndrome Revisited. *Circulation* 138, 929–944 (2018).
40. Rangaswami, J. *et al.* Cardiorenal Syndrome: Classification, Pathophysiology, Diagnosis, and Treatment Strategies: A Scientific Statement From the American Heart Association. *Circulation* 139, 840–878 (2019).
41. Ronco, C. Cardiorenal Syndromes: Definition and Classification. *Contributions to Nephrol.* 164, 33–38 (2010).
42. Gnanaraj, J. & Radhakrishnan, J. Cardio-renal syndrome. *F1000Research* 5, 1–10 (2016).
43. Liu, S. Heart-kidney interactions: mechanistic insights from animal models. *Am. J. Physiol. Renal Physiol.* 316, 974–985 (2019).
44. Moe, G. Heart failure with multiple comorbidities. *Curr. Opin. Cardiol.* 31, 209–216 (2016).
45. Wouters, O. J., O'Donoghue, D. J., Ritchie, J., Kanavos, P. G. & Narva, A. S. Early chronic kidney disease: diagnosis, management and models of care. *Nat. Rev. Nephrol.* 11, 491–502 (2015).
46. Thomas, R., Kanso, A. & Sedor, J. R. Chronic kidney disease and its complications. *Prim. Care* 35, 329–344 (2008).
47. Mihai, S. *et al.* Inflammation-related mechanisms in chronic kidney disease prediction, progression, and outcome. *J. Immunol. Res.* 2180373, 1–16 (2018).
48. Linhart, C. *et al.* Systemic inflammation in acute cardiorenal syndrome: an observational pilot study. *ESC Hear. Fail.* 5, 920–930 (2018).
49. Van Linthout, S. & Tschöpe, C. Inflammation – Cause or Consequence of Heart Failure or Both? *Curr. Heart Fail. Rep.* 14, 251–265 (2017).
50. Franssen, C. *et al.* Myocardial Microvascular Inflammatory Endothelial Activation in Heart Failure With Preserved Ejection Fraction. *JACC. Heart Fail.* 4, 312–324 (2016).
51. Vitiello, L. *et al.* Microvascular inflammation in atherosclerosis. *IJC Metab. Endocr.* 3, 1–7 (2014).
52. Mohammed, S. F. *et al.* Coronary microvascular rarefaction and myocardial fibrosis in heart failure with preserved ejection fraction. *Circulation* 131, 550–559 (2015).
53. Ma, Z. G., Yuan, Y. P., Wu, H. M., Zhang, X. & Tang, Q. Z. Cardiac fibrosis: new insights into the pathogenesis. *Int. J. Biol. Sci.* 14, 1645–1657 (2018).
54. Rieder, F. *et al.* Inflammation-induced endothelial-to-mesenchymal transition: A novel mechanism of intestinal fibrosis. *Am. J. Pathol.* 179, 2660–2673 (2011).
55. Wesseling, M., Sakkars, T. R., de Jager, S. C. A., Pasterkamp, G. & Goumans, M. J. The morphological and molecular mechanisms of epithelial/endothelial-to-mesenchymal transition and its involvement in atherosclerosis. *Vascul. Pharmacol.* 106, 1–8 (2018).
56. Zeisberg, E. M. *et al.* Endothelial-to-mesenchymal transition contributes to cardiac fibrosis. *Nat. Med.* 13, 952–961 (2007).
57. Xu, X. *et al.* Endocardial fibroelastosis is caused by aberrant endothelial to mesenchymal transition. *Circ. Res.* 116, 857–866 (2015).
58. Redza-Dutordoir, M. & Averill-Bates, D. A. Activation of apoptosis signalling pathways by reactive oxygen species. *Biochim. Biophys. Acta Mol. Cell Res.* 1863, 2977–2992 (2016).
59. Wang, Y., Gallant, R. C. & Ni, H. Extracellular matrix proteins in the regulation of thrombus formation. *Curr. Opin. Hematol.* 23, 280–287 (2016).
60. van den Born, B.-J. H. *et al.* Endothelial dysfunction, platelet activation, thrombogenesis and fibrinolysis in patients with hypertensive crisis. *J. Hypertens.* 29, 922–927 (2011).

61. Cerinic, M. M. et al. Blood coagulation, fibrinolysis, and markers of endothelial dysfunction in systemic sclerosis. *Semin. Arthritis Rheum.* 32, 285–295 (2003).
62. Hornig, B. & Drexler, H. Endothelial function and bradykinin in humans. *Drugs* 54, 42–47 (1997).
63. Ancion, A., Tridetti, J., Nguyen Trung, M.-L., Oury, C. & Lancellotti, P. A Review of the Role of Bradykinin and Nitric Oxide in the Cardioprotective Action of Angiotensin-Converting Enzyme Inhibitors: Focus on Perindopril. *Cardiol. Ther.* 8, 179–191 (2019).
64. Sandoo, A., van Zanten, J. J. C. S. V., Metsios, G. S., Carroll, D. & Kitas, G. D. The endothelium and its role in regulating vascular tone. *Open Cardiovasc. Med. J.* 4, 302–312 (2010).
65. Ohba, K. et al. Microvascular Coronary Artery Spasm Presents Distinctive Clinical Features With Endothelial Dysfunction as Nonobstructive Coronary Artery Disease. *J. Am. Heart Assoc.* 1, e002485 (2012).
66. Mohammed, S. F., Majure, D. T. & Redfield, M. M. Zooming in on the Microvasculature in Heart Failure With Preserved Ejection Fraction. *Circ. Heart Fail.* 9, e003272 (2016).
67. Heymans, S. et al. Inflammation as a therapeutic target in heart failure? A scientific statement from the Translational Research Committee of the Heart Failure Association of the European Society of Cardiology. *Eur. J. Heart Fail.* 11, 119–129 (2009).
68. Dick, S. A. & Epelman, S. Chronic Heart Failure and Inflammation: What Do We Really Know? *Circ. Res.* 119, 159–176 (2016).
69. Chung, E. S., Packer, M., Lo, K. H., Fasanmade, A. A. & Willerson, J. T. Randomized, double-blind, placebo-controlled, pilot trial of infliximab, a chimeric monoclonal antibody to tumor necrosis factor- α , in patients with moderate-to-severe heart failure: results of the anti-TNF Therapy Against Congestive Heart Failure. *Circulation* 107, 3133–3140 (2003).
70. Anker, S. D. & Coats, A. J. S. How to RECOVER from RENAISSANCE? The significance of the results of RECOVER, RENAISSANCE, RENEWAL and ATTACH. *Int. J. Cardiol.* 86, 123–130 (2002).
71. Ridker, P. M. et al. Anti-inflammatory Therapy with Canakinumab for Atherosclerotic Disease. *N. Engl. J. Med.* 377, 1119–1131 (2017).
72. Luan, H. H. et al. GDF15 Is an Inflammation-Induced Central Mediator of Tissue Tolerance. *Cell* 178, 1231–1244 (2019).



PART I

Vascular inflammation and renal dysfunction in atherosclerosis



2

The morphological and molecular mechanisms of epithelial/endothelial-to-mesenchymal transition and its involvement in atherosclerosis

Vascular pharmacology 2018; 106:1-8

M. Wesseling^{1,2*}, T. R. Sakkars^{1*}, S. C.A. de Jager^{1,3}, G. Pasterkamp², M.J. Goumans⁴

*These authors contributed equally to the manuscript

¹ Laboratory of Experimental Cardiology, University Medical Center Utrecht, Utrecht, The Netherlands

² Laboratory of Clinical Chemistry and Histology, University Medical Center Utrecht, Utrecht, The Netherlands

³ Laboratory of Translational Immunology, University Medical Center Utrecht, Utrecht, The Netherlands

⁴ Molecular Cell Biology, Leiden University Medical Center, Leiden, The Netherlands

Abstract

Cell transdifferentiation occurs during cardiovascular development or remodeling either as a pathologic feature in the progression of disease or as a response to injury. Endothelial-to-Mesenchymal Transition (EndMT) is a process that is classified as a specialized form of Epithelial-to-Mesenchymal Transition (EMT), in which epithelial cells lose their epithelial characteristics and gain a mesenchymal phenotype. During transdifferentiation, cells lose both cell-cell contacts and their attachment to the basement membrane. Subsequently, the shape of the cells changes from a cuboidal to an elongated shape. A rearrangement of actin filaments facilitates the cells to become motile and prime their migration into the underlying tissue. EMT is a key process during embryonic development, wound healing and tissue regeneration, but has also been implicated in pathophysiological processes, such organ fibrosis and tumor metastases. EndMT has been associated with additional pathophysiological processes in cardiovascular related diseases, including atherosclerosis. Recent studies prove a significant role for EndMT in the progression and destabilization of atherosclerotic plaques, as a consequence of EndMT-derived fibroblast infiltration and the increased secretion of matrix metalloproteinase respectively. In this review we will discuss the essential molecular and morphological mechanisms of EMT and EndMT, along with their common denominators and key differences. Finally, we will discuss the role of EMT/EndMT in developmental and pathophysiological processes, focusing on the potential role of EndMT in atherosclerosis in more depth.

Introduction

In the past decades, the discovery of non-myeloid stem cells and their ability to differentiate into different cell lineages has been of great significance in the research field of developmental biology, regenerative medicine and cancer development. Mature epithelial cells may acquire remarkable cell plasticity and transdifferentiate into mesenchymal cells, a biological process called Epithelial-to-Mesenchymal Transition (EMT). During this process, epithelial cells lose their strong cell-cell contact as well as their attachment with the basement membrane upon degradation and deconstruction of cellular junctions^{1,2}. Subsequently, the epithelial cells fail to retain their apical-basal polarity and gain a new polarity, termed as front-rear polarity. In this transition to front-rear polarity, the cytoskeleton reorganizes from cortical to parallel contractile actin fibers, which changes the cell shape in such a way that the cells become motile and start to migrate into the underlying tissue^{3,4}. As a consequence of the change in cell shape, the cell starts to remodel the surrounding extracellular matrix (ECM). This remodeling indicates the appearance of an epithelial-derived mesenchymal cell. When a cell expresses mesenchymal markers, but still contains some epithelial features, it is called intermediate EMT¹. All these morphological changes are regulated by multiple signaling pathways, which activate EMT specific transcription factors, contributing to a new gene expression pattern⁵. EMT is involved in several fundamental processes during embryonic development, including wound healing, regeneration and heart development, but also in pathophysiological processes, such as organ fibrosis and cancer⁶.

In more recent studies, a similar process is described for the endothelium, where endothelial cells undergo the same transition, called Endothelial-to-Mesenchymal Transition (EndMT). EndMT has similar morphological and molecular characteristics as EMT, gives rise to the same mesenchymal phenotype and is involved in similar developmental and pathophysiological processes². However, despite these similarities, key differences with respect to the molecular mechanisms that drive the transition of EndMT have been described⁷. Interestingly, EndMT has been suggested to be involved in the pathophysiological process of cardiovascular diseases^{8,9}.

In this review, the essential molecular mechanisms that drive EMT and its involvement in developmental and pathophysiological processes are described. Subsequently, we will discuss the common denominators and key differences of EMT and EndMT. Finally, we will outline the role of EndMT in cardiovascular disease, where its potential involvement in atherosclerosis is discussed in more depth (Figure 1a).

EndMT a form of EMT

The morphological and molecular processes of EndMT can be compared to EMT, as endothelial cells are a specialized form of epithelial cells with the same characteristics and both can acquire a mesenchymal phenotype. There are however some important differences between EndMT and EMT⁷. The main structure of adherens junctions in endothelial cells is VE-cadherin, instead of E-cadherin (CDH1) in other epithelial cells (Table 1).

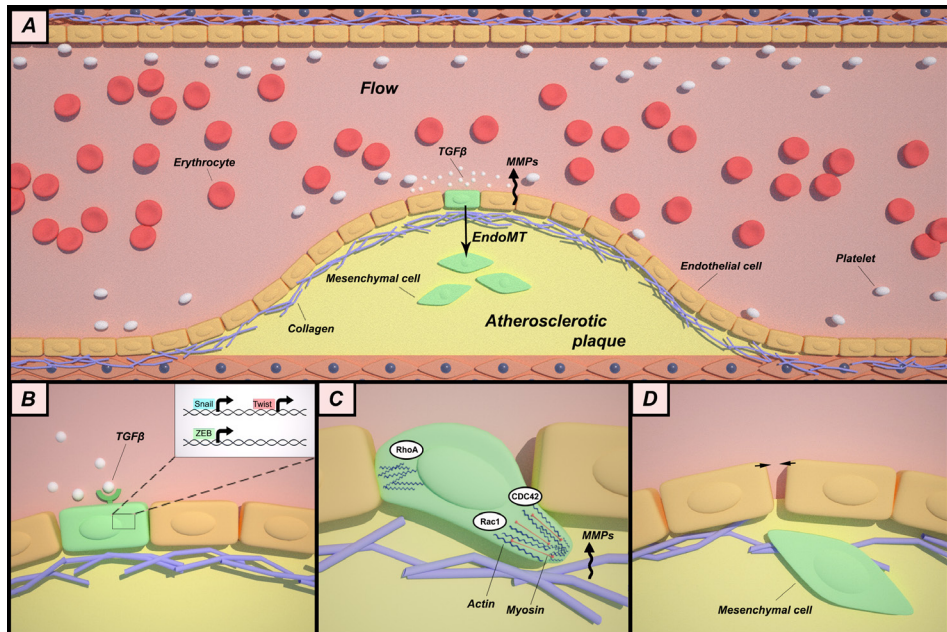


Figure 1. The role of EndMT in the pathophysiology process of atherosclerosis.

a) A large vessel with an atherosclerotic plaque is illustrated. Upon TGF- β stimulation the endothelial cells in the cap of the plaque undergo endothelial-to-mesenchymal transition (EndMT), resulting in transdifferentiated mesenchymal cells. The EndMT-derived fibroblasts are characterized by their increased secretion of MMPs which correlates with the formation of unstable plaques. b) TGF- β stimulation contributes to a new gene expression pattern in which specific EndMT transcription factors are activated in the nucleus of the endothelial cell. Snail, ZEB and Twist are upregulated which initiates the transdifferentiation towards a mesenchymal cell type. c) After the degradation of cell adhesion junctions, the shape of the cell changes switching from an apical-basal polarity to a front-rear polarity. At the rear side of the cell RhoA is upregulated, promoting actomyosin contractility and retraction, while in the front side of the cell, CDC42 and Rac1 are upregulated which results in actin polarization and the formation membrane protrusions. The increased expression of MMPs and mesenchymal integrins enables the cell to remodel the surrounding ECM and become motile. d) After a complete EndMT, the endothelial cell has become a fully differentiated invasive mesenchymal cell.

Endothelial cells also express fewer tight junctions. Furthermore, the main component of the intermediate filaments in epithelial cells is cytokeratin, which via EMT is replaced by vimentin, while endothelial cells already contain vimentin as its basic intermediate filament component (Table 1). Finally, endothelial cells express specific surface proteins when compared to other epithelial cells, such as PECAM (CD31), VE-cadherin and VEGFR2, while epithelial surface markers, include E-cadherin, claudins, occludins, desmoplakin and cytokeratin (Table 1). As a consequence, the molecular and biochemical signaling also vary between EndMT and EMT. Fibroblast growth factor (FGF) signaling is a central player in the maintenance of the endothelial phenotype and function, and its downregulation is key for the initiation of EndMT (Table 1)¹⁰. Despite these critical differences, transforming growth factor (TGF)- β signaling is still identified as the most essential signaling pathway steering both EMT as EndMT.

Table 1. Differences between EMT and EndMT on a cellular level.

	EMT	EndMT
Adherens junctions	• E-cadherin (CDH1)	• VE-cadherin (CD144) • Fewer tight junctions
Intermediate filaments	• Cytokeratin	• Vimentin
Surface markers	• Claudins, occludins, desmoplakin and cytokeratin	• PECAM (CD31), VEGFr
Molecular signaling	• TGF- β	• TGF- β with additional FGF downregulation

Abbreviations: PECAM, platelet endothelial cell adhesion molecule; VEGFr, vascular endothelial growth factor receptor; TGF- β , transforming growth factor beta; FGF, fibroblast growth factor.

TGF- β signaling

At the top of the regulatory network of transcription factors and target genes, the growth factor signaling pathways are located. These pathways are responsible for the induction and progression of all the cellular changes that occur during EMT and EndMT. A signaling pathway is initiated by binding of a ligand to the transmembrane receptor, leading to kinase activation, phosphorylation of intracellular signaling molecules and finally increased or reduced expression of target genes involved in mesenchymal differentiation. There are various potent factors able to induce these target genes alone or in combination, for example growth factors like Wnt, Notch, EGF, FGF, but also hypoxia and environmental influences like obesity^{11,12}. However, the most dominant signaling pathway involved in mesenchymal transformation is the TGF- β signaling pathway (Figure 1a)^{2,12}. TGF- β regulates transcription via multiple downstream signaling pathways, of which Smad signaling is the most important one (Figure 2). The TGF- β family is divided in three subfamilies, which consist of the three mammalian TGF- β isoforms, activins and BMPs¹³. TGF- β family members bind to a heterotetrameric receptor complex consisting of two type-II receptors and two type-I receptors (Figure 2). The type-II receptors can be divided in five different types and the type-I receptor, also referred to as activin receptor-like kinase (ALK), in seven different ones, all binding ligands of the TGF- β superfamily, albeit with different preference and affinity (Figure 2). In endothelial cells, TGF- β binds, besides the TGF- β type I receptor ALK5, to an additional type I receptor, called activin receptor-like kinase 1 (ALK1)^{14,15}. The homodimeric transmembrane proteins betaglycan and endoglin function as a co-receptor and facilitate binding of the different TGF- β ligands to the TGF- β receptor complex (Figure 2)¹³. TGF- β initiates signaling by first binding to the type-II receptor, which then recruits the type-I receptor and phosphorylates its serine/threonine domain¹⁶. This domain forms a docking side for multiple signaling proteins and transcription factors, which form the initiating factors of multiple TGF- β induced signaling pathways involved in EMT and EndMT. The most relevant signaling pathways will be discussed, beginning with the Smad signaling pathway.

The activated TGF- β receptor complex transduces its signal by phosphorylating Smad transcription factors, which subsequently translocate into the nucleus and bind to promoters of EMT and EndMT inducing genes (Figure 2)^{17,18}. These genes include the

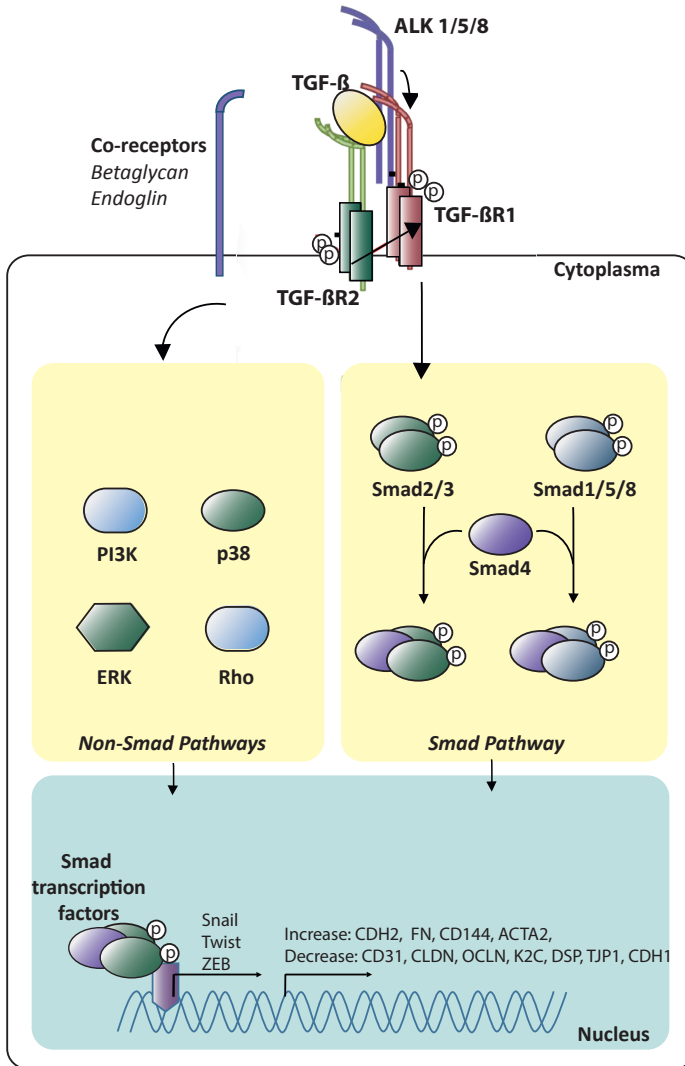


Figure 2. TGF- β signaling.

Upon TGF- β ligand binding to a heterotetrameric complex of two TGF β RII receptors and two type I receptors, the type I receptor kinase is activated by the type 2 receptor, followed by activation of intracellular Smad and non-Smad pathways, which in turn translocate to the nucleus to regulate the expression of transcription factors like SNAIL, TWIST and ZEB. These transcription factors will in turn increase and decrease the expression of several genes involved in EndMT, as depicted in the figure. The co-receptors Betaglycan and endoglin facilitate binding and modulate signaling.

key transcription factor families Snail, Twist and ZEB (Figure 2)¹⁹. Additionally, TGF- β also regulates EMT and EndMT via other signaling pathways, called non-Smad signaling, for example via the activation of signaling proteins involved in cytoskeletal rearrangement (Figure 2)^{2,12}. Consequently, TGF- β signaling activates the Rho GTPases: RhoA, RAC1 and CDC42. Furthermore, TGF- β signaling activates the Phosphatidylinositol 3-kinase (PI3K). Remarkably, the addition of the PI3K inhibitor LY294002 prevents the TGF- β induced transcriptional responses, deconstruction of ZO-1, activation of AKT, phosphorylation of Smad2 and cell migration, indicating the important role of TGF- β signaling via PI3K in EMT²⁰. The inhibition of AKT via siRNA's leads to the downregulation of Snail and the maintenance of the epithelial phenotype²¹. Additionally, AKT phosphorylates and inactivates GSK3 β , thereby preventing Snail1 from being degraded²².

Transcription factors regulating EMT and EndMT

All cellular changes that occur during the mesenchymal transition, such as junction loss, polarity transition and cytoskeleton reorganization, are controlled at the DNA level by transcription factors. The three key transcription factors regulating EMT and/or EndMT are: Snail, Twist and ZEB, as well as the transcription cofactors YAP and TAZ^{12,23,24} (Figure 1b). During the transition, these transcription factors bind alone or together to the promoter of target genes and/or regulating each other's expression to repress the expression of epithelial genes and stimulate the expression of mesenchymal genes.

Snail

The Snail family of zinc-finger transcription factor consists of three members: Snail, Slug and Smuc, respectively Snail1, Snail2 and Snail3⁵. Snail1 plays a pivotal role in cell transition as it interacts with multiple transcription factors and signaling proteins involved in the downregulation and upregulation of respectively epithelial, endothelial and mesenchymal features. For instance, the interaction of Snail1 with Smad3 and Smad4 results in the repression of transcription of the E-cadherin and occludin promoter²⁵. While, Snail downregulates claudin (CLDN), occludin (OCLN), desmoplakin (DSP) and cytokeratin (K2C), it upregulates mesenchymal features like N-cadherin (CDH2), collagen and fibronectin (FN) (Figure 2)². As Snail is key regulator of both EMT and EndMT, several signaling pathways control the activity, degradation and localization of Snail within the cell to modulate its activity².

Twist

The Twist transcription factor is important for morphogenesis by determining the final differentiation status of cell lineages during development²⁶. Just like Snail, Twist is a key regulator in mesenchymal differentiation, as it interacts with multiple signaling proteins and transcription factors involved in the downregulation of epithelial genes and the upregulation of mesenchymal genes². Many of the downstream targets for Twist are

similar to those of the Snail transcription factor, such as the downregulation of CDH1, which encodes for the transmembrane protein E-cadherin²⁷.

ZEB

The zinc finger E-box binding homeobox (ZEB) transcription factor is a key regulator of development in all kinds of tissues. It includes two paralogs, the family members ZEB1 and ZEB2, which contain zinc finger domains at both ends of the protein, required for DNA binding at the E-motif of target genes⁵. They also contain a homeodomain, a Smad-binding domain and a CTBP-binding domain. Just as Snail and Twist, the ZEB transcription factor forms a central component in multiple signaling pathways leading to the repression or activation of target genes facilitating EMT and EndMT², for example, downregulating ZO1 (TJP1), and upregulating fibronectin (FN), N-cadherin (CDH2) and MMPs (Figure 2). Additionally, ZEB plays an important role in down regulating the expression of the critical EMT protein E-cadherin²⁸. As mentioned before, transcription factors in EMT also regulate each other's expression and often work. This is indeed the case for ZEB1, since ZEB1 is a downstream transcriptional target of the cooperating transcription factors Snail1 and Twist²⁹.

YAP/TAZ

Transcriptional co-activators yes-associated protein (YAP) and PDZ binding domain (TAZ, also known as WWTR1) are two core proteins in the Hippo signaling pathway²⁴. Inactivation of the Hippo signaling pathway consisting of kinases, will result in hyperphosphorylation and translocation of YAP/TAZ to the nucleus^{24,30}. In the nucleus, transcriptional co-activators YAP/TAZ interact with DNA binding co-factors Tead1-4 and Smad's regulating downstream genes³¹. In EMT, overexpression of YAP/TAZ is associated with genes involved in loss of cell-cell and cell-ECM interactions^{24,30}. Furthermore, the interaction of YAP1 with Tead and Smad2/3/4 results in more potent TGF- β signaling and Snail, Twist and ZEB regulation²⁴.

Epithelial-to-Mesenchymal Transition (EMT)

Epithelium forms one of the most prevalent cell types of several tissues in the human body³². The most important functions of epithelial cells are protecting the underlying tissue from toxins and pathogens, exchange of chemicals and nutrients and contraction of epithelial tubes. Epithelial cells form a single or multiple layer of cells that are tightly packed via intercellular junctions and attached to a basement membrane via its basal surface. This basement membrane attaches epithelial tissue to the underlying connective tissue and provides structural support. Because most epithelial tissues lack blood vessels, epithelial cells depend on oxygen and nutrients from connective tissue. The basement membrane also causes the epithelial cells to display an apical-basal polarity which means that the organelles, but also other proteins and molecules, are not equally divided within

the epithelial cell. The basal pole is at the side of the cell lining the connective tissue and the apical pole is located at the other end of the cell, usually lining a surface or lumen. Prior to explaining the specific role of EMT in disease and tissue remodeling, we first describe the morphological and molecular changes that occur during this complex transition, beginning with the loss of cell junctions and the loss of apical-basal polarity.

Loss of cell junctions and apical-basal polarity in epithelial cells

Epithelial cells contain multiple adhesive structures, such as tight junctions, adherens junctions, gap junctions, desmosomes and hemidesmosomes which enable communication between cells and provide stabilization and integrity of the epithelial lining. EMT/EndMT triggers the deconstruction of these adhesive structures by degrading specific adhesion proteins, processes that are independent of TGF- β /Smad signaling or transcription factors mentioned above.

Tight junctions are the first lateral adhesion molecules that are deconstructed in an early state of EMT. The major structural proteins of tight junctions are the transmembrane proteins occludin and claudin, which are located at the most apical side of the junctional complex³². The intracellular proteins responsible for polarizing the occludins and claudins at the apical side of the cell are ZO-1 and ZO-2. The deconstruction of tight junctions in EMT is initiated by activation of the TGF- β signaling, leading to the degradation and decreased expression of the transmembrane proteins occludins and claudins, followed by the downregulation of ZO-1 and ZO-2^{1,33}. In EndMT, tight junctions are degraded in the same way, and Claudin 5 forms the major target³⁴.

The main structural component of adherens junctions in epithelium is E-cadherin, and VE-cadherin in endothelium. E-cadherin is a transmembrane glycoprotein which functions in a calcium dependent way³². The extracellular domain of E-cadherin provides adhesion to neighboring cells (also expressing E-cadherin on their cell surface), whereas the highly conserved intracellular domain is connected to actin filaments. This indicates that the regulation of E-cadherin in adherens junctions also modulates the localization of the cytoskeleton. During the transition, E-cadherin is endocytosed or proteolytic digested by the E3-ubiquitin-ligase Hakai³⁵. Additionally, cleavage of the cytoplasmic domain of E-cadherin by γ -secretase also results in loss of cellular adhesion, in which the cleaved cytoplasmic fragment interacts with p120 catenin³⁶. The E-cadherin fragment and p120 catenin are translocated to the nucleus where they modulate the expression of genes involved in EMT. Finally, multiple signaling pathways are activated that ultimately cause E-cadherin expression to be repressed. The degradation and decreased expression of E-cadherin forms a hallmark event in the transition from epithelial to mesenchymal cells. As a consequence of the reduced expression of E-cadherin, β -catenin accumulates in the cytoplasm and is either degraded or translocated to the nucleus where it functions as a transcription factor and modulate, among others, the expression of genes involved in EMT⁴. As gene expression is modulated, E-cadherin is degraded, and the expression of the mesenchymal adhesion protein N-cadherin is induced³⁷. Contrary to the high affinity of E-cadherin in epithelial cell-cell adhesion, N-cadherin has a weak interaction capacity,

allowing the cells to migrate. This 'cadherin switch' causes epithelial cells to lose their adhesive characteristics and gain mesenchymal features like motility.

In EndMT, the adherens junctions need to be degraded, following the same mechanism in EMT, respectively via VE-cadherin which is very similar to E-cadherin³⁸. Another important marker for adherens junction removal in EndMT is the degradation of the platelet endothelial cell adhesion molecule, PECAM1 (CD31)³⁸. Adherens junctions are crucial for the regulation of all the other cell junctions, like Gap junctions, and stay in close contact with desmosomes, the appearance and regulation of which are very similar³⁹. Gap junction channels are formed through the interactions of connexins between two neighboring cells. During EMT, the gap junction channels are disrupted because of the downregulation of connexins⁴⁰. The breakdown of the complete epithelial junctional complex initiates the loosening of cell-cell contacts and promotes the transition of epithelial cells to mesenchymal cells.

Cytoskeleton reorganization, front-rear polarity and migration

One main characteristic of mesenchymal cells is their motility and migratory abilities. For transiting epithelial and endothelial cells to gain this motility, a reorganization of the cytoskeleton is needed, in which the highly dynamic actin skeleton plays a key role. The actin skeleton localized close to the plasma membrane is called the cell cortex³². The cell cortex regulates plasma membrane behavior and can form specialized extensions, for example microvilli that enlarge the surface of epithelial cells in the intestine and promote nutrient absorption. The actin skeleton is also capable of forming membrane protrusions involved in cell motility, like lamellipodia and filopodia.

During EMT, these membrane protrusions are required for cell motility and the degradation of extracellular matrix around the cell, promoting cell migration⁴ (Figure 1c). At the opposite side of the cell the formation of actin stress fibers and cell contraction are characteristics of EMT (Figure 1c). Actin remodeling is regulated by the Rho family of GTP-binding proteins, like RhoA, Cdc42 and Rac1. RhoA controls cell-cell adhesion by the formation of actin stress fibers, whereas Cdc42 and Rac1 promote motility by the formation of lamellipodia and filopodia (Figure 1c). These Rho GTPases are tightly regulated by guanine nucleotide exchange factors (GEFs), GTPase-activating proteins (GAPs) and guanine nucleotide dissociation inhibitors (GDIs)⁴¹.

During the reorganization of the cytoskeleton, the intermediate EMT cells gain a front-rear polarity². In the transition from apical-basal polarity to front-rear polarity, the cytoskeleton is completely reorganized in such a way that the cells gain a front side which will form the leading edge of the cell and a rear side which will form the tail of the cell. Cdc42 and Rac1 are located at the front side of the cell stimulating actin polarization and the formation of membrane extensions, such as lamellipodia and filopodia, and RhoA is located at the rear side of the cell promoting actomyosin contractility and retraction (Figure 1c). A key initiator of this asymmetric distribution is PI3K, which is activated by Rac1 and on its turn recruits Cdc42 and Rac1-GEFs to the front side of the cell⁴². Rac1 then stimulates the recruitment of integrins to the leading edge of the cell. Transition to

a front-rear polarity causes the cells to lose their adhesion junctions at the rear side of the cell and break down ECM at the front side of the cell, becoming migratory and invasive mesenchymal cells.

Extracellular matrix (ECM) remodeling and cellular invasiveness

For the transiting epithelial and endothelial cells to become invasive mesenchymal cells, the capacity of breaking down and remodel ECM is essential. The family of integrins plays an important role in this process. Integrins are transmembrane proteins that consist of an alpha and beta subunit and form the connection between the cytoskeleton and ECM, activating signaling pathways within the cell upon binding to the ECM^{4,32}. During the transition, integrins associated with the basement membrane are degraded and mesenchymal integrins interacting with the new ECM surrounding are induced (Figure 1c)². For example, the expression of mesenchymal $\beta 1$ integrins is enhanced which, depending on the α chain, augment affinity to fibronectin and/or collagen type 1, stimulating cell migration and the deconstruction of E-cadherin⁴³⁻⁴⁶.

This compositional change of integrins, such as the increased expression of $\alpha v\beta 6$ integrins, correlates with the upregulation of several matrix metalloproteinases (MMPs), essential for ECM degradation and remodeling, but also cleavage of cell surface receptors like E-cadherin^{2,47}. MMP-2 and MMP-9 are most involved in these invasive processes as they break down the major ECM component collagen. Sometimes the breakdown of ECM exposes a latent growth factor, which can be activated by specific integrins, like the $\alpha v\beta 6$ integrin that activates latent TGF- β released from the ECM⁴⁸. Subsequently, the $\alpha v\beta 6$ integrin expressing cells can transduce this signal when expressing the TGF- β receptors, activate downstream signaling, which in turn promotes ECM remodeling via upregulation of the matrix proteins collagen type 1 and fibronectin and increase of the expression of TIMPs to inhibit ECM breakdown.

EMT in development and disease

EMT can be divided in three different subtypes depending on the biological context in which it transits^{6,11}. EMT type 1 is associated with oocyte implantation and embryonic development. EMT type 2 is involved in wound healing, tissue regeneration and the pathophysiological process of organ and tissue fibrosis. These processes are initiated as a response to inflammation or a traumatic injury, in which repair and regeneration play a fundamental role. Macrophages and fibroblasts mediate tissue repair by rearranging the ECM via the secretion of MMPs and the deposition of ECM components, especially collagen type 1. After approximately two weeks, the damaged and inflamed tissue is repaired and replaced. However, when inflammation persists, it will lead to a chronic response where fibroblasts keep proliferating, leading to a continuous deposition of

collagen causing organ fibrosis. It was previously believed that all these activated disease-related fibroblasts were either derived from resident fibroblasts or the bone marrow. Interestingly, in kidney fibrosis, only 35% of the fibroblasts originate from these sources while 65% of the activated fibroblast in renal fibrosis are derived via EMT type 2, include approximately 30-35% of the cells derived via EndMT⁴⁹⁻⁵². These proportions are likely to vary between different organs and phases of fibrosis; but do indicate the importance of EMT in the development of tissue fibrosis. Finally, EMT type 3 occurs in the invasive and metastatic processes during cancer^{6,11,53}.

While this EMT classification distinguishes between totally different biological and pathophysiological processes, the morphological and molecular changes are similar: junction loss, polarity change, cytoskeleton rearrangement and different expression of EMT genes regulated by transcription factors and signaling pathways. Beside transcriptional control and signaling pathways, also posttranscriptional, posttranslational and epigenetic control by noncoding RNAs have been associated with the epithelial to mesenchymal phenotypic changes¹¹.

EndMT is implicated in the same pathological processes as EMT, such as cancer progression and organ fibrosis of e.g. kidney and heart^{38,49}. While EndMT is well known for its critical role for proper heart development, such as the development of the heart valves and septa from endocardial cells^{54,55}, in more recent studies, EndMT has also been implicated in pathological processes during cardiovascular diseases, such as myocardial infarction³⁸, portal hypertension¹⁰, pulmonary hypertension⁵⁶ and vascular graft failure^{57,58}. All of these pathological conditions include features of inflammation and suggests a linkage of EndMT to the cardiovascular pathology of atherosclerosis.

EndMT in atherosclerosis

Atherosclerosis is a lipid storage disorder, with features of chronic inflammation. It is initiated by endothelial damage caused by modified LDL, hypertension, difference in shear stress and infectious micro-organisms. As a consequence, endothelial cells increase their permeability to lipoproteins, expression of adhesion molecules and the release of inflammatory cytokines. Subsequently, white blood cells are recruited into the tunica intima where they phagocytose the oxidized lipoproteins and become foam cells. Next, mesenchymal cells, such as fibroblasts and smooth muscle cells, infiltrate the fatty streak and secrete ECM components like collagen and fibronectin, leading to the formation of a fibrous cap. The active atherosclerotic lesion contains activated endothelium with migrating cells of fibroblastic lineage: an environment where there could be a biological call for EndMT.

As mentioned above, TGF- β signaling is identified as the key signaling pathway for the initiation and progression of EndMT. Upstream pathways of TGF- β signaling are of interest to unravel the potential mechanisms that could induce EndMT in atherosclerotic disease. FGF signaling maintains the endothelial phenotype and function, while

inhibition of FGF signaling initiates EndMT. Interestingly, repression of endothelial FGF signaling by knocking out the FGF adaptor protein FRS2 or the FGF1 receptor, leads to the activation of TGF- β signaling and subsequent EndMT^{57,59}. FGF signaling is downregulated by inflammatory cytokines, such as TNF- α , IFN- γ and IL-1 β which in turn can activate TGF- β signaling⁵⁷. Interestingly, the same cytokines are involved in the progression of atherosclerosis, which implicates the possible involvement of EndMT in this disease.

Increased plaque formation associates with EndMT

On the basis of the above mentioned hypothesis, Chen *et al.* (2015) conducted a study design with mice as the *in vivo* model⁸. In this experimental study *Apoe*^{-/-} mice were created with a deletion of the FRS2 α adaptor protein, important for transmitting the signal from the FGF receptor to its downstream targets. The development of atherosclerosis in these FRS2 α ^{ECKO} mice was compared to control *Apoe*^{-/-} mice still expressing FRS2 α . After 4 weeks on high fat diet, increased number of atherosclerotic lesions were found in the aortic arch, thoracic and abdominal aorta, and aortic root of the FRS2 α ^{ECKO} mice when compared to control mice. Additionally, FRS2 α ^{ECKO} mice had increased secretion of fibronectin and expression of adhesion molecules, such as ICAM-1 and VCAM-1 in the atherosclerotic lesion. After 16 weeks on high fat diet, the atherosclerotic lesions further increased in the FRS2 α ^{ECKO} mice with an 84% higher plaque burden. Furthermore, immunostaining showed increased recruitment of macrophages, but also a significant increased expression of EndMT markers, such as p-Smad2, α SMA, Notch3 and collagen, and an increased number of endothelial cells undergoing EndMT. Chen *et al.* additionally executed immunostaining for EndMT markers in left coronary arteries (LCAs) of human patients with coronary artery disease (CAD), which were divided in four different groups: patients with mild CAD (intima/media ratio <0.2), moderate CAD (intima/media ratio 0.2-1), severe CAD (intima/media ratio >1) and a control group, patients with normal LCAs (no neointima). Immunostaining for the FGF receptor 1 in the LCA's showed a FGFR1 expression of 81% absence of disease, subsequently decreasing with CAD severity. In contrast, the expression of the TGF- β signaling marker p-Smad2 was approximately 13% in absence of disease and increased significantly with CAD severity. Additionally, endothelial cells expressing FGFR1 and p-Smad2 showed strong negative and positive relationship with the intima/media ratio, respectively. When the FGFR1 expression was compared to the p-Smad2 expression an inverse relationship was observed. Finally, many more additional EndMT and inflammatory markers were measured in human endothelial cells according to this study design and all gave the same significantly outcome.

These results indicate a strong involvement of EndMT in atherosclerosis and suggest EndMT as the link between the elevated inflammatory cytokines, and the increased mesenchymal cell appearance and recruitment of cell in the neointima with increased secretion of ECM components and adhesion molecules, leading to the formation of atherosclerotic plaques. These mesenchymal cells include plaque-associated fibroblasts and smooth muscle cells which play an important role in regulating inflammation,

secretion of ECM components and therefore stable plaque formation⁶⁰. A similar outcome was found by Moonen *et al.*, (2015), which also suggested that EndMT contributes to neointimal hyperplasia, a process characterized as an initial stage of atherosclerosis, in which mesenchymal cells are recruited into the neointima and tunica intima via proliferation and migration⁶¹. Instead of studying EndMT because of increased inflammatory cytokine levels, Moonen *et al.*, focused on EndMT as the link between the degree of shear stress and the increased recruitment of mesenchymal cells. They found that uniform laminar shear stress (LSS) inhibits EndMT in an ERK5-dependent manner, while disturbed flow, measured in different shear-stress gradients, resulted in increased neointimal hyperplasia upon EndMT induction⁶¹.

EndMT-derived fibroblasts in plaques

Although suggesting that they are derived via EndMT, neither Chen *et al.*, nor Moonen *et al.*, determined the origin of the mesenchymal cells^{8,61}. Their origin remained unclear until Evrad *et al.* (2016) performed a lineage tracing experiment for endothelial cells to prove that EndMT-derived fibroblasts are indeed common in atherosclerotic plaques⁹. After 8, 18 and 30 weeks on a high fat diet, a significant number of cells in the atherosclerotic plaque were derived from endothelial cells and now expressed fibroblast markers, demonstrating the involvement of EndMT. Moreover, after 30 weeks 45% of the fibroblasts were derived from endothelial cells, which suggests that 3-9% of the total intimal plaque consists of transiting cells (EndMT) and possibly endothelial-derived fibroblasts. To further determine if the transiting cells indeed underwent EndMT to form more mature fibroblasts, endothelial-derived cells which expressed fibroblast markers were selected based on their lack of VE-cadherin expression, a specific endothelial marker. The results showed that 10% of the fibroblasts were derived from endothelial cells and did not express VE-cadherin, indicating a more mature fibroblast phenotype. The same experiment was also performed with markers associated with myofibroblasts and smooth muscle cells, but the endothelial-derived cells co-expressed 10-fold lower levels of these markers compared to the fibroblast markers.

EndMT-derived fibroblasts correlate with plaque instability

Evrad *et al.* next studied EndMT involvement in human atherosclerosis⁹. In this study design two different types of plaques were compared based on their classification: plaque type V (fibroatheroma) and plaque type VI (complex plaque with unstable characteristics, possibly thrombus). EndMT was again defined by cells expressing both endothelial markers, like PECAM and fibroblast markers, like FSP-1. Multiple endothelial and mesenchymal marker combinations were used. For each combination the proportion of cells undergoing EndMT was significantly higher in the plaque type V. Additionally, an

inverted relationship was observed between fibrous cap formation and the proportion of cells undergoing EndMT. These data suggest a direct correlation between EndMT and the appearance of unstable plaques and plaque ruptures⁹.

These results indicate that fibroblasts derived from endothelial cells have different functions compared to fibroblasts derived from myofibroblast lineages⁹. To study these different effector functions with respect to plaque instability and rupture, the expression of ECM genes was compared between bona fide fibroblast and EndMT derived fibroblasts. This experiment showed a significantly higher expression of collagen genes and a significantly lower expression of MMP genes in bona fide fibroblasts, compared to the EndMT derived fibroblast. Conversely, the expression of MMP genes is significantly higher and the collagen expression is significantly lower in EndMT derived fibroblasts⁹. MMP levels were also significantly higher in conditioned media collected from EndMT derived fibroblasts. Remarkably, when the protein level was compared between the lysates of EndMT derived fibroblast and bona fide fibroblasts, the MMP activity was significantly higher in EndMT derived fibroblasts. This study suggests a correlation between EndMT and plaque instability⁹.

Conclusion

The transition from epithelial/endothelial to mesenchymal cells (EMT/EndMT) is a gradual and complex process depending on many morphological and molecular changes, which are all crucial for EMT/EndMT completion. EMT and EndMT are involved in many developmental and pathophysiological processes, ranging from embryonic development to cancer progression. Additionally, EndMT has also been implicated in several cardiovascular diseases, such as myocardial infarctions and hypertension. In more recent literature, EndMT was linked to the pathophysiological process of atherosclerosis, suggesting an important contribution of EndMT in plaque progression and instability. Future research will address the potential of targeting molecular signaling pathways essential for EndMT initiation and progression hopefully providing new treatment modalities.

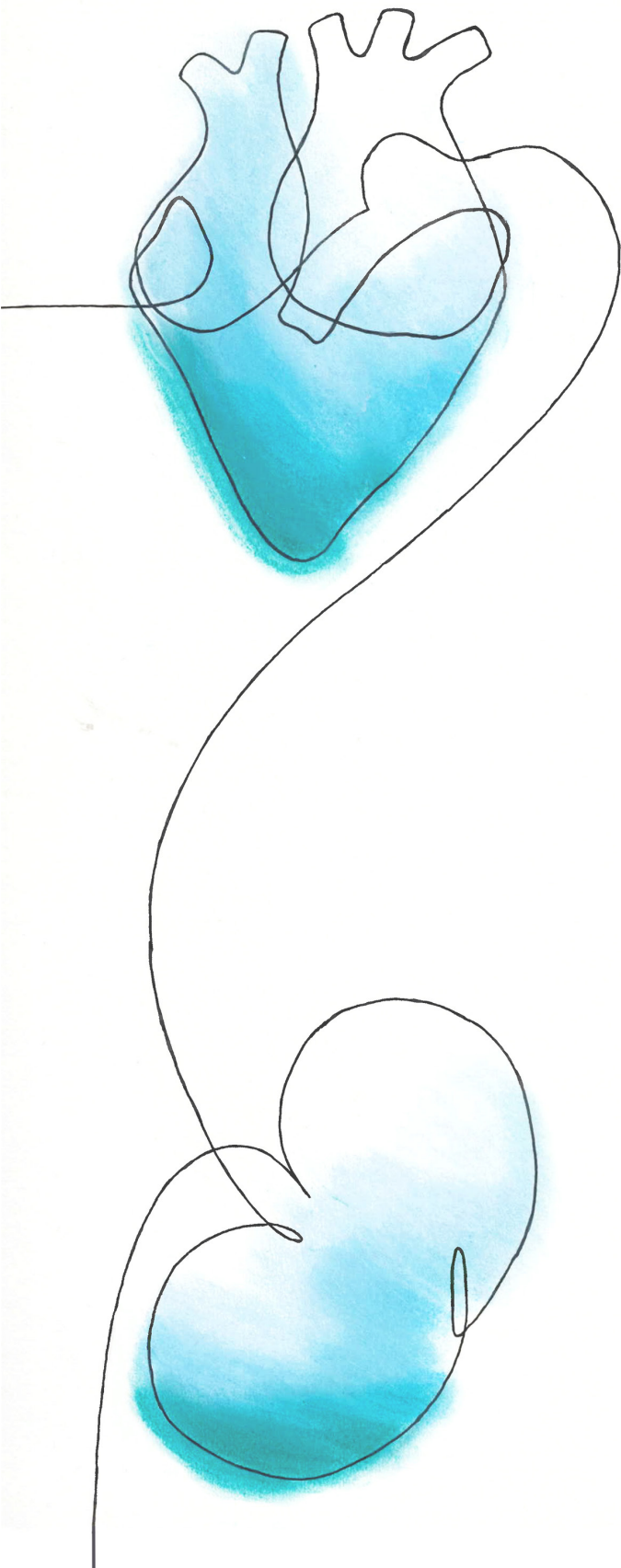
Acknowledgements

The authors gratefully acknowledge Arjan Barendrecht for the design and production of Figure 1. We acknowledge support from the Netherlands CardioVascular Research Initiative: An initiative with support of the Dutch Heart Foundation, CVON2014-11 RECONNECT.

References

1. Huang, R. Y. J., Guilford, P. & Thiery, J. P. Early events in cell adhesion and polarity during epithelial-mesenchymal transition. *J. Cell Sci.* **125**, 4417–4422 (2012).
2. Lamouille, S., Xu, J. & Derynck, R. Molecular mechanisms of epithelial-mesenchymal transition. *Nat. Rev. Mol. Cell Biol.* **15**, 178–196 (2014).
3. Mayor, R. & Etienne-Manneville, S. The front and rear of collective cell migration. *Nat. Rev. Mol. Cell Biol.* **17**, 97–109 (2016).
4. Yilmaz, M. & Christofori, G. EMT, the cytoskeleton, and cancer cell invasion. *Cancer Metastasis Rev.* **28**, 15–33 (2009).
5. Xu, J., Lamouille, S. & Derynck, R. TGF- β -induced epithelial to mesenchymal transition. *Cell Res.* **19**, 156–172 (2009).
6. Kalluri, R. & Weinberg, R. A. The basics of epithelial-mesenchymal transition. *J. Clin. Invest.* **119**, 1420–1428 (2009).
7. Potenta, S., Zeisberg, E. & Kalluri, R. The role of endothelial-to-mesenchymal transition in cancer progression. *Br. J. Cancer* **99**, 1375–1379 (2008).
8. Chen, P. Y. et al. Endothelial-to-mesenchymal transition drives atherosclerosis progression. *J. Clin. Invest.* **125**, 4514–4528 (2015).
9. Evrard, S. M. et al. Endothelial to mesenchymal transition is common in atherosclerotic lesions and is associated with plaque instability. *Nat. Commun.* **7**, (2016).
10. Kitao, A. et al. Endothelial to mesenchymal transition via transforming growth factor- β 1/smad activation is associated with portal venous stenosis in idiopathic portal hypertension. *Am. J. Pathol.* **175**, 616–626 (2009).
11. Nieto, M. A. Epithelial plasticity: A common theme in embryonic and cancer cells. *Science (80-.)*. **342**, (2013).
12. Zheng, H. & Kang, Y. Multilayer control of the EMT master regulators. *Oncogene* **33**, 1755–1763 (2014).
13. Goumans, M. J. & ten Dijke, P. TGF- β signaling in control of cardiovascular function. *Cold Spring Harb. Perspect. Biol.* **10**, (2018).
14. Oh, S. et al. Activin receptor-like kinase 1 modulates transforming growth factor- β 1 signaling in the regulation of angiogenesis. *Natl. Acad. Sci.* **97**, 2626–2631 (2000).
15. Goumans, M. J. et al. Balancing the activation state of the endothelium via two distinct TGF- β type I receptors. *EMBO J.* **21**, 1743–1753 (2002).
16. Massagué, J. TGF β signalling in context. *Nat. Rev. Mol. Cell Biol.* **13**, 616–630 (2012).
17. Valcourt, U., Kowanz, M., Niimi, H., Heldin, C. H. & Moustakas, A. TGF- β and the Smad signaling pathway support transcriptomic reprogramming during epithelial-mesenchymal cell transition. *Mol. Biol. Cell* **16**, 1987–2002 (2005).
18. Feng, X.-H. & Derynck, R. Specificity and versatility in TGF- β signaling through Smads. *Annu. Rev. Cell Dev. Biol.* **21**, 659–693 (2005).
19. Thuault, S. et al. Transforming growth factor-beta employs HMGA2 to elicit epithelial-mesenchymal transition. *J. Cell Biol.* **174**, 175–183 (2006).
20. Bakin, A. V., Tomlinson, A. K., Bhowmick, N. A., Moses, H. L. & Arteaga, C. L. Phosphatidylinositol 3-Kinase Function Is Required for Transforming Growth Factor-Mediated Epithelial to Mesenchymal Transition and Cell Migration. *J. Biol. Chem.* **275**, 36803–36810 (2000).
21. Lamouille, S., Subramanyam, D., Belloch, R. & Derynck, R. Regulation of epithelial-mesenchymal and mesenchymal-epithelial transitions by microRNAs. *Curr. Opin. Cell Biol.* **25**, 200–2207 (2013).
22. Zhou, B. P. et al. Dual regulation of Snail by GSK-3 β -mediated phosphorylation in control of epithelial-mesenchymal transition. *Nat. Cell Biol.* **6**, 931–940 (2004).
23. Peinado, H., Olmeda, D. & Cano, A. Snail, ZEB and bHLH factors in tumour progression: An alliance against the epithelial phenotype? *Nature Reviews Cancer* **7**, 415–428 (2007).
24. Zhang, H. et al. Yap1 Is required for endothelial to mesenchymal transition of the atrioventricular cushion. *J. Biol. Chem.* **289**, 18681–18692 (2014).
25. Vincent, T. et al. A SNAIL1-SMAD3/4 transcriptional repressor complex promotes TGF- β mediated epithelial-mesenchymal transition. *Nat. Cell Biol.* **11**, 943–950 (2009).
26. Chen, Z. F. & Behringer, R. R. twist is required in head mesenchyme for cranial neural tube morphogenesis. *Genes Dev.* **9**, 686–699 (1995).
27. Yang, J., Mani, S., Donaher, J., Cell, S. R.- & 2004, U. Twist, a master regulator of morphogenesis, plays an essential role in tumor metastasis. *J. Biol. Chem.* **289**, 18681–18692 (2014).
28. Eger, A. et al. DeltaEF1 is a transcriptional repressor of E-cadherin and regulates epithelial plasticity in breast cancer cells. *Oncogene* **24**, 2375–2385 (2005).
29. Dave, N. et al. Functional cooperation between Snail1 and twist in the regulation of ZEB1 expression during epithelial to mesenchymal transition. *J. Biol. Chem.* **286**, 12024–12032 (2011).
30. Li, Z. et al. The Hippo transducer TAZ promotes epithelial to mesenchymal transition and cancer stem cell maintenance in oral cancer. *Mol. Oncol.* **9**, 1091–1105 (2015).

31. Ramjee, V. et al. Epicardial YAP/TAZ orchestrate an immunosuppressive response following myocardial infarction. *J. Clin. Invest.* **127**, 899–911 (2017).
32. Mescher, A. L. *Junqueira's basic histology: text and atlas.* (Mcgraw-hill, 2013).
33. Umeda, K., Ikenouchi, J., Katahira-Tayama, S., Cell, K. F.- & 2006, U. ZO-1 and ZO-2 independently determine where claudins are polymerized in tight-junction strand formation. *Cell* **126**, 741–754 (2006).
34. Kokudo, T. et al. Snail is required for TGF β -induced endothelial-mesenchymal transition of embryonic stem cell-derived endothelial cells. *J. Cell Sci.* **121**, 3317–3324 (2008).
35. Fujita, Y. et al. Hakai, a c-Cbl-like protein, ubiquitinates and induces endocytosis of the E-cadherin complex. *Nat. Cell Biol.* **4**, 222–231 (2002).
36. Marambaud, P. et al. A presenilin-1/ γ -secretase cleavage releases the E-cadherin intracellular domain and regulates disassembly of adherens junctions. *EMBO J.* **21**, 1948–1956 (2002).
37. Wheelock, M. J., Shintani, Y., Maeda, M., Fukumoto, Y. & Johnson, K. R. Cadherin switching. *Journal of Cell Science* **121**, 727–735 (2008).
38. Zeisberg, E. M. et al. Endothelial-to-mesenchymal transition contributes to cardiac fibrosis. *Nat. Med.* **13**, 952–961 (2007).
39. Meng, W. & Takeichi, M. Adherens junction: molecular architecture and regulation. *Cold Spring Harb. Perspect. Biol.* **1**, Article a002899 (2009).
40. Bax, N. A. M. et al. Epithelial-to-mesenchymal transformation alters electrical conductivity of human epicardial cells. *J. Cell. Mol. Med.* **15**, 2675–2683 (2011).
41. Schmidt, A. & Hall, A. Guanine nucleotide exchange factors for Rho GTPases: Turning on the switch. *Genes Dev.* **16**, 1587–1609 (2002).
42. Nelson, W. J. Remodeling epithelial cell organization: transitions between front-rear and apical-basal polarity. *Cold Spring Harb. Perspect. Biol.* **1**, Article a000513 (2009).
43. Yang, X., Pursell, B., Lu, S., Chang, T. K. & Mercurio, A. M. Regulation of β 4-integrin expression by epigenetic modifications in the mammary gland and during the epithelial-to-mesenchymal transition. *J. Cell Sci.* **122**, 2473–2480 (2009).
44. Maschler, S. M. et al. Tumor cell invasiveness correlates with changes in integrin expression and localization. *Oncogene* **24**, 2032–2041 (2005).
45. Mise, N. et al. Zyxin is a transforming growth factor- β (TGF- β)/Smad3 target gene that regulates lung cancer cell motility via integrin α 5 β 1. *J. Biol. Chem.* **287**, 31393–31405 (2012).
46. Koenig, A., Mueller, C., Hasel, C., Adler, G. & Menke, A. Collagen Type I Induces Disruption of E-Cadherin-Mediated Cell-Cell Contacts and Promotes Proliferation of Pancreatic Carcinoma Cells. *Cancer Res* **66**, 4662–71 (2006).
47. Nistico, P., Nistico, P., Bissell, M. J. & Radisky, D. C. Epithelial-Mesenchymal Transition: General Principles and Pathological Relevance with Special Emphasis on the Role of Matrix Metalloproteinases. *Cold Spring Harb. Perspect. Biol.* **4**, Article a011908 (2012).
48. Sheppard, D. Integrin-mediated activation of latent transforming growth factor β . *Cancer Metastasis Rev.* **24**, 395–402 (2005).
49. Zeisberg, E., Potenta, S., Sugimoto, H., Zeisberg, M. & Kalluri, R. Fibroblasts in kidney fibrosis emerge via endothelial-to-mesenchymal transition. *Am Soc Nephrol* **19**, 2282–2287 (2008).
50. Iwano, M. et al. Evidence that fibroblasts derive from epithelium during tissue fibrosis. *Am Soc Clin Investig* **110**, 341–350 (2002).
51. Rastaldi, M. et al. Epithelial-mesenchymal transition of tubular epithelial cells in human renal biopsies. *Kidney Int.* **62**, 137–146 (2002).
52. Kalluri, R. & Neilson, E. G. Epithelial-mesenchymal transition and its implications for fibrosis. *J. Clin. Invest.* **112**, 1776–1784 (2003).
53. Thiery, J. P. Epithelial-mesenchymal transitions in tumour progression. *Nat. Rev.* **2**, 442 (2002).
54. Markwald, R. R., Fitzharris, T. P. & Manasek, F. J. Structural development of endocardial cushions. *Am. J. Anat.* **148**, 85–119 (1977).
55. Kisanuki, Y. et al. Tie2-Cre transgenic mice: a new model for endothelial cell-lineage analysis in vivo. *Dev. Biol.* **230**, 230–242 (2001).
56. Piera-Velazquez, S., Mendoza, F. A. & Jimenez, S. A. Endothelial to Mesenchymal Transition (EndoMT) in the Pathogenesis of Human Fibrotic Diseases. *J. Clin. Med.* **5**, 45 (2016).
57. Chen, P. et al. FGF regulates TGF- β signaling and endothelial-to-mesenchymal transition via control of let-7 miRNA expression. *Cell Rep.* **2**, 1684–1696 (2012).
58. Cooley, B. C. et al. TGF-beta signaling mediates endothelial-to-mesenchymal transition (EndMT) during vein graft remodeling. *Sci. Transl. Med.* **227**, (2014).
59. Chen, P.-Y., Qin, L., Tellides, G. & Simons, M. Fibroblast growth factor receptor 1 is a key inhibitor of TGF β signaling in the endothelium. *Sci. Signal* **7**, (2014).
60. Mori, H. et al. Coronary Artery Calcification and its Progression: What Does it Really Mean? *JACC. Cardiovascular imaging* **11**, 127–142 (2018).
61. Moonen, J. R. et al. Endothelial-to-mesenchymal transition contributes to fibro-proliferative vascular disease and is modulated by fluid shear stress. *Cardiovasc. Res.* **108**, 377–386 (2015).



3

Impaired kidney function is associated with intraplaque hemorrhage in patients undergoing carotid endarterectomy

Atherosclerosis 2017; 266:128-135

M. Wesseling^{1*}, I.D. van Koeverden^{1*}, G.W. van Lammeren², S.W. van der Laan¹, S. Haitjema¹, J.P.M. de Vries², H.M. den Ruijter¹, S.C.A. de Jager¹, I. Hofer¹, P. Blankestijn⁴, M. Verhaar⁴, D.P.V. de Kleijn³, G.J. de Borst³, G. Pasterkamp¹

* These authors contributed equally to the manuscript

¹Laboratory of Experimental Cardiology, University Medical Center Utrecht, Utrecht, The Netherlands

²Department of Vascular Surgery, St. Antonius Hospital, Nieuwegein, The Netherlands

³Department of Vascular Surgery, University Medical Center Utrecht, Utrecht, The Netherlands

⁴Department of Nephrology, University Medical Center Utrecht, Utrecht, The Netherlands

Abstract

Previously we showed that patients undergoing carotid endarterectomy have an increased risk for major atherosclerotic events in the presence of moderate or poor kidney function. Acceleration of vascular inflammatory responses is considered to be causally involved in progression of atherogenesis and poor outcome in chronic kidney disease patients. The association between kidney function and plaque composition has not been thoroughly investigated yet. The aim of this study was to investigate the association between kidney function and atherosclerotic plaque composition in patients undergoing carotid endarterectomy.

Atherosclerotic plaques harvested from 1796 patients who underwent carotid endarterectomy were immunohistochemically stained for, macrophages, smooth muscle cells, calcifications, collagen, microvessels, lipid core size and intraplaque hemorrhage. Cytokines were measured in plaque and plasma and associated with kidney function. Quantitative proteomics were performed on 40 carotid plaques and associated with kidney function.

Decreased kidney function was associated with increased odds ratio of intraplaque hemorrhage, OR 1.15 (95%CI; 1.02-1.29, $p=0.024$) and increased odds ratio of fibrous-atheromatous plaques (plaques with lipid core presenting more than 10% of total plaque surface) OR 1.21 (95%CI; 1.07-1.38, $p=0.003$) per decrease of 20 points in eGFR. Proteomics revealed that decreased kidney function was associated with upregulation of the classical pathway of the complement system and the intrinsic pathway of the coagulation system.

Decreased kidney function was associated with plaque hemorrhage but not with inflammatory plaque characteristics. Our data suggests that other pathways than the inflammation-pathway are involved in plaque vulnerability and poor outcome in patients with decreased kidney function.

Introduction

Chronic kidney disease (CKD) and cardiovascular disease (CVD) are profound problems increasingly diagnosed in the elderly patient in Western society today¹. Due to large interactions between the heart, blood vessels and kidney function these three are intrinsically bound and together form the cardio-renal-axis.

The pivotal role of inflammation in development of atherosclerosis and kidney failure has been clearly established^{2,3}. Beside inflammation various other plaque features are described that might be associated with MACE, such as neovascularization, calcium deposition, and vessel wall remodeling⁴. Autopsy studies showed that decreased kidney function associated with vascular calcifications and smooth muscle cell apoptosis. In patients with manifestations of cerebrovascular disease, CKD is an important risk factor for future major cardiovascular events (MACE)⁵. In patients with end-stage renal disease mortality rate after myocardial infarction from cardiac causes is approximately 40% at one year, 51% at two years and 70% at five years⁶.

In hemodialysis patients, oxidative stress and a state of chronic inflammation have been described as a cause and a consequence of atherogenesis^{7,8}. Recent ongoing clinical trials show promising results targeting chronic inflammation for improvement of vascular function^{9,10}. Inflammation is an established contributor to atherosclerotic disease, however it is not clear to what extent decreased kidney function contributes to atherosclerotic inflammation, and whether it is associated with different plaque characteristics⁹⁻¹¹.

Current evidence on associations of CKD with atherosclerotic plaque characteristics is scarce, obtained post-mortem or obtained with small sample sizes. We report associations of CKD with plaque characteristics in a large cohort that represent viable patients. This patient domain is rapidly growing in size due to improved survival rates following a cardiovascular event. We hypothesized that decreased kidney function is associated with increased inflammatory plaque characteristics which may explain the increased risk for adverse secondary manifestations in this patient group.

We present analyses of a cohort of 1796 patients with advanced atherosclerosis who underwent CEA with a normal distribution of glomerular filtration rate and completed three year follow-up. We studied histological characteristics of the harvested carotid plaques, together with pro- and anti-inflammatory plasma and plaque protein levels. In addition, a quantitative proteomic analysis was performed to examine the plaque proteome in relation to kidney function.

Patients and Methods

Athero-Express biobank study

The Athero-Express Biobank is world's largest ongoing atherosclerotic plaque biobank and started on March 24th, 2002 in the University Medical Center Utrecht and the St. Antonius Hospital Nieuwegein in the Netherlands¹². Study design has been reported before, but in short, atherosclerotic plaques of patients undergoing CEA are harvested

and subjected to histological staining and protein extraction. Between April 2002 and August 2015, 2281 patients undergoing CEA at one of our institutions were included in the Athero-Express. Patients were considered eligible for inclusion in the current study when both plaque histology and eGFR were available. 118 patients were excluded for the current analyses due to missing eGFR and another 337 patients due to missing information on plaque histology. The first three years after surgery, all patients were contacted annually for their medical status. If any adverse events were reported, information was gathered at the respective hospitals or general practitioner.

Kidney function estimation

An estimation of the glomerular filtration rate (eGFR) is considered a reliable measure for kidney function¹³. For all patients, eGFR was calculated with the modification for diet (MDRD) formula and expressed in ml/min/1.73m². Serum creatinine was measured in peripheral blood, withdrawn before surgery. Patients were classified based on their kidney function according to the international guidelines of the National Kidney Foundation (KDOQI)^{14,15}: eGFR ≥ 90 ml/min/1.73m² (CKD stage 1: normal kidney function), eGFR 60-89 ml/min/1.73m² (CKD stage 2: mildly impaired kidney function), eGFR 30-59 ml/min/1.73m² (CKD stage 3: moderately impaired kidney function). In our cohort only 30 patients were identified with severely impaired kidney function and end stage kidney disease (CKD stage 4 and 5: eGFR < 30 ml/min/1.73m²). We considered this patient group too small to compare with the other groups and was therefore excluded from the current study.

Atherosclerotic plaque assessment

After CEA all atherosclerotic plaques were immediately processed. The culprit lesion was divided into segments of 5 mm thickness along the longitudinal axis. The segment with the largest plaque burden was chosen as culprit lesion and subjected to histological examination. A detailed description of atherosclerotic plaque assessment has been reported previously and has been added to the supplemental methods^{12,16-18}.

Inflammatory plaque and plasma proteins

To investigate if plaque protein levels associate with kidney function, cytokine levels were measured in randomly selected subgroups with a normal distribution of eGFR. Cytokines, interleukins and matrix metalloproteinases (MMP) were selected based on known influence on plaque progression and stability. The selection of protein markers in plasma was based on the previously selected markers that were measured in plaque. Circulating inflammatory marker high-sensitive C-reactive protein (hsCRP) was added to this essay to gain knowledge on the general inflammatory status of the patients. All used kits and essays are added to the supplemental methods.

Quantitative Plaque Proteomics

Quantitative proteomics measurements were performed in carotid plaques from 40 patients, including 20 patients suffering from MACE during three years of follow-up

and 20 age and sex matched controls without MACE during three years of follow-up. The methods of the quantitative proteomics experiment have been reported in detail previously¹⁹. In short, proteins were isolated from carotid atherosclerotic plaques and peptides were separated with high-performance liquid chromatography using a SCX column in 15 salt fractions. Bioworks 3.3 was used to generate a list of identified proteins per salt fraction. Proteins that were detectable in at least 32 of all 40 investigated plaques were included for analysis. Proteins detected with quantitative proteomics were correlated with eGFR using Pearson's correlation tests. Proteins that showed significant correlations ($p < 0.05$) with eGFR were entered into Ingenuity Pathways Analysis (Ingenuity® Systems, "http://www.ingenuity.com/").

Clinical outcome

To confirm previously reported associations between kidney failure and adverse outcome during follow-up after CEA⁵ we analyzed the impact of CKD on outcome in the current study cohort. Primary endpoint of interest consisted of all major manifestations of CVD including myocardial infarction, stroke and cardiovascular death. Secondary endpoint of interest was all-cause mortality. Definitions of endpoints were previously described^{5,12}. Two members of the outcome assessment committee validated endpoints. If no consensus was reached, a third observer was consulted for final judgment of the endpoint.

Statistical analysis

Data were inspected for patterns of missing values. The proportion of randomly missing values for baseline characteristics varied between 0-5%. Missing values were imputed using multiple imputation to prevent limitation of incomplete case analyses in multivariable regression analyses²⁰. Differences in binary characteristics between the three groups were analyzed with Pearson's Chi square. Differences in continuous parameters between the groups were calculated with One-Way ANOVA or Pearson correlation tests where appropriate. To investigate independent associations between histological plaque characteristics and kidney function, and to correct for potential confounders, we conducted multivariable linear and binary logistic regression models for continuous and binomial plaque characteristics respectively. Non-normally distributed quantitative histological parameters, including macrophages and SMCs, required logarithmic transformation, to enter them into linear regression models. Impact of CKD on clinical outcome was studied with Cox proportional hazard models. We corrected for all baseline characteristics that showed an association with kidney function ($p < 0.10$) in all multivariable analyses. To assess associations between kidney function groups and various protein levels measured in plaque and plasma, UNIANOVA with correction for multiple confounders was used. Proteins detected with quantitative plaque proteomics were correlated to eGFR using Pearson correlation tests. To assess whether sex stratification was necessary, interaction terms were built into the model. SPSS 21.0 (SPSS Inc, Chicago, Illinois, USA) was used for all statistical analyses.

Results

Patient characteristics

Baseline characteristics of the 1796 included patients before CEA are reported in table 1. The percentage of patients with relevant comorbidities at baseline increased with every decrease in kidney function. Patients with moderately and mildly impaired kidney function were older, and were more frequently: female, treated for hypertension and had a higher prevalence of coronary artery disease as compared to patients with normal kidney function. The percentage of diabetic patients was highest in the moderately impaired kidney function group but surprisingly enough lowest in the mildly impaired kidney function group. Clinical presentation did not differ between kidney function groups. TIAs were most prevalent in all kidney function groups directly followed by stroke. Other clinical presentation were ocular symptoms and asymptomatic carotid stenosis. Prescription of anticoagulants, diuretics, beta-blockers and ACE-inhibitors significantly increased with decreasing kidney function. There were no differences observed in the percentage of statins and antiplatelet-drug-use across our cohort. Total cholesterol, HDL and LDL cholesterol significantly declined concomitantly with declining kidney function.

Plaque characteristics and kidney function

After correcting for possible confounders, IPH was more frequently observed in patients with decreased kidney function, OR 1.15 (95% CI; 1.02-1.29, $p=0.024$) per decrease of 20 points in eGFR (Table 2). Fibrous-atheromatous plaques (plaques with lipid core presenting more than 10% of total plaque surface) were more often observed in patients with impaired kidney function, OR 1.21 (95% CI; 1.07-1.38, $p=0.003$) per decrease of 20 points in eGFR. For continuous measures of plaque characteristics an association with eGFR was found with the percentage of smooth muscle cell staining ($p=0.001$) in univariate analysis, however not in multivariate analysis. No significant association was found between eGFR and macrophage staining. In addition, large lipid core (plaques with lipid core covering more than 40% of total plaque surface), moderate/heavy calcifications, collagen staining and the number of micro vessels were not associated with eGFR. In figure 1 a typical example of a carotid plaque with IPH is depicted characterized by heavy glycoporphine staining central in the plaque specimen.

Inflammatory protein markers in plaque and kidney function

We examined the relation between various inflammatory protein markers in plaque and kidney function (Table 3, Supplemental figure 1). Levels of chemokine RANTES (CCL5) increased in plaques from patients with impaired kidney function ($p=0.030$). The levels of pro-inflammatory chemokine monocyte chemoattractant protein-1 (MCP-1), Osteoprotegerin (OPG) and vascular endothelial growth factor A (VEGFA) were not associated with eGFR. The interleukin analysis in plaque, varied between kidney function groups but did not consistently increase with decreasing kidney function (Table 3). No statistically significant associations were observed for plaque MMP2, MMP8 and MMP9 with eGFR.

Table 1. Baseline characteristics of patients with normal kidney function (eGFR \geq 90 ml/min/1.73 m²), mildly impaired kidney function (eGFR 60-89 ml/min/1.73 m²) and moderately impaired kidney function (eGFR 30-59 ml/min/1.73 m²).

Patient characteristics	eGFR \geq 90 ml/min/1.73 m ²	eGFR 60-89 ml/min/1.73 m ²	eGFR 30-59 ml/min/1.73 m ²	p-value
	(n=340)	(n=988)	(n=468)	
eGFR in mL/min/1.73 m ² [median; IQR]	98.4 [93.5-107.0]	74.1 [67.5-81.4]	50.7 [42.8-55.5]	<0.001
Sex, male n (%)	253(74.4)	685(69.3)	288(61.5)	<0.001
Age, years [median; IQR]	65 [57-71]	69 [62-75]	74 [68-79]	<0.001
BMI [median; IQR]	25.8 [23.5-28.1]	26.0 [24.1-28.4]	26.1 [24.1-28.7]	0.132
Current smoker, n (%)	159(48.5)	322(33.2)	122(26.8)	<0.001
Diabetes mellitus, n (%)	84(24.7)	201(20.3)	135(28.8)	0.001
Treated hypertension, n (%)	220(67.7)	693(71.8)	369(81.6)	<0.001
Treated hypercholesterolaemia, n (%)	209(66.6)	614(67.0)	284(68.4)	0.832
History of CAD, n (%)	80(23.6)	296(30.0)	195(41.8)	<0.001
Triglycerides in mmol/l [median; IQR]	1.40 [1.06-1.98]	1.40 [1.04-2.00]	1.40 [1.00-2.10]	0.942
Total cholesterol in mg/dL [median; IQR]	4.97 [4.00-5.70]	4.68 [3.90-5.60]	4.40 [3.50-5.23]	<0.001
HDL in mmol/l [median; IQR]	1.15 [0.94-1.39]	1.13 [0.92-1.41]	1.07 [0.87-1.34]	0.001
LDL in mmol/l [median; IQR]	2.93 [2.20-3.60]	2.71 [2.07-3.42]	2.50 [1.80-3.10]	<0.001
Clinical presentation				
Ø Asymptomatic, n (%)	41(12.1)	129(13.2)	76(16.3)	0.172
Ø Ocular, n (%)	59(17.5)	154(15.7)	67(14.3)	0.488
Ø TIA, n (%)	131(38.8)	447(45.7)	198(42.4)	0.075
Ø Stroke, n (%)	107(31.7)	249(25.4)	126(27.0)	0.085
Pre-operative medication use				
Statin use, n (%)	252(74.1)	753(76.4)	356(76.2)	0.692
Antiplatelet use, n (%)	312(91.8)	870(88.3)	410(88.0)	0.169
Anti-coagulant use, n (%)	24(7.1)	119(12.1)	74 (15.8)	0.001
Diuretic use, n (%)	89(26.2)	308(31.2)	236(50.5)	<0.001
RAAS medication use, n (%)	144(42.4)	4782(48.9)	284(60.8)	<0.001
Betablocker use, n (%)	119(35.0)	437(44.3)	248(53.1)	<0.001

Abbreviations: BMI, Body Mass Index; CAD, Coronary Artery Disease; PAOD, Peripheral Arterial Occlusive Disease; eGFR, estimated Glomerular Filtration Rate; TIA, Transient Ischemic Attack; RAAS, Renin Angiotensin Aldosterone System. Bold values were considered statistically significant with a p<0.05.

Table 2. Histological atherosclerotic plaque characteristics of 1796 carotid plaques.

Binominal carotid plaque characteristics	p-value Univariate	Odds ratio Unadjusted	p-value Multivariate	Odds ratio adjusted
Presence of lipid core $\geq 40\%$, % (n)	0.498	1.039 [0.931-1.159]	0.303	1.074 [0.937-1.231]
Presence of lipid core $\geq 10\%$, % (n)	0.035	1.117 [1.008-1.239]	0.003	1.213 [1.067-1.379]
Moderate/heavy calcifications, % (n)	0.106	1.082 [0.984-1.189]	0.867	0.990 [0.882-1.112]
Moderate/heavy collagen, % (n)	0.835	0.987 [0.876-1.113]	0.882	0.989 [0.854-1.145]
Presence of intraplaque hemorrhage, % (n)	0.097	1.085 [0.985-1.195]	0.024	1.145 [1.018-1.289]
Continuous carotid plaque characteristics	p-value	Beta Unadjusted	p-value adjusted	Beta Adjusted
Mean number of microvessels per hotspot	0.304	0.026 [-0.019-0.060]	0.419	0.024 [-0.028-0.067]
% of positive macrophage staining per plaque	0.217	-0.030 [0.036-0.008]	0.354	-0.026 [-0.040-0.014]
% of positive SMC staining per plaque	0.001	-0.078 [-0.078- -0.019]	0.124	-0.043 [-0.062-0.008]

Odds ratios and regression coefficients represent the risk per decrease of 20 points eGFR. Multivariate analysis corrected for sex, age, smoking status, diabetes mellitus, hypertension, history of CAD, lipid levels, anticoagulant therapy, Beta blocker use, diuretics use, RAAS medications. Abbreviations: CI, confidence interval; SMC, Smooth Muscle Cell. Bold values were considered statistically significant with a $p < 0.05$.

Inflammatory protein levels in plasma and kidney function

In plasma, the moderately impaired kidney function group had a higher osteoprotegerin level when ($p < 0.002$) compared to the normal and mildly impaired kidney function groups (Table 4, Supplemental figure 1). Lastly the hsCRP levels giving an overall impression of the inflammatory state of a patient were decreased in the mildly impaired kidney function group compared to the normal and moderately impaired kidney failure group ($p = 0.022$) (Table 4, Supplemental figure 1).

Plaque proteome pathway analysis and kidney function

Mean eGFR among the 40 patients included in the proteomic analysis was $65.8 (\pm 22.8)$ ml/min/1.73m². Plaque proteomics resulted in detection of peptides that identified 3873 proteins. Overall, 565 of 3873 proteins (14.6%) were detectable in at least 32 of 40 plaques ($\geq 80\%$). Of these 565 proteins, 105 (18.6%) correlated with eGFR with a p -value < 0.05 (Supplemental table 1). The (relative) quantitative values of these 105 associated proteins were uploaded into Ingenuity pathway analyses. Pathway analyses revealed that a decrease in eGFR was inversely associated with proteins involved in the intrinsic pathway of the coagulation system (Supplemental table 2 + Figure 2). In addition, proteins of the classic complement pathway were also associated with decreased kidney function (Supplemental figure 3).

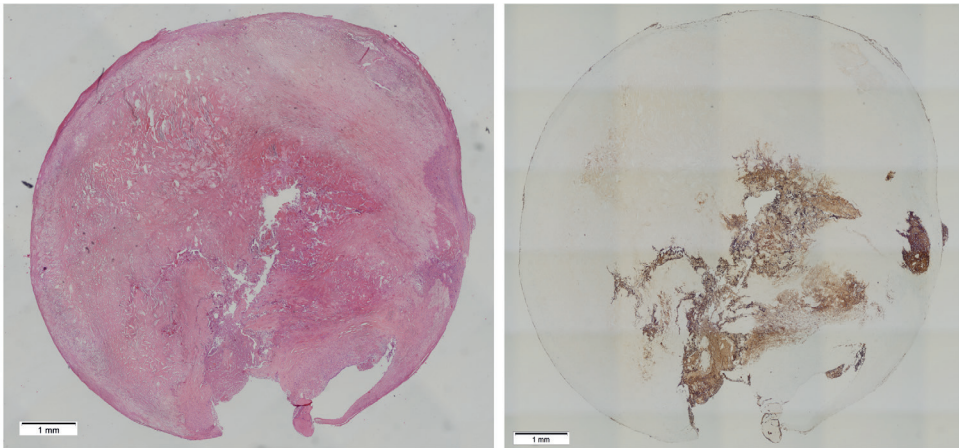


Figure 1. Typical example of an atherosclerotic plaque with intraplaque hemorrhage.

Left panel, typical example of an atherosclerotic plaque with intraplaque hemorrhage quantified using Hematoxylin and eosin staining. Bar, 1mm. Right panel showing same atherosclerotic plaque with glycophorine staining depicting intraplaque residues of erythrocytes. Bar, 1mm.

Clinical outcome and kidney function

To confirm previously described observations that impaired kidney function is associated with adverse cardiovascular outcome after carotid endarterectomy, we performed survival analyses within the current cohort (Figure 2 + 3). In total 1573 patients completed three year follow-up or endured a major endpoint, 151 patients (8.8%) were lost to follow-up. In a cox proportional hazards analysis, patients with moderately impaired kidney function have a 1.75 HR (95% CI 1.08-2.85, $p=0.024$) for major adverse cardiovascular events (MACE) during 3-year follow-up compared to patients with normal kidney function. All-cause mortality associated with the moderately impaired kidney function group HR 1.85 (95% CI 1.05-3.26, $p=0.035$) in both univariate and multivariate analysis after correcting for possible confounders (age, sex, smoking status, diabetes, hypertension, history of coronary artery disease, symptom status and lipid levels).

Discussion

To our knowledge, this is the first large atherosclerotic plaque study reporting on associations between kidney function and atherosclerotic plaque composition. We observed a higher prevalence of fibrous-atheromatous lesions and intraplaque hemorrhage in patients with decreased kidney function. These histological plaque features are considered to characterize the vulnerability of atherosclerotic lesions. In our cohort of patients undergoing carotid endarterectomy, we confirmed that impaired kidney function associated with poor outcome during follow up. However, we could

Table 3. Plaque protein levels in patients with normal kidney function (eGFR ≥ 90 ml/min/1.73 m²), mildly impaired kidney function (eGFR 60-89 ml/min/1.73 m²) and moderately impaired kidney function (eGFR 30-59 ml/min/1.73 m²).

Plaque protein	n	eGFR ≥ 90 ml/min/1.73 m ²	eGFR 60-89 ml/min/1.73 m ²	eGFR 30-59 ml/min/1.73 m ²	P-value
RANTES (pg/ug)	597	1.19 [1.12-1.26]	1.30 [1.26-1.35]	1.28 [1.22-1.35]	0.030
OPG (pg/ml)	581	906.87 [778.40-1056.96]	818.93 [757.64-885.70]	759.00 [674.36-854.68]	0.207
MCP-1 (pg/ug)	1176	1.40 [1.34-1.45]	1.44 [1.41-1.47]	1.44 [1.40-1.49]	0.384
VEGFA (ng/ml)	564	555.57 [357.25-864.13]	471.07 [370.94-598.76]	564.53 [394.98-806.96]	0.642
Interleukin 4 (pg/ml)	552	35.30 [22.33-55.83]	67.90 [54.02-85.27]	42.31 [29.97-59.68]	0.010
Interleukin 5 (pg/ml)	552	50.96 [33.42-77.70]	81.37 [65.96-100.41]	51.99 [37.86-71.38]	0.023
Interleukin 6 (pg/ml)	552	26.21 [18.27-37.58]	36.67 [30.64-43.89]	25.92 [19.76-33.98]	0.054
Interleukin 8 (pg/ml)	552	48.04 [29.62-77.91]	42.14 [33.11-53.60]	42.56 [29.58-61.21]	0.890
Interleukin 10 (pg/ml)	552	9.55 [6.82-13.38]	14.00 [11.84-16.54]	10.99 [8.55-14.15]	0.069
Interleukin 12 (pg/ml)	552	24.93 [15.95-38.98]	46.43 [37.15-57.99]	34.09 [24.36-47.70]	0.030
MMP 2 activity*	587	5.10 [4.68-5.55]	5.35 [5.13-5.58]	5.17 [4.84-5.52]	0.483
MMP 8 activity*	587	5.72 [4.92-6.65]	5.98 [5.54-6.45]	6.69 [5.96-7.52]	0.196
MMP 9 activity*	587	1.79 [1.65-1.94]	1.92 [1.84-1.99]	1.96 [1.85-2.09]	0.193

Values presented as mean [95% CI]. Associations are corrected for sex, age and year of surgery. Abbreviations: OPG, Osteoprotegerin; MCP-1, monocyte chemoattractant protein-1; VEGFA, Vascular endothelial growth factor A; MMP, Matrix metalloproteinase. * Values represent arbitrary units corrected for total protein content. Bold values were considered statistically significant with a $p < 0.05$.

not find supportive evidence for a role of inflammation as neither inflammatory plaque characteristics nor inflammatory plaque proteins were associated with decreased kidney function.

Table 4. Plasma protein levels in patients with normal kidney function (eGFR \geq 90 ml/min/1.73 m²), mildly impaired kidney function (eGFR 60-89 ml/min/1.73 m²) and moderately impaired kidney function (eGFR 30-59 ml/min/1.73 m²).

Plasma protein	n	eGFR \geq 90 ml/min/1.73 m ²	eGFR 60-89 ml/min/1.73 m ²	eGFR 30-59 ml/min/1.73 m ²	P-value
RANTES (ng/ml)	1028	3.82 [3.57-4.09]	3.77 [3.63-3.92]	3.85 [3.63-4.07]	0.841
OPG (ng/ml)	1054	1.77 [1.67-1.87]	1.74 [1.68-1.80]	1.93 [1.84-2.01]	0.002
MCP-1 (pg/ml)	580	85.54 [69.93-104.61]	91.29 [82.25-101.26]	80.72 [69.05-94.40]	0.429
VEGFA (pg/ml)	902	440.54 [367.10-529.16]	416.13 [377.28-458.59]	410.76 [354.08-476.09]	0.830
hsCRP (ug/ml)	1055	4.21 [3.58-4.94]	3.66 [3.35-4.00]	4.53 [3.96-5.18]	0.022

Values presented as mean [95% CI]. Associations are corrected for sex, age and year of surgery. Abbreviations: OPG, Osteoprotegerin; MCP-1, monocyte chemoattractant protein-1; VEGFA, Vascular endothelial growth factor A. Bold values were considered statistically significant with a P<0.05.

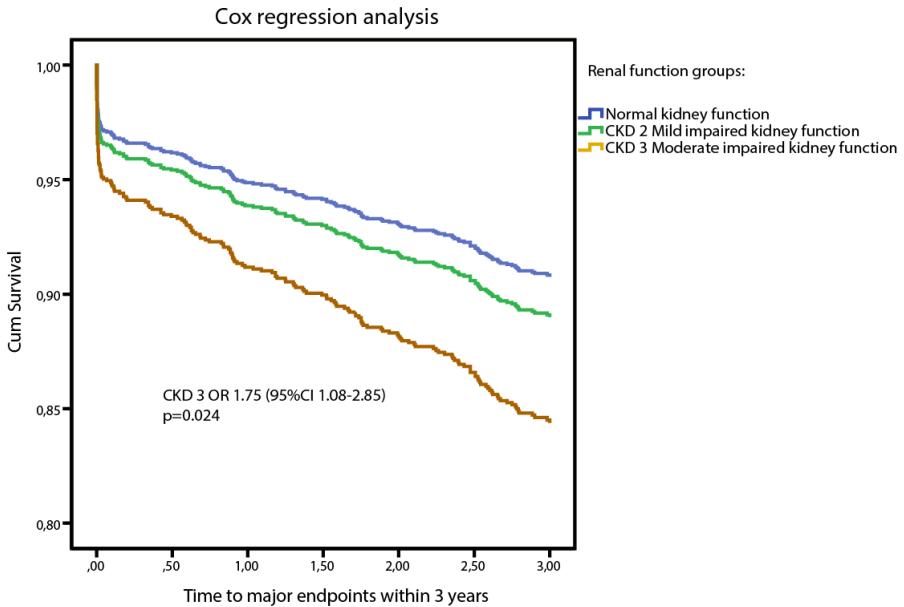


Figure 2. Hazard curves for CKD and major cardiovascular events after carotid endarterectomy. Major cardiovascular events during 3 year follow-up. CKD 3 OR 1.75 (95% CI 1.08-2.85, p=0.024) corrected for age, sex, smoking status, diabetes, hypertension, history of coronary artery disease, symptom status, and lipid levels.

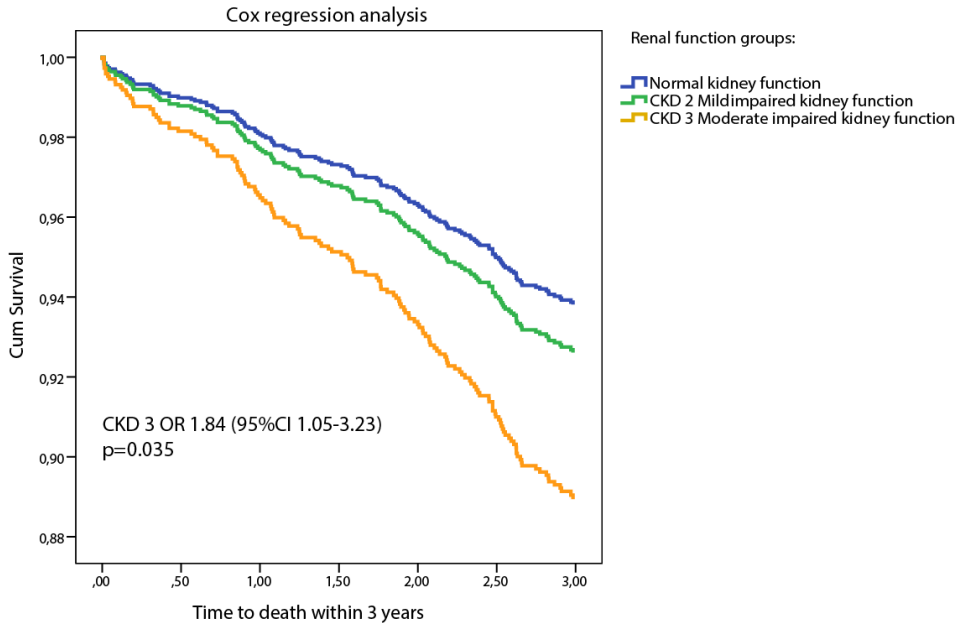


Figure 3. Hazard curves for all-cause mortality after carotid endarterectomy.

Death during 3 year follow-up. CKD 3 OR 1.84 (95% CI 1.05-3.23, $p=0.035$) corrected for age, sex, smoking status, diabetes, hypertension, history of coronary artery disease, symptom status, and lipid levels.

We found that plaque hemorrhage was increasingly prevalent in patients with impaired kidney function^{18,21}. Plaque hemorrhage is believed to result from disrupted microvessels that are formed in response to plaque growth. In atherosclerotic plaques there is a relative shortage of support tissue such as collagen and extracellular components which results in leaky or disrupted endothelial linings of newly formed microvessels^{22,23}. Earlier work within our biobank revealed that plaque hemorrhage is the only histological plaque feature that independently predicts MACE during follow-up, yet this finding was restricted to males only²⁴. We tested whether the increased risk for MACE in CKD patients may be explained by the increased incidence of plaque hemorrhage, but found that both plaque hemorrhage and CKD are independent risk factors. This implicates that CKD is associated with MACE through alternative mechanisms.

We hypothesized that inflammation could be such an alternative mechanism, as disease progression in both atherosclerosis and CKD are strongly driven by inflammatory processes. However, associations of decreased kidney function with inflammatory histological plaque features were absent or inconsistent. Neither did we find an association between CKD and calcifications, a characteristic that is commonly used as reported as a strong prognostic marker of coronary atherosclerotic plaque burden. In Autopsy studies a high prevalence of calcifications of the vessel wall among patients with CKD has been reported which is considered a strong prognostic marker of coronary

atherosclerotic plaque burden. In both univariate and multivariate regression models such association were not found suggesting that other underlying mechanisms such as plaque hemorrhage are responsible for accelerated progression of atherosclerotic plaques in patients with CKD^{6,25,26}.

In addition, we investigated the plaque proteome of patients with and without CKD. These analyses revealed that patients with decreased kidney function have an up regulation of the classical complement pathway and the intrinsic coagulation pathway. The classical complement system has been suggested to have a stabilizing effect on plaques by promoting clean-up of apoptotic cells and cell debris, and hereby removing the inflammatory triggers within the arterial wall^{27,28}. Although the complement pathway was upregulated in CKD patients, this was contradictory with our histology results which showed increased risk of plaque features that are considered to represent a vulnerable atherosclerotic plaque type in patients with CKD. Pathway analyses also revealed alterations in the coagulation pathway, which is in line with previous reports that showed patients with CKD have altered coagulation pathways²⁹. Furthermore, alterations in coagulation are in line with our main finding that plaque hemorrhage was more prevalent in patients with CKD. These results will have to be interpreted with caution, since we observed differences in the prescription of anti-coagulants and aspirin between kidney function groups in the current cohort. To correct for differences in medication-use possibly driving our effect we added anticoagulant-use to the multivariate model. Moreover, when we tested the association of anticoagulant-use with presence of intraplaque hemorrhage, such association was not found (*data not included*).

Our results are of clinical relevance, as recent clinical trials show a possible therapeutic target in inhibition of inflammation. In a relatively small cohort of 42 CKD patients, IL-1 inhibition improved the brachial artery flow-mediated dilatation⁹. Targeting IL-1 β in a high-risk cardiovascular patient cohort of more than 500 patients decreased levels of hsCRP and IL-6 after four months of follow-up¹⁰. Targeting inflammation in CKD patients has resulted in beneficial short-term results on vascular function however no long-term effects of anti-inflammatory drugs in CKD patients have been published until date. Moreover data on decreased manifestations of CVD such as MI, stroke and cardiovascular death in patients treated with anti-inflammatory drugs are still lacking. We found inconsistent associations between decreased kidney function and systemic inflammatory proteins. This contradicts earlier studies that showed a significant increase in systemic inflammatory proteins³⁰. Our data suggests that increased systemic inflammation is not the primary cause for increased risk of CVD. Highlighting the lack of robust data on the long-term effect of anti-inflammatory drugs in CKD patients combined with the absence of a role for inflammation in the present study, our findings suggest that targeting the inflammatory pathway in CKD patients would not result in a significant decrease in morbidity and mortality.

Since no strong consistent associations was found between eGFR and inflammatory plaque markers additional analyses is performed for all patients that had a major cardiovascular adverse event during three year follow-up. Since we hypothesized that

inflammation is a key driver of increased morbidity and mortality during follow-up in patients with decreased kidney function, we aimed to investigate the associations between plaque histology and eGFR in this subset of our cohort. In total 235 patients (13.5%) developed a major cardiovascular adverse event during follow-up and associations of plaque characteristics and inflammatory plaque proteins with eGFR are reported in supplemental table 3 and 4. No associations of eGFR with binominal or continuous plaque characteristics were observed for patients that developed a major cardiovascular event during three year follow-up. No consistent increase in inflammatory plaque proteins was observed with decreasing kidney function. A statistically significant difference between Interleukin 4, 5 and 12 was observed between different kidney function groups however these differences did not show a gradual decline or increase over different kidney function groups.

This study suffers from several limitations. First, we describe a large cohort of patients that underwent CEA, with a wide variation in eGFR. However, because patients had to be fit for surgery, only few patients with end stage kidney failure or dialysis could be identified. Conclusions concerning atherosclerotic plaque composition and inflammatory status for this highly vulnerable patient group can therefore not be inferred from this study. However the distribution of kidney function in our cohort is a good reflection of elderly patients in the general population affected by atherosclerotic disease. Second, eGFR estimated by the MDRD equation has its limitations. Ideally eGFR would have been measured at multiple time points so patients are grouped based on multiple measurements narrowing the chance that patients are wrongfully classified. Last, no measures of urinary protein excretion were available which can potentially drive cardiovascular outcomes during follow-up in our cohort.

In conclusion, in patients suffering from carotid artery disease, decreased kidney function was associated with intraplaque hemorrhage and poor secondary outcome but not with inflammatory histological plaque characteristics after carotid endarterectomy. Furthermore, the current data suggests that plaque complement and coagulation pathways are involved in subsequent poor outcome in patients with decreased kidney function and severe atherosclerotic disease. Our data suggests that mechanisms other than inflammation explain the poor cardiovascular outcome in patients with impaired kidney function following carotid endarterectomy. Future efforts on reducing cardiovascular disease burden in CKD patients may not merely address the reduction of inflammation driven disease progression. The current study shows that other effectors such as intraplaque hemorrhage offer potential therapeutic targets to reduce atherosclerotic disease progression in CKD patients.

Conflict of interest

All authors report no conflicts of interest relevant to this article.

Acknowledgements

Supported by Dutch Heart Foundation, CVON 2014-11 RECONNECT.

References

1. Shlipak, M. G. *et al.* Cardiovascular disease risk status in elderly persons with renal insufficiency. *Kidney Int.* **62**, 997–1004 (2002).
2. Ross, R. Inflammation or Atherogenesis. *N. Engl. J. Med.* **340**, 115–126 (1999).
3. Tedgui, A. & Mallat, Z. Cytokines in atherosclerosis: pathogenic and regulatory pathways. *Physiol. Rev.* **86**, 515–81 (2006).
4. Hansson, G. K., Libby, P. & Tabas, I. Inflammation and plaque vulnerability. *J. Intern. Med.* **278**, 483–493 (2015).
5. Van Lammeren, G. W. *et al.* Decreased kidney function: An unrecognized and often untreated risk factor for secondary cardiovascular events after carotid surgery. *Stroke* **42**, 307–312 (2011).
6. Herzog, C. A., Ma, J. Z. & Collins, A. J. Poor long-term survival after acute myocardial infarction among patients on long-term dialysis. *N Engl J Med* **339**, 799–805 (1998).
7. Merino, A. *et al.* Microinflammation and endothelial damage in hemodialysis. *Contrib. Nephrol.* **161**, 83–88 (2008).
8. Pawlak, K., Naumnik, B., Brzóska, S., Pawlak, D. & Myśliwiec, M. Oxidative Stress - A Link between Endothelial Injury, Coagulation Activation, and Atherosclerosis in Haemodialysis Patients. *Am. J. Nephrol.* **24**, 154–161 (2004).
9. Nowak, K. L. *et al.* IL-1 Inhibition and Vascular Function in CKD. *J. Am. Soc. Nephrol.* **28**, 971–980 (2017).
10. Ridker, P. M. *et al.* Effects of interleukin-1 inhibition with canakinumab on hemoglobin A1c, lipids, C-reactive protein, interleukin-6, and fibrinogen a phase IIb randomized, placebo-controlled trial. *Circulation* **126**, 2739–2748 (2012).
11. Walther, C. P. & Navaneethan, S. D. Inflammation as a Therapeutic Target To Improve Vascular Function in Kidney Disease. *J. Am. Soc. Nephrol.* ASN.2016111173 (2017).
12. Verhoeven, B. A. N. *et al.* Athero-express: Differential atherosclerotic plaque expression of mRNA and protein in relation to cardiovascular events and patient characteristics. Rationale and design. *Eur. J. Epidemiol.* **19**, 1127–1133 (2004).
13. Stevens, L. A., Coresh, J., Greene, T. & Levey, A. S. Assessing Kidney Function — Measured and Estimated Glomerular Filtration Rate. *N Engl J Med* **354**, 2473–2483 (2006).
14. National Kidney Foundation. K/DOQI clinical practice guidelines for chronic kidney disease: evaluation, classification, and stratification. *Am J Kidney Dis* **39**, S1–S26 (2002).
15. Eknoyan, G. Meeting the challenges of the new K/DOQI guidelines. *Am J Kidney Dis* **41**, 3–10 (2003).
16. Hellings, W. E. *et al.* Intraobserver and interobserver variability and spatial differences in histologic examination of carotid endarterectomy specimens. *J. Vasc. Surg.* **46**, 1147–1154 (2007).
17. Davies, M. J., Richardson, P. D., Woolf, N., Katz, D. R. & Mann, J. Risk of thrombosis in human atherosclerotic plaques: role of extracellular lipid, macrophage, and smooth muscle cell content. *Br. Heart J.* **69**, 377–381 (1993).
18. Virmani, R. *et al.* Atherosclerotic plaque progression and vulnerability to rupture: Angiogenesis as a source of intraplaque hemorrhage. *Arterioscler. Thromb. Vasc. Biol.* **25**, 2054–2061 (2005).
19. De Kleijn, D. P. V. *et al.* Local atherosclerotic plaques are a source of prognostic biomarkers for adverse cardiovascular events. *Arterioscler. Thromb. Vasc. Biol.* **30**, 612–619 (2010).
20. Janssen, K. J. M. *et al.* Missing covariate data in medical research: To impute is better than to ignore. *J. Clin. Epidemiol.* **63**, 721–727 (2010).
21. Hellings, W. E. *et al.* Composition of Carotid Atherosclerotic Plaque Is Associated With Cardiovascular Outcome: A Prognostic Study. *Circulation* **121**, 1941–1950 (2010).
22. Sluimer, J. C. *et al.* Thin-Walled Microvessels in Human Coronary Atherosclerotic Plaques Show Incomplete Endothelial Junctions. Relevance of Compromised Structural Integrity for Intraplaque Microvascular Leakage. *J. Am. Coll. Cardiol.* **53**, 1517–1527 (2009).
23. Kolodgie, F. D. *et al.* Intraplaque hemorrhage and progression of coronary atheroma. *N. Engl. J. Med.* **349**, 2316–2325 (2003).
24. Vrijenhoek, J. E. *et al.* Gender is strongly associated with the presence of atherosclerotic plaque hemorrhage and an effect modifier in the relation between plaque hemorrhage and cardiovascular outcome. *Circulation* **126**, 2011–2012 (2012).
25. Sarnak, M. J. *et al.* Kidney Disease as a Risk Factor for Development of Cardiovascular Disease. *Circulation* **108**, 2154–2169 (2003).
26. Ritz, E. & McClellan, W. M. Overview: Increased Cardiovascular Risk in Patients with Minor Renal Dysfunction: An Emerging Issue with Far-Reaching Consequences. *J. Am. Soc. Nephrol.* **15**, 513–516 (2004).
27. Oksjoki, R., Kovanen, P. T. & Pentikäinen, M. O. Role of complement activation in atherosclerosis. *Curr. Opin. Lipidol.* **14**, 477–482 (2003).

28. Oksjoki, R. et al. Complement regulation in human atherosclerotic coronary lesions. Immunohistochemical evidence that C4b-binding protein negatively regulates the classical complement pathway, and that C5b-9 is formed via the alternative complement pathway. *Atherosclerosis* **192**, 40–48 (2007).
29. Lutz, J., Menke, J., Sollinger, D., Schinzel, H. & Thürmel, K. Haemostasis in chronic kidney disease. *Nephrol. Dial. Transplant* **29**, 29–40 (2014).
30. Hiramoto, J. S. et al. Inflammation and coagulation markers and kidney function decline: the Multi-Ethnic Study of Atherosclerosis (MESA). *Am J Kidney Dis* **60**, 225–232 (2012).

Supplemental methods

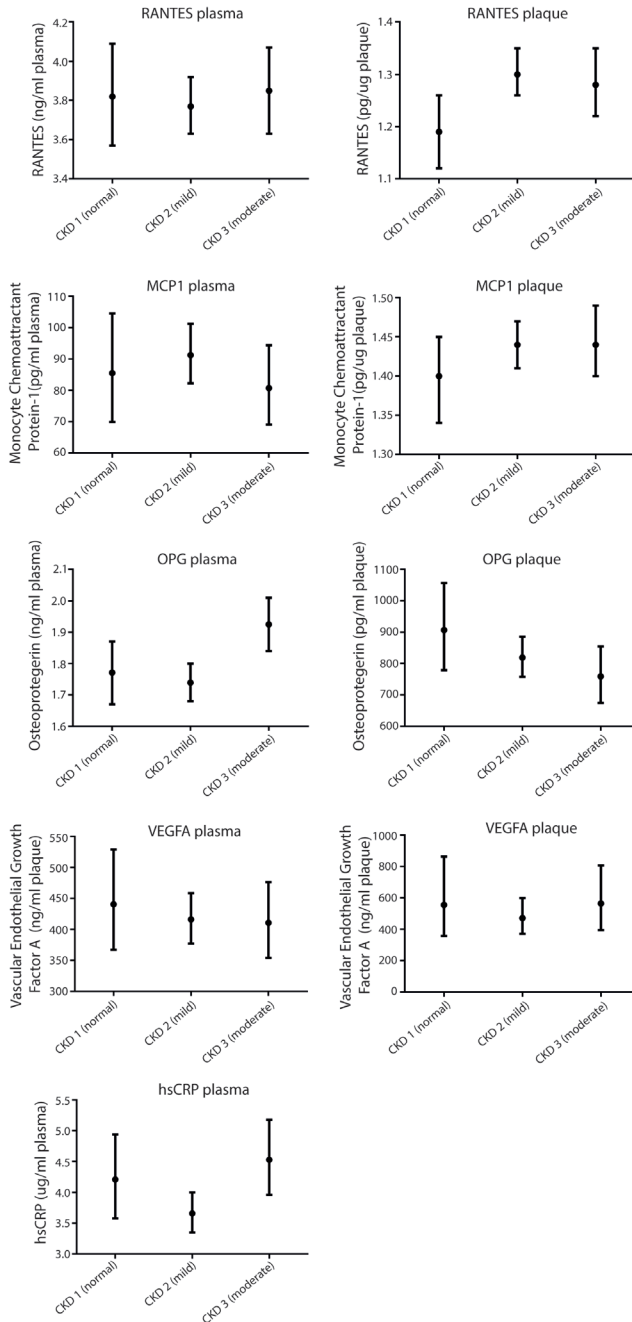
Specimens were stained with CD68 for macrophages, alpha-actin for smooth muscle cells (SMC), picro-sirius Red (PSR) for collagen, hematoxylin eosin (HE) for general overview including calcifications, CD34 for microvessels and HE and fibrin for plaque hemorrhages. Macrophage content and SMC content were measured quantitatively using computerized analyses using AnalySIS 3.2 software (Soft Imaging Systems GmbH, Münster, Germany), and reported as percentage positive staining per plaque area. Microvessels in the plaque were scored quantitatively in three hotspots and reported as an average number of vessels per hot spot. In addition, presence of collagen and calcification was scored semiquantitatively as no/minor or moderate/heavy staining, according to the following criteria: 1. no or minor staining along part of the luminal border of the plaque, or a few scattered spots within the lesion; 2. moderate or heavy staining along the entire luminal border or evident parts within the lesion. Size of the lipid core was visually estimated as a percentage of total plaque area using HE and PSR staining. A carotid plaque with a lipid core covering >40% of the plaque surface was considered as an atheromatous plaque, a carotid plaque with a lipid core covering >10% and <40% was considered a fibrous-atheromatous plaque and a lipid core covering <10% of the plaque surface was considered a fibrous plaque. Intraplaque hemorrhage was defined as a hemorrhage within the plaque without signs of cap rupture and no continuum to a luminal thrombus, and was scored as present or absent. Intraobserver and interobserver variability were examined previously and showed good reproducibility (κ 0.6-0.9).

Inflammatory plaque proteins

Cytokine protein levels were determined in atherosclerotic plaque isolates after Tripure (Roche) protein isolation. Osteoprotegerin (n=581) and RANTES (n=597) levels were measured with Multiplex Immunoassay (Bioplex, Biorad Laboratories, Hercules, USA). MCP-1 (n=1,176) was measured at the in-house Luminex core facility, and VEGFA (n=564) was measured with ELISA (Bender MedSystems, Vienna, Austria). Levels of Interleukin-4 (IL-4), IL-5, IL-6, IL-8, IL-10, and IL-12 in a selected cohort of 552 patients were quantified by Fluorescent Bead Immunoassay 810FF (Bendermed Systems, Vienna, Austria). Additionally to the cytokines and interleukins, we measured MMPs which are considered to have an effect on plaque stability. Activities of MMP2, 8 and 9 within the atherosclerotic specimens were quantified with biotrak activity assays RPN 2635 (Amersham Biosciences Buckinghamshire, UK).

Inflammatory plasma proteins

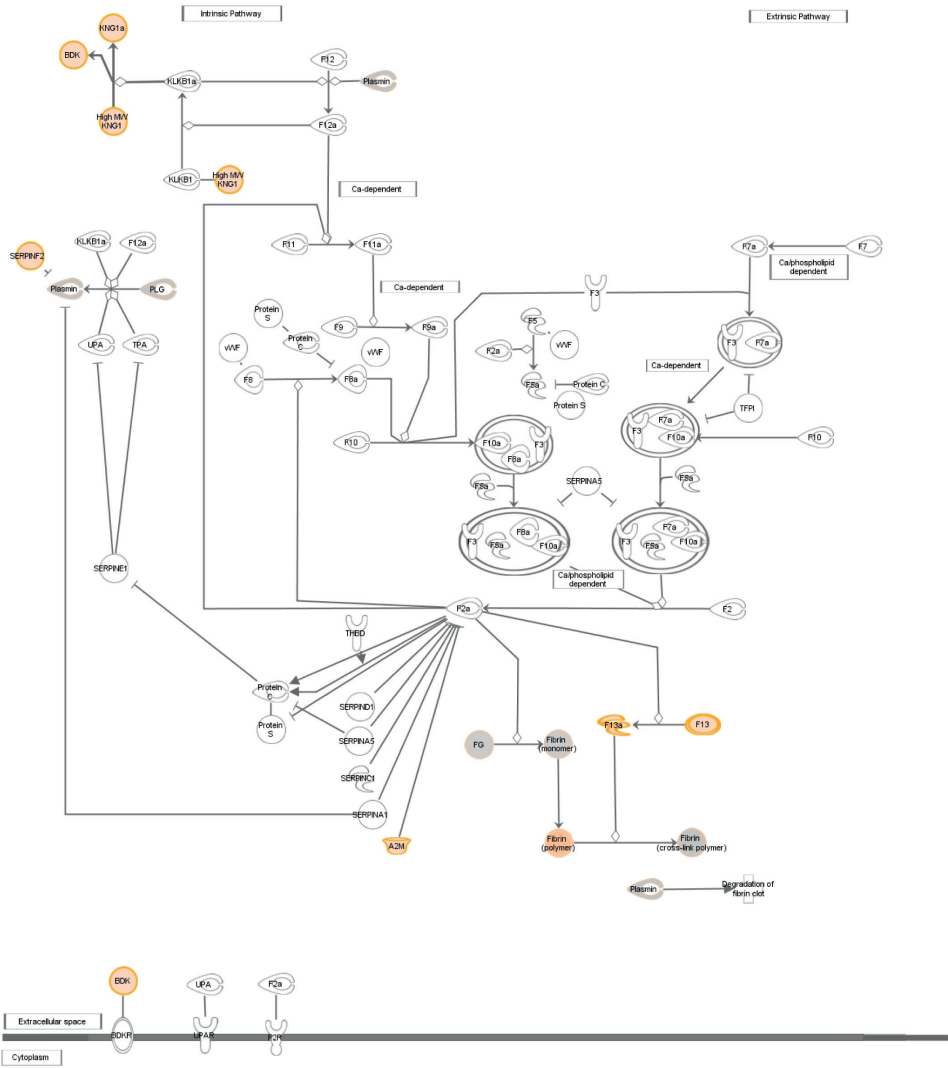
In plasma the proteins, MCP-1 (n=580), RANTES (n=1028), VEGFA (n=902), Osteoprotegerin (n=1054) and circulating hsCRP (n=1055) were measured. ELISAs were performed for quantification of hsCRP (Mouse anti-human CRP, DY1707; Streptavidin-mono-HRP, P0397, Dako), OPG (mouse anti-human OPG, MAB8051, R&D Systems; biotinylated goat anti-human OPG, BAF805 (DY805), R&D Systems; streptavidin-mono-



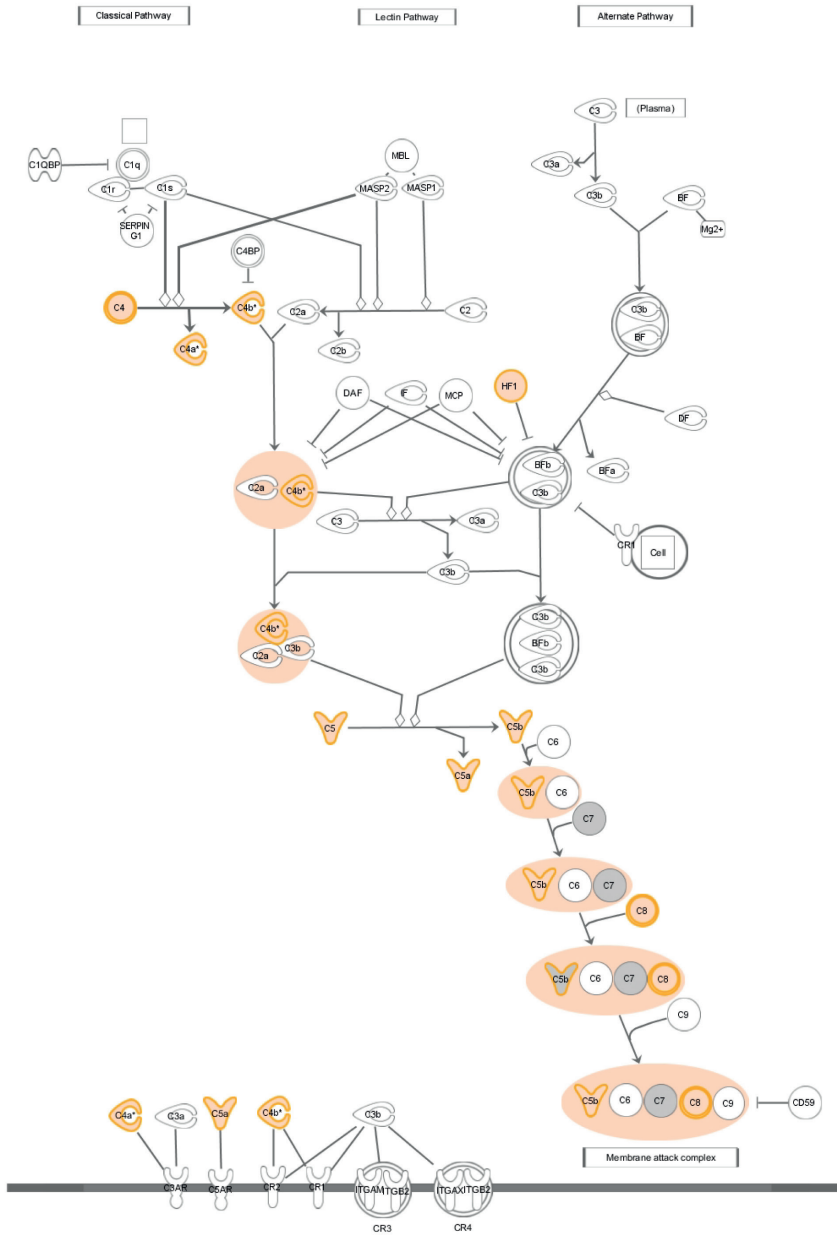
Supplemental figure 1.

Plaque and plasma protein levels in patients with normal kidney function (CKD1), mildly impaired kidney function (CKD2) and moderately impaired kidney function (CKD3)
 Values are presented as median with interquartile range.

HRP, P0397, Dako) and RANTES (anti-hCCL5/Rantes, MAB278, R&DSystems; anti-hRantes, AB-278-NA, R&Dsystems; Rabbit anti-Goat-HRP, P0449, Dako) levels. MCP-1 and VEGFA are measured at the Luminex core facility, UMC Utrecht.



Supplemental figure 2. Pathway derived from Ingenuity Pathway analysis. Coagulation system and upregulation of intrinsic pathway with decreasing eGFR. Color indicates a significant correlation. Source: Path Designer, Ingenuity System, Inc. All rights reserved.



Supplemental figure 3. Pathway derived from Ingenuity Pathway analysis. Complement system and upregulation of classical pathway with decreasing eGFR. Color indicates a significant correlation. Source: Path Designer, Ingenuity System, Inc. All rights reserved.

Supplemental table 1. Alphabetically ordered list of plaque proteins correlated with eGFR in 40 patients.

ID	Pearsons r	p- value	ID	Pearsons r	p- value	ID	Pearsons r	p- value	ID	Pearsons r	p- value
A2M	-0.466	0.002	CLEC11A	-0.351	0.026	IGKV1_5	-0.424	0.006	SOD2	-0.327	0.040
ACTR2	-0.388	0.013	CLU	-0.451	0.003	IGL@	-0.359	0.023	SPTAN1	-0.337	0.034
ACTR3	-0.363	0.021	CP	-0.383	0.015	PI00387116.1	-0.508	0.001	SPTBN5	-0.385	0.014
ANXA2	-0.385	0.014	CPB2	-0.385	0.014	IQGAP1	-0.415	0.008	STAB1	-0.357	0.024
ANXA7	-0.327	0.040	CPNE3	-0.339	0.033	KNG1	-0.468	0.002	STOM	-0.362	0.022
APOA4	-0.418	0.007	CST3	-0.533	<0.001	LAMA4	-0.412	0.008	SYNE1	-0.368	0.020
APOB	-0.396	0.011	CTSB	-0.516	0.001	LAMB1	-0.347	0.028	TCP1	-0.369	0.019
APOC3	-0.341	0.031	CTSD	-0.403	0.010	LAP3	-0.320	0.044	THBS2	-0.454	0.003
APOD	-0.338	0.033	DST	-0.324	0.041	LCP1	-0.315	0.048	TNC	-0.326	0.040
APOE	-0.351	0.026	EEF1G	-0.323	0.042	LGALS3BP	-0.424	0.006	TPI1	-0.343	0.030
ARHGD1B	-0.359	0.023	EHD4	-0.360	0.023	LRRCS9	-0.399	0.011	TUBA1B	-0.421	0.007
ARPC2	-0.387	0.014	F13A1	-0.515	0.001	LYZ	-0.346	0.029	TUBA4A	-0.388	0.013
ATL3	-0.367	0.020	FGA	-0.289	0.071	MDH2	-0.465	0.002	TXN	-0.422	0.007
ATP5B	-0.340	0.032	FLII	-0.323	0.042	MSN	-0.316	0.047	UGP2	-0.340	0.032
ATP5O	-0.350	0.027	GNB2L1	-0.457	0.003	P4HB	-0.408	0.009	VDAC1	-0.352	0.026
C4A	-0.418	0.007	GSTP1	-0.348	0.028	PGK1	-0.314	0.049	VDAC3	-0.317	0.046
C4B	-0.424	0.006	HADHA	-0.384	0.014	PKM2	-0.412	0.008	VTN	-0.359	0.023
C5	-0.357	0.024	HK1	-0.348	0.028	PLG	-0.380	0.016	YWHAE	-0.400	0.010
C7	-0.349	0.027	HNRNPA2B	-0.389	0.013	PLTP	-0.418	0.007	YWHAQ	-0.366	0.020
C8G	-0.424	0.006	HPR	-0.418	0.007	PRDX1	-0.331	0.037			
CAP1	-0.314	0.049	HSP90AA1	-0.335	0.034	RNASE3	-0.334	0.035			
CBR1	-0.436	0.005	HSP90B1	-0.341	0.031	S100A4	-0.333	0.036			
CCT3	-0.403	0.010	HSPA5	-0.323	0.042	SERPINE2	-0.511	0.001			
CD109	-0.382	0.015	HSPA8	-0.369	0.019	SERPINF1	-0.408	0.009			
CFH	-0.345	0.029	IGHM	-0.393	0.012	SERPINF2	-0.316	0.047			
CFL1	-0.365	0.021	IGKC	-0.378	0.016	SLPI	-0.374	0.017			

Supplemental table 2. Ingenuity pathway Analysis results reveals enrichment of the coagulation and complement system.

Pathway	Molecules	-log(p-value)	Ratio
Coagulation System	KNG1,F13A1,A2M,SERPINF2	4.66	4/28 (0.143)
Complement System	C4A/C4B,CFH,C8G,C5	4.48	4/31 (0.129)

Supplemental table 3. Histological atherosclerotic plaque characteristics of patients that did develop major adverse cardiovascular events during three year follow-up (n=235).

Binominal carotid plaque characteristics	P-value	Odds ratio	[95%CI]		P-value Multivariate	Odds ratio	[95%CI]	
	Univariate	unadjusted				adjusted		
Presence of lipid core \geq 40%. % (n)	0.991	0.998	0.749	1.330	0.898	1.026	0.688	1.531
Presence of lipid core \geq 10%. % (n)	0.290	1.161	0.880	1.531	0.499	1.127	0.797	1.592
Moderate/heavy calcifications. % (n)	0.715	1.048	0.815	1.347	0.873	0.974	0.703	1.349
Moderate/heavy collagen. % (n)	0.889	1.023	0.743	1.409	0.456	0.840	0.531	1.328
Presence of intraplaque hemorrhage. % (n)	0.832	1.029	0.792	1.337	0.122	1.326	0.927	1.896
Continuous carotid plaque characteristics	P-value	Beta	[95%CI]		P-value adjusted	Beta	[95%CI]	
		Unadjusted				Adjusted		
Mean number of microvessels per hotspot	0.959	-0.003	-0.106	0.101	0.891	-0.012	-0.136	0.118
% of positive macrophage staining per plaque	0.671	0.029	-0.046	0.072	0.663	-0.015	-0.085	0.055
% of positive SMC staining per plaque	0.216	-0.085	-0.125	0.028	0.921	0.008	-0.070	0.078

Odds ratios and regression coefficients represents the risk per decrease of 20 points eGFR. Multivariate analysis corrected for sex, age, smoking status, diabetes mellitus, hypertension, history of CAD, lipid levels, anticoagulant therapy, Beta blocker use, diuretics use and RAAS medications. Abbreviations: CI, confidence interval; SMC, Smooth Muscle Cell.

Supplemental table 4. Plaque and plasma protein levels in patients with normal kidney function (eGFR \geq 90 ml/min/1.73 m²), mildly impaired kidney function (eGFR 60-89 ml/min/1.73 m²) and moderately impaired kidney function (eGFR 30-59 ml/min/1.73 m²) of patients with major adverse cardiovascular events during three year follow-up.

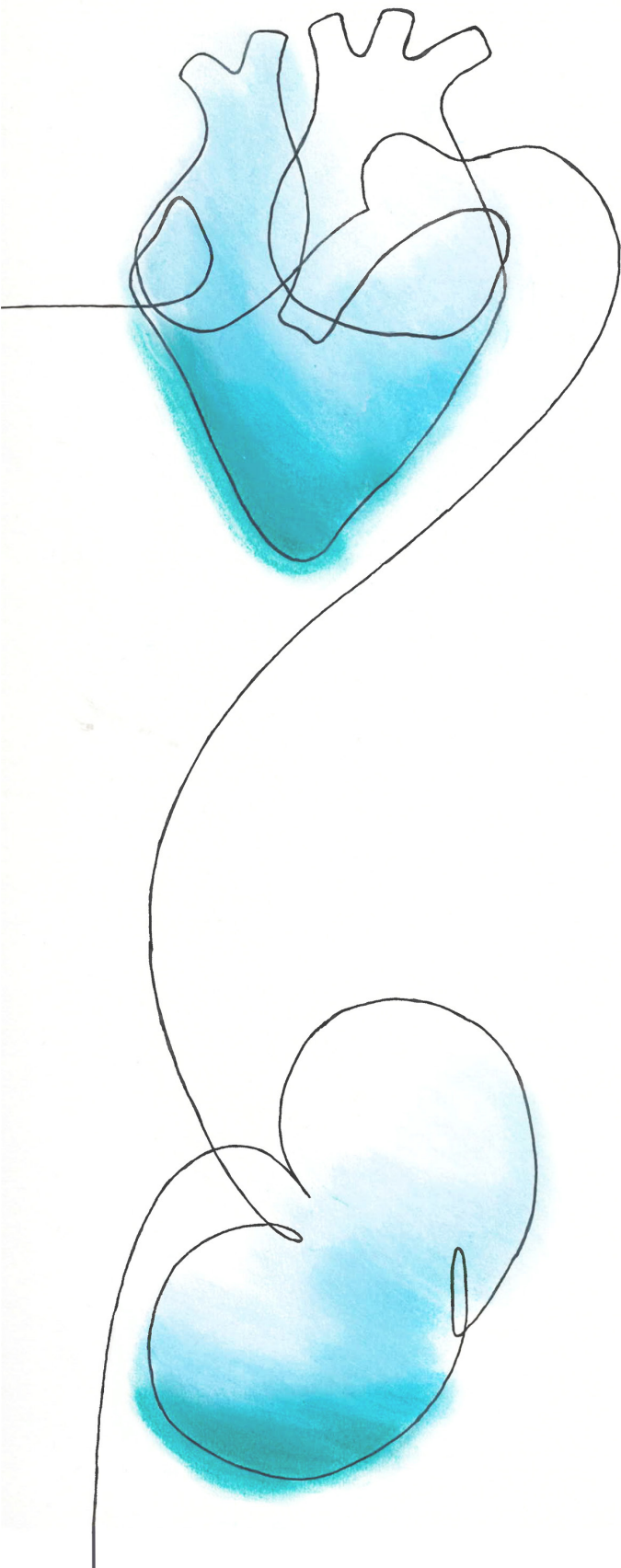
Plaque protein	n	eGFR \geq 90 ml/ min/1.73 m ²	eGFR 60-89 ml/ min/1.73 m ²	eGFR 30-59 ml/ min/1.73 m ²	P-value
Interleukin 4 (pg/ml)	78	40.94 [12.81-130.93]	127.10 [68.15-237.14]	13.29 [6.12-28.87]	<0.001
Interleukin 5 (pg/ml)	78	57.69 [12.92-185.54]	127.10 [67.91-237.91]	34.85 [15.98-76.03]	0.041
Interleukin 6 (pg/ml)	78	32.23 [12.14-85.51]	37.30 [22.10-62.96]	32.62 [17.01-62.60]	0.935
Interleukin 8 (pg/ml)	78	88.59 [24.57-319.16]	51.21 [25.75-101.88]	26.15 [11.12-61.57]	0.276
Interleukin 10 (pg/ml)	78	15.99 [6.14-41.57]	20.72 [12.58-34.12]	7.61 [4.10-14.13]	0.055
Interleukin 12 (pg/ml)	78	32.01 [9.17-111.79]	74.14 [37.90-144.98]	21.50 [9.33-49.52]	0.071
RANTES (pg/ug)	71	1.10 [0.87-1.39]	1.36 [1.21-1.53]	1.29 [1.15-1.45]	0.271
OPG (pg/ml)	79	809.97 [567.37-1115.68]	991.28 [800.79 - 1227.62]	915.07 [709.82-1197.19]	0.601
MCP-1 (pg/ug)	138	1.37 [1.13-1.67]	1.50 [1.36-1.66]	1.54 [1.39-1.70]	0.608
VEGFA (ng/ml)	79	551.15 [150.22-2022.70]	400.21 [185.06-865.01]	594.67 [244.37-1447.16]	0.789
Plasma protein					
RANTES (ng/ml)	112	3.97 [2.87-5.49]	4.41 [3.75-5.18]	3.90 [3.27-4.65]	0.571
OPG (ng/ml)	110	2.48 [2.05-2.91]	1.91 [1.69-2.13]	1.97 [1.74-2.21]	0.065
MCP-1 (pg/ml)	79	93.50 [51.23-170.69]	98.49 [68.65-141.42]	77.01 [50.14-118.34]	0.702
VEGFA (pg/ml)	96	648.72 [318.47-1321.62]	520.61 [388.08-697.93]	504.21 [359.62-706.65]	0.823
hsCRP (ug/ml)	112	8.18 [3.90-17.13]	3.89 [2.69-5.62]	5.20 [3.47-7.77]	0.169

Corrected for age, sex and year of surgery. Values are presented as mean with [95% confidence interval]. Abbreviations: OPG, Osteoprotegerin; MCP-1, monocyte chemoattractant protein-1; VEGFA, Vascular endothelial growth factor A.



PART II

The underlying pathophysiology of cardiac remodeling



4

High renin expression in the absence of kidney injury in the murine trans aortic constriction model

In revision. American Journal of Physiology: Renal Physiology

M. Wesseling^{1,2}, E. Mulder¹, M.A.D. Brans¹, M. Bulthuis³, G. Pasterkamp²,
M.C. Verhaar⁴, H. van Goor³, J.A. Joles^{4*}, S.C.A. de Jager^{1,5*†}

* authors contributed equally

¹ Laboratory for Experimental Cardiology, University Medical Center Utrecht, Utrecht, the Netherlands

² Laboratory for Clinical Chemistry and Haematology, University Medical Center Utrecht, Utrecht, the Netherlands

³ Pathology and Medical Biology, University Medical Center Groningen, Groningen, the Netherlands

⁴ Department of Nephrology and Hypertension, University Medical Center Utrecht, Utrecht, the Netherlands

⁵ Laboratory for Translational Immunology, University Medical Center Utrecht, Utrecht, the Netherlands

Abstract

Cardiorenal syndrome type 2 is characterized by kidney failure as consequence of heart failure and affects >50% of heart failure patients. Murine transverse aortic constriction (TAC) is a heart failure model, where pressure overload is induced on the heart without systemic hypertensive consequences. Whether renal function is altered in this model is debated, and if so, at which time post-TAC renal dysfunction starts to contribute to worsening of cardiac function. We therefore studied the effects of progressive heart failure on the kidney in the absence of chronically elevated systemic blood pressure and renal perfusion pressure.

A total of 129 C57BL/6J mice were exposed to TAC using a minimally invasive technique and followed from 3 to 70 days post-TAC. Cardiac function was determined with 3D ultrasound and showed a gradual decrease in stroke volume over time. Renin expression in the kidney increased with heart failure, suggestive of the presence of hypoperfusion. In addition, plasma urea levels, a surrogate marker for renal dysfunction, were increased post-TAC. However, neither structural abnormalities in the kidneys, nor albuminuria were present at any time-point post-TAC.

In conclusion, progressive heart failure associated with increased renin expression, but only mildly affected renal function without inducing structural injury. In combination, these data suggest that heart failure alone does not contribute to kidney dysfunction in mice.

Introduction

Cardiorenal syndrome (CRS) is a clinical characterization of patients with both heart and kidney failure where CRS type 2 describes chronic kidney disease (CKD) as consequence of heart failure^{1,2}. Especially in a non-ischemic heart failure population, patients often suffer from CKD^{3,4}. Indeed, over 50% of all heart failure patients show a certain degree of CKD which has been associated with increased mortality rates^{4,5}.

A generally accepted model to study adverse cardiac remodeling in heart failure is transverse aortic constriction (TAC). Cardiac remodeling in this model is characterized by early structural changes due to inflammation and fibrosis, and results in left ventricular hypertrophy^{6,7}. Consequently, the functional capacity of the heart deteriorates as end systolic and diastolic volumes increase and stroke volume is reduced⁸. As the kidneys are downstream of the heart, it is reasonable to assume that they experience hypoperfusion in the TAC model, due to a reduced stroke volume. From the two kidney one clip model (2k1c) it has been established that renal hypoperfusion leads to local renin-angiotensin system (RAS) stimulation consequently leading to various systemic effects, including aldosterone release⁹. Little information is available on deterioration of kidney function in the TAC model, although RAS stimulation has been documented to exacerbate heart failure progression after TAC^{10,11}.

TAC has been proven to be a relevant preclinical model for chronic non-ischemic heart failure, however for CRS Type 2 this is debated^{10,12-15}. Based on the reduced stroke volume in the TAC model and increased renin expression in the 2k1c model we hypothesized that in the TAC model, hypoperfusion in the kidneys directly leads to renin activation and in the long-term renal hypofiltration, fibrosis and atrophy, as has been shown by us and others for the clipped kidney in the 2k1c model^{9,16}. To identify acute and progressive effects of heart failure on the kidney, we aim to establish the expression of renin in relation to presence of structural and functional deterioration of the kidney in a mouse TAC model. As no systemic hypertension is present in this model, it allows dissociation of direct effects of acute and chronic heart failure from acute and persistently increased renal perfusion pressure on acute and chronic kidney injury, respectively^{17,18}.

Methods

Animals

Male and female C57BL/6J mice were used, originally obtained from the Jackson laboratory and kept in our breeding facility. Animals were housed under standard conditions in filter top cages with 12h light/dark cycle. Mice received standard chow and water ad libitum. Researchers and technicians were blinded for animal groups, respective operations, data acquisition and analysis. Mice, aged 9-12 weeks, were included in the study with a starting weight between 20-30 gram. All mice were randomly assigned to follow-up time after TAC as described¹⁹. Supplemental figure 1a shows a flowchart with

animals used per experimental group, mice excluded based on flow ratios, and mice lost during follow up. For each time point we included at least 5 male and 5 female TAC mice. We included a total of 129 mice and finally analyzed 13 baseline (no surgery) and 94 TAC mice.

Transverse aortic constriction

All animal experiments were performed according to the 'Guide for the care and use of Laboratory Animals'. Experiments were approved by the Animal Experiments Committee of the University Medical Center Utrecht (Utrecht, the Netherlands) and reported according to the Arrive guidelines²⁰. Surgery was performed by an experienced surgeon in a dedicated mouse operation room. Mice were anesthetized by intraperitoneal (i.p.) injection of medetomidine hydrochloride (1.0 g/kg body weight), midazolam (Dormicum®, Roche, 10.0 mg/kg) and fentanyl (Janssen-Cilag, 0.1 mg/kg). Mice were intubated and ventilated on a rodent ventilator (Minivent, Hugo Sachs Electronics, Germany) with an oxygen-air ratio of 1:1 (175 strokes/minute, 250 µl stroke volume). Via a thoracic incision between the upper left sternal border in the second intercostal space, a ligature was placed around the transverse aorta between the right and left common carotid arteries. Constriction was standardized by placing a 7-0 silk suture around a blunt 27-gauge needle which was subsequently removed.

Echocardiography

For transthoracic 3D-echocardiography we used the Vevo 2100 System with a 22-35 MHz transducer (MS550D; VisualSonics Inc., Toronto, Canada), to assess cardiac function by structural and functional parameters. The mice underwent echocardiography at baseline, day 7 and at termination, under the inhalation of 2% isoflurane in a mixture of oxygen/air of 1:1. At day 7 echocardiography was performed to confirm correct placement of the ligation by Doppler flow measurements on the carotid arteries (Supplemental figure 1b). Only animals with a flow ratio (between left and right carotid) >5 were included in the study. At baseline and termination, two-dimensional echocardiography images were recorded on the short and long axis of the heart at multiple levels in both end systole and end diastole with use of respiratory triggering. The VevoLab software (Fujifilm; VisualSonics Inc.) was used for analyses on cardiac flow and volumes.

Tissue collection

Mice were sacrificed at baseline, 3, 7, 14, 21, 28, 35, 42, 56, or 70 days after TAC (Supplemental figure 1c). When possible, urine was collected directly before termination, by fixation of the mice and bladder stimulation by hand, and stored at -20°C until further analysis. Mice were terminated by exsanguination after i.p. administration of overdose sodium pentobarbital (60 g/kg). Blood was collected in EDTA-coated tubes via orbital puncture for plasma collection and stored at -80°C until further analysis. The vascular system was flushed with 5 ml phosphate-buffered saline (PBS) via right ventricular puncture. Heart weight and tibia length was assessed. The kidneys were cut in half

longitudinally, and half of the kidney was snap-frozen in liquid nitrogen for RNA isolation. The other half was fixed in 4% paraformaldehyde for 24h, and subsequently embedded in paraffin for histology.

Urea measurements in plasma

In the plasma samples we determined urea levels with the Urea CT* FS** according to manufacturer's protocol (DiaSys Diagnostic Systems, GmbH, Germany).

Albumin measurements in urine

In order to measure albumin levels in urine animals were placed in metabolic cages overnight (15h) to collect urine at day 3, 7 and 14 (Supplemental figure 2). Before placement in metabolic cages animals underwent a TAC procedure as described above. Mice were taken off chow and put on 15% glucose supplemented water overnight in order increase drinking and consequential urine secretion. During the same period mice were deprived of food. On day 14 animals were sacrificed and urine was collected and stored at -20°C. Albumin levels were determined using a Mouse Albumin Elisa kit according to manufacturer's protocol (Bethyl laboratories Inc., Bioke, Leiden, the Netherlands). To correct for variation in urine concentration we determined urine osmolarity using an Osmometer (3320 Osmometer, Advanced instruments Inc, Norwood, MA, US).

Histology

From the paraffin embedded kidneys, 3 µm sections were cut and fixed on glass slides (X-tra™ Adhesive, Surgipath, Leica Biosystems, UK). Sections are deparaffinized and stained for Periodic Acid-Schiff (PAS) to evaluate glomerular and tubular morphology. Furthermore, sections were stained for renin as described previously⁹. Both PAS and renin immunohistochemistry analysis was performed on the scanned slides with Image Scope (v12.3.2.8013 Aperio, Leica Biosystems Imaging, Inc., Buffalo Grove, IL). Renin positive cells were counted in all glomeruli of one renal cross section. Subsequently, the number renin positive cells were corrected for the total number of glomeruli per renal cross section, since the juxtaglomerular apparatus was not visible in all glomeruli. Analysis was performed in a blinded fashion by two independent observers.

Statistics

For statistical analysis, we used one-way ANOVA followed by Dunnett's multiple comparisons test (all TAC groups were compared to the baseline group) performed with GraphPad (Prism 8.0.1 for Windows, GraphPad Software, San Diego, CA). Data is shown as mean±SD. For associations we used linear regression. $p < 0.05$ was considered significant.

Results

Gradual adverse cardiac remodeling upon TAC

To induce heart failure, mice were subjected to pressure overload by TAC. Heart weight to tibia length ratio were determined as an indication of cardiac remodeling and was progressively and significantly increased compared to control (baseline) mice from 21 days post-TAC ($p < 0.0001$, Figure 1a). Stroke volume decreased, starting at day 3 ranging till day 70 with no progressive deterioration over time (Figure 1b). In line, increased end systolic volume, end diastolic volume and reduced contraction (measured as global longitudinal strain) together with a decreased EF confirm structural remodeling with reduced cardiac function over time after TAC (Table 1). We were unable to calculate cardiac output in our model, as the heart rate was influenced by the used anesthetics.

Renin expression and its association to cardiac function

A decrease in stroke volume can lead to hypoperfusion of the kidney and consequently affect renal function. Due to hypoperfusion the intrarenal RAS will be activated. With immunohistochemistry, renin expression in renal juxtaglomerular cells was evaluated to establish RAS activation in response to the reduced blood flow upon TAC (Figure 2a, black arrows indicate renin staining). Analysis showed a mild progressive increase of renin in the juxtaglomerular apparatus, reaching statistical significance from 35 days post-TAC vs. control (day 35, 56 and 70 $p < 0.05$) (Figure 2b). Taken together, these results suggest gradual RAS activation in response to the initial direct reduction in renal blood flow after TAC.

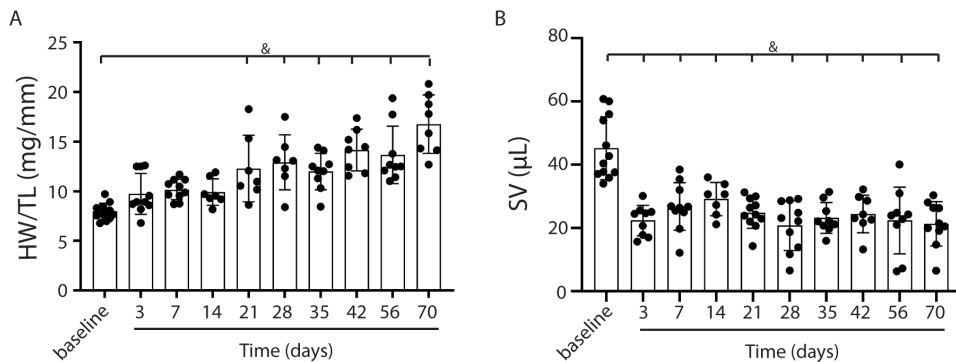


Figure 1. Cardiac function and weight in TAC mice over time.

A gradual increase in heart weight to tibia length ratio over time, indicating the presence of cardiac remodeling post-TAC (a). Stroke volume decreases over time vs. baseline (b). Mean \pm SD. &= $p < 0.0001$. HW/TL; Heart weight / Tibia length.

Table 1. Echocardiography variables.

Time (days)	n	ESV			EDV			SV			EF			Strain		
		mean (sd)	adjusted p value	mean (sd)	adjusted p value	mean (sd)	adjusted p value	mean (sd)	adjusted p value	mean (sd)	adjusted p value	mean (sd)	adjusted p value	mean (sd)	adjusted p value	
Base-line	15	16.24 (3.99)	-	48.57 (9.62)	-	45.23 (9.91)	-	67.99 (5.38)	-	-17.82 (1.99)	-	-	-	-	-	
3	7	38.58 (11.66)	0.0068	60.66 (10.22)	0.3101	22.37 (4.81)	< 0.0001	37.33 (10.58)	< 0.0001	-12.96 (4.03)	< 0.0001	< 0.0001	-12.96 (4.03)	< 0.0001	0.018	
7	10	30.21 (7.36)	0.15	56.59 (11.30)	0.7121	26.84 (7.51)	< 0.0001	47.08 (8.33)	< 0.0001	-10.928 (4.32)	< 0.0001	< 0.0001	-10.928 (4.32)	< 0.0001	< 0.0001	
14	9	28.87 (7.24)	0.2806	59.14 (10.20)	0.4246	29.17 (5.25)	0.0001	51.42 (7.60)	0.0025	-11.50 (1.23)	0.0002	0.0002	-11.50 (1.23)	0.0002	0.0002	
21	11	44.60 (19.37)	0.0001	69.91 (19.01)	0.0035	24.77 (4.88)	< 0.0001	37.94 (10.44)	< 0.0001	-8.29 (2.92)	< 0.0001	< 0.0001	-8.29 (2.92)	< 0.0001	< 0.0001	
28	11	44.97 (17.18)	0.0001	65.74 (12.71)	0.032	20.75 (7.86)	< 0.0001	33.53 (17.63)	< 0.0001	-10.80 (3.66)	< 0.0001	< 0.0001	-10.80 (3.66)	< 0.0001	< 0.0001	
35	8	40.74 (12.27)	0.0023	63.63 (13.68)	0.1087	23.16 (4.88)	< 0.0001	36.87 (8.37)	< 0.0001	-8.37 (3.22)	< 0.0001	< 0.0001	-8.37 (3.22)	< 0.0001	< 0.0001	
42	10	44.75 (18.66)	< 0.0001	77.46 (16.20)	0.0011	24.45 (5.93)	< 0.0001	40.37 (16.55)	< 0.0001	-7.94 (5.19)	< 0.0001	< 0.0001	-7.94 (5.19)	< 0.0001	< 0.0001	
56	8	62.77 (25.51)	< 0.0001	85.34 (17.42)	< 0.0001	22.40 (10.54)	< 0.0001	28.61 (15.73)	< 0.0001	-7.25 (2.28)	< 0.0001	< 0.0001	-7.25 (2.28)	< 0.0001	< 0.0001	
70	9	78.87 (28.13)	< 0.0001	98.76 (24.80)	< 0.0001	21.34 (7.04)	< 0.0001	22.17 (12.16)	< 0.0001	-6.70 (3.46)	< 0.0001	< 0.0001	-6.70 (3.46)	< 0.0001	< 0.0001	

P-values are presented compared with baseline values. Abbreviations, ESV; End systolic volume, EDV; End diastolic volume, SV; Stroke volume, EF; Ejection Fraction.

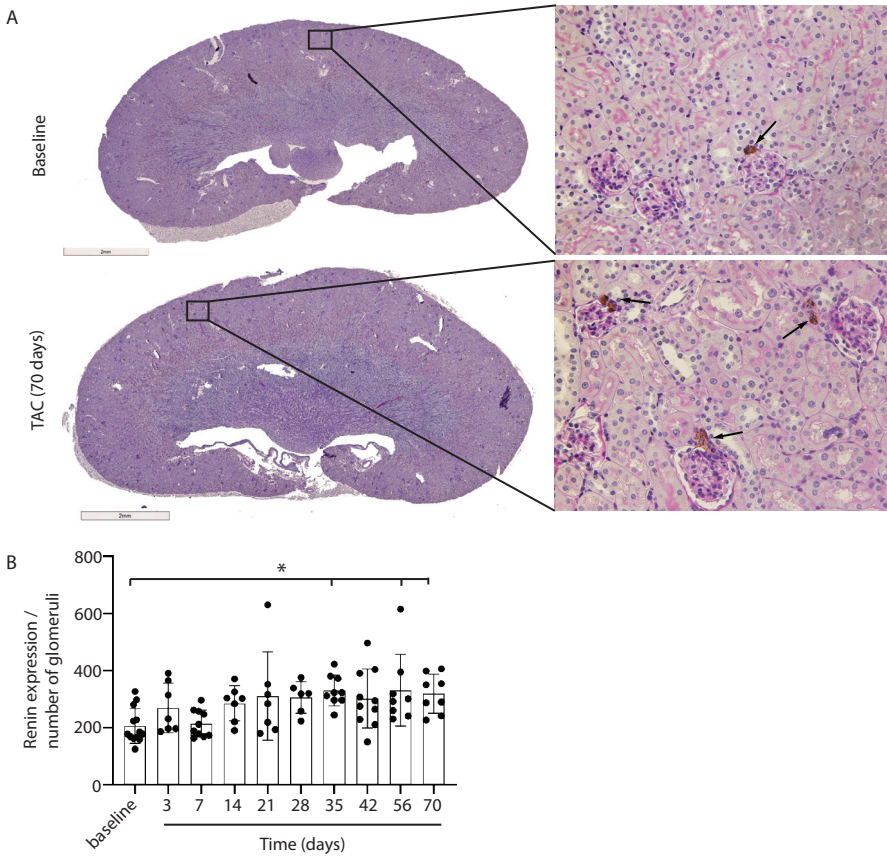


Figure 2. Renal renin expression after TAC.

Representative figures of renin expression at baseline and after 3 to 70 days of TAC (a). Renin expression is visible in the juxtaglomerular cells close to the glomeruli (arrows). Renin expression, corrected for the number of glomeruli present in the section, is increased from day 35 compared to baseline (b). Mean±SD, * $p < 0.05$.

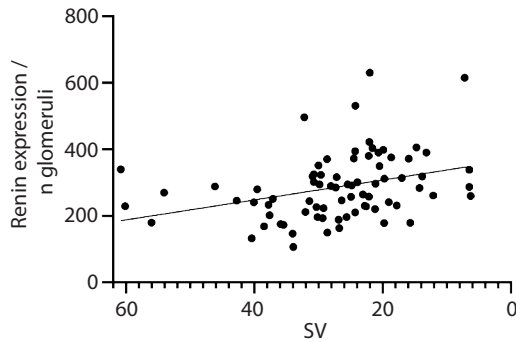


Figure 3. Renin expression increases upon reduced cardiac function.

Renin expression (relative to the number of glomeruli) is significantly correlated to a lower stroke volume after TAC ($p < 0.003$). SV; Stroke volume.

Next, we investigated the relation between renin expression and cardiac function in order to associate the presence of renal hypoperfusion with decreasing stroke volume. A significant positive association is present for renin expression and decreasing stroke volume ($p=0.0029$, Figure 3). Although both sexes were included in our study, we did not observe any differences in renin expression between males and females.

Kidney function and structure

As a measure for kidney function we assessed glomerular function, morphological changes and albuminuria in mice exposed to TAC. A mild and stable increase in urea levels was observed over time after TAC compared to baseline (day 7, $p<0.01$; day 28, 35 and 70, $p<0.05$) (Figure 4a). The increase in urea suggests a mildly reduced renal glomerular filtration as possible consequence of TAC. No fibrosis, sclerosis or an indication of infiltrating immune cells was observed in either the glomerular or tubulo-interstitial compartments upon TAC at any timepoint (Figure 4b). Incidentally, we did observe some random protein casts in the kidney medulla with no apparent relation to duration of TAC ($n=28/107$, ranging from day 0 till day 70). No differences in albuminuria could be observed between early and late timepoints after TAC (Figure 4c). As we were unable to obtain enough urine from all mice and were not in possession of baseline samples, we included 10 additional mice to collect urine with metabolic cages. Again, no differences were observed for albumin excretion post-TAC compared to baseline (Figure 4d). Although both sexes were included in our study, we did not observe any differences in kidney function and structure between males and females (data not shown). To summarize, despite the severe cardiac remodeling after prolonged exposure to TAC, there is no indication of structural damage or kidney dysfunction after prolonged exposure to TAC.

Discussion

As the influence of the cardiorenal axis in the TAC heart failure model¹⁵ is debated we evaluated renal function and structure in relation to renin expression in the TAC model over time. We are the first to provide an elaborate TAC study of progressive heart failure allowing us to assess both, acute and progressive effects of heart failure on renal function in relation to renin expression. Our results indicate that in the TAC model, hypoperfusion of the kidneys occurs as cardiac stroke volume decreases and renin expression increases over time. This indicates that the RAS is activated in a response to reduced renal blood flow. In addition, increased renin levels significantly associate with reduced stroke volume. Despite very severe heart failure upon prolonged TAC we did not detect functional and structural abnormalities in the kidneys. Taken together, our results indicate that in the murine TAC model the kidneys remain intact independent of worsening cardiac function, possibly as a consequence of renin activation.

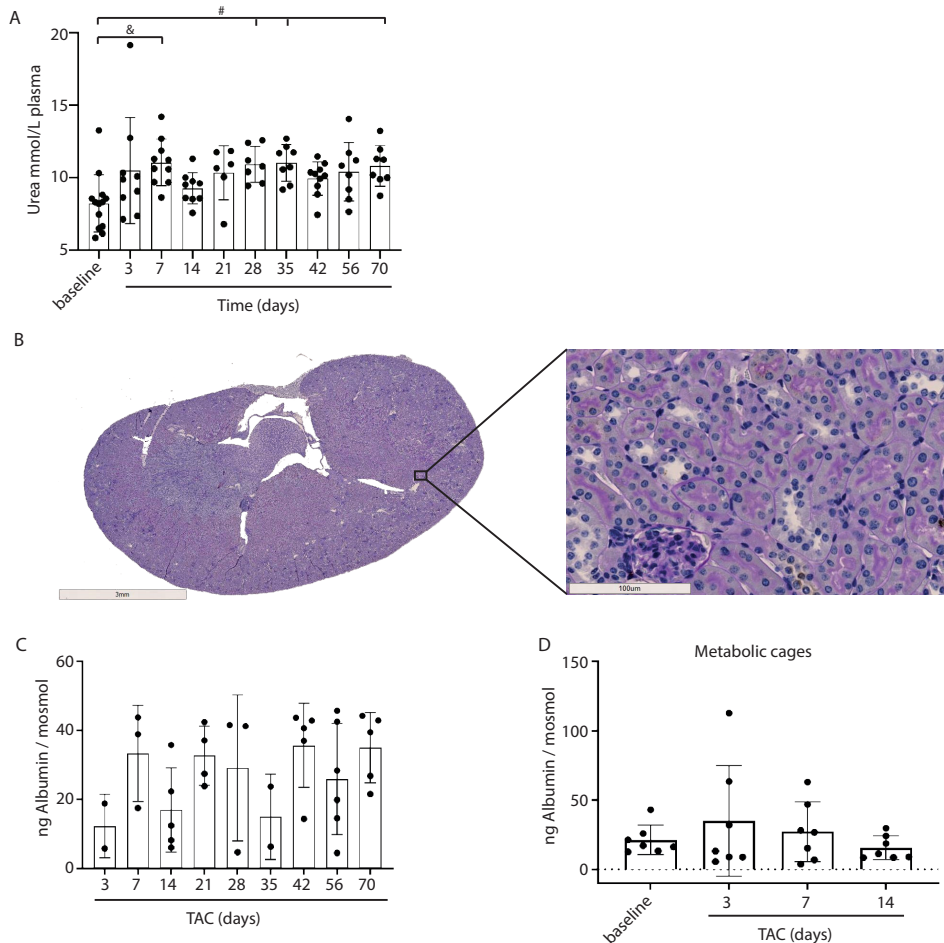


Figure 4. Kidney morphology, signs of damage and albumin levels.

Urea levels in plasma were significantly upregulated over time after TAC versus baseline (a). No structural abnormalities were observed in glomeruli and tubuli (PAS staining) (b). No increase in urinary albumin levels could be observed after TAC (c). Urine albumin levels (corrected for osmolality) post-TAC were not different from baseline (metabolic cages) (d). Mean \pm SD. # $p < 0.05$; & $p < 0.01$.

It has previously been shown that a strongly reduced stroke volume can activate RAS, leading to increased inflammation and severe renal fibrosis^{21,22}. For example Li *et al*, reported RAS activation due to cardiac pressure overload 18 weeks post-TAC¹⁰, where Zhao already reported increased albuminuria and structural abnormalities after 8 weeks of TAC²². However, contradictory results have also been described, for instance Tan *et al*, show that after 10 weeks TAC, only a mild renal pathology is present which didn't associate with the progressive cardiac remodeling post-TAC¹⁵. This is in line with others who showed no signs of kidney fibrosis 4 weeks post TAC in a model with mild, moderate

and severe aortic constriction¹³. However, none of these studies included sequential time series to evaluate the start and progression of renal dysfunction in TAC mice. Here, in a longitudinal study, we show that kidney function and structure remain normal up till 10 weeks post-TAC. However, our model might be too mild to induce renal dysfunction already after 70 days, but longer survival is difficult as mice do suffer from severe cardiac dysfunction.

Although we observe a preserved renal function after TAC, we cannot ignore the consequences that high renin levels may have on the heart and kidney via RAS activation¹⁰. For example, Angiotensin II (Ang II) is known to induce renal and cardiac fibrosis. As renin plays an important role in the Ang II production, increased renin levels have a direct consequence on cardiac fibrosis formation and renin is reported to affect renal perfusion²³⁻²⁵. Therapeutic intervention of RAS can interrupt this vicious circle. Indeed, treatment with Angiotensin-converting enzyme inhibitors (ACEi) and Angiotensin II receptor blockers (ARB) are proven to be protective for heart failure and prevent left ventricular stiffness in humans, most likely as a direct consequence of reduced Ang II levels²⁶. In addition ACE inhibition results in an improved cardiac and renal function in mice after TAC^{25,27}.

When using the TAC model to study heart failure it is important to take the cardiorenal axis into account, patients with a reduced cardiac function often also experience CKD²⁸⁻³¹, as it has been suggested that a decline in kidney function directly contributes to further deterioration of cardiac function in patients^{32,33}. Several papers have indicated a good animal model that properly represents the clinical manifests off CRS is lacking^{15,34,35}. Attempts have been made to developed such a CRS models, for instance showing adverse cardiac remodeling in a severe CKD model thereby mimicking aspects of CRS4 in patients³⁶. Others have shown an experimental model of dual insults that combine myocardial infarction or doxorubicin induced dilated cardiomyopathy, followed by 5/6 subtotal nephrectomy, thereby mimicking patients with preexisting chronic heart failure and asymptomatic renal dysfunction^{37,38}. One could also argue that the TAC model represents primary renal malfunction (decreased renal perfusion due to reduced SV, leading to renin secretion and angiotensin formation), followed by gradual development of angiotensin II dependent chronic heart failure, therefore modelling CRS3. However further studies are needed to gain insights into the variety of bidirectional pathway interactions between heart and kidney, like hemodynamic, humoral, metabolic and cell mediated communication in animal models to overcome the current limitations of the existing models^{32,35}.

In conclusion, we show that progressive heart failure within our TAC model only mildly affects renal function without inducing major structural abnormalities. Our results do not support the hypothesis that heart failure due to acute cardiac pressure overload leads to rapid progressive deterioration of kidney function. Indeed, our data suggest that the TAC model is suitable to test the function of novel proteins in or therapeutics for heart failure without an influence of kidney dysfunction other than renin release.

Acknowledgements

We gratefully acknowledge Adele Dijk, Petra van de Kraak, Melanie van de Kaa and Petra de Bree for their technical support for this extensive mice study.

Conflict of interest

The authors declared they do not have anything to disclose regarding conflict of interest with respect to this manuscript.

Financial support

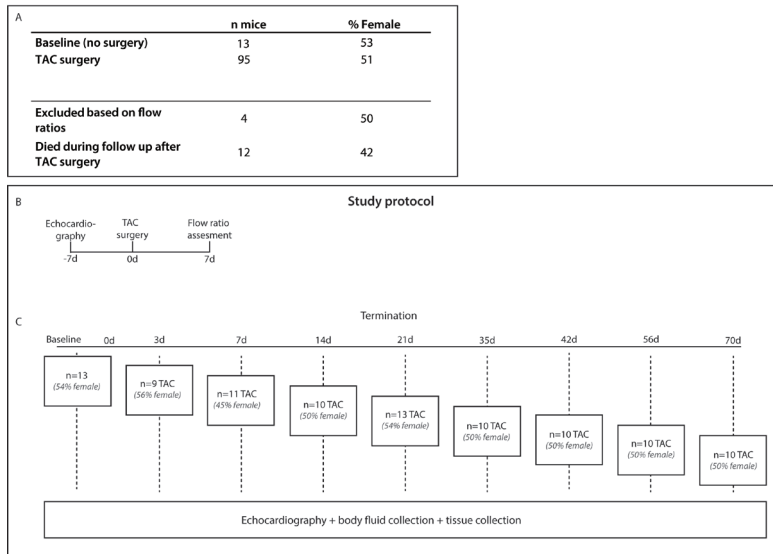
This study was supported by the Netherlands Cardiovascular Research Initiative: An initiative with support of the Dutch Heart Foundation [CVON2014-11 RECONNECT].

References

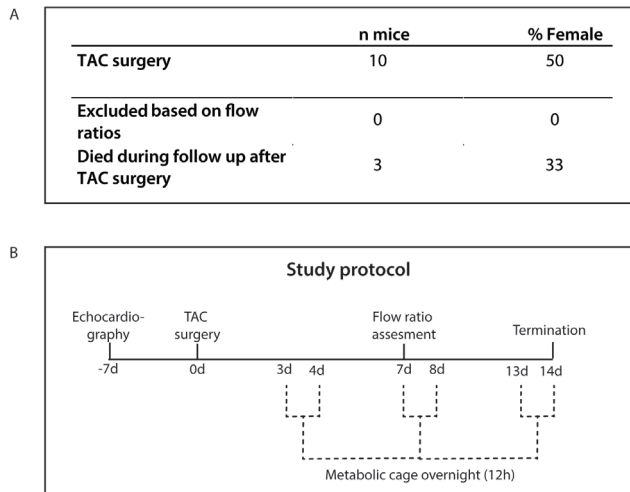
1. Zannad, F. & Rossignol, P. Cardiorenal Syndrome Revisited. *Circulation* **138**, 929–944 (2018).
2. Rangaswami, J. et al. Cardiorenal Syndrome: Classification, Pathophysiology, Diagnosis, and Treatment Strategies: A Scientific Statement From the American Heart Association. *Circulation* **139**, 840–878 (2019).
3. Schefold, J. C., Filippatos, G., Hasenfuss, G., Anker, S. D. & Von Haehling, S. Heart failure and kidney dysfunction: Epidemiology, mechanisms and management. *Nat. Rev. Nephrol.* **12**, 610–623 (2016).
4. van Deursen, V. M. et al. Co-morbidities in patients with heart failure: an analysis of the European Heart Failure Pilot Survey. *Eur. J. Heart Fail.* **16**, 103–111 (2014).
5. Hillege, H. L. et al. Renal function as a predictor of outcome in a broad spectrum of patients with heart failure. *Circulation* **113**, 671–678 (2006).
6. Gross, D. *Animal Models in Cardiovascular Research*. (Springer, 2019).
7. Furihata, T. et al. The experimental model of transition from compensated cardiac hypertrophy to failure created by transverse aortic constriction in mice. *IJC Hear. Vasc.* **11**, 24–28 (2016).
8. Hampton, C. et al. Early echocardiographic predictors of outcomes in the mouse transverse aortic constriction heart failure model. *J. Pharmacol. Toxicol. Methods* **84**, 93–101 (2017).
9. Krebs, C. et al. Antihypertensive therapy upregulates renin and (pro)renin receptor in the clipped kidney of Goldblatt hypertensive rats. *Kidney Int.* **72**, 725–730 (2007).
10. Li, Z. et al. Hydrogen Sulfide Attenuates Renin Angiotensin and Aldosterone Pathological Signaling to Preserve Kidney Function and Improve Exercise Tolerance in Heart Failure. *JACC. Basic to Transl. Sci.* **3**, 796–809 (2018).
11. Rockman, H. A., Wachhorst, S. P., Mao, L. & Ross, J. ANG II receptor blockade prevents ventricular hypertrophy and ANF gene expression with pressure overload in mice. *Am. J. Physiol. - Hear. Circ. Physiol.* **266**, 35–36 (1994).
12. Kamal, F. A. et al. G Protein-Coupled Receptor-G-Protein $\beta\gamma$ -Subunit Signaling Mediates Renal Dysfunction and Fibrosis in Heart Failure. *J. Am. Soc. Nephrol.* **28**, 197–208 (2017).
13. Richards, D. A. et al. Distinct Phenotypes Induced by Three Degrees of Transverse Aortic Constriction in Mice. *Sci. Rep.* **9**, 5844 (2019).
14. Zhao, Y. et al. Wnt/ β -catenin signaling mediates both heart and kidney injury in type 2 cardiorenal syndrome. *Kidney Int.* **95**, 815–829 (2019).
15. Tan, W. S. et al. Modeling heart failure risk in diabetes and kidney disease: limitations and potential applications of transverse aortic constriction in high-fat-fed mice. *Am. J. Physiol. Regul. Integr. Comp. Physiol.* **314**, 858–869 (2018).
16. Cheng, J. et al. Temporal analysis of signaling pathways activated in a murine model of two-kidney, one-clip hypertension. *Am. J. Physiol. Physiol.* **297**, 1055–1068 (2009).
17. Han, S. W. & Ryu, K. H. Renal dysfunction in acute heart failure. *Korean Circ. J.* **41**, 565–74 (2011).
18. ter Maaten, J. M. et al. Connecting heart failure with preserved ejection fraction and renal dysfunction: the role of endothelial dysfunction and inflammation. *Eur. J. Heart Fail.* **18**, 588–598 (2016).
19. De Haan, J. J. et al. Complement 5a Receptor deficiency does not influence adverse cardiac remodeling after pressure-overload in mice. *Sci. Rep.* **7**, 17045 (2017).
20. Sert, N. P. du et al. The ARRIVE guidelines 2019: updated guidelines for reporting animal research. *bioRxiv* **703181**, (2019).
21. Rudomanova, V. & Blaxall, B. C. Targeting GPCR-G $\beta\gamma$ -GRK2 signaling as a novel strategy for treating cardiorenal pathologies. *Biochim. Biophys. Acta. Mol. basis Dis.* **1863**, 1883–1892 (2017).
22. Zhao, Y. et al. Wnt/ β -catenin signaling mediates both heart and kidney injury in type 2 cardiorenal syndrome. *Kidney Int.* **95**, 815–829 (2019).
23. Schrotten, N. F. & Gaillard, C. A. J. M. New roles for renin and prorenin in heart failure and cardiorenal crosstalk. *Heart Fail. Rev.* **17**, 191–201 (2012).
24. Passier, R. C. J. J., Smits, J. F. M., Verluyten, M. J. A. & Daemen, M. J. A. P. Expression and localization of renin and angiotensinogen in rat heart after myocardial infarction. *Am. J. Physiol.* **271**, 40–43 (1996).
25. Chinnakkannu, P. et al. Suppression of angiotensin II-induced pathological changes in heart and kidney by the caveolin-1 scaffolding domain peptide. *PLoS One* **13**, e0207844 (2018).
26. Wright, J. W., Mizutani, S. & Harding, J. W. Pathways involved in the transition from hypertension to hypertrophy to heart failure. Treatment strategies. *Heart Fail. Rev.* **13**, 367–75 (2008).
27. Wang, X. et al. The effects of different angiotensin II type 1 receptor blockers on the regulation of the ACE-AngII-AT1 and ACE2-Ang(1–7)-Mas axes in pressure overload-induced cardiac remodeling in male mice. *J. Mol. Cell. Cardiol.* **97**, 180–190 (2016).
28. Patel, K. K. et al. Characteristics and Outcomes of Patients With Aortic Stenosis and Chronic Kidney Disease. *J. Am. Heart Assoc.* **8**, (2019).

29. Zaleska-Kociecka, M., Dabrowski, M. & Stepinska, J. Acute kidney injury after transcatheter aortic valve replacement in the elderly: Outcomes and risk management. *Clin. Interv. Aging* **14**, 195–201 (2019).
30. Kumar, V. & Seth, A. Transcatheter aortic valve replacement: Protect the kidneys to protect the patient. *Catheter. Cardiovasc. Interv.* **93**, 749–750 (2019).
31. Harada, M., Miyashita, Y., Ichikawa, T. & Kobayashi, M. A Case of Rapid Progressive Kidney Dysfunction with Severely Calcified Stenotic Aorta. *Case Reports Nephrol. Dial.* **8**, 253–260 (2018).
32. Hewitson, T. D., Holt, S. G. & Smith, E. R. Animal Models to Study Links between Cardiovascular Disease and Renal Failure and Their Relevance to Human Pathology. *Front. Immunol.* **6**, 465 (2015).
33. Gnanaraj, J. & Radhakrishnan, J. Cardio-renal syndrome. *F1000Research* **5**, 1–10 (2016).
34. Liu, S. Heart-kidney interactions: mechanistic insights from animal models. *Am. J. Physiol. Renal Physiol.* **316**, 974–985 (2019).
35. Szymanski, M. K., de Boer, R. A., Navis, G. J., van Gilst, W. H. & Hillege, H. L. Animal models of cardiorenal syndrome: a review. *Heart Fail. Rev.* **17**, 411–20 (2012).
36. Verhulst, A., Neven, E. & D’Haese, P. C. Characterization of an Animal Model to Study Risk Factors and New Therapies for the Cardiorenal Syndrome, a Major Health Issue in Our Aging Population. *Cardiorenal Med.* **7**, 234–244 (2017).
37. Liu, S. et al. Subtotal nephrectomy accelerates pathological cardiac remodeling post-myocardial infarction: implications for cardiorenal syndrome. *Int. J. Cardiol.* **168**, 1866–80 (2013).
38. Chua, S. et al. The cardioprotective effect of melatonin and exendin-4 treatment in a rat model of cardiorenal syndrome. *J. Pineal Res.* **61**, 438–456 (2016).

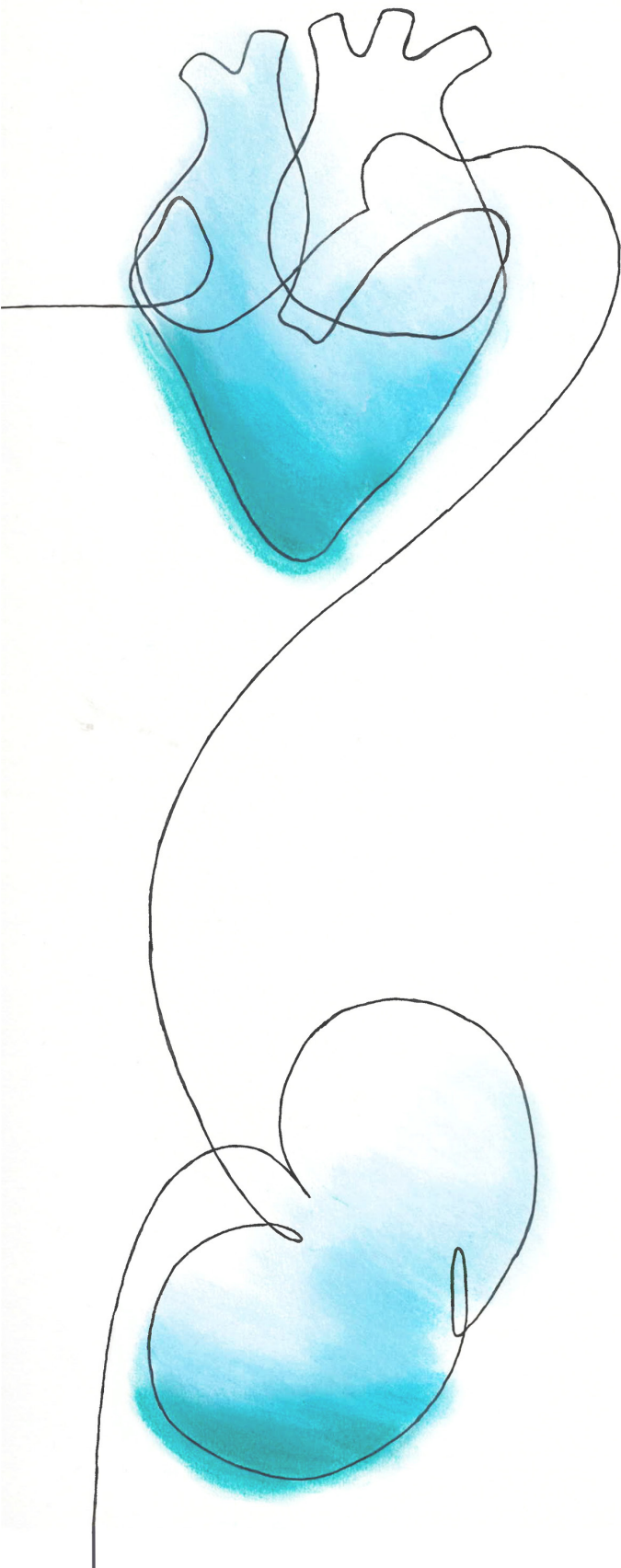
Supplemental



Supplemental figure 1. Study protocol TAC mice. A) number of mice included as control (no surgery) and TAC surgery. In addition, the number of mice that were excluded based on the carotid doppler flow measurements, no TAC present and the number of mice that are lost during follow up as direct consequence of surgery. No mice were lost during later stages of the experiments. B) Start of the experiments. C) termination protocol.



Supplemental figure 2. Study protocol TAC mice on metabolic cages. A) number of mice included for TAC surgery. In addition, the number of mice that were excluded based on the carotid doppler flow measurements, failed TAC, or lost during follow up as direct consequence of surgery. B) The study protocol showing when the mice were in metabolic cages overnight.



5

Sex-specific cardiac remodeling in mice undergoing transverse aortic constriction

In preparation

M. Wesseling^{1,2,5}, M. Hulsbos¹, M. A.D. Brans¹, R.J.G. Hartman¹, P. van de Kraak¹, H.M. den Ruijter¹, G. Pasterkamp², M.J. Goumans⁵, S.C.A. de Jager^{1,6*}

¹Laboratory for Experimental Cardiology, University Medical Center Utrecht, Utrecht, the Netherlands

²Laboratory for Clinical Chemistry and Haematology, University Medical Center Utrecht, Utrecht, the Netherlands

³Pathology and medical biology, University Medical Center Groningen, Groningen, the Netherlands

⁴Nephrology, University Medical Center Utrecht, Utrecht, the Netherlands

⁵Cell and Chemical Biology, Leiden University Medical Center Leiden, the Netherlands

⁶Laboratory for Translational Immunology, University Medical Center Utrecht, Utrecht, the Netherlands

Abstract

In heart failure, men more often present with heart failure with reduced ejection fraction whereas diastolic heart failure with preserved ejection fraction is more prevalent in women. The mechanisms underlying these sex differences in the pathophysiology of heart failure remain poorly understood. We studied sex differences in cardiac remodeling, using the murine transverse aortic constriction (TAC) model.

Male (n=56) and female mice (n=57) were studied up till 70 days post-TAC. Echocardiography was performed at termination to evaluate differences in cardiac function, and immunohistochemistry used to assess structural differences, i.e. fibrosis and cardiomyocyte hypertrophy. Plasma was drawn at termination where after Olink proteomics were performed to measure circulating plasma proteins between the male and female mice.

We observed both functional and structural differences between the two sexes upon the same degree of pressure overload. In male mice, characteristics of progressive eccentric remodeling were observed, whereas female mice showed more concentric remodeling. Cardiomyocyte hypertrophy was present in both sexes without any differences. Masson's trichrome staining of cardiac tissue confirmed a correlation between fibrosis and deteriorating cardiac function in both males and females. However, when assessing regional fibrosis of the left ventricle, perivascular fibrosis was more pronounced in female compared to male mice, while interstitial fibrosis was not different between the sexes. Furthermore, increased expression of circulating inflammatory related proteins, such as interleukin (IL)-1 β

and C-C Motif Chemokine Ligand 2 (CCL2) was observed in plasma over time both in males and females. Pathway analysis, revealed that vascular dysfunction, including endothelial to mesenchymal transition (EndMT), was specifically upregulated in female mice. These data underscore the importance to stratify mouse data by sex in the TAC model. Future research will focus on elucidating the key processes underlying the differences in eccentric and concentric cardiac remodeling between the sexes.

Introduction

Currently, at least 37.7 million people worldwide suffer from heart failure^{1,2}. The risk to develop heart failure is estimated to further elevate as the incidence of comorbidities, like kidney failure, hypertension and diabetes are expected to increase in the aging population³⁻⁵. The clinical guidelines separate heart failure patients on left ventricular ejection fraction (LVEF)⁶, being heart failure with preserved ejection fraction (HFpEF, LVEF $\geq 50\%$) or heart failure with reduced ejection fraction (HFrEF, LVEF $\leq 40\%$)⁶. The cumulative incidence of heart failure is roughly similar between men and women, however HFrEF is mostly observed in man whereas women more often present HFpEF^{3,7-9}. HFpEF is hallmarked by diastolic dysfunction, valvular pathology and comorbidities such as hypertension and aging^{7,9,10}. However, since women are often underrepresented in clinical studies and sex-stratified data is scarce, sex differences in the progression and onset of chronic heart failure might still be unknown nowadays^{11,12}.

Myocardial remodeling following cardiac volume or pressure overload, leads to alterations in cardiac architecture, caused by increased collagen synthesis and fibrotic tissue formation, resulting in decreased cardiac function^{11,13}. Cardiac remodeling can be classified either in eccentric or concentric hypertrophy, both initiated to preserve ejection fraction (EF). Eccentric remodeling is characterized by progressive dilation of the left ventricle (LV) and loss of cardiac mass, associated with an increase in apoptosis and more cardiomyocyte hypertrophy^{11,14}. Furthermore, eccentric remodeling is more prevalent among men with an initial preservation of the stroke volume^{11,14}. Concentric remodeling is characterized by an increase in wall thickness thereby compromising cavity size¹¹. Recently, studies on sex differences in aortic stenosis patients have revealed the presence of more diffuse and focal myocardial fibrosis in females compared to males, resulting in LV stiffening and reduced cardiac function^{13,15,16}. In the murine TAC model, representing chronic non ischemic heart failure, a ligation is placed around the aortic arch between the left and right common carotid artery thereby decreasing the arterial lumen and inducing cardiac pressure overload¹⁷. The model is characterized by low grade inflammation, left ventricular hypertrophy and a gradual increase of fibrosis, resulting in a reduced cardiac function¹⁷.

In the current study, we compare cardiac remodeling at numerous time points, ranging from 3 to 70 days after TAC, to assess differences in the progression towards heart failure in male and female mice. We hypothesize that sex-specific pathophysiological processes are induced in mice resulting in distinct phenotypes of cardiac remodeling between the two sexes.

Methods

Animals

Male and female C57BL/6J mice (age 9-12 weeks old, weight 20-30 gram) were obtained from the Jackson laboratory¹⁸ and bred in our breeding facility. All mice received standard chow and water ad libitum and were housed under standard conditions using a filter top cage with 12h light/dark cycle. In a 16 month period, all mice were randomly assigned to experimental groups of transverse aortic constriction (TAC) surgery and survival times (3-70 days) as described previously¹⁹. The primary outcome variable is the reduced cardiac function as seen by an increased end systolic volume (ESV) and end diastolic volume (EDV). With a sample size calculation based on the primary outcome variables, a minimal of 5 male and female mice were included per group, with a total of 108 mice, consisting of 13 baseline (no surgery) and 95 TAC mice. A flowchart showing animals used per experimental group, mice excluded or lost during follow up post-TAC is provided in supplemental figure 1. No mice were excluded based on previously established human endpoints, which included a weight loss of >10% over the experimental time period, visual indications of pain and stress like pulled back ears or any condition interfering with daily activities (e.g. eating or drinking). All animal experiments were approved by the Animal Experiments Committee of the University Medical Center Utrecht (Utrecht, the Netherlands) and performed conform to the 'Guide for the care and use of Laboratory Animals'. All surgeries, data acquisitions and analysis are performed in a blinded fashion.

Transverse aortic constriction (TAC)

An experienced surgeon performed the TAC procedure in a dedicated mouse operation room. Mice were anesthetized by intraperitoneal (i.p.) injection of medetomidine hydrochloride (1.0 g/kg body weight), midazolam (Dormicum®, Roche, 10.0 mg/kg) and fentanyl (Janssen-Cilag, 0.1 mg/kg). Mice were intubated and ventilated on a rodent ventilator (minivent, Hugo Sachs Electronics, Germany) with a 1:1 oxygen-air ratio (175 strokes/minute, 250 µl stroke volume). With a minimal invasive incision between the upper left sternal border in the second intercostal space, a ligature was placed around the aorta between the right and left common carotid arteries. The ligation was placed with a 7-0 silk suture around a blunt 27-gauge needle which was subsequently removed.

Echocardiography

At baseline, day 7 and at termination, mice underwent echocardiography under the inhalation of anesthesia (2% isoflurane) in a mixture of 1:1 oxygen/air. To assess cardiac function by structural and functional parameters we used the Vevo 2100 System with a 22-35 MHz transducer (MS550D) (VisualSonics Inc., Toronto, Canada), for transthoracic 3D-echocardiography. Doppler flow measurements in the carotid arteries, was performed to confirm correct placement of the ligation, at day 7 echocardiography. A total of 6 mice (3 male and 3 female) were excluded based on a flow ratio ≤ 5 between the left and right

carotid artery. Three-dimensional images were obtained on the short and long axis of the heart at multiple levels in both end systole and end diastole with use of respiratory triggering, at baseline and termination. For further analyses on cardiac flow and volumes we used the Vevo® 2100 software (Fujifilm VisualSonics Inc., Toronto, Canada). In addition to flow and volumes we used speckle-tracking analysis software to assess the global longitudinal strain (Vevo Strain, Fujifilm VisualSonics Inc., Toronto, Canada).

Tissue and sample collection

Mice were sacrificed either at baseline, or 3, 7, 14, 21, 28, 35, 42, 56, 70 days after TAC (Supplemental figure 1c) by exsanguination after i.p. administration of an overdose Pentobarbital (60 g/kg). Via orbital puncture, blood was collected in an EDTA coated tube for plasma collection. The vascular system was flushed with 5 ml phosphate-buffered saline (PBS) via right ventricular puncture. After heart and left tibia collection, the heart weight and tibia length were assessed. The heart was longitudinal cut in half, where after one half of the heart was fixed in 4% paraformaldehyde for 24h, and subsequently embedded in paraffin for histological analysis. The other half, was again longitudinal cut in two parts and both snap-frozen in liquid nitrogen for further analysis. All blood and tissue samples were stored at -80 until further analysis.

Histology

Paraffin embedded hearts were cut in 3 µm thick sections. Before staining, the sections are deparaffinized (2x 10 minutes in Ultraclear (1466, Sakura), 2x 5 minutes in 100% EtOH, (4099.9005 Klinipath), 2x 5 minutes in 96% EtOH (Klinipath), 2x 5 minutes in 70% EtOH (Klinipath), 5 minutes in Demi H₂O). To observe the general morphology of the cardiac tissue, an H&E staining was performed. Slides were stained with Hematoxyline (4085.9002, Klinipath) for 5 minutes and with Eosin (341973R, Eosin) for 2 minutes. To assess cardiac hypertrophy, antigen retrieval was performed by 20 minutes boiling in citrate buffer (sodium citrate tribasic dehydrate, 6132-04-3, Sigma-Aldrich) followed by staining with Wheat Germ Agglutinin (WGA-FITC 1:40, L4895, Sigma Aldrich) for 30 minutes at room temperature (RT) staining to assess cell size. Nuclei were stained with Hoechst (1:10.000, 33342(H1399), Thermo Scientific). Collagen was stained with Masson's Trichrome (HT15-1KT, Sigma Aldrich), according to the manufacturers protocol. For analysis, tissue slides were scanned with a 20x objective on a microscope (Olympus BX53) and analyzed with cellSence imaging software (Olympus Life Science Solutions, Hamburg, Germany). Except the WGA staining which was analyzed with Image J (version 1.47, National Institute of Health, USA). The number analyzed for each staining is provided in the representative figure legend.

Olink proteomics

The Mouse Exploratory panel of the Olink Multiplex platform (Olink Proteomics AB, Uppsala, Sweden) was used within Arcadia (Utrecht, the Netherlands) for analysis of high-abundance proteins in plasma samples. Both male and female plasma samples of

0, 7, 35- and 70-days post-TAC were used in this analysis. Gene ontology enrichment analysis on the Olink data was performed and visualized using clusterProfiler (v3.10.0)²⁰ in R(v3.5.1).

Statistical analysis

For statistical analysis, we used one-way ANOVA followed by Dunnett's multiple comparisons test (all TAC groups were compared to the baseline group) performed with GraphPad (Prism 8.0.1 for Windows, GraphPad Software, San Diego, CA). Data is shown as mean±SD. $p < 0.05$ was considered significant.

Results

Baseline characteristics of male and female mice

56 male and 57 female mice between 9 and 11 weeks of age were included for comparative analysis on cardiac remodeling after induced pressure overloaded heart failure. At baseline, male mice were heavier compared to female mice (male 26.9 ± 1.9 grams vs female 21.6 ± 1.3 grams, $p=0.01$, Supplemental figure 2a). However, for both male and female mice, the increase in total body weight over the experimental time was similar ($p > 0.999$) (Supplemental figure 2c). Tibia length, indicative of body size, was larger in male mice compared to female mice at baseline (female 17.62 ± 0.04 mg/mm vs male 17.88 ± 0.08 mg/mm, $p < 0.001$) (Supplemental figure 2b). The heart weight/tibia length (HW/TL) did not differ between male and female mice at baseline ($p=0.163$), indicating that hearts of male mice were bigger compared to female hearts, suggesting a possible difference in the left ventricular volume. However, at baseline, the end diastolic volume (EDV) and end systolic volume (ESV) were not different between the sexes (ESV $p > 0.999$, EDV $p=0.7452$) (Figure 1c and 1f). Accordingly, at baseline the global longitudinal strain (GLS) and ejection fraction (EF) showed no differences between male and female mice (Figure 1i and Table 2).

Cardiac dysfunction over time post-TAC

To induce chronic heart failure, an aortic ligation is placed to induce pressure overload in the left ventricle. At 7 days, the right and left carotid flow is measured to determine a flow ratio representative of the aortic constriction size. No difference was observed in flow ratio between sexes (male 12.8 ± 7.9 vs female 11.8 ± 6.6 , $p=0.57$, Supplemental figure 2d), suggesting both male and female mice experience the same degree of aortic constriction and pressure overload. To study cardiac function over time, we assessed the ESV, EDV and GLS in baseline and post-TAC mice (Figure 1). Overall, ESV (Figure 1a-c) and EDV (Figure 1d-f) increased over time for both male and female mice. In males, an increase in ESV was observed already at day 3 ($46.26 \text{ ul} \pm 10.92$ compared to baseline $17.39 \text{ ul} \pm 4.91$, $p < 0.01$), followed by a fluctuating, though progressive increase over time post-TAC (Figure 1a + Table 1a). After 70 days, males display a severe increased

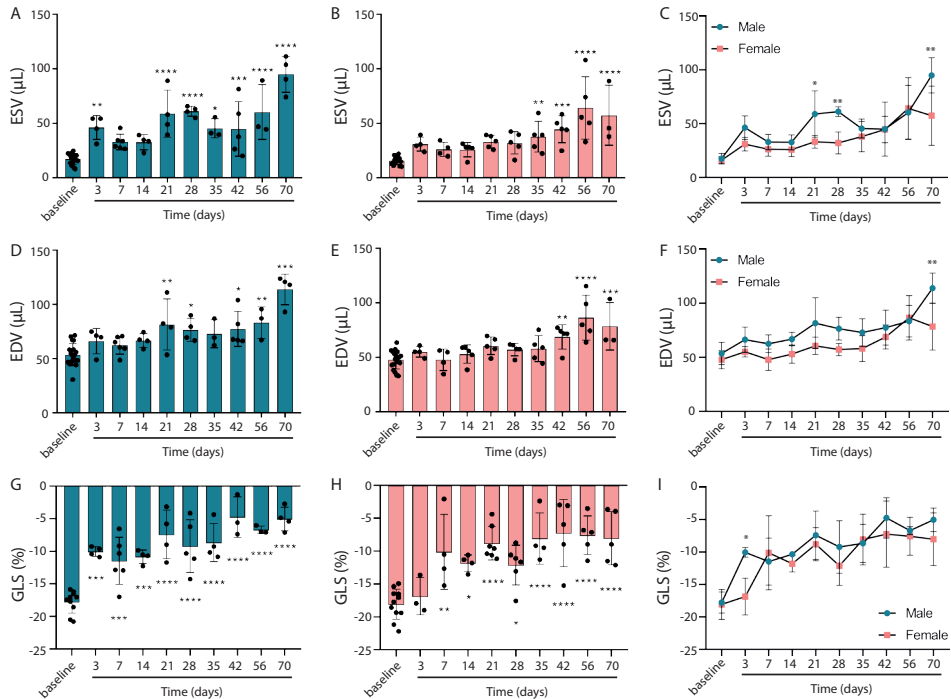


Figure 1. Reduced cardiac function after induction of pressure overload in male and female mice.

An increase in ESV and EDV over time post-TAC is indicative of a worse cardiac function in both males and females. a) In males, a progressive though fluctuating increase in end systolic volumes is present. b) In females this increase in volume is less progressive and is only significantly present after several days post-TAC (35 days-70 days). c) male and female increase over time, shows slight differences in progression. In both, male (d) and female (e) mice, there is only slightly increased EDV over time. f) only at 70 days a difference in EDV is observed between males and females. g) The progressive increased strain in males starts at day 3. h) Similar results are present for the female mice, although they have a more preserved strain in the first days compared to males (i). ESV; end systolic volume, EDV; end diastolic volume, GLS; global longitudinal strain. Mean±SD (*= $p>0.05$, **= $p>0.01$, ***= $p>0.001$, ****= $p>0.0001$)

ESV ($95 \text{ ul} \pm 16.4$ compared to baseline $17 \text{ ul} \pm 4.9$, $p<0.001$), which is less sustained in females ($57 \text{ ul} \pm 27.5$ compared to baseline $16 \text{ ul} \pm 3.5$, $p<0.001$) (Figure 1a and b + Table 1a and b). In both male and female mice, the EDV gradually increases over time, however less extensive than the ESV (Figure 1d and e). After 70 days, the EDV in males more than doubled (114 ± 14.0 compared to baseline 54 ± 10.3 , $p<0.001$), whereas females exhibit a 60% increase in EDV (79 ± 21.8 compared to baseline 48 ± 8.4 , $p<0.001$) (Table 1a and b). The calculated EF post-TAC was significantly decreased in both males (70 days 17 ± 8.4 compared to baseline 68 ± 7.5 , $p<0.001$) and females (70 days 29 ± 14.3 compared to baseline 66 ± 8.2 , $p<0.001$) (Table 1a and b). When comparing the EDV, ESV and EF of male and female mice at the different time points, male and female mice showed a similar cardiac function (Figure 1c, f and i). Interestingly, after 70 days, both EDV and ESV were significantly reduced in females, compared to males (EDV $p<0.01$, ESV $p<0.01$).

Table 1. Echo parameters at baseline and post-TAC in males and females.

A									
Time (days)	n	ESV (ul)		EDV (ul)		EF (%)		GLS (%)	
		mean (sd)	adjusted p value	mean (sd)	adjusted p value	mean (sd)	adjusted p value	mean (sd)	adjusted p value
Base-line	15	17.39 (4.91)	-	53.59 (10.34)	-	67.54 (7.54)	-	-17.79 (1.63)	-
3	4	46.26 (10.92)	0.0013	66.27 (11.70)	0.448	30.74 (6.01)	<0.0001	-10.04 (0.74)	0.0002
7	6	32.89 (7.12)	0.0971	62.47 (8.16)	0.6867	47.25 (8.85)	0.0001	-11.47 (3.63)	0.0004
14	4	32.65 (6.90)	0.2447	66.85 (6.32)	0.3906	47.65 (6.12)	0.0134	-10.35 (0.44)	0.0007
21	4	58.93 (21.48)	<0.0001	81.58 (23.47)	0.0016	28.45 (7.51)	<0.0001	-7.41 (3.73)	<0.0001
28	4	61.14 (4.51)	<0.0001	76.48 (10.54)	0.0147	19.22 (9.63)	<0.0001	-9.22 (4.04)	<0.0001
35	4	45.50 (8.80)	0.0074	72.91 (12.78)	0.1284	37.60 (4.57)	<0.0001	-8.66 (2.94)	<0.0001
42	5	44.95 (25.13)	0.0007	77.46 (16.20)	0.0037	31.01 (10.97)	<0.0001	-4.75 (3.12)	<0.0001
56	3	60.33 (25.18)	<0.0001	83.41 (14.55)	0.0033	28.83 (20.17)	<0.0001	-6.70 (0.60)	<0.0001
70	4	94.98 (16.39)	<0.0001	113.95 (14.03)	<0.0001	16.80 (8.36)	<0.0001	-5.03 (1.81)	<0.0001

B									
Time (days)	n	ESV (ul)		EDV (ul)		EF (%)		GLS (%)	
		mean (sd)	adjusted p value	mean (sd)	adjusted p value	mean (sd)	adjusted p value	mean (sd)	adjusted p value
Base-line	15	15.97 (3.46)	-	47.75 (8.44)	-	65.99 (8.24)	-	-18.07 (2.32)	-
3	7	30.90 (6.37)	0.2193	55.06 (4.80)	0.8774	43.93 (10.45)	0.0022	-16.86 (2.84)	0.9975
7	10	26.19 (6.46)	0.6757	47.77 (9.96)	1.0000	46.81 (8.81)	0.0103	-10.11 (5.71)	0.002
14	9	25.85 (6.58)	0.6101	52.96 (8.43)	0.9687	49.01 (5.77)	0.0312	-11.81 (1.25)	0.0236
21	11	33.13 (5.88)	0.0579	60.58 (8.05)	0.1812	45.53 (3.69)	0.0018	-8.79 (2.54)	<0.0001
28	11	23.03 (10.23)	0.0904	57.15 (5.68)	0.5459	44.97 (13.56)	0.0013	-12.12 (3.03)	0.0104
35	8	37.89 (14.05)	0.0066	58.05 (11.93)	0.4287	36.44 (10.57)	<0.0001	-8.08 (3.92)	<0.0001
42	10	44.55 (12.33)	0.0002	68.79 (11.12)	0.0033	35.99 (11.96)	<0.0001	-7.23 (5.10)	<0.0001
56	8	64.24 (28.54)	<0.0001	86.51 (20.51)	<0.0001	28.49 (15.14)	<0.0001	-7.57 (2.93)	<0.0001
70	9	57.38 (27.54)	<0.0001	78.50 (21.75)	0.0004	29.32 (14.29)	<0.0001	-8.032 (4.06)	<0.0001

The mean echo parameters for each time point post-TAC in males (a) and female (b) mice. ESV; end systolic volume, EDV; end diastolic volume, EF; ejection fraction, GLS; Global longitudinal strain. Mean±SD are presented. P-value ≤0.05 is considered significant.

Overall, these results demonstrate a similar reduced cardiac function in mice, although at early phases post-TAC cardiac dysfunction in males seem to be more severe when compared to females.

The analysis of the GLS to determine cardiac wall deformation induced by ventricular pressure changes, showed a deteriorated GLS in both male and female mice post-TAC. The progression of deteriorated GLS appeared slightly different between males and females. Compared to baseline, males show an severely affected GLS starting at day 3 (-17.79 ± 1.63 vs baseline -10.04 ± 0.74 , $p < 0.001$), where in females the GLS deteriorates mildly progressive starting at day 7 post-TAC (-18.07 ± 2.32 vs baseline 10.11 ± 5.71 , $p < 0.002$) (Figure 1g and h + Table 1a and b). After 70 days, both female mice ($-8.03\% \pm 4.06$ compared to baseline $-18.07\% \pm 2.32$, $p < 0.001$) and male mice ($-5.03\% \pm 1.81$ compared to baseline $-17.79\% \pm 1.63$ $p < 0.001$) show a severely reduced GLS (Table 1a and b). Comparing male and female mice at each individual time point shows only a significant difference after 3 days ($p = 0.046$, Figure 1i). Overall, the results show an increased cardiac wall deformation induced by pressure and thereby reduced systolic function in both males and females over time.

Adverse cardiac remodeling post-TAC

Cardiac remodeling is depicted by an increase in the heart weight/tibia length (HW/TL) ratio. After 70 days, a significant increased HW/TL ratio was observed in both male (18.36 ± 2.94 mg/mm compared to baseline 8.48 ± 0.74 mg/mm, $p < 0.001$) and female mice (15.17 ± 2.18 mg/mm compared to baseline 7.54 ± 0.59 mg/mm, $p < 0.001$) (Figure 2a and b, Table 2). Moreover, after 70 days the HW/TL ratio in males is almost similar to the one in females (18.36 ± 2.94 mg/mm vs 15.17 ± 2.18 mg/mm). Comparing male and female progression in HW/TL, no differences were observed (Figure 2c). Congruent with the functional echo data, the HW/TL increase appears more gradual in females than in males over time, which suggests a distinct type of cardiac remodeling (Figure 2a and b). In order to visualize the global structural cardiac remodeling, we performed hematoxylin and eosin (HE) staining. Interestingly, males showed eccentric cardiac remodeling over time, illustrated by enlargement of the left ventricular wall and an increase in left ventricular cavity size (Figure 2d). Female mice showed concentric remodeling up till 70 days, demonstrated by an increase in left ventricular wall thickness, but a similar overall heart size, which leads to reduced ventricular volumes reduced (Figure 2e). Combined, the HW/TL and HE indicate adverse cardiac remodeling in both male and female mice with indications of respectively concentric and eccentric remodeling.

Cardiac hypertrophy post-TAC

Both eccentric and concentric remodeling are associated with an increase in overall cardiac dimensions and cardiomyocyte hypertrophy is a known denominator of this increase in size. To assess if cardiac hypertrophy drives the phenotypic difference in cardiac remodeling between male and female mice post-TAC, a wheat germ agglutinin (WGA) staining to analyze cell size was performed (Figure 3a). At 70 days, a significant

increase in cardiomyocyte cell size in both males ($242 \pm 37 \mu\text{m}^2$ in at baseline and $424 \pm 77 \mu\text{m}^2$ at 70 days after TAC, $p < 0.001$) (Figure 3a, b and e) and females ($230 \pm 25 \mu\text{m}^2$ in at baseline and $354 \pm 33 \mu\text{m}^2$ at 70 days after TAC, $p < 0.001$) (Figure 3a, c and e) was observed. Interestingly, cardiomyocyte cell size measurements were not significantly different between male and female mice (Figure 3d), suggesting that the observed differences in eccentric and concentric cardiac remodeling is not due to distinct cardiomyocyte hypertrophy.

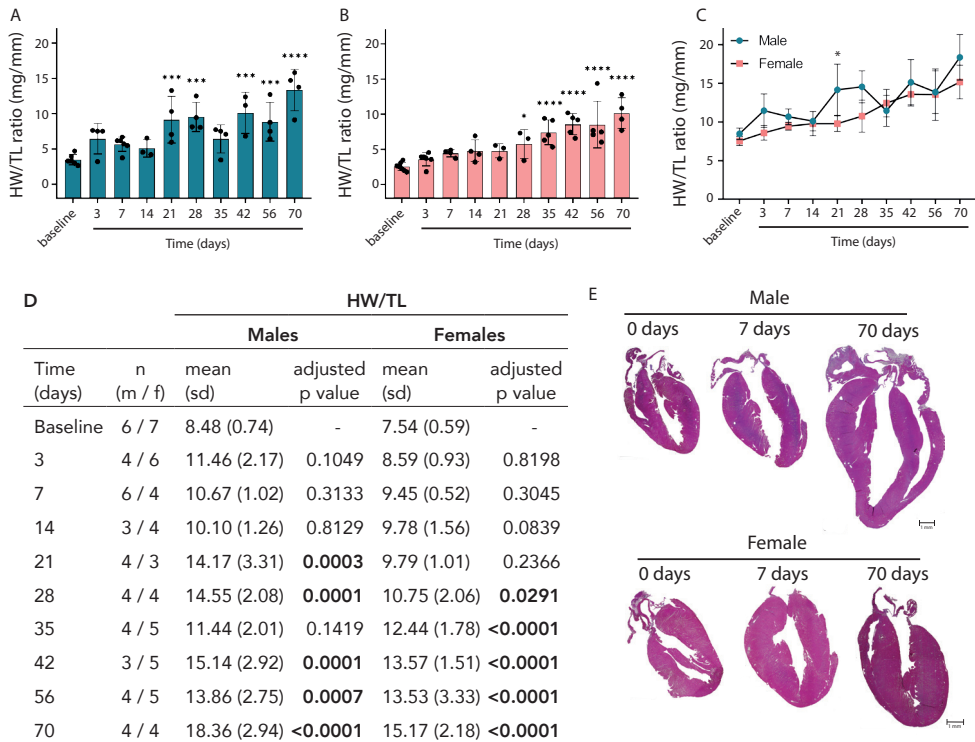


Figure 2. Adverse cardiac remodeling upon TAC differs between males and females.

a) Upon TAC, a progressive increase in Heart Weight/Tibia Length (HW/TL) in males is present. b) A more gradual but still progressive increase in HW/TL ratio in females. c) comparison of male and female progression in HW/TL over time. d) This table represents the mean \pm SD of the HW/TL ratio's at baseline and over time. e) Representative pictures of the HE staining for males and females show a difference in cardiac remodeling, eccentric in males and concentric in females over time. * $p > 0.05$, ** $p > 0.01$, *** $p > 0.001$, **** $p > 0.0001$. Mean \pm SD

Fibrosis

Cardiac fibrosis is an adverse effect of cardiac remodeling, affecting both compliance and stiffness of the left ventricle. To determine the localization and quantify the degree of cardiac fibrosis in both male and female mice, Masson's Trichrome staining was performed (Figure 4). Both interstitial and vascular fibrosis were assessed by quantitative

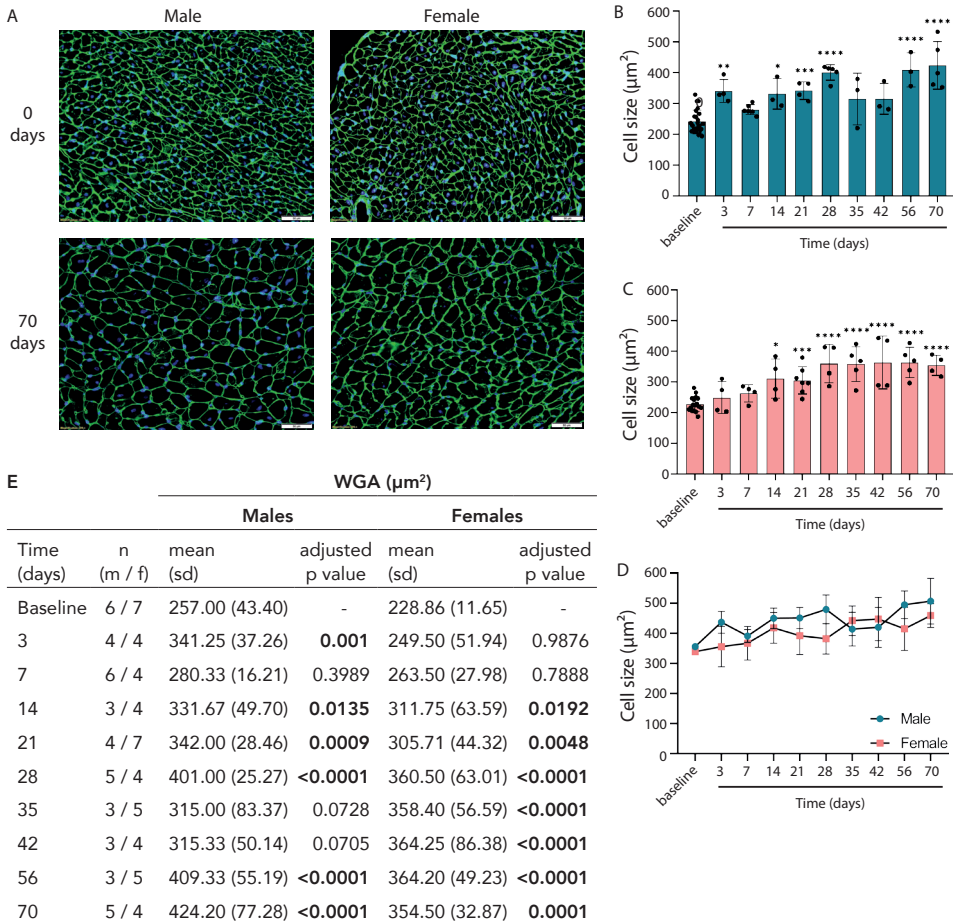
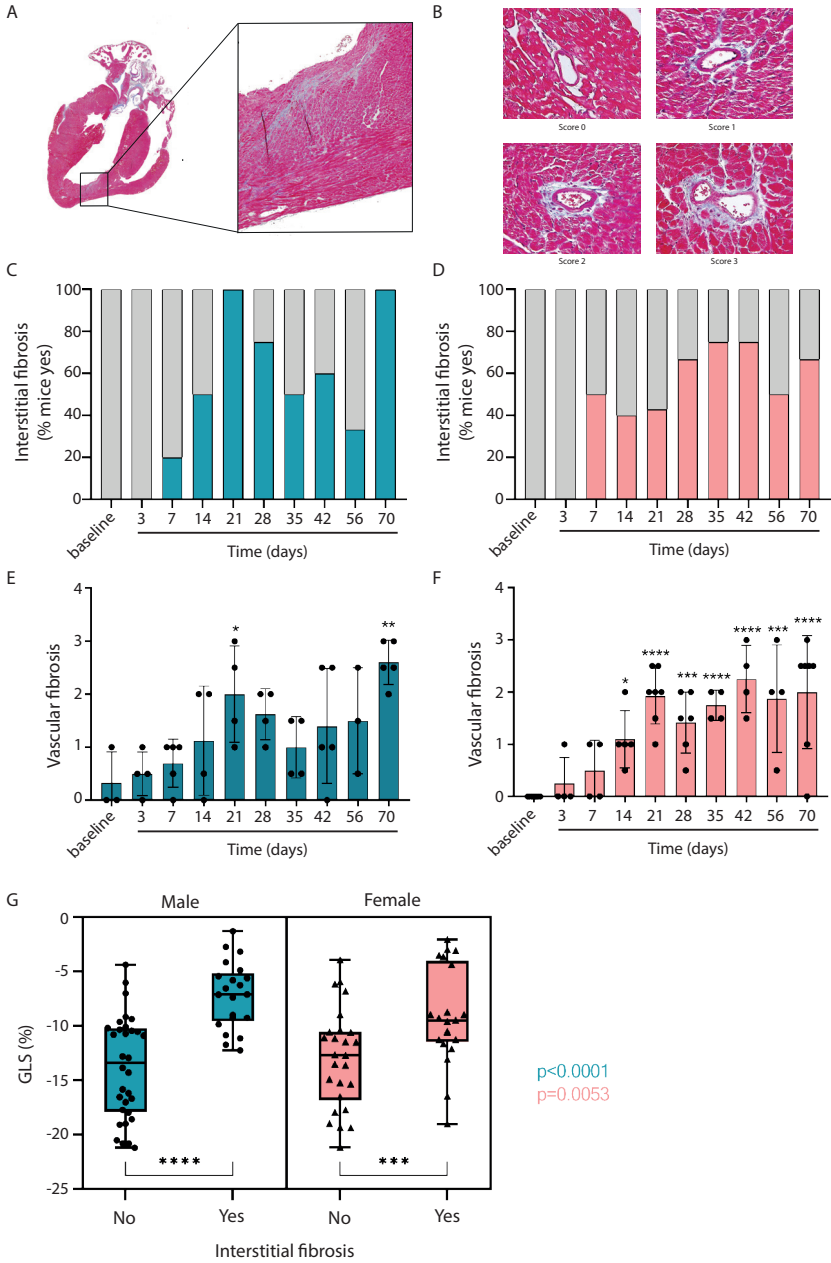


Figure 3. Cardiomyocyte hypertrophy is similar between sexes.

a) Representative images of the WGA staining which delimiting the cell membrane needed for calculation of the cell size. Quantification of the WGA staining shows an increase over time in cardiomyocyte cell size in both male (b) and female (c) mice, and no differences between male and female mice (d). e) All the n, mean and p values of the cardiomyocyte cell size are presented for both male and female mice over time. Mean \pm SD. *p>0.05, **p>0.01, ***p>0.001, ****p>0.0001.

scoring (Figure 4a and b). Interstitial fibrosis in both male and female mice was observed from day 7 post-TAC onwards (Figure 4c and d), but no sex differences in interstitial fibrosis could be observed over time. Both male and females showed a significant increase in vascular fibrosis starting at day 21 (Figure 4e and f). Although males show a large variation, females show a more profound non-progressive increase in vascular fibrosis from 21-70 days. Noteworthy, considering strain to be a good parameter for cardiac wall deformation induced by pressure, we plotted the strain against interstitial fibrosis which is a major determinant of cardiac wall stiffening (Figure 4g). Our results showed a



positive correlation between GLS and interstitial fibrosis in males ($p < 0.001$) and females ($p = 0.005$) (Figure 4g). Combined these results suggest that interstitial fibrosis does not the major cause for sex differences in concentric and eccentric remodeling, although, vascular fibrosis is more profoundly present in females compared to males. Therefore, we next decided to investigate alternative mechanisms potentially compromising vascular function specifically in female mice, which may enhance the risk of heart failure.

Olink biomarker panel analysis

Specific systemic factors (i.e., inflammatory cytokines) have been suggested to negatively affect vascular function²¹. In order to discover underlying pathophysiological processes in heart failure explaining the sex difference in eccentric and concentric remodeling, we performed an Olink biomarker analysis in peripheral blood. We measured the circulating protein levels of 92 well-known biomarkers, such as lipoprotein lipase (LpL), transforming growth factor (TGF)- β , Interleukin 6 (IL6) and Troponin. As such, Troponin levels were increased especially in males (Figure 5a), indicative of cardiac injury.

At baseline, the expression of several proteins, including Contactin 4 (CNTN4), Cadherin 6 (CDH6), Interleukin 1 (IL1)- α and S100 calcium binding protein A4 (S100-A4) were found different in males compared to females (Supplemental table 1). Using Gene Ontology to analyze biological processes with the proteins that were different at baseline, revealed increased protein levels in male mice associated with cardiac growth, including processes involving mesenchymal and cardiomyocytes growth (Figure 5d), while in contrast, females displayed an enrichment in protein levels related to endothelial function and responses to endotoxins (i.e. lipopolysaccharide) (Supplemental table 1, Figure 5d). Furthermore, levels of several proteins were increased over time post-TAC in both sexes, such as Interleukin 23 receptor (IL23r)(Figure 5b), Interleukin 1 β (IL1 β) and Rantes (CCL5). Interleukin 1 α (IL1 α) and Cysteine rich transmembrane BMP regulator (CRIM1), among others, were specifically increased in male mice, while Transforming growth factor β receptor 3 (TGF β 3) was increased in female mice (Figure 5c, Supplemental table 2).

Next we performed pathway analysis on the measured levels of circulating proteins post-TAC to identify differentially expressed pathways in male versus female mice (Figure 5e). With heart failure progression, both sexes show inflammatory activation linked to increased myeloid and leukocyte chemotaxis (Figure 5e). In male mice (with eccentric remodeling), the upregulated proteins are primarily associated to organismal homeostasis (Figure 5e) this includes pathways involved in water, iron, tissue, temperature and energy homeostasis. As cardiac remodeling involves molecular, cellular and interstitial changes, the activation of homeostasis related pathways would suggest compensatory mechanisms are activated to antagonize the dysregulation in cardiac tissue. On the other hand, the activation of homeostasis related pathways may also be the consequence of the systemic effects of heart failure. In female mice (with concentric remodeling), the increased protein levels are primarily associated to pathways related to endothelial to mesenchymal transition (EndMT) (Figure 5e). As postulated in HFpEF, concentric remodeling in woman is associated with an increase in vascular dysfunction²². These

results suggest that inflammation is a common denominator for heart failure progression in both male and female mice. While cardiac remodeling in males is mostly associated to efforts maintaining tissue homeostasis, females present with enhanced vascular dysfunction in concentric remodeling. Overall, the circulating protein levels in male and female mice differ at baseline and over time post-TAC. Pathway analysis has identified specific pathophysiological pathways activated in males with concentric remodeling and females with concentric remodeling. Future research should establish the contribution of these pathways to disease progression.

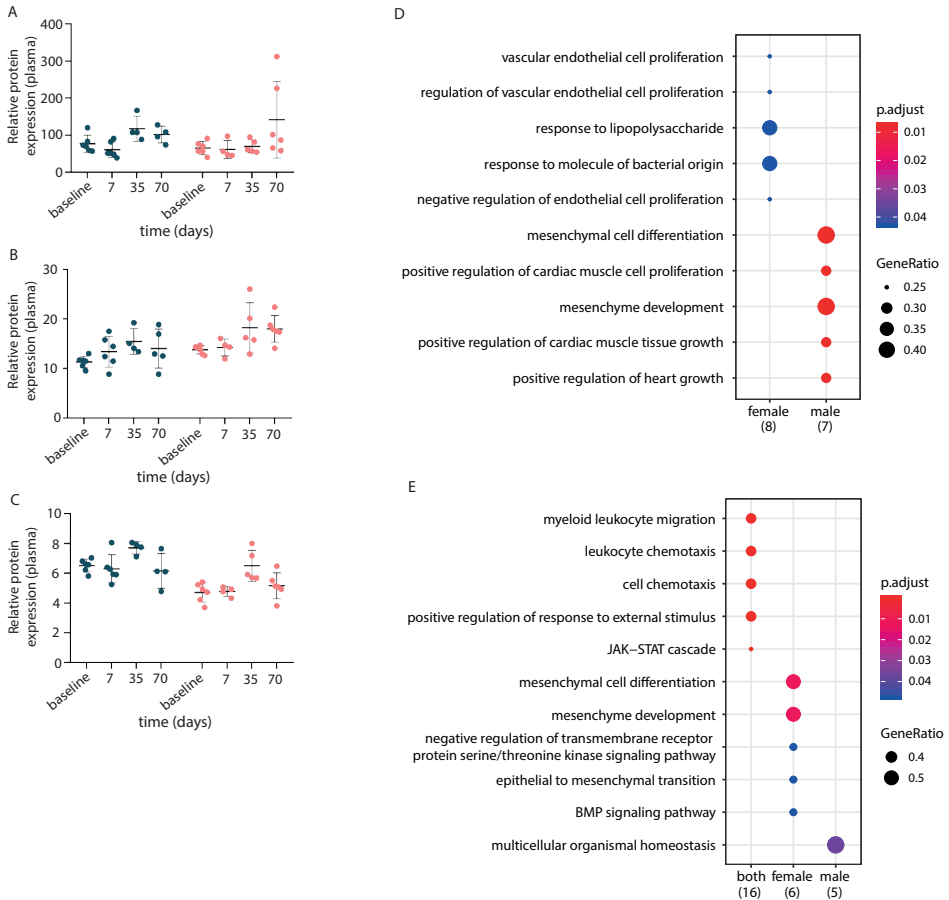


Figure 5. Sex specific pathways based on protein expression determined with Olink. a) Troponin levels are increased in males over time indicative of cardiac injury. b) Interleukin 23r expression increases over time for both males and females. c) The baseline levels of TGF-β receptor 3 are higher in males compared to females. A dot plot is shown for Gene Ontology enrichments at baseline (d) and over time post-TAC (e). The terms are present in the rows, the gene sets are allocated in the column. Color indicates significance, while the size of the dot indicates the ratio of the genes that are present from the entire set that is tested. The number indicates the number of genes used for the analysis. Mean±SD.

Discussion

Left ventricular hypertrophy and sex-specific cardiac remodeling are associated with adverse cardiovascular outcomes. Although sex differences are observed in cardiac remodeling^{23,24}, the underlying pathophysiological processes are largely unknown. Within this extensive longitudinal mice study, we assessed the effect of biological sex on cardiac remodeling and function upon pressure overload induced heart failure. Although cardiac function in both sexes was deteriorated, we found striking differences in cardiac remodeling phenotypes between the two sexes. While male mice primarily show eccentric remodeling, female mice display concentric remodeling upon pressure overload. We assessed cardiomyocyte hypertrophy and interstitial fibrosis as two major components of cardiac remodeling, but did not observe differences between male and female mice. However, female mice did show a more pronounced perivascular fibrosis upon heart failure progression. We used an exploration biomarker panel to support the identification of potential underlying pathophysiological mechanisms explaining the sex differences in perivascular fibrosis and cardiac remodeling. Interestingly, cardiac remodeling was associated with vascular dysfunction in female mice, while in male mice it is primarily associated to tissue homeostasis.

As expected, after TAC a reduced cardiac function is observed in both sexes. However, our results do suggest that female mice heart failure development is less progressive during early phases after the induction of pressure overload. This is in line with previous reports showing preservation of cardiac function in early heart failure of rat and murine pressure overload models in females compared to males^{25,26}. It has been suggested that, in female hearts subjected to metabolic pathways are more efficiently regulated than in male mice, thereby protecting them against early onset heart failure induced by pressure overload²⁶. Furthermore, an earlier induction of matrix production has been observed in male compared to female heart²⁶, in response to early heart failure induced by pressure overload. Despite this relative protection in early heart failure, this does not occur during the progressive stage of heart failure, as compensatory mechanisms to maintain cardiac function when changing towards maladaptive cardiac remodeling²⁶. Nonetheless, female rats with progressive heart failure, still have a better LV function due to preservation of the ventricular-arterial coupling²⁵. Accordingly, the risk of disease progression and worse outcome are higher in males compared to females with established heart failure²⁷. Combined, this may explain the differences in male and female early onset heart failure. However, cardiac remodeling is already in early post-TAC phases present in female mice, although they maintain a better cardiac function.

In addition to differences in cardiac function, we observed striking sex differences in cardiac remodeling. Males show eccentric remodeling while females show concentric remodeling upon pressure overload. This has been previously reported by other groups using different heart failure models^{25,28,29}. In spontaneous hypertensive rats, males showed a larger increase in cardiac geometry with an earlier induced reduction in cardiac function compared to females²⁸. In rats with ascending aortic stenosis induced pressure

overload, cardiac gene expression suggested that the contractile functional reserve was decreased in male animals²⁹. While these studies clearly implicate a difference between cardiac remodeling in male and female animals, we are the first to provide clear data on differences in eccentric vs concentric remodeling.

In cardiac remodeling, cardiac hypertrophy is classified based on the increasing geometries of the heart and individual size of cardiomyocytes. Eccentric hypertrophy and dilation of the cardiovascular wall, is associated with lengthening of the cardiomyocytes³⁰. Concentric hypertrophy and thickening of the cardiac wall, is associated with thickening of the cardiomyocytes³⁰. However, despite distinct eccentric remodeling in male mice and concentric remodeling in female mice were observed, we did not identify sex-specific differences in cardiomyocyte hypertrophy. Another important factor known to associate with sex in cardiac remodeling is apoptosis³¹. In murine cardiac dysfunction, it is known that females are better protected from apoptotic death signals compared to males³¹. Histological analysis in post mortem material of healthy and ischemic heart failure patients, revealed that less cardiomyocyte apoptosis is present in females compared to males^{32,33}. Combined, in absence of sex differences in interstitial fibrosis and hypertrophy in our model, reduced apoptosis in females might be a possible explanation for the increased wall thickness compared to male mice. However, it has also been shown that apoptosis induced upon pressure overload primarily affects non-cardiomyocytes and does correlate with the degree of hypertrophy, but not with a reduced cardiac function³⁴. Furthermore, the increase in wall thickness in concentric remodeling may also be caused by increased cardiomyocyte proliferation instead of reduced apoptosis. Therefore, future research should establish the contribution of apoptosis and cellular proliferation in cardiac remodeling of the murine TAC model.

Both pre-clinical studies and observational clinical studies have observed/reported sex specific cardiac remodeling in response to different types of injury, such as aging, pressure and volume overload or MI. Already in 1992, a debate on the role of sex-associated differences in cardiac remodeling induced by pressure overload was ongoing in patients with aortic stenosis³⁵. Patients with severe aortic stenosis showed sex differences in left ventricular remodeling with preservation of function in females, and an increase in left ventricle wall thickness and mass in males^{24,36}. Both papers suggested an underlying role for female hormones, such as estrogens, in the protection against eccentric cardiac remodeling^{24,36}. Although estrogens are known to protect against left ventricular hypertrophy, this is not likely to explain the complete difference in cardiac remodeling as post-menopausal women with reduced estrogen levels, have the same risk for adverse cardiac remodeling as males^{11,23}. Therefore, future research should focus on estrogen (ER) and estrogen receptors (ER α and ER β) in both male and female mice post-TAC to elucidate if estrogen affects adverse cardiac remodeling and contributes to concentric remodeling in female mice.

In the current study, female mice show more profound perivascular fibrosis and circulating proteins related to endothelial dysfunction. These results are in line with current paradigms suggesting that chronic cardiac dysfunction and remodeling in women

are driven by vascular dysfunction²². Coronary microvascular dysfunction, defined as a reduced coronary flow and endothelial dysfunction, is associated with worse outcome in female heart failure patients³⁷. We found an upregulation of endothelial to mesenchymal transition (EndMT) related pathways, such as Wnt and BMP signaling in female mice, which associated to the pathogenesis of human fibrotic diseases³⁸. During EndMT, endothelial cells become mesenchymal cells able to produce collagens which could explain the more profound perivascular fibrosis observed in the female mice. However, the exact role of EndMT in the pathogenesis of cardiac perivascular fibrosis is still controversial and not fully understood³⁸. Some reports show that EndMT contributes to interstitial fibrosis and vascular rarefaction^{39,40}, whereas others point at the over activation of resident fibroblast lineages becoming myofibroblasts⁴¹. in response to pressure overload induced cardiac fibrosis. Therefore, endothelial dysfunction and EndMT should be assessed in the TAC model. Furthermore, specific proteins and pathways responsible for endothelial dysfunction in females should be unraveled to provide new insights in concentric remodeling in females.

A potential limitation in this study is the similar size of the needle used for the ligation on the aortas in both male and female mice. We recognize that male mice may have a larger sized aorta at baseline, as they are bigger than females (shown by increased body weight and tibia length) and as such possibly also have increased cardiac dimensions. This may have resulted in a greater degree of constriction in males, explaining the difference in the type of cardiac remodeling (eccentric vs concentric) in male compared to female animals. However, no differences in ESV and EDV were observed when assessing baseline echocardiographic parameters. Furthermore, the flow ratio indicative of the constriction size was not different between sexes. These observations indicate that the degree of constriction was similar and both male and female mice experienced the same extent of pressure overload. Furthermore, the global longitudinal strain, which is indicative of the systolic pressure on the left ventricular wall, is similar in males and females at baseline and shows a similar degree of decline over time, again implying that both sexes experience similar pressure overload²⁹. Although it is known that ligation size affects the degree of heart failure and cardiac remodeling⁴², we have found no indications of differences in ligation between sexes. Since we cannot completely rule out that the difference of cardiac remodeling is not related to degree of constriction we will evaluate the effect of a less severe aortic constriction in both sexes. We expect this approach will confirm that the differences we observe, related to concentric and eccentric remodeling, are explained by biological sex differences independent of the aortic constriction.

Conclusion

Currently there is limited information regarding sex-specific pathophysiological processes underlying cardiac remodeling in heart failure⁴³. Using a TAC model of heart failure, we demonstrate sex differences in pathophysiological pathways that might

explain the alternate cardiac remodeling in male (eccentric remodeling) and female mice (concentric remodeling). Further research will be needed to elucidate which if the differentially regulated pathways and candidate factors identified are essential drivers for sex-specific cardiac remodeling. Based on our O-link discovery array, we suggest that vascular dysfunction leading to perivascular fibrosis may be a major determinant for adverse cardiac remodeling in females. Future research into the degree of vascular dysfunction in female heart failure will not only contribute to better understanding of female disease, but may also aid the identification of novel female specific targets to prevent adverse cardiac remodeling.

Acknowledgements

We gratefully acknowledge Emma Mol, Patricia van den Hoogen, Danny Elbersen, Eva Mulder and Judith de Haan for their technical support for this mice study.

Conflict of Interest

None declared.

Financial support

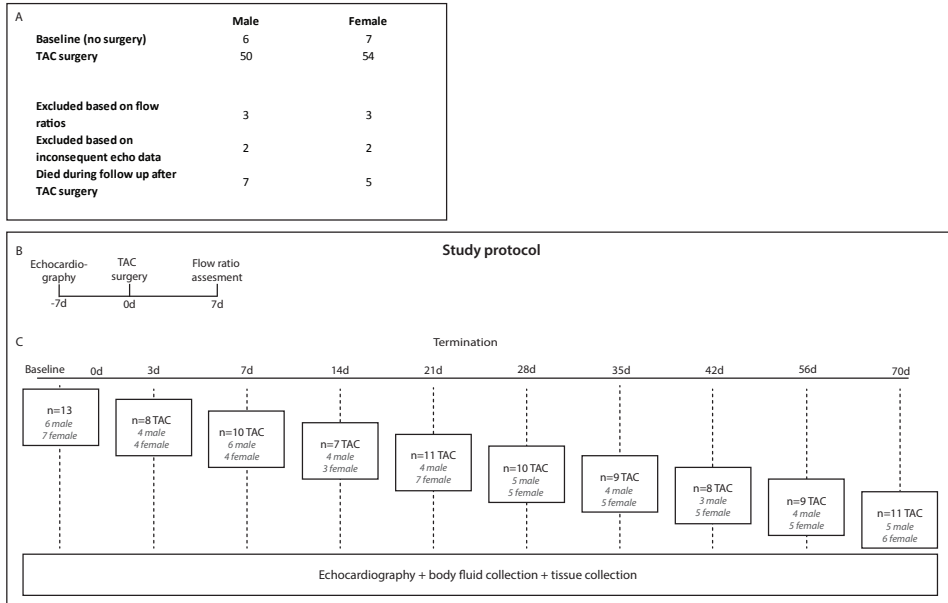
This study was supported by the Netherlands Cardiovascular Research Initiative: An initiative with support of the Dutch Heart Foundation [CVON2014-11 RECONNECT]

References

1. Ponikowski, P. et al. Heart failure: preventing disease and death worldwide. *ESC Hear. Fail.* **1**, 4–25 (2014).
2. Shah, K. S. et al. Heart Failure With Preserved, Borderline, and Reduced Ejection Fraction: 5-Year Outcomes. *J. Am. Coll. Cardiol.* **70**, 2476–2486 (2017).
3. Bui, A. L., Horwich, T. B. & Fonarow, G. C. Epidemiology and risk profile of heart failure. *Nat. Rev. Cardiol.* **8**, 30–41 (2011).
4. Messerli, F. H., Rimoldi, S. F. & Bangalore, S. The Transition From Hypertension to Heart Failure: Contemporary Update. *JACC. Heart Fail.* **5**, 543–551 (2017).
5. van der Wal, H. H., van Deursen, V. M., van der Meer, P. & Voors, A. A. *Comorbidities in Heart Failure. Handbook of experimental pharmacology* vol. 243 (2017).
6. Ponikowski, P. et al. 2016 ESC Guidelines for the Diagnosis and Treatment of Acute and Chronic Heart Failure. *Rev. Española Cardiol.* **69**, 1167 (2016).
7. Meyer, S. et al. Sex differences in new-onset heart failure. *Clin. Res. Cardiol.* **104**, 342–50 (2015).
8. Ho, J. E. et al. Discriminating clinical features of heart failure with preserved vs. reduced ejection fraction in the community. *Eur. Heart J.* **33**, 1734–41 (2012).
9. Lam, C. S. P., Donal, E., Kraigher-Krainer, E. & Vasan, R. S. Epidemiology and clinical course of heart failure with preserved ejection fraction. *Eur. J. Heart Fail.* **13**, 18–28 (2011).
10. Ziaean, B. & Fonarow, G. C. Epidemiology and aetiology of heart failure. *Nat. Rev. Cardiol.* **13**, 368–378 (2016).
11. Piro, M., Della Bona, R., Abbate, A., Biasucci, L. M. & Crea, F. Sex-related differences in myocardial remodeling. *J. Am. Coll. Cardiol.* **55**, 1057–65 (2010).
12. Crousillat, D. R. & Ibrahim, N. E. Sex Differences in the Management of Advanced Heart Failure. *Curr. Treat. Options Cardiovasc. Med.* **20**, 88 (2018).
13. Tastet, L. et al. Sex-Related Differences in the Extent of Myocardial Fibrosis in Patients With Aortic Valve Stenosis. *JACC Cardiovasc. Imaging* **In press**, (2019).
14. Zhang, X.-P. et al. Increased apoptosis and myocyte enlargement with decreased cardiac mass; distinctive features of the aging male, but not female, monkey heart. *J. Mol. Cell. Cardiol.* **43**, 487–491 (2007).
15. Zacharias, M. et al. Clinical epidemiology of heart failure with preserved ejection fraction (HFpEF) in comparatively young hospitalized patients. *Int. J. Cardiol.* **202**, 918–921 (2016).
16. Aurigemma, G. P., Silver, K. H., McLaughlin, M., Mauser, J. & Gaasch, W. H. Impact of chamber geometry and gender on left ventricular systolic function in patients > 60 years of age with aortic stenosis. *Am. J. Cardiol.* **74**, 794–798 (1994).
17. deAlmeida, A. C., van Oort, R. J. & Wehrens, X. H. T. Transverse aortic constriction in mice. *J. Vis. Exp.* **38**, 1729 (2010).
18. The Jackson Laboratory. <https://www.jax.org/jax-mice-and-services>.
19. De Haan, J. J. et al. Complement 5a Receptor deficiency does not influence adverse cardiac remodeling after pressure-overload in mice. *Sci. Rep.* **7**, 17045 (2017).
20. Yu, G., Wang, L.-G., Han, Y. & He, Q.-Y. clusterProfiler: an R package for comparing biological themes among gene clusters. *OMICS* **16**, 284–287 (2012).
21. Zhang, C. The role of inflammatory cytokines in endothelial dysfunction. *Basic Res. Cardiol.* **103**, 398–406 (2008).
22. Paulus, W. J. & Tschöpe, C. A novel paradigm for heart failure with preserved ejection fraction: comorbidities drive myocardial dysfunction and remodeling through coronary microvascular endothelial inflammation. *J. Am. Coll. Cardiol.* **62**, 263–71 (2013).
23. DeLeon-Pennell, K. Y. & Lindsey, M. L. Somewhere over the sex differences rainbow of myocardial infarction remodeling: hormones, chromosomes, inflammasome, oh my. *Expert Rev. Proteomics* **16**, 1–8 (2019).
24. Kostkiewicz, M., Tracz, W., Olszowska, M., Podolec, P. & Drop, D. Left ventricular geometry and function in patients with aortic stenosis: gender differences. *Int. J. Cardiol.* **71**, 57–61 (1999).
25. Ruppert, M. et al. Pressure-volume analysis reveals characteristic sex-related differences in cardiac function in a rat model of aortic banding-induced myocardial hypertrophy. *Am. J. Physiol. Hear. Circ. Physiol.* **315**, 502–511 (2018).
26. Witt, H. et al. Sex-specific pathways in early cardiac response to pressure overload in mice. *J. Mol. Med.* **86**, 1013–1024 (2008).
27. Follath, F. Nonischemic heart failure: epidemiology, pathophysiology, and progression of disease. *J. Cardiovasc. Pharmacol.* **33**, 31–35 (1999).
28. Pfeffer, J. M., Pfeffer, M. A., Fletcher, P., Fishbein, M. C. & Braunwald, E. Favorable effects of therapy on cardiac performance in spontaneously hypertensive rats. *Am. J. Physiol. Hear. Circ. Physiol.* **242**, 776–784 (1982).

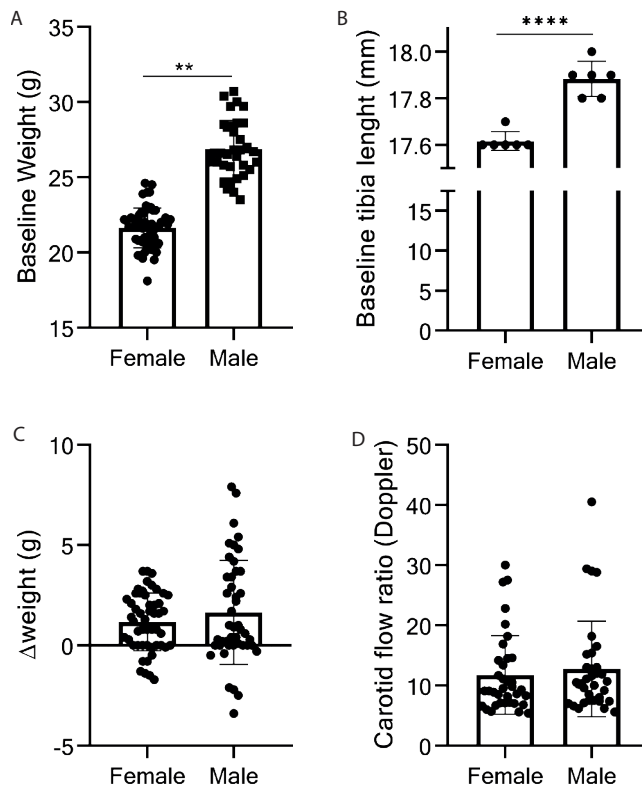
29. Weinberg, E. O. *et al.* Gender differences in molecular remodeling in pressure overload hypertrophy. *J. Am. Coll. Cardiol.* **34**, 264–273 (1999).
30. Kehat, I. & Molkentin, J. D. Molecular pathways underlying cardiac remodeling during pathophysiological stimulation. *Circulation* **122**, 2727–2735 (2010).
31. Guerra, S. *et al.* Myocyte death in the failing human heart is gender dependent. *Circ. Res.* **85**, 856–866 (1999).
32. Biondi-Zoccai, G. G. L. *et al.* Reduced post-infarction myocardial apoptosis in women: a clue to their different clinical course? *Hear. Br. Card. Soc.* **91**, 99–101 (2005).
33. Mallat, Z. *et al.* Age and gender effects on cardiomyocyte apoptosis in the normal human heart. *Journals Gerontol. Ser. A, Biol. Sci. Med. Sci.* **56**, 719–723 (2001).
34. Gelpi, R. J. *et al.* Apoptosis in severe, compensated pressure overload predominates in nonmyocytes and is related to the hypertrophy but not function. *Am. J. Physiol. Hear. Circ. Physiol.* **300**, 1062–1068 (2011).
35. Buttrick, P. & Scheuer, J. Sex-associated differences in left ventricular function in aortic stenosis of the elderly. *Circulation* **86**, 1336–1338 (1992).
36. Carroll, J. D. *et al.* Sex-associated differences in left ventricular function in aortic stenosis of the elderly. *Circulation* **86**, 1099–1107 (1992).
37. Garcia, M., Mulvagh, S. L., Merz, C. N. B., Buring, J. E. & Manson, J. E. Cardiovascular Disease in Women: Clinical Perspectives. *Circ. Res.* **118**, 1273–1293 (2016).
38. Piera-Velazquez, S., Mendoza, F. A. & Jimenez, S. A. Endothelial to Mesenchymal Transition (EndoMT) in the Pathogenesis of Human Fibrotic Diseases. *J. Clin. Med.* **5**, 45 (2016).
39. Goumans, M. J., van Zonneveld, A. J. & ten Dijke, P. Transforming Growth Factor β -Induced Endothelial-to-Mesenchymal Transition: A Switch to Cardiac Fibrosis? *Trends Cardiovasc. Med.* **18**, 293–298 (2008).
40. Zeisberg, E. M. *et al.* Endothelial-to-mesenchymal transition contributes to cardiac fibrosis. *Nat. Med.* **13**, 952–961 (2007).
41. Moore-Morris, T. *et al.* Resident fibroblast lineages mediate pressure overload-induced cardiac fibrosis. *J. Clin. Invest.* **124**, 2921–2934 (2014).
42. Richards, D. A. *et al.* Distinct Phenotypes Induced by Three Degrees of Transverse Aortic Constriction in Mice. *Sci. Rep.* **9**, 5844 (2019).
43. Taylor, A. L. Heart failure in women. *Curr. Heart Fail. Rep.* **12**, 187–195 (2015).

Supplemental



Supplemental figure 1. Mice included in the study and study protocol.

a) male and female mice included in the study and number of mice subjected to TAC surgery. b) study protocol for baseline assessment of cardiac function and flow ratio assessment to establish correct placement of the ligation after 7 days. c) study protocol with number of mice terminated over time at which echocardiography is performed and body fluids and tissues are collected.



Supplemental figure 2. Baseline characteristics male and female mice.

Weight at baseline is higher in males compared to females (a), as well as the tibia length (b). The weight increase over time during the experiment was not different between male and female mice (c). The carotid flow, representative of the aortic constriction is not different between the male and female mice (d).

Supplemental table 1. Circulating proteins higher at baseline in either males or females.

Higher level at baseline			
Abbreviation	Factor	Male	Female
S100-A4	S100 calcium binding protein A4	x	
GFRa1	GDNF family receptor a1	x	
ppp1r2	Protein phosphatase inhibitor 2	x	
Adam23	Disintegrin and metallopeptidase domain 23	x	
CCN1	Cyr61; Cysteine rich angiogenic inducer	x	
Ntf3	Neurotrophin 3	x	
ErbB4	Tyrosine protein kinase receptor ErbB4	x	
Vsig2	V-set and immunoglobulin domain containing protein 2	x	
Tgfβr3	Transforming growth factor β receptor 3	x	
IL23r	Interleukin 23 receptor		x
Cxcl9	CXC motif chemokine 9		x
Wisp1	WNT1 inducible signaling pathway protein1		x
CDH6	Cadherin 6		x
Cntn4	Contactin 4		x
Ghrl	Appetite regulating hormone		x
IL1α	Interleukin 1 α		x
CCl2	CC ligand 2		x

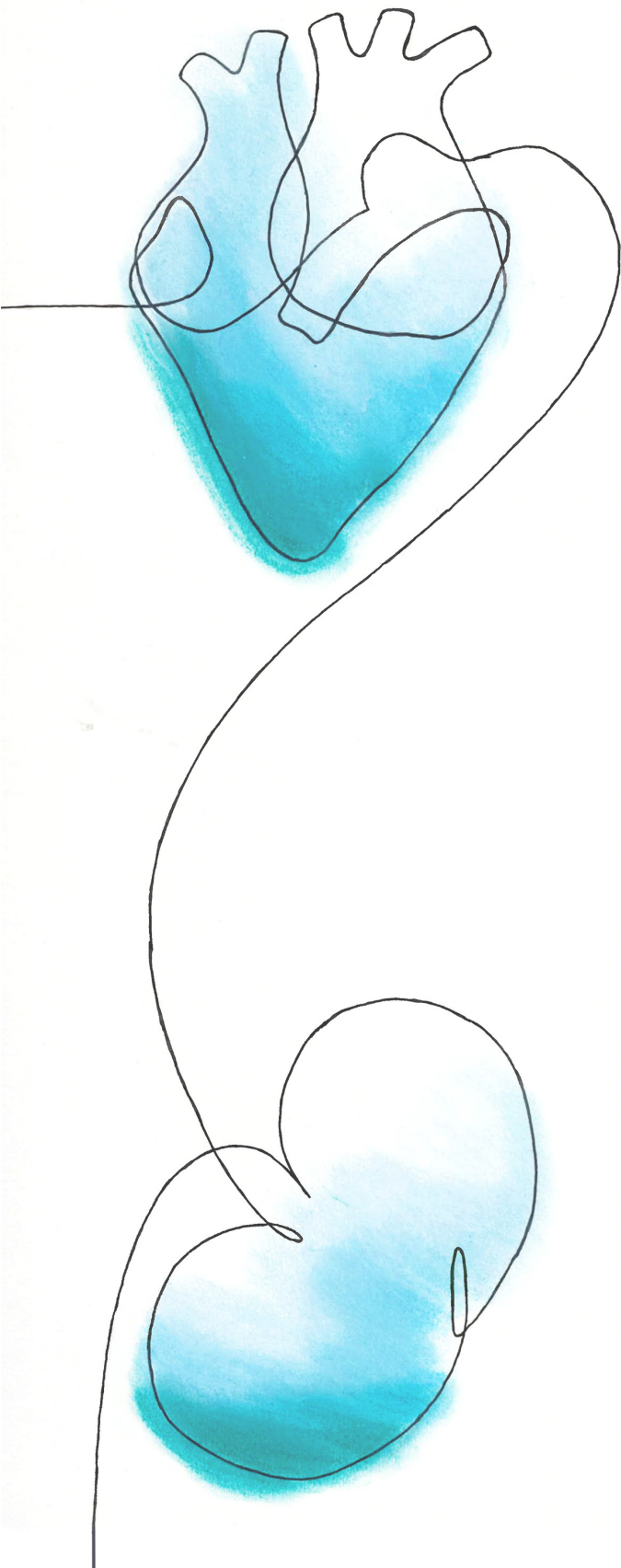
Supplemental table 2. Circulating protein levels increasing over time-post TAC (0-70 days) in either males, females or both sexes.

Abbreviation	Factor	Increase over time (0-70 days)		
		Male	Female	Both
Gcg	Glucagon			x
CCl5	Rantes			x
IL1 β	Interleukin 1 β			x
Notch3	Neurogenic locus notch homolog protein 3			x
Adam23	Disintegrin and metallopeptidase domain 23			x
CCn1	Cyr61; cysteine rich angiogenic inducer			x
CCL2	CC ligand 2			x
ErbB4	ErbB4; receptor tyrosine protein kinase erbb4			x
Vegfd	Vascular endothelial growth factor D			x
Ntf3	Neurotrophin 3			x
Ccl20	C-C motif chemokine 20			x
Igsf3	Immunoglobulin superfamily member 3			x
IL23r	Interleukin 23 receptor			x
LGMMN	Legumain, cyteine protease			x
CSF2	Granulocyte macrophage colony stimulating factor			x
IL17f	Interleukin 17f			x
Tnni3	Troponin 1		x	
Tgf β 3	Transforming growth factor B receptor 3		x	
CXCL1	Growth regulated alpha protein		x	
Lpl	Lipoprotein lipase		x	
Fstl3	Follistatin related protein 3		x	
Gdnf	Glial derived neurotrophic factor		x	
S100-A4	S100 calcium binding protein A4		x	
Crim1	Cysteine Rich Transmembrane BMP Regulator 1	x		
IL1 α	Interleukin 1 α	x		
Foxo1	Foxo1	x		
Apbb1ip	Amyloid Beta Precursor Protein Binding Family B Member 1 Interacting Protein	x		
Tpp1	Tripeptidyl peptidase 1	x		



PART III

GDF15 as biomarker and target





GDF15 in adverse cardiac remodeling: from biomarker to causal player

Accepted in ESC Heart Failure

M. Wesseling^{1,2}, J.H.C. de Poel¹, S.C.A. de Jager^{1,3}

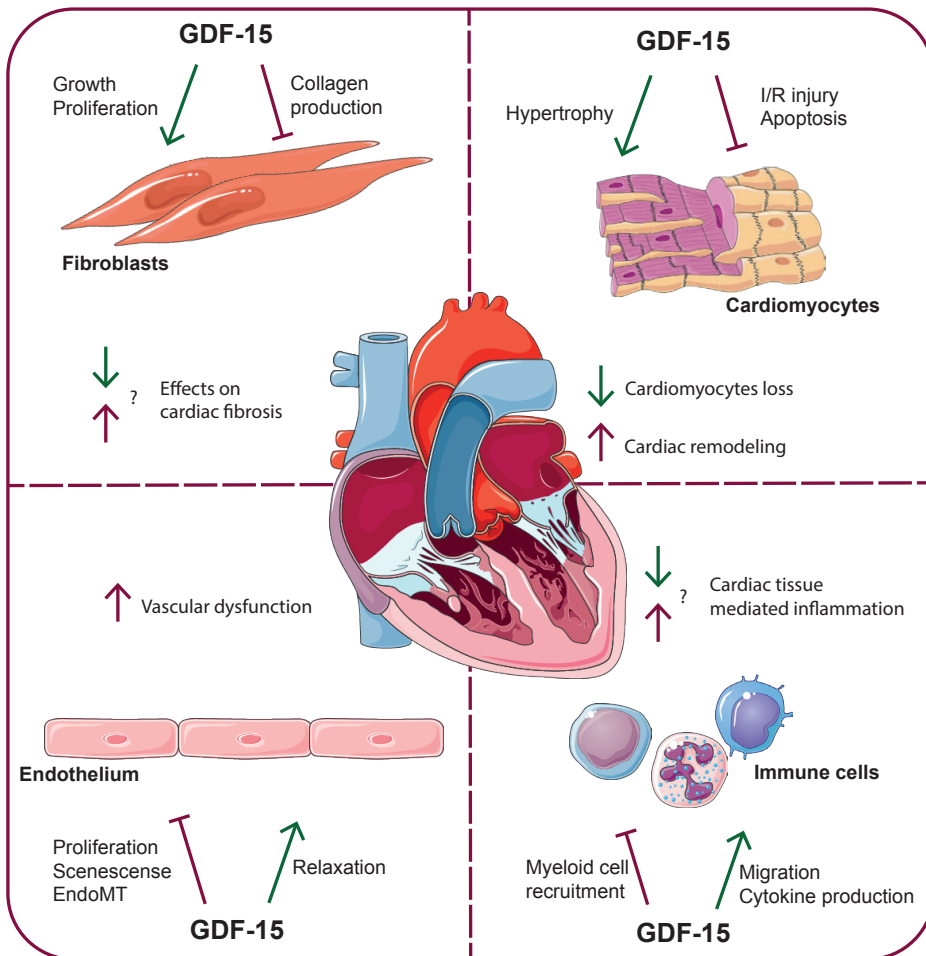
¹Laboratory for Experimental Cardiology, University Medical Centre Utrecht, Utrecht, The Netherlands

²Laboratory for Clinical Chemistry and Hematology, University Medical Centre Utrecht, Utrecht, The Netherlands

³Laboratory for Translational Immunology, University Medical Centre Utrecht, Utrecht, The Netherlands

Abstract

Heart failure is a growing health issue as a negative consequence of improved survival upon myocardial infarction, unhealthy lifestyle and the aging of our population. The large and complex pathology underlying heart failure make diagnosis and especially treatment very difficult. There is an urgent demand for discriminative biomarkers to aid disease management of heart failure. Studying cellular pathways and pathophysiological mechanisms contributing to disease initiation and progression is crucial for understanding the disease process and will aid to identification of novel biomarkers and potential



Graphical abstract. Proposed effects of GDF15 in adverse cardiac remodeling.

GDF15 is known to affect cardiovascular cells by stimulation or inhibition of cellular processes. The effects of GDF15 are either beneficial or detrimental during adverse cardiac remodeling. (Figure constructed from Servier medical art, <https://smart.servier.com/>)

therapeutic targets. Growth differentiation factor 15 (GDF15) is a proven valuable biomarker for different pathologies, including cancer, type 2 diabetes and cardiovascular diseases. Although the prognostic value of GDF15 in heart failure is robust, the biological function of GDF15 in adverse cardiac remodeling is not fully understood. GDF15 is a distant member of the TGF- β family and involved in various biological processes including inflammation, cell cycle and apoptosis. However more research is suggesting a role in fibrosis, hypertrophy and endothelial dysfunction. As GDF15 is a pleiotropic protein, elucidating the exact role of GDF15 in complex disease processes has proven to be a challenge. In this review we provide an overview of the role GDF15 plays in various intra- and extracellular processes underlying heart failure and we touch upon crucial points that need consideration before GDF15 can be integrated as a biomarker in standard care or when considering GDF15 for therapeutic intervention.

Background

The mortality rates related to cardiovascular disease (CVD) have increased worldwide, since 2015 one in three deaths worldwide is a consequence of a CVD¹. Heart failure is a growing health issue as a negative consequence of improved survival upon myocardial infarction (MI), unhealthy lifestyle and the aging of our population². Therefore, the European Society of Cardiology recently updated their criteria defining heart failure by including extra cardiac organ co-morbidities like diabetes, hypertension and kidney dysfunction^{3,4}. These new criteria show the complexity of heart failure throughout the patient population.

Heart failure cannot be classified as a single disease, multiple underlying causes including hypertension, vascular calcification or MI, show that heart failure better fits the description of a syndrome rather than a disease^{5,6}. Furthermore, apart from underlying cardiac pathologies, extra-cardiac pathologies such as cardiorenal syndrome and anemia contribute to the development of heart failure^{7,8}. Disease progression is further accelerated by aging, diabetes, and hypertension as they cause endothelial dysfunction, left ventricular hypertrophy and vascular disease⁹⁻¹¹.

A key process underlying heart failure is cardiac remodeling as response to injury, like inflammation, volume and pressure overload. In response to injury, the heart compensate for the loss of cardiac output by remodeling of the myocardium. Cardiac remodeling is characterized by molecular, cellular and structural changes that manifest in morphological changes of heart size, shape, and function^{12,13}. The mechanisms underlying cardiac remodeling are not fully understood, as they vary from apoptosis, oxidative stress and inflammation to changes in energy metabolism and contractile proteins^{5,12,13}. Severe remodeling of cardiac tissue associates with progressive worsening of cardiac function eventually increasing mortality risk in patients, this highlights the need for assessment of cardiac remodeling to monitor disease and therapy adjustment where needed.

The demand for biomarkers that improve disease management of heart failure patients is increasing¹⁴. Although no curative therapy for heart failure is available, co-morbidities influence disease progression and contribute to worsening of cardiac function. Proper biomarkers would allow to routinely assess disease progression and in case of heart failure which includes many co-morbidities, inform on their presence to combine this information and maintain optimal treatment for the patient.

Elevated protein expression of circulating growth differentiation factor 15 (GDF15) are correlated to many pathological conditions, mainly being different types of cancer but also metabolic diseases such as obesity and diabetes¹⁵⁻¹⁸. GDF15 is easily detectable in blood, however concentration vary with age and gender^{15,19-21}. For instance, we have shown that circulating levels of GDF15 can serve as strong independent predictor for cardiovascular events in woman but not in men²². Although GDF15 has a sex-dependent prognostic value in heart failure patients²³, the prognostic value of GDF15 is not standardly analyzed for males and females separately to increase accuracy²⁴⁻²⁶. Elevated serum levels of GDF15 were also associated with enhanced cardiovascular disease development, progression and mortality both in disease and general population^{17,27-31}. In line, experimental murine ischemia/reperfusion injury models show an rapid increase in circulating and tissue GDF15 levels upon cardiac injury that remained elevated for several days^{27,32}. Moreover, GDF15 has been proven to be a valuable biomarker for heart failure, apart from the existing cardiac markers such as natriuretic peptides, ST2, high-sensitivity troponin, and procalcitonin^{19,33,34}, as it can serve as independent biomarker for survival and outcome^{35,36}. GDF15 has been linked to the incidence, progression and prognosis of heart failure as biomarker for acute and chronic cellular stress^{28,35}. In line, Roche Diagnostics developed a commercial assay that provided robust data of GDF15 levels in serum and plasma under routine conditions²¹. To implement GDF15 as biomarker in standard clinical practice, we need to understand which pathophysiological process(es) are associated with increased levels in order to adjusted disease management accordingly.

Besides its biomarker function, GDF15 may have a causal role in heart failure, something we need to elucidate before GDF15 can become the new discovered target for therapeutic therapy. As GDF15 is an active player in many pathophysiological processes^{16,37}, understanding its molecular basis, biological mechanism, and receptor activity in heart tissue could help elucidating its role in the onset and progression of heart failure. Therefore the aim of this review is to summarize current literature regarding biomarker function and causal role of GDF15 relevant in heart function and adverse cardiac remodeling. We describe the molecular background of GDF15, followed by an overview of effects on intra and extra cellular processes associated with pathophysiological mechanisms driving heart failure. Lastly based on all this information, we will touch upon future perspectives and current needs in the GDF15 cardiac research field.

Growth differentiation factor 15

Growth differentiation factor 15 (GDF15), also termed macrophage inhibitory cytokine 1 (MIC-1) is a divergent member of the transforming growth factor (TGF)- β family^{37,38}. The TGF- β family consists of TGF- β isoforms, activins and bone morphogenetic proteins (BMPs), and are best known for their effects on tissue homeostasis, cell proliferation and differentiation³⁹. Although GDF15 belongs to this TGF- β superfamily and shares homology with bone morphogenetic proteins (BMPs), its major functions are not completely identical. GDF15 is robustly expressed by placenta and prostate tissue, while in other tissues expression is very low^{15,17,37,40}. However, under pathophysiological conditions like cellular stress and tissue injury, GDF15 can be produced and secreted by many various cell types like macrophages, vascular smooth muscle cells, endothelial cells and cardiomyocytes¹⁵⁻¹⁸ in organs such as kidney, heart and liver.

GDF15 receptor identification

Knowing GDF15 is rapidly produced and secreted by various tissue and cells, one of the most urgent questions is to which receptor GDF15 binds and which intracellular signaling cascades are activated. It was recently established that GDF15 can bind with high affinity to the GDNF family receptor α -like (GFRAL) receptor⁴¹⁻⁴⁴. GFRAL is mainly located in the central nervous system⁴⁵ and binding and signaling of GDF15/GFRAL axis leads to a decreased food intake and subsequent weight loss^{46,47}. This discovery helped unravel a role for GDF15 on activation of certain metabolic pathways and increases knowledge about possible therapeutic use of GDF15 in obesity and weight loss⁴³.

To our knowledge, expression of the GFRAL receptor has only been found in the central nervous system leaving the question to which primary receptor GDF15 binds in the periphery still open⁴⁸. So far, studies have reported GDF15 binding to the TGF- β II receptor⁴⁹, ALK receptors^{17,49,50}, and some indicate binding to tyrosine or serine/threonine receptors⁵¹. The discovery of GFRAL provided important insight in the signaling capabilities of GDF15 via non TGF- β related receptors and suggests signaling of GDF15 beyond the TGF- β receptor family may be very important in the periphery as well. As such, exploring the possible cardiac signaling receptors of GDF15 in cardiomyocytes, fibroblasts and endothelial cells may provide more insights in mechanistic effects and possible therapeutic targeting of GDF15 during progressive heart failure.

Regulation of GDF15 on the genetic level

GDF15 is located on chromosome 19p12-13.1, with a length of 2.746 base pairs containing two exons separated by an intron^{15,52} (Figure 1). Various gene polymorphisms (SNPs) are suggested to affect GDF15 expression, for example rs888663 and rs1054564 located upstream of the GDF15 gene⁵³⁻⁵⁵ are associated with cardiovascular diseases⁵⁶⁻⁵⁸. Contradictory, no effect of SNPs increasing GDF15 transcription activity⁵⁷ in cardiovascular diseases are also present^{59,60}. In addition, SNPs in the miRNAs (miR) regulating GDF15 expression are suggested to be important as well, an example is miR SNP rs1054564 in

the 3'UTR of the GDF15 transcript, which causes allele-specific translational repression via has-miR-1233-3p⁶¹. Furthermore, miRSNP rs1054564 is associated with reduced levels of circulating GDF15 in a Taiwanese cardiovascular disease population⁶². They suggest GDF15 to be a major genetic determinant of the GDF15 concentration⁶²

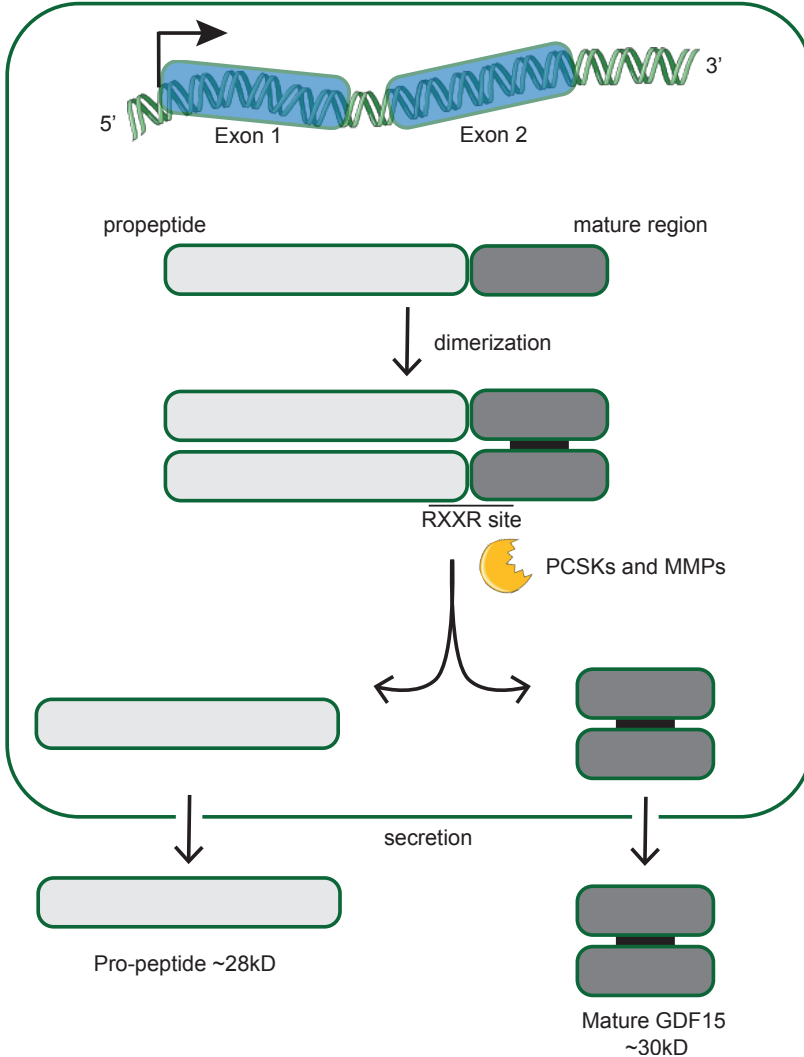


Figure 1. GDF15 transcription and maturation.

Originating from two exons, GDF15 is synthesized as polypeptide consisting of a propeptide and a mature region. Between two mature regions, a homodimer is formed by an interchain disulfide bond. The propeptide plays an important role in intracellular trafficking and secretion. PCSKs and MMPs are able to cleave the pro-GDF15 polypeptide at the RXXR cleave site, thereby forming a biological active mature GDF15. After cleavage, both the propeptide and mature GDF15 are secreted. (Figure adapted from Servier medical art, <https://smart.servier.com/>)

Production of GDF15

Originating from two exons, GDF15 is synthesized as a polypeptide (pre-pro-GDF15) which consists of a signal peptide, a pro-peptide and a mature region^{42,63} (Figure 1). The GDF15 polypeptide is biologically inactive and forms a homodimers through a interchain disulfide bond at the C terminus in the endoplasmic reticulum⁶⁴. The N-terminal side contains the signaling peptide important for secretion and intracellular trafficking⁴². Once located in the endoplasmic reticulum the polypeptide is cleaved by the serine proteinases pro-protein convertase subtilisin/kexin-types (PCSKs)⁶⁵. PCSK 3, 5 and 6 are able to recognize and remove the signaling peptide of the GDF15 polypeptide and therefore essential in the formation of a biologically active GDF15⁶⁶. In addition to PCSKs, GDF15 can also be processed by matrix metalloproteinase (MMP)-26⁶⁷ (Figure 1). The presence of GDF15 and MMP-26 in placental development suggests that MMP-26 is just as important as PCSKs in the processing and maturation of GDF15. Besides serine and matrix metalloproteinases, there are also cysteine proteinases⁶⁸, all involved in extracellular proteolysis⁶⁹ and further research should elucidate their possible contribution to GDF15 maturation. After cleavage of the pro-GDF15 domain, both a mature GDF15 protein and the remaining pro-peptide are secreted (Figure 1). Pro-GDF15 is secreted into the extracellular matrix and is stored in latent stromal ECM stores⁶⁴. Under stress conditions, latent pro-GDF15 from the storage pools is cleaved to its active mature form. Bauskin *et al.*, found that the pro-peptide of pro-GDF15 is responsible for this cleaving and signaling to increase circulating serum levels of GDF15 upon demand^{64,70}. Whether these storage pools are present or activated in cardiac tissue during the progression of heart failure has not been clarified, but it may contribute to increased GDF15 secretion into the circulation during heart failure. As previously reported that an increase in these stromal stores of GDF15 associate with disease outcome of prostate cancer patients, it could be very relevant to investigate the presence of stores in cardiac tissue⁶⁴. Therefore, histopathological assessment of GDF15 in cardiac tissue of heart failure patients could indicate the increased GDF15 production and storage, possibly predictive of disease severity and outcome.

GDF15 as a causal player in adverse remodeling

GDF15 can be produced by almost every cell type in the periphery under stress conditions and can have an influence on numerous cell types^{71,72}. Depending on the state of cells and the microenvironment present, GDF15 can both have beneficial or adverse effects on several different cellular processes^{16,44}. Most pathophysiological and mechanistic effects of GDF15 are observed in cancers, however also inflammation, hypertrophy and fibrosis in organ dysfunction are under direct influence of GDF15^{16,44}. Below we describe the most important cellular mechanisms that can be influenced in cardiac cells by GDF15 and are related to the onset and progression of heart failure.

Effect of GDF15 on cardiomyocytes

The loss of cardiomyocyte as a consequence of apoptosis and the very low proliferation rate of cardiomyocyte are highly important mechanisms in the development of heart failure. Studying interactions of GDF15 with cell cycle processes, have so far gained most insights from the cancer research field. Elevation of circulating GDF15 levels have been associated with increased apoptosis and reduced cell proliferation in solid tumours^{73,74}. Multiple oncogenic studies propose GDF15 to play a role in cell growth arrest and apoptosis, either via p53-dependent or p53-independent mechanisms⁷⁵⁻⁷⁷. In line, as mentioned above, Jones *et al.* identified a P53 regulated miR embedded in the GDF15 intron gene, able to reduce cell proliferation and desensitize cells to DNA damage-induced apoptosis in a human colorectal cancer cells line⁷⁸. Moreover, as GDF15 is also a downstream target of p53, early growth response 1 (EGR-1), and Akt/GSK-3 β , there is a feedback loop for the effect of GDF15 plays in cell growth arrest and apoptosis^{73,75,76,79,80}. Nevertheless, knowing that GDF15 is pleotropic, opposing studies showed that an increase in GDF15 is able to induce proliferation of cervical and malignant glioma cancer cells^{81,82}. Relating to cardiomyocytes, GDF15 is associated with protection against ischemia reperfusion and angiotensin II, NO, or TGF- β_1 induced apoptosis^{83,84}. Even more interesting, GDF15 is associated with ERBB2 and CyclinD1 in cervical cancer cell proliferation⁸⁵, both known factors to induce cardiomyocyte proliferation⁸⁶⁻⁸⁸. In line, recently the Hippo-YAP pathway gained special attention in regards to cardiac regeneration as potential therapeutic target^{89,90}. Moreover, interplay between Hippo-YAP and TGF- β pathways are known to be involved in tissue homeostasis⁹¹⁻⁹³. This suggests that GDF15, as TGF- β family member, may affect the Hippo-YAP pathway, thereby possibly targeting cardiomyocyte proliferation. To conclude, the effect of GDF15 on proliferation and apoptosis is relevant to study in cardiomyocytes to maintain high number of viable and functional cardiomyocytes in order to maintain cardiac output. Cardiac hypertrophy is characterized by an increase in heart size and a loss of sufficient cardiac output as cardiomyocytes enlarge as consequence of a pathophysiological stimuli⁹⁴. Elevated circulating GDF15 levels positive correlate with thickness of the posterior wall of the left ventricle, interventricular septum, and left ventricular mass^{51,95,96}. Mechanistically, GDF15 is reported to have a pro-hypertrophic effect on cardiomyocytes, that attenuates cardiac hypertrophy via PI3K and ERK signaling pathways, thereby affecting transcription via the Smad1 pathway^{83,97,98}. However it has also been described that GDF15 can protect against hypertrophy through Smad dependent pathways⁹⁷. Moreover, it has been shown that GDF15 can inhibit the activation of endothelial growth factor receptor (EGFr) thereby attenuating hypertrophic responses in a Smad independent manner⁹⁶. Furthermore, in animal models mesenchymal stem cell treatment showed beneficial paracrine effects via induction of GDF15 secretion, thereby reducing hypertrophy and left ventricular remodeling^{99,100}. Concluding, both pro- and anti-hypertrophic effect of GDF15 are described suggesting a mediating role of GDF15 in cardiac hypertrophic responses dependent on the environmental circumstances. It

remains unclear if Smad dependent signaling pathways dominate other pathways in GDF15 mediated hypertrophic responses.

Effect of GDF15 on endothelial cells

Endothelial dysfunction is crucial mediator of impaired coronary and systemic perfusion and reduced cardiac capacity via directly negatively affect cardiac remodeling and cardiomyocyte function^{101,102}. Endothelial dysfunction in patients with chronic heart failure is associated with increased mortality¹⁰³. Increased adhesion molecule expression, reduced anticoagulant properties, and imbalanced production of vasodilating and vasoconstriction substances all lead to endothelial dysfunction¹⁰⁴. There are sufficient indications that GDF15 causes endothelial dysfunction by impairing vascular contraction and relaxation, that consequently could have an large impact on the function of the heart. Not only by inducing large artery disease but also microvascular disease which is associated with a deteriorating cardiac function¹⁰⁵. Mechanistically, Mazagova *et al.* showed that the vascular contractility in response to vasoconstrictor agents were repressed under presence of GDF15, suggesting that GDF15 effects the NO system in endothelial cells¹⁰⁴. Indeed others show that increased levels of GDF15 are important for NO release in endothelial cells that will result in reduced vasodilation¹⁰⁶. Furthermore, it has been shown that GDF15 can induce proliferation of endothelial cells during angiogenesis¹⁰⁷ but also endothelial senescence via ROS pathway activation, implicating endothelial function loss^{108,109}.

Recently various studies have addressed the contribution of Epithelial-mesenchymal transition (EMT) and endothelial to mesenchymal transition (EndMT) to the inflammation and fibrosis response in tissue repair, implicated to play a role in pathological processes of heart failure^{110,111}. It is well established, that the TGF- β pathway plays an important role in E(nd)MT and thereby cell migration and fibrosis as expression of respectively MMPs and collagens are upregulated during this process. It has been shown that GDF15 inhibits TGF- β I target genes thereby diminished cell migration as result of suppressed EMT in bone tumor epithelial cells¹¹². This data supports the notion that GDF15 has a potential anti-migratory effect on endothelial cells¹¹³. However, contradictory results are found that display E(nd)MT progression and increased cell migration promoted by GDF15, through activation of the TGF- β pathway in a paracrine and autocrine signaling manner^{76,114,115}.

Effect of GDF15 on fibroblasts

In cardiac pathologies, during repair and regenerative processes following upon tissue injury, an excessive amount of fibrous connective tissue is formed consisting of ECM deposition, including collagen, fibronectin and laminin^{116,117}. This myocardial fibrosis is an integral component leading to both functional impairment and arrhythmogenesis¹¹⁸⁻¹²¹. Various studies show associations between GDF15 and cardiac fibrosis, collagen turnover and collagen depositions in respectively heart failure, myocardial infarction and atherosclerosis^{49,122,123}. However, the exact source of this increased GDF15 production has not been clearly identified. Lok and colleagues showed that cardiac tissue itself

was not the main source of GDF15 production in cardiac fibrosis, but suggest systemic oxidative stress to increase GDF15 in different cells and organs¹²², while Kempf *et al.*, show that GDF15 is expressed and secreted in cardiomyocytes subjected to ischemia/reperfusion injury, through a nitrosative stress-dependent signaling pathway³². GDF15 is recently identified as a possible inhibitor of fibroblasts growth via repression of TGF- β signaling and oncogenic protein N-Myc, reducing fibroblast activation and fibrosis in chronic kidney disease and pulmonary fibrosis^{124,125}. These result, suggest the possibility of using GDF15 as therapeutic to delay progression of fibrosis¹²⁴. However, contrary results have also been found in gastric cancer, suggesting that GDF15 stimulates the activation and proliferation of fibroblasts and therefore playing an important role in fibrosis progression¹²⁶. Considering the anti- and pro-fibrotic effects of GDF15 described, using GDF15 as possible therapeutic target for cardiac fibrosis relies on further research to discover specific effects of GDF15 on cardiac related fibrosis.

Effect of GDF15 on resident and infiltrating inflammatory cells

As GDF15 is a family member of TGF- β and an inflammatory cytokine secreted upon injury, it is opposed to be an mediator of tissue inflammation¹²⁷. The balance in resident and infiltrating inflammatory cells varies depending on acute and chronic heart failure, with respectively monocytes and macrophages and later reparative monocytes and T cell infiltration^{128,129}. In acute heart failure upon MI, the necrotic area is controlled by inflammatory cells like neutrophils, monocytes and macrophages thereby prone to cardiac rupture^{130,131}. Kempf *et al.* showed an anti-inflammatory role of GDF15 after an MI, as the infarct border zone increased GDF15 expression, thereby inhibited myeloid cell recruitment and protecting the myocardium from cardiac rupture¹³². In chronic heart failure for example heart failure with preserved ejection fraction (HFpEF), the increase in GDF15 is thought to reflect the inflammatory response as systemic low grade inflammation is a central pathophysiologic mechanism¹⁰⁵. In chronic heart failure, an increasing amount of infiltrating inflammatory cells are present in cardiac tissue, the same accounts for GDF15 levels with progression of the disease. For example, macrophages express GDF15 during inflammatory responses contributing to the inflammatory activity of activated macrophages¹³³. In line, a lack of GDF15 resulted in impaired macrophage migration and monocyte recruitment and a downregulation of pro-inflammatory cytokines such as IFN- γ ^{49,134}. This suggests that circulating GDF15 reflects the inflammatory status of the patient, and reduction of GDF15 as therapeutic intervention may be useful to attenuate macrophage inflammation in CVD.

Discussion and future perspective

With this review we aimed to summarize the current knowledge about GDF15 in heart failure and define the most vital questions that should be addressed in the coming years. Over the last years GDF15 gained more and more interest in the cardiovascular field

as it hold promise as a valuable biomarker. It has been shown that GDF15 has cardio-protective properties mostly through anti-apoptotic, anti-hypertrophic, anti-fibrotic and anti-inflammatory actions. However, an increase in GDF15 concentrations has also been associated with pro-apoptotic, pro-hypertrophic, pro-fibrotic and pro-inflammatory responses including a worse prognosis and higher mortality rates among heart failure patients. However, a causal role for GDF15 in adverse cardiac remodeling remains to be elucidated, whether GDF15 plays an adaptive or maladaptive role in heart failure patients is still poorly understood. Summarizing on the data included in this review we propose that GDF15 may be a valuable therapeutic target in heart failure as it is involved in several key processes in the pathobiology of heart failure.

Added value of GDF15 as a heart failure biomarker?

Currently it has been well established that GDF15 level are increased during CVD development, progression, and can prognosticate disease progression³¹. However, the availability of a reliable diagnostic test for routine clinical use and the complementary relevant cut-off values are lacking. With the recent development of a diagnostic GDF15 kit by Roche the first steps towards a clinical biomarker approach are made²¹. However, it remains unclear what the specific implications are when heart failure patients have increased levels of GDF15, as we cannot connect the level to a specific pathophysiological contributor to disease progression, like cardiac fibrosis. Therefore, we need more information on the causal role of GDF15 before the specific biomarker function of GDF15 in clinical care can be established. For example, it has been reported that after LVAD implantation in patients with advanced heart failure GDF15 levels decrease^{122,135}. This indicates that the elevation of GDF15 in heart failure patients is reversible upon treatment. A pharmacological treatment with vasodilator hormone human relaxin-2 (Serelaxin) was able to lower GDF15 levels in patients with acute heart failure^{136,137}. This indicates cardiac stress reduction due to treatment thereby improving heart function and consequently downregulation of GDF15 levels and insinuates GDF15 may be an interesting biomarker for treatment responsiveness.

When looking for future therapeutic intervention options or clinical discriminative biomarkers to aid to prediction and guide treatment, it is of crucial importance to gain more insight in the specific signaling effects of GDF15 within cardiac tissue. Elucidating the balance in GDF15 concentration needed for normal pathophysiological function, thereby needing to either increasing or decreasing the GDF15 levels is needed to provide a beneficial effect on cardiac function.

GDF15 as therapeutic intervention for heart failure

Before GDF15 can become a therapeutic option we need to elucidate on the possible options for intervention. For example, inhibiting or enhancing GDF15 production, post transcriptional regulation, receptor ligand binding, and protein interactions. Although cardiomyocytes are the functional cellular cardiac component, these cells have proven to be difficult targets¹³⁸ as endothelial cells form the functional barrier between the

circulating levels and cardiac tissue. Therefore a more relevant cell type for targeting via receptor interaction would be endothelial cells, especially as endothelial dysfunction can be reversible¹³⁹. In this manner modulation of fibrotic responses could be made possible. GDF15 receptor inhibition is where potential lies, as shown with the GFRAL receptor in the blood brain barrier, which yield beneficial treatment potential for obesity^{42,43}. A logical druggable target are receptors as they are easily accessible for biologicals, however for heart failure this will remain complex due to the lack of known cardiac receptor for GDF15. Therefore, emphasizing more research into the specific cardiac receptor for GDF15 is crucial.

Microvascular intervention

To the best of our knowledge no research has been performed into the role of GDF15 on cardiac tissue calcification, something less prevalent but nevertheless interesting as it plays a major role in conduction disturbances in cardiac tissue¹⁴⁰. In line, HFpEF is associated with microvascular vascular stiffness and microvascular calcification^{141,142}. Well established are coronary artery calcifications associated with heart failure as it increases the risk for cardiovascular events^{143,144}. Until now preventive treatment for calcification is not possible due to lack of knowledge about the underlying mechanism¹⁴⁵⁻¹⁴⁷. GDF15 is associated with the presence of carotid artery calcification²², increased expression resulted in reduced atherosclerotic lesion formation¹⁴⁸, and absence of GDF15 in leukocytes resulted in stable lesion formation¹⁴⁹. From patients and animal studies we know that endothelial dysfunction leads to increased vascular calcification via BMP pathway activation^{150,151}, addressing endothelial cells as possible target to reduce calcification. Therefore the role of GDF15 in vascular calcification and stiffness could give valuable information towards unraveling the mechanism behind heart failure.

Conclusion

With this review we aimed to display the potential behind GDF15 beyond a biomarker function as it is involved in many pathophysiological processes in heart failure. The future of GDF15 as therapeutic target lies in additional cardiac specific research unraveling the causal effect of GDF15 in cardiac dysfunction on a cellular and molecular level.

Funding

This work was supported by Netherlands Cardiovascular Research Initiative: An initiative with support of the Dutch Heart Foundation (CVON2014-11 RECONNECT and Queen of Hearts Program 2013T084]

References

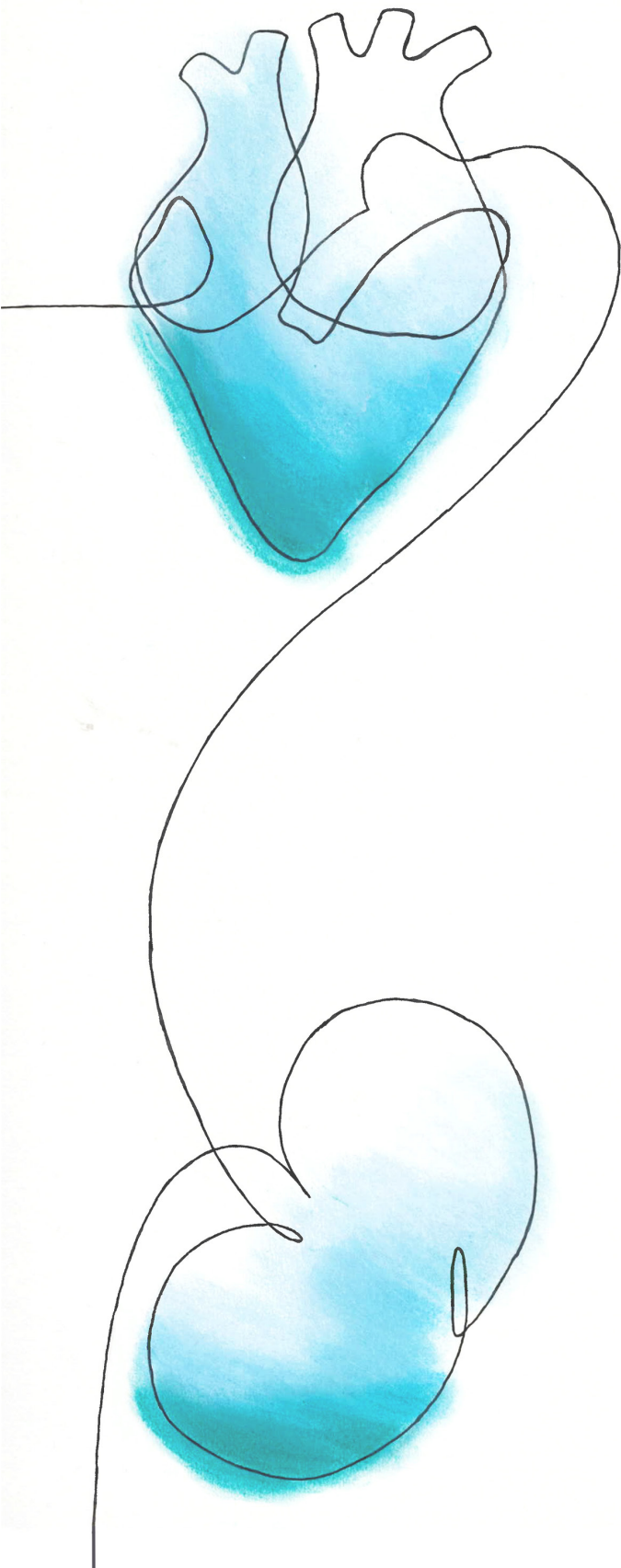
1. Lozano, R. et al. Global and regional mortality from 235 causes of death for 20 age groups in 1990 and 2010: a systematic analysis for the Global Burden of Disease Study 2010. *Lancet* **380**, 2095–2128 (2012).
2. Bleumink, G. et al. Quantifying the heart failure epidemic: prevalence, incidence rate, lifetime risk and prognosis of heart failure The Rotterdam Study. *Eur. Heart J.* **25**, 1614–1619 (2004).
3. Crespo-Leiro, M. G. et al. Advanced heart failure: a position statement of the Heart Failure Association of the European Society of Cardiology. *Eur. J. Heart Fail.* **20**, 1505–1535 (2018).
4. Ponikowski, P. et al. 2016 ESC Guidelines for the diagnosis and treatment of acute and chronic heart failure. *Eur. Heart J.* **37**, 2129–2200 (2016).
5. Shah, A. M. & Mann, D. L. In search of new therapeutic targets and strategies for heart failure: recent advances in basic science. *Lancet* **378**, 704–12 (2011).
6. The Lancet. Heart failure: the need for improved treatment and care. *Lancet* **392**, 451 (2018).
7. Ronco, C., Haapio, M., House, A. A., Anavekar, N. & Bellomo, R. Cardiorenal Syndrome. *J. Am. Coll. Cardiol.* **52**, 1527–1539 (2008).
8. Anand, I. S. Anemia and Chronic Heart Failure. *J. Am. Coll. Cardiol.* **52**, 501–511 (2008).
9. Strait, J. B. & Lakatta, E. G. Aging-Associated Cardiovascular Changes and Their Relationship to Heart Failure. *Heart Fail. Clin.* **8**, 143–164 (2012).
10. Dhingra, R. & Vasani, R. S. Diabetes and the risk of heart failure. *Heart Fail. Clin.* **8**, 125–33 (2012).
11. Frohlich, E. D. & Susic, D. Pressure Overload. *Heart Fail. Clin.* **8**, 21–32 (2012).
12. Frohlich, E. D. Risk Mechanisms in Hypertensive Heart Disease. *Hypertension* **34**, 782–789 (1999).
13. Azevedo, P. S., Polegato, B. F., Minicucci, M. F., Paiva, S. A. R. & Zornoff, L. A. M. Cardiac Remodeling: Concepts, Clinical Impact, Pathophysiological Mechanisms and Pharmacologic Treatment. *Arq. Bras. Cardiol.* **106**, 62–9 (2016).
14. Eitel, I. et al. Growth-differentiation factor 15 as predictor of mortality in acute reperfused ST-elevation myocardial infarction: insights from cardiovascular magnetic resonance. *Heart* **97**, 632–640 (2011).
15. Corre, J., Hébraud, B. & Bourin, P. Concise review: growth differentiation factor 15 in pathology: a clinical role? *Stem Cells Transl. Med.* **2**, 946–52 (2013).
16. Breit, S. N. et al. The TGF- β superfamily cytokine, MIC-1/GDF15: A pleiotropic cytokine with roles in inflammation, cancer and metabolism. *Growth Factors* **29**, 187–195 (2011).
17. Adela, R. & Banerjee, S. K. GDF-15 as a Target and Biomarker for Diabetes and Cardiovascular Diseases: A Translational Prospective. *J. Diabetes Res.* **2015**, 490842 (2015).
18. Koopmann, J. et al. Serum macrophage inhibitory cytokine 1 as a marker of pancreatic and other periampullary cancers. *Clin. Cancer Res.* **10**, 2386–92 (2004).
19. Kempf, T. et al. Circulating Concentrations of Growth-Differentiation Factor 15 in Apparently Healthy Elderly Individuals and Patients with Chronic Heart Failure as Assessed by a New Immunoradiometric Sandwich Assay. *Clin. Chem.* **53**, 284–291 (2006).
20. Dominguez-Rodriguez, A., Abreu-Gonzalez, P., Hernandez-Baldero, I. F., Avanzas, P. & Bosa-Ojeda, F. Change in growth differentiation factor 15, but not C-reactive protein, independently predicts major cardiac events in patients with non-ST elevation acute coronary syndrome. *Mediators Inflamm.* **2014**, 929536 (2014).
21. Wollert, K. C. et al. An Automated Assay for Growth Differentiation Factor 15. *J. Appl. Lab. Med.* **1**, 510–521 (2017).
22. Gohar, A. et al. Circulating GDF-15 levels predict future secondary manifestations of cardiovascular disease explicitly in women but not men with atherosclerosis. *Int. J. Cardiol.* **241**, 430–436 (2017).
23. Meyer, S. et al. Neurohormonal and clinical sex differences in heart failure. *Eur. Heart J.* **34**, 2538–2547 (2013).
24. Zelniker, T. A. et al. Prognostic role of GDF-15 across the spectrum of clinical risk in patients with NSTEMI-ACS. *Clin. Chem. Lab. Med.* **57**, 1084–1092 (2019).
25. Benes, J. et al. The Role of GDF-15 in Heart Failure Patients With Chronic Kidney Disease. *Can. J. Cardiol.* **35**, 462–470 (2019).
26. Yin, J. et al. Increased Growth Differentiation Factor 15 Is Associated with Unfavorable Clinical Outcomes of Acute Ischemic Stroke. *Clin. Chem.* **65**, 569–578 (2019).
27. Wollert, K. C. et al. Prognostic Value of Growth-Differentiation Factor-15 in Patients With Non-ST-Elevation Acute Coronary Syndrome. *Circulation* **115**, 962–971 (2007).
28. Wollert, K. C. & Kempf, T. Growth Differentiation Factor 15 in Heart Failure: An Update. *Curr. Heart Fail. Rep.* **9**, 337–345 (2012).
29. Bonaca, M. P. et al. Growth Differentiation Factor-15 and Risk of Recurrent Events in Patients Stabilized After Acute Coronary Syndrome. *Arterioscler. Thromb. Vasc. Biol.* **31**, 203–210 (2011).
30. Tzikas, S. et al. GDF-15 predicts cardiovascular events in acute chest pain patients. *PLoS One* **12**, e0182314 (2017).
31. Wollert, K. C., Kempf, T. & Wallentin, L. Growth Differentiation Factor 15 as a Biomarker in Cardiovascular Disease. *Clin. Chem.* **63**, 140–151 (2017).

32. Kempf, T. et al. The Transforming Growth Factor- β Superfamily Member Growth-Differentiation Factor-15 Protects the Heart From Ischemia/Reperfusion Injury. *Circ. Res.* **98**, 351–360 (2006).
33. Kurmani, S. & Squire, I. Acute Heart Failure: Definition, Classification and Epidemiology. *Curr. Heart Fail. Rep.* **14**, 385–392 (2017).
34. Wettersten, N. & Maisel, A. S. Biomarkers for Heart Failure: An Update for Practitioners of Internal Medicine. *Am. J. Med.* **129**, 560–567 (2016).
35. Kempf, T. & Wollert, K. C. Growth-Differentiation Factor-15 in Heart Failure. *Heart Fail. Clin.* **5**, 537–547 (2009).
36. Kempf, T. et al. Growth-differentiation factor-15 improves risk stratification in ST-segment elevation myocardial infarction. *Eur. Heart J.* **28**, 2858–2865 (2007).
37. Bootcov, M. R. et al. MIC-1, a novel macrophage inhibitory cytokine, is a divergent member of the TGF- β superfamily. *Proc. Natl. Acad. Sci. U. S. A.* **94**, 11514–9 (1997).
38. Harris, P. & Ralph, P. Human leukemic models of myelomonocytic development: a review of the HL-60 and U937 cell lines. *J. Leukoc. Biol.* **37**, 407–22 (1985).
39. Massagué, J. TGF β signalling in context. *Nat. Rev. Mol. Cell Biol.* **13**, 616–630 (2012).
40. Yokoyama-Kobayashi, M., Saeki, M., Sekine, S. & Kato, S. Human cDNA encoding a novel TGF- β superfamily protein highly expressed in placenta. *J. Biochem.* **122**, 622–6 (1997).
41. Xiong, Y. et al. Long-acting MIC-1/GDF15 molecules to treat obesity: Evidence from mice to monkeys. *Sci. Transl. Med.* **9**, eaan8732 (2017).
42. Mullican, S. E. & Rangwala, S. M. Uniting GDF15 and GFRAL: Therapeutic Opportunities in Obesity and Beyond. *Trends Endocrinol. Metab.* **29**, 560–570 (2018).
43. Yang, L. et al. GFRAL is the receptor for GDF15 and is required for the anti-obesity effects of the ligand. *Nat. Med.* **23**, 1158–1166 (2017).
44. Emmerson, P. J. et al. The metabolic effects of GDF15 are mediated by the orphan receptor GFRAL. *Nat. Med.* **23**, 1215–1219 (2017).
45. Yamaguchi, K. et al. Peroxisome proliferator-activated receptor ligand MCC-555 suppresses intestinal polyps in ApcMin/+ mice via extracellular signal-regulated kinase and peroxisome proliferator-activated receptor-dependent pathways. *Mol. Cancer Ther.* **7**, 2779–2787 (2008).
46. Macia, L. et al. Macrophage Inhibitory Cytokine 1 (MIC-1/GDF15) Decreases Food Intake, Body Weight and Improves Glucose Tolerance in Mice on Normal & Obesogenic Diets. *PLoS One* **7**, e34868 (2012).
47. Chrysovergis, K. et al. NAG-1/GDF-15 prevents obesity by increasing thermogenesis, lipolysis and oxidative metabolism. *Int. J. Obes.* **38**, 1555–1564 (2014).
48. Mullican, S. E. et al. GFRAL is the receptor for GDF15 and the ligand promotes weight loss in mice and nonhuman primates. *Nat. Med.* **23**, 1150–1157 (2017).
49. de Jager, S. C. A. et al. Growth differentiation factor 15 deficiency protects against atherosclerosis by attenuating CCR2-mediated macrophage chemotaxis. *J. Exp. Med.* **208**, 217–225 (2011).
50. Unsicker, K., Spittau, B. & Krieglstein, K. The multiple facets of the TGF- β family cytokine growth/differentiation factor-15/macrophage inhibitory cytokine-1. *Cytokine Growth Factor Rev.* **24**, 373–384 (2013).
51. Xue, H. et al. The association of growth differentiation factor-15 with left ventricular hypertrophy in hypertensive patients. *PLoS One* **7**, e46534 (2012).
52. Eling, T. E., Baek, S. J., Shim, M. & Lee, C. H. NSAID activated gene (NAG-1), a modulator of tumorigenesis. *J. Biochem. Mol. Biol.* **39**, 649–55 (2006).
53. Jiang, J. et al. A Meta-Analysis of Genome-Wide Association Studies of Growth Differentiation Factor-15 Concentration in Blood. *Front. Genet.* **9**, (2018).
54. Ho, J. E. et al. Clinical and Genetic Correlates of Growth Differentiation Factor 15 in the Community. *Clin. Chem.* **58**, 1582–1591 (2012).
55. Cheung, C.-L., Tan, K. C. B., Au, P. C. M., Li, G. H. Y. & Cheung, B. M. Y. Evaluation of GDF15 as a therapeutic target of cardiometabolic diseases in human: A Mendelian randomization study. *EBioMedicine* **41**, 85–90 (2019).
56. Jing, R., Liu, Q., Xie, Q. & Qian, Z. Correlation between GDF 15 gene polymorphism and the collateral circulation in acute non-ST segment elevated myocardial infarction. *Int. J. Clin. Exp. Med.* **8**, 14383–7 (2015).
57. Wang, X. et al. The haplotype of the growth-differentiation factor 15 gene is associated with left ventricular hypertrophy in human essential hypertension. *Clin. Sci.* **118**, 137–145 (2009).
58. Chen, X. et al. Correlation between GDF-15 gene polymorphism and the formation of collateral circulation in acute ST-elevation myocardial infarction. *Rev. Assoc. Med. Bras.* **63**, 1049–1054 (2017).
59. Chen, Z. et al. Study of the association between growth differentiation factor 15 gene polymorphism and coronary artery disease in a Chinese population. *Mol. Biol. Rep.* **38**, 5085–5091 (2011).
60. Cheung, C.-L., Tan, K. C. B., Au, P. C. M., Li, G. H. Y. & Cheung, B. M. Y. Evaluation of GDF15 as a therapeutic target of cardiometabolic diseases in human: A Mendelian randomization study. *EBioMedicine* **41**, 85–90 (2019).

61. Teng, M.-S. et al. A GDF15 3' UTR variant, rs1054564, results in allele-specific translational repression of GDF15 by hsa-miR-1233-3p. *PLoS One* **12**, e0183187 (2017).
62. Hsu, L.-A. et al. Growth Differentiation Factor 15 May Predict Mortality of Peripheral and Coronary Artery Diseases and Correlate with Their Risk Factors. *Mediators Inflamm.* Article ID 9398401 (2017).
63. Zimmers, T. A. et al. Growth differentiation factor-15/macrophage inhibitory cytokine-1 induction after kidney and lung injury. *Shock* **23**, 543–8 (2005).
64. Bauskin, A. R. et al. The Propeptide Mediates Formation of Stromal Stores of PROMIC-1: Role in Determining Prostate Cancer Outcome. *Cancer Res.* **65**, 2330–2336 (2005).
65. Seidah, N. G., Sadr, M. S., Chrétien, M. & Mbikay, M. The multifaceted proprotein convertases: their unique, redundant, complementary, and opposite functions. *J. Biol. Chem.* **288**, 21473–81 (2013).
66. Li, J. J. et al. Growth Differentiation Factor 15 Maturation Requires Proteolytic Cleavage by PCSK3, -5, and -6. *Mol. Cell. Biol.* **38**, (2018).
67. Li, S. et al. Maturation of Growth Differentiation Factor 15 in Human Placental Trophoblast Cells Depends on the Interaction With Matrix Metalloproteinase-26. *J. Clin. Endocrinol. Metab.* **99**, E2277–E2287 (2014).
68. Chapman, H. A., Riese, R. J. & Shi, G.-P. Emerging roles for cysteine proteases in human biology. *Annu. Rev. Physiol.* **59**, 63–88 (1997).
69. Arturo, G.-T. et al. Extracellular Proteases in Atherosclerosis and Restenosis. *Arterioscler. Thromb. Vasc. Biol.* **25**, 1119–1127 (2005).
70. Bauskin, A. R. et al. The TGF- β Superfamily Cytokine MIC-1/GDF15: Secretory Mechanisms Facilitate Creation of Latent Stromal Stores. *J. Interf. Cytokine Res.* **30**, 389–397 (2010).
71. Böttner, M. et al. Characterization of the rat, mouse, and human genes of growth/differentiation factor-15/macrophage inhibiting cytokine-1 (GDF-15/MIC-1). *Gene* **237**, 105–11 (1999).
72. Böttner, M., Suter-Crazzolaro, C., Schober, A. & Unsicker, K. Expression of a novel member of the TGF- β superfamily, growth/differentiation factor-15/macrophage-inhibiting cytokine-1 (GDF-15/MIC-1) in adult rat tissues. *Cell Tissue Res.* **297**, 103–110 (1999).
73. Liu, T. et al. Macrophage inhibitory cytokine 1 reduces cell adhesion and induces apoptosis in prostate cancer cells. *Cancer Res.* **63**, 5034–40 (2003).
74. Chen, S.-J. et al. Prostate-derived factor as a paracrine and autocrine factor for the proliferation of androgen receptor-positive human prostate cancer cells. *Prostate* **67**, 557–571 (2007).
75. Li, P.-X. et al. Placental Transforming Growth Factor- β Is a Downstream Mediator of the Growth Arrest and Apoptotic Response of Tumor Cells to DNA Damage and p53 Overexpression. *J. Biol. Chem.* **275**, 20127–20135 (2000).
76. Baek, S. J., Kim, K. S., Nixon, J. B., Wilson, L. C. & Eling, T. E. Cyclooxygenase inhibitors regulate the expression of a TGF-beta superfamily member that has proapoptotic and antitumorigenic activities. *Mol. Pharmacol.* **59**, 901–8 (2001).
77. Schiegnitz, E. et al. GDF 15 as an anti-apoptotic, diagnostic and prognostic marker in oral squamous cell carcinoma. *Oral Oncol.* **48**, 608–614 (2012).
78. Jones, M. F. et al. Growth differentiation factor-15 encodes a novel microRNA 3189 that functions as a potent regulator of cell death. *Cell Death Differ.* **22**, 1641–1653 (2015).
79. Lee, S.-H. et al. ESE-1/EGR-1 pathway plays a role in tolfenamic acid-induced apoptosis in colorectal cancer cells. *Mol. Cancer Ther.* **7**, 3739–3750 (2008).
80. Yamaguchi, K., Lee, S.-H., Eling, T. E. & Baek, S. J. Identification of Nonsteroidal Anti-inflammatory Drug-activated Gene (NAG-1) as a Novel Downstream Target of Phosphatidylinositol 3-Kinase/AKT/GSK-3 β Pathway. *J. Biol. Chem.* **279**, 49617–49623 (2004).
81. Li, S., Ma, Y.-M., Zheng, P.-S. & Zhang, P. GDF15 promotes the proliferation of cervical cancer cells by phosphorylating AKT1 and Erk1/2 through the receptor ErbB2. *J. Exp. Clin. Cancer Res.* **37**, 80 (2018).
82. Roth, P. et al. GDF-15 Contributes to Proliferation and Immune Escape of Malignant Gliomas. *Clin. Cancer Res.* **16**, 3851–3859 (2010).
83. Heger, J. et al. Growth differentiation factor 15 acts anti-apoptotic and pro-hypertrophic in adult cardiomyocytes. *J. Cell. Physiol.* **224**, 120–126 (2010).
84. Kempf, T. et al. The Transforming Growth Factor- β Superfamily Member Growth-Differentiation Factor-15 Protects the Heart From Ischemia/Reperfusion Injury. *Circ. Res.* **98**, 351–360 (2006).
85. Li, S., Ma, Y.-M., Zheng, P.-S. & Zhang, P. GDF15 promotes the proliferation of cervical cancer cells by phosphorylating AKT1 and Erk1/2 through the receptor ErbB2. *J. Exp. Clin. Cancer Res.* **37**, 80 (2018).
86. D'Uva, G. et al. ERBB2 triggers mammalian heart regeneration by promoting cardiomyocyte dedifferentiation and proliferation. *Nat. Cell Biol.* **17**, 627–38 (2015).
87. Leach, J. P. & Martin, J. F. Cardiomyocyte Proliferation for Therapeutic Regeneration. *Curr. Cardiol. Rep.* **20**, 63 (2018).
88. Li, J. et al. Alpha-catenins control cardiomyocyte proliferation by regulating Yap activity. *Circ. Res.* **116**, 70–9 (2015).

89. Wang, J., Liu, S., Heallen, T. & Martin, J. F. The Hippo pathway in the heart: pivotal roles in development, disease, and regeneration. *Nat. Rev. Cardiol.* **15**, 672–684 (2018).
90. Ikeda, S. & Sadoshima, J. Regulation of Myocardial Cell Growth and Death by the Hippo Pathway. *Circ. J.* **80**, 1511–1519 (2016).
91. Pefani, D.-E. et al. TGF- β Targets the Hippo Pathway Scaffold RASSF1A to Facilitate YAP/SMAD2 Nuclear Translocation. *Mol. Cell* **63**, 156–166 (2016).
92. Szeto, S. G. et al. YAP/TAZ Are Mechanoregulators of TGF- β -Smad Signaling and Renal Fibrogenesis. *J. Am. Soc. Nephrol.* **27**, 3117–3128 (2016).
93. Ben Mimoun, S. & Mauviel, A. Molecular mechanisms underlying TGF- β /Hippo signaling crosstalks – Role of baso-apical epithelial cell polarity. *Int. J. Biochem. Cell Biol.* **98**, 75–81 (2018).
94. Tardiff, J. C. Cardiac hypertrophy: stressing out the heart. *J. Clin. Invest.* **116**, 1467–70 (2006).
95. Kou, H. et al. Association between growth differentiation factor 15 and left ventricular hypertrophy in hypertensive patients and healthy adults. *Clin. Exp. Hypertens.* **40**, 8–15 (2018).
96. Xu, X. et al. Growth Differentiation Factor (GDF)-15 Blocks Norepinephrine-induced Myocardial Hypertrophy via a Novel Pathway Involving Inhibition of Epidermal Growth Factor Receptor Transactivation. *J. Biol. Chem.* **289**, 10084–10094 (2014).
97. Xu, J. et al. GDF15/MIC-1 Functions As a Protective and Antihypertrophic Factor Released From the Myocardium in Association With SMAD Protein Activation. *Circ. Res.* **98**, 342–350 (2006).
98. Ago, T. & Sadoshima, J. GDF15, a Cardioprotective TGF- β Superfamily Protein. *Circ. Res.* **98**, 294–297 (2006).
99. Zhang, Y. et al. Potent Paracrine Effects of human induced Pluripotent Stem Cell-derived Mesenchymal Stem Cells Attenuate Doxorubicin-induced Cardiomyopathy. *Sci. Rep.* **5**, 11235 (2015).
100. Wehman, B. et al. Mesenchymal stem cells preserve neonatal right ventricular function in a porcine model of pressure overload. *Am. J. Physiol. Circ. Physiol.* **310**, H1816–H1826 (2016).
101. Bauersachs, J. & Widdler, J. D. Endothelial dysfunction in heart failure. *Pharmacol. Rep.* **60**, 119–26.
102. Lam, C. S. P. & Lund, L. H. Microvascular endothelial dysfunction in heart failure with preserved ejection fraction. *Heart* **102**, 257–9 (2016).
103. Alem, M. M. Endothelial Dysfunction in Chronic Heart Failure: Assessment, Findings, Significance, and Potential Therapeutic Targets. *Int. J. Mol. Sci.* **20**, (2019).
104. Mazagova, M. et al. Growth differentiation factor 15 impairs aortic contractile and relaxing function through altered caveolar signaling of the endothelium. *Am. J. Physiol. Circ. Physiol.* **304**, H709–H718 (2013).
105. Paulus, W. J. & Tschöpe, C. A Novel Paradigm for Heart Failure With Preserved Ejection Fraction. *J. Am. Coll. Cardiol.* **62**, 263–271 (2013).
106. Lind, L. et al. Growth-differentiation factor-15 is an independent marker of cardiovascular dysfunction and disease in the elderly: results from the Prospective Investigation of the Vasculature in Uppsala Seniors (PIVUS) Study. *Eur. Heart J.* **30**, 2346–2353 (2009).
107. Wang, S. et al. Growth differentiation factor 15 promotes blood vessel growth by stimulating cell cycle progression in repair of critical-sized calvarial defect. *Sci. Rep.* **7**, 9027 (2017).
108. Park, H., Kim, C.-H., Jeong, J.-H., Park, M. & Kim, K. S. GDF15 contributes to radiation-induced senescence through the ROS-mediated p16 pathway in human endothelial cells. *Oncotarget* **7**, 9634–44 (2016).
109. Wu, Q. et al. Cigarette Smoke Induces Human Airway Epithelial Senescence via Growth Differentiation Factor 15 Production. *Am. J. Respir. Cell Mol. Biol.* **55**, 429–38 (2016).
110. Zeisberg, E. M. et al. Endothelial-to-mesenchymal transition contributes to cardiac fibrosis. *Nat. Med.* **13**, 952–961 (2007).
111. Li, Y., Lui, K. O. & Zhou, B. Reassessing endothelial-to-mesenchymal transition in cardiovascular diseases. *Nat. Rev. Cardiol.* **15**, 445–456 (2018).
112. Min, K.-W. et al. NAG-1/GDF15 accumulates in the nucleus and modulates transcriptional regulation of the Smad pathway. *Oncogene* **35**, 377–88 (2016).
113. Min, K.-W., Zhang, X., Imchen, T. & Baek, S. J. A peroxisome proliferator-activated receptor ligand MCC-555 imparts anti-proliferative response in pancreatic cancer cells by PPAR γ -independent up-regulation of KLF4. *Toxicol. Appl. Pharmacol.* **263**, 225–232 (2012).
114. Li, C. et al. GDF15 promotes EMT and metastasis in colorectal cancer. *Oncotarget* **7**, 860–72 (2016).
115. Jiang, G., Liu, C. & Zhang, W. IL-17A and GDF15 are able to induce epithelial-mesenchymal transition of lung epithelial cells in response to cigarette smoke. *Exp. Ther. Med.* **16**, 12–20 (2018).
116. Liu, Y. Cellular and molecular mechanisms of renal fibrosis. *Nat. Rev. Nephrol.* **7**, 684–696 (2011).
117. Duffield, J. S. Cellular and molecular mechanisms in kidney fibrosis. *J. Clin. Invest.* **124**, 2299–2306 (2014).
118. Travers, J. G., Kamal, F. A., Robbins, J., Yutzey, K. E. & Blaxall, B. C. Cardiac Fibrosis. *Circ. Res.* **118**, 1021–1040 (2016).
119. Brown, R. D., Ambler, S. K., Mitchell, M. D. & Long, C. S. THE CARDIAC FIBROBLAST: Therapeutic Target in Myocardial Remodeling and Failure. *Annu. Rev. Pharmacol. Toxicol.* **45**, 657–687 (2005).
120. Khan, R. & Sheppard, R. Fibrosis in heart disease: understanding the role of transforming growth factor-beta1 in cardiomyopathy, valvular disease and arrhythmia. *Immunology* **118**, 10–24 (2006).

121. Janicki, J. S. & Brower, G. L. The role of myocardial fibrillar collagen in ventricular remodeling and function. *J. Card. Fail.* **8**, S319–S325 (2002).
122. Lok, S. I. *et al.* Circulating growth differentiation factor-15 correlates with myocardial fibrosis in patients with non-ischaemic dilated cardiomyopathy and decreases rapidly after left ventricular assist device support. *Eur. J. Heart Fail.* **14**, 1249–1256 (2012).
123. Wang, F.-F. *et al.* Correlation between growth differentiation factor-15 and collagen metabolism indicators in patients with myocardial infarction and heart failure. *J. Geriatr. Cardiol.* **13**, 88–93 (2016).
124. Kim, Y.-I., Shin, H.-W., Chun, Y.-S. & Park, J.-W. CST3 and GDF15 ameliorate renal fibrosis by inhibiting fibroblast growth and activation. *Biochem. Biophys. Res. Commun.* **500**, 288–295 (2018).
125. Kim, Y.-I. *et al.* Epithelial cell-derived cytokines CST3 and GDF15 as potential therapeutics for pulmonary fibrosis. *Cell Death Dis.* **9**, 506 (2018).
126. Ishige, T. *et al.* Combined Secretomics and Transcriptomics Revealed Cancer-Derived GDF15 is Involved in Diffuse-Type Gastric Cancer Progression and Fibroblast Activation. *Sci. Rep.* **6**, 21681 (2016).
127. Luan, H. H. *et al.* GDF15 Is an Inflammation-Induced Central Mediator of Tissue Tolerance. *Cell* **178**, 1231–1244 (2019).
128. Frangogiannis, N. G. Regulation of the inflammatory response in cardiac repair. *Circ. Res.* **110**, 159–73 (2012).
129. Frangogiannis, N. G. The inflammatory response in myocardial injury, repair, and remodelling. *Nat. Rev. Cardiol.* **11**, 255–65 (2014).
130. Frangogiannis, N. G. The Mechanistic Basis of Infarct Healing. *Antioxid. Redox Signal.* **8**, 1907–1939 (2006).
131. Gao, X.-M. *et al.* Infarct size and post-infarct inflammation determine the risk of cardiac rupture in mice. *Int. J. Cardiol.* **143**, 20–28 (2010).
132. Kempf, T. *et al.* GDF-15 is an inhibitor of leukocyte integrin activation required for survival after myocardial infarction in mice. *Nat. Med.* **17**, 581–588 (2011).
133. Schlittenhardt, D. *et al.* Involvement of growth differentiation factor-15/macrophage inhibitory cytokine-1 (GDF-15/MIC-1) in oxLDL-induced apoptosis of human macrophages in vitro and in arteriosclerotic lesions. *Cell Tissue Res.* **318**, 325–333 (2004).
134. Bonaterra, G. A. *et al.* Growth differentiation factor-15 deficiency inhibits atherosclerosis progression by regulating interleukin-6-dependent inflammatory response to vascular injury. *J. Am. Heart Assoc.* **1**, e002550 (2012).
135. Ahmad, T. *et al.* Effects of Left Ventricular Assist Device Support on Biomarkers of Cardiovascular Stress, Fibrosis, Fluid Homeostasis, Inflammation, and Renal Injury. *JACC Hear. Fail.* **3**, 30–39 (2015).
136. Metra, M. *et al.* Effects of serelaxin in subgroups of patients with acute heart failure: results from RELAX-AHF. *Eur. Heart J.* **34**, 3128–3136 (2013).
137. Cotter, G. *et al.* Growth differentiation factor 15 (GDF-15) in patients admitted for acute heart failure: results from the RELAX-AHF study. *Eur. J. Heart Fail.* **17**, 1133–1143 (2015).
138. Eschenhagen, T. *et al.* Cardiomyocyte Regeneration. *Circulation* **136**, 680–686 (2017).
139. Celermajer, D. S. Endothelial dysfunction: does it matter? Is it reversible? *J. Am. Coll. Cardiol.* **30**, 325–33 (1997).
140. Pillai, I. C. L. *et al.* Cardiac Fibroblasts Adopt Osteogenic Fates and Can Be Targeted to Attenuate Pathological Heart Calcification. *Cell Stem Cell* **20**, 218–232 (2017).
141. Cheng, H.-M., Wang, J.-J. & Chen, C.-H. The Role of Vascular Calcification in Heart Failure and Cognitive Decline. *Pulse* **5**, 144–153 (2017).
142. Nance, J. W., Crane, G. M., Halushka, M. K., Fishman, E. K. & Zimmerman, S. L. Myocardial calcifications: Pathophysiology, etiologies, differential diagnoses, and imaging findings. *J. Cardiovasc. Comput. Tomogr.* **9**, 58–67 (2015).
143. Lala, A. & Desai, A. S. The role of coronary artery disease in heart failure. *Heart Fail. Clin.* **10**, 353–365 (2014).
144. Madhavan, M. V. *et al.* Coronary Artery Calcification: Pathogenesis and Prognostic Implications. *J. Am. Coll. Cardiol.* **63**, 1703–1714 (2014).
145. Bakhshi, H. *et al.* Progression of Coronary Artery Calcium and Incident Heart Failure: The Multi-Ethnic Study of Atherosclerosis. *J. Am. Heart Assoc.* **6**, (2017).
146. Leening, M. J. G. *et al.* Coronary Calcification and the Risk of Heart Failure in the Elderly. *JACC Cardiovasc. Imaging* **5**, 874–880 (2012).
147. Liu, W. *et al.* Current understanding of coronary artery calcification. *J. Geriatr. Cardiol.* **12**, 668–75 (2015).
148. Johnen, H. *et al.* Increased expression of the TGF- β superfamily cytokine MIC-1/GDF15 protects ApoE $^{-/-}$ mice from the development of atherosclerosis. *Cardiovasc. Pathol.* **21**, 499–505 (2012).
149. de Jager, S. C. A. *et al.* Growth differentiation factor 15 deficiency protects against atherosclerosis by attenuating CCR2-mediated macrophage chemotaxis. *J. Exp. Med.* **208**, 217–225 (2011).
150. Yao, Y. *et al.* A role for the endothelium in vascular calcification. *Circ. Res.* **113**, 495–504 (2013).
151. Sánchez-Duffhues, G. *et al.* Inflammation induces endothelial-to-mesenchymal transition and promotes vascular calcification through downregulation of BMPR2. *J. Pathol.* **247**, 333–346 (2019).





GDF15 as a marker and mediator of vascular dysfunction in heart failure of non-ischemic origin

In preparation

M. Wesseling^{1,2}, G. Sanchez-Duffhues³, J.J. de Haan¹, J. Tromp⁴,
T.C.L. Bracco Gartner^{1,5,6}, L. Bosch¹, M.A.D. Brans¹, S.J. Lee⁷, J.P.G. Sluiter^{1,6,8},
G. Pasterkamp^{2,8}, A.A. Voors⁴, M.J. Goumans³, S.C.A. de Jager^{1,9}

¹Laboratory of Experimental Cardiology, University Medical Center Utrecht, Utrecht, The Netherlands

²Centraal Diagnostisch Laboratorium, University Medical Center Utrecht, Utrecht, The Netherlands

³Department of Cell and Chemical Biology, Leiden University Medical Center, Leiden, The Netherlands

⁴Department of Cardiology, University Medical Centre Groningen, Groningen, The Netherlands

⁵Department of Cardiothoracic Surgery, University Medical Center Utrecht, Utrecht, the Netherlands

⁶UMC Utrecht Regenerative Medicine Center, Circulatory Health Laboratory, Utrecht, The Netherlands

⁷Department of Molecular Biology and Genetics, The Johns Hopkins University School of Medicine, Baltimore, USA

⁸Utrecht University, Utrecht, The Netherlands

⁹Laboratory of Translational Immunology, University Medical Center Utrecht, Utrecht, The Netherlands

Abstract

For proper disease management of heart failure patients of non-ischemic origin, mostly being heart failure with preserved ejection fraction (HFpEF) patients, there is an emerging demand for improved diagnostics and therapeutic interventions. Increased circulating levels of growth differentiation factor 15 (GDF15) have been associated with worse outcome in heart failure patients. However, whether GDF15 is causally involved in the pathobiology of heart failure has not been fully clarified. It is pivotal to reveal the potential causal role of GDF15 in underlying pathophysiological processes, as this will strengthen the potential of GDF15 prior to application in primary clinical care .

We show that high circulating GDF15 levels are associated with increased mortality and rehospitalization in heart failure patients of non-ischemic origin derived from the BIOSTAT-CHF cohort. In order to unveil the causative role of GDF15 in cardiac disease, we used a murine pressure overload-induced model for heart failure. We found that reduced cardiac function is accompanied by increased circulating and myocardial levels of GDF15. Furthermore, we used genetically ablated GDF15^{-/-} mice, subjected to transverse aortic constriction (TAC) to investigate the contribution of GDF15 to cardiac failure. We observed that already one-week post-TAC, cardiac remodeling and global deformation of the myocardium were significantly deteriorated in GDF15^{-/-} mice after TAC compared to the WT littermate controls. These initial differences continued into severely aggravated adverse cardiac remodeling in the GDF15^{-/-} mouse during the course of 42 days follow-up. In line, the heart weight /tibia length (HW/TL) ratio was more profoundly increased in the GDF15^{-/-} mice than in the WT mice, whereas no obvious differences in cardiomyocyte hypertrophy and global fibrosis were observed. Interestingly, focused on the cardiac microvasculature revealed a higher perivascular collagen content in GDF15^{-/-} mice compared to the WT littermates. This increase in perivascular fibrosis is indicative of endothelial dysfunction and suggestive of Endothelial to Mesenchymal transition (EndMT) as a primary underlying process. Indeed, in the same cells, fibroblast and endothelial specific markers were found co-localized in the heart of GDF15^{-/-} mice. Next, preliminary *in vitro* experiments using human Endothelial Colony Forming Cells (ECFCs), revealed that overexpression of GDF15 partially inhibits the induction of EndMT in response to pro-inflammatory cytokines tumor necrosis factor (TNF)- α and transforming growth factor (TGF)- β , thereby suggesting a protective effect of GDF15.

In summary, our results indicate that GDF15 levels are highly elevated in response to cardiac failure to prevent endothelial dysfunction in cardiac microvessels and eventually perivascular fibrosis. Future research will need to establish the protective effect of GDF15 and unravel the specific mechanisms of action of GDF15 on endothelial cells behavior.

Introduction

Growth differentiation factor 15 (GDF15), also known as macrophage inhibitory cytokine (MIC)-1, is a cytokine and distant member of the transforming growth factor (TGF)- β family¹. Genetic mutations in genes encoding for components of the TGF- β signaling pathway are often related to cardiovascular diseases (CVD)^{2,3}. Noteworthy, highly circulating GDF15 levels are associated with worse outcome in various CVDs⁴⁻⁹. In a multi biomarker approach, several studies have addressed the benefits of GDF15 in risk stratification and prognostication of patients with heart failure¹⁰⁻¹⁴. Moreover, in the development of adverse left ventricular remodeling and heart failure high GDF15 levels constitute a risk factor of worse outcome and death^{12,15-18}. For disease management of heart failure, there is an emerging demand for improved diagnostics and therapeutic interventions. In order to include GDF15 in primary clinical care in its full potential, either at biomarker or therapeutic intervention, it is pivotal to first perform comprehensive preclinical research to reveal the role of GDF15 in underlying pathophysiological processes.

GDF15 has been described to be involved in a wide range of processes, including inflammation, apoptosis, matrix remodeling and cardiomyocyte hypertrophy¹⁹. For instance, GDF15 inhibits the infiltration of neutrophils and macrophages into the heart upon myocardial infarction^{20,21}, and partially blocks cardiomyocyte apoptosis^{22,23}. The direct role of GDF15 on cardiomyocyte hypertrophy is still controversial. As such, it has been reported that *in vitro* stimulation of cardiomyocytes with GDF15 increases hypertrophy²², while others have demonstrated that GDF15 can inhibit norepinephrine induced hypertrophy²⁴. Likewise, cardiac specific overexpression of GDF15 *in vivo* inhibits cardiomyocyte hypertrophy induced by pressure-overload²⁵.

There is an ongoing debate at the potential to target endothelial cells for cardiovascular disease management, including possible treatment of the wide spectrum of heart failure^{26,27}. Reduced nitric oxide (NO) availability, impaired vascular dilatation and increased inflammatory response, contribute to endothelial dysfunction, favoring heart failure progression and eventually, leading to a fundamental impact on mortality²⁶. Endothelial to mesenchymal transition (EndMT) has appeared as a form of endothelial plasticity contributing to the onset and development of an increasing number of postnatal disorders²⁸, including cardiac fibrosis²⁹. Noteworthy, EndMT can be induced in response to several stimuli, like inflammation^{28,30}. Luan *et al.* have recently shown that GDF15 plays an important role as mediator in inflammation driven tissue tolerance to damage³¹. Indeed, GDF15 has been demonstrated to prevent cardiac damage and failure through promotion of survival in the acute phase of inflammation³¹. Therefore, there is accumulative evidence suggesting that GDF15 is an important determinant in fibrotic response mechanisms following a local inflammation.

As aforementioned, circulating GDF15 levels are elevated in patients with heart failure, which positively correlate with increased mortality. Whether GDF15 is involved in the pathogenesis of heart failure or if it is a consequence reflecting the severity of disease

inflammatory state of the heart remains unknown. In this study, we investigated the role of GDF15 in heart failure of non-ischemic origin using *in vivo* and *in vitro* models of disease. We hypothesized that deficiency of GDF15 would accelerate inflammation induced vascular dysfunction, including EndMT and consequently aggravate adverse cardiac remodeling.

Methods

Patient population and selection

The BIOlogy Study to Tailored Treatment in Chronic Heart Failure (BIOSTAT-CHF) index cohort is a multicenter, multinational, prospective, observational study which included 2516 patients with worsening signs and/or symptoms of heart failure³². Patients included were considered to be on suboptimal medical treatment and the majority of patients were hospitalized for acute heart failure. Inclusion criteria were 18 years or older, cardiac dysfunction, and currently under treatment but not for evidence based therapies³². Medical records, demographics, physical examination, blood collection and median follow-up of 21 months was available³². Blood was drawn at inclusion. The primary clinical outcome of this study was all-cause mortality and/or heart failure hospitalization within 2 years. The secondary outcome of this study was all-cause mortality at 2 years. The BIOSTAT-CHF validation cohort consisted of 1738 patients from Scotland, UK (6 centers). The BIOSTAT-CHF index and validation cohort are well matched cohorts as previously reported³³, i.e. a median follow-up of 21 months and similar secondary outcomes were present.

Animals

To establish the circulating GDF15 levels in a mouse model during heart failure, a mixed population of male and female C57BL/6J mice were used (age 9-12 weeks old, weight 20-30 gram), originally obtained from the Jackson laboratory³⁴ and bred in our breeding facility. To investigate the causal role of GDF15 in heart failure, we used female GDF15^{-/-} (KO) and their wildtype (C57Bl/6J background) littermates (age 11-13 weeks, weight 18-24 gram, Supplementary figure 1,2). All mice received standard chow and water ad libitum and were housed under filter top cages with a light/dark cycle of 12/12 hours. The researcher who performed surgery on block-random assigned animals was blinded for animal groups (blocking factor was day of surgery). Technicians and observers, who were blinded for animal groups, performed the respective operations, data acquisition and analyses. All surgeries were done in a dedicated mouse operation room. All animal experiments were approved by the Ethical Committee on Animal Experimentation of the University Medical Center Utrecht (Utrecht, the Netherlands) and conform to the 'Guide for the care and use of laboratory animals.

Transverse aortic constriction

Transverse aortic constriction surgeries were performed in a dedicated mouse operation room by an experienced surgeon as previous reported³⁵. Anesthesia was induced by

intraperitoneal (i.p.) injection of medetomidine hydrochloride (1.0 g/kg body weight), midazolam (Dormicum®, Roche, 10.0 mg/kg) and fentanyl (Janssen-Cilag, 0.1 mg/kg). Mice were intubated and connected to a respirator with a 1:1 oxygen-air ratio (175 strokes/minute, 250 µl stroke volume). A core body temperature of 37 °C was maintained during surgery by continuous rectal temperature monitoring and an automatic heating blanket. To place the transverse aortic constriction, the aortic arch was reached between two ribs after a midline incision in the anterior neck. The TAC was placed between brachiocephalic artery and the left common artery against a blunt 27-gauge needle with a 7-0 suture followed by prompt removal of the needle. Sham operated mice underwent the same procedure without aortic binding. Correct placement of the TAC was confirmed after one week by Doppler flow measurements of the carotid arteries (only flow ratio between left and right carotid >5 were considered successful and included). For 1 week survival, 9 WT and 9 GDF15^{-/-} mice got TAC surgery and 3 WT and 3 GDF15^{-/-} were sham operated, none of the mice died during 1 week follow-up. For 6 weeks survival, 18 WT and 17 GDF15^{-/-} got TAC surgery and 6 WT and GDF15^{-/-} were sham operated. As a consequence of the disease model 11 animals were lost during follow-up and final analysis was done on 13 WT TAC, 12 GDF15^{-/-} TAC, 6 WT sham and 5 GDF15^{-/-} sham (Details can be found in Supplemental figure 3).

Echocardiography

To assess cardiac geometry and function, echocardiography was used. For the TACtime study echocardiography was performed at termination. For the GDF15^{-/-} study, at baseline, 7, 14, 35 and 42 days after TAC echocardiography was performed. During echo procedure, mice were under anesthesia by inhalation of 2.0% isoflurane in a mixture of oxygen/air (1:1). Heart rate, respiration and rectal temperature were constantly monitored and body temperature was kept between 36.0 and 38.0 °C using heating lamps. Three-dimensional reconstruction echo images were made from two-dimensional images that were recorded on the short axis of the heart at multiple levels in both end systole as in end diastole, with respiratory triggering. To analyze global longitudinal strain, Vevo strain speckle-tracking software was used. Image acquisition and analyses were performed using the dedicated Vevo® 2100 System and Software (Fujifilm Visual Sonics Inc., Toronto, Canada).

Termination

Mice were exsanguinated after being anesthetized using sodium pentobarbital (60.0 g/kg). Blood was collected through orbital puncture in EDTA coated tubes for plasma collection. The vascular system was flushed with 5 mL phosphate-buffered saline (PBS) through right ventricular puncture. Heart weight and tibia length was assessed. Half of the heart was formalin-fixed for 24 hours and afterwards embedded in paraffin. The other half snap-frozen in liquid nitrogen for RNA and protein isolation.

GDF15 measurement

Human GDF15

The levels GDF15 were measured for 2300 patients using electrochemiluminescence on a cobas e411 analyzer, using standard methods³⁶ (Roche Diagnostics GmbH, Mannheim, Germany).

Murine GDF15

To assess the circulating GDF15 levels in progressive heart failure, GDF15 was measured in our large study characterizing cardiac remodeling in the TAC model (*manuscript in preparation*). In short, 104 mice underwent a TAC surgery and at different time points post-TAC (3, 7, 14, 21, 28, 35, 42, 56, 70) mice were terminated. Furthermore, 13 mice were terminated at baseline (no surgery). Final analysis was performed on 101 mice (baseline + post-TAC). GDF15 levels are measured with a mGDF15 ELISA (MGD150, Quantikine ELISA, R&D systems Inc., USA).

Primary cell isolation and cell culture

For primary cell isolation, human fetal tissue was obtained following parental permission using standard informed consent procedures. Peripheral blood samples for primary cell isolation were withdrawn after a written informed consent. The process was approved by the ethics committees of the Leiden University Medical Center, the Netherlands. This is in accordance with the principles outlined in the Declaration of Helsinki.

Human Endothelial colony-forming cells (hECFCs) represent an easy source of fully functional and highly proliferative endothelial cells. The hECFC isolation protocol requires a withdrawal of 30 to 60mL of peripheral blood in citrate-treated collection tubes. The ECFCs are isolated as previously described³⁷. In short, prediluted blood (1:1 with prewarmed 1xPBS) was centrifuged at 740g for 30 min with Ficoll Paque Plus (GE Healthcare Europe GmbH, Eindhoven, The Netherlands), to separate a fraction containing mononuclear cells (MNCs). After several wash steps with M199 (Lonza, Verviers, Belgium) supplemented with 0.1% penicillin/streptomycin (Invitrogen, Leek, The Netherlands), cells are resuspended in complete EGM-2 (Lonza) supplemented with 20% Fetal Bovine Serum (FBS) and 0.1% penicillin–streptomycin and seeded into 48-well plates precoated with 3µg/cm² human collagen type I (#C7624, Sigma Aldrich). After 24 hours, nonadherent cells were carefully removed and fresh medium was added to each well. From this moment, the medium is replaced every day and supernatants discarded. ECFC colonies with regular cobblestone morphology appear within 3 to 4 weeks. Isolated ECFCs are then maintained in EGM-2 (Lonza) supplemented with 10% FBS and 0.1% penicillin/streptomycin (Invitrogen). All experiments were performed with cells grown to near-confluency between passage 6 and 8.

Human fetal Cardiac fibroblasts were isolated in subsequently performed procedure as previously published. After subtraction of Sca-1 positive cells, the remaining dissolved heart tissue was plated overnight on tissue culture treated plastic to allow fibroblast

to adhere. hFCF were cultured in fibroblast medium (FM) containing DMEM (4.5 g/L glucose; Gibco), 10% FBS, and 1% P/S. Cells were cultured until 90% confluency and passaged in a 1:3 ratio before experimental use at passage 4–7. Cells were maintained at 5% CO₂, 20% O₂, 37°C, in a humidified atmosphere.

Lentiviral production, transduction and generation of a GDF15 over-expression construct

Lentiviral vectors were produced in HEK293T cells as previously described³⁸. Human GDF15 (NM_004864) coding sequence was amplified by PCR from 1 µg of RNA from HUVECs using the oligos hGDF15EcoRV-FW: ATAGGATATCATGCCCGGGCAAGAACTCAG and hGDF15XhoI-RV: CTATCTCGAGTCATATGCAGTGGCAGTCTT. Amplified DNA was subsequently digested with EcoRV and XhoI and ligated into a previously described lentiviral pLV-IRES-Puro vector. The obtained pLV-GDF15 vector was confirmed by Sanger sequencing. Stable hECFCs infected with either control (empty) viruses or pLV-GDF15 were selected by adding puromycin (1 µg/mL) for 48 hours two days after infection.

EndMT assays

hECFCs were seeded at confluence in 12-well plates (for qPCR) or Lab-Tek II chamber slides (for immunofluorescence) in EBM2 complete medium containing 2% FBS. Next day, the cells were stimulated with the indicated ligands for 24 h in EBM2 complete medium containing 10% FBS, and endothelial and mesenchymal-specific markers were analyzed by RT-qPCR or immunofluorescent labeling.

Fibroblast activation assay

To study the effects of GDF15 on cardiac fibroblast activation, hFCF were used in a 3D hydrogel model as previously reported³⁹. In short, hFCFs were cultured in a 3D gelatin methacryloyl hydrogel in fibroblast medium. Thereafter, cells were stimulated with 1 and 10 ng GDF15, a kind gift of Dr. Marko Hyvönen (University of Cambridge, UK), 1 ng TGF-β3, a kind gift of Dr. Joachim Nickel, (Universitätsklinikum Würzburg, Germany) and 1 ng BMP9 (R&D systems.) for 7 days. At day 7, specific markers for fibroblast activation were analyzed by RT-qPCR.

Histology

Mouse tissue

Paraffin embedded murine hearts were cut in 5 µm thick sections. Before staining, sections were deparaffinized 2x 8 minutes in Ultraclear (1466, Sakura), 2x 5 minutes in 100% EtOH (4099.9005, Klinipath), 2x 5 minutes in 96% EtOH (Klinipath), 5 minutes in 70% EtOH (Klinipath), 5 minutes in Demi H₂O). For immunofluorescent staining's, antigen retrieval was performed by boiling in citrate buffer for 20 minutes. To examine cell size, Wheat Germ Agglutinin (WGA) staining was performed. WGA-FITC labeled antibody

was incubated (1:40, L4895, Sigma Aldrich) for 30 minutes at room temperature (RT). To visualize blood vessels (both micro and macro), a double staining for α Smooth Muscle Actin (α SMA) and CD31 was performed. Mouse anti- α SMA-FITC (1:400, clone 1A4, F3777, Sigma) was used for 1 hour at RT and Rabbit-anti-mouse CD31 (1:1500, Santa Cruz, sc-1506, 0.5 mg/ml) overnight at 4°C followed by polyclonal goat-anti-rabbit biotin (1:200, Vector, BA1000) for 30 min at RT and Streptavidin-Alexa 555 (1:1000, Invitrogen, S21381) for 1 hour at RT. Due to technical problems with embedding of some of the tissues were unsuitable for reliable histological assessment. We therefore included an additional set of 12 WT and 12 KO mice exposed to TAC (42 days follow-up) with the specific aim to supplement the histological assessment of fibrosis and presence of EndMT. No differences in cardiac function or remodeling are found with mice previously mentioned (*data not shown*). Quantification of collagen density was performed using a Masson's Trichrome staining. Collagen density analysis was done with a semi quantitative analysis.

Immunofluorescent labeling of cultured cells

ECFCs grown on coverslips were fixed with 4% formaldehyde for 30 min at room temperature, washed with glycine for 5 min, permeabilized with 0.2% Triton X-100, and blocked in PBS containing 5% BSA for 1 h. The cells were incubated overnight at 4°C with primary antibody in blocking solution with gentle shaking. Next day, the cells were washed five times in washing buffer (PBS containing 0.05% Tween-20 and 1% BSA) and incubated with secondary antibody (Alexa-Fluor FITC goat anti-mouse IgG, Alexa-Fluor 555 anti-rabbit IgG; Invitrogen; 1:200) or with phalloidin-488 (1:100) in PBS with 0.5% BSA for 1 h. Finally, the cells were washed five times in washing buffer and mounted in Prolong Gold containing DAPI (Invitrogen). Preparations were imaged in a Leica SP5 confocal scanning laser microscope. The antibodies used are described in supplemental table 1.

Quantitative real-time RT-PCR (qPCR)

Mouse tissue

For total RNA extraction, murine hearts were mechanically disrupted in 1 ml TriPure (Roche), (extracellular) debris was removed by centrifugation at 12.000 x g for 10 min. Next, 200 μ L of chloroform was added to the supernatant and the aqueous phase was separated by centrifugation at 12.000 x g for 15 min. The liquid phase (~350 μ L) was mixed 1:1 with 70% ethanol and further processed to obtain RNA. 500ng of RNA was reverse transcribed using RevertAid First Strand cDNA Synthesis Kits (Biorad, Veenendaal). Quantitative PCR (qPCR) experiments were performed using SYBR Green (Bio-Rad, Veenendaal, The Netherlands) and a Bio-Rad CFX Connect device. Threshold cycle values (Ct) were analyzed and expression was quantified using the 2^{-ddCt} method. A list of used primers can be found in supplemental table 1.

Cell culture

For both ECFCs and fCFs, total RNA extraction was performed using NucleoSpin RNA II (Machery Nagel, Düren, Germany). The hfCF-laden GelMA hydrogels were mechanically disrupted in 1 ml TriPure (Roche), (extracellular) debris was removed by centrifugation at 12.000 x g for 10 min. Next, 200 µL of chloroform was added to the supernatant and the aqueous phase was separated by centrifugation at 12.000 x g for 15 min. The liquid phase (~350 µL) was mixed 1:1 with 70% ethanol and transferred to the isolation column after which the manufacturer's instructions were followed.

500ng of RNA was reverse transcribed using RevertAid First Strand cDNA Synthesis Kits (Fermentas/Thermo Fisher Scientific, Freemont, CA, USA). Quantitative PCR (qPCR) experiments were performed using SYBR Green (Bio-Rad, Veenendaal, The Netherlands) and a Bio-Rad CFX Connect device. Threshold cycle values (Ct) were corrected for baseline expression of house hold genes (s28 and GAPDH) and expression was quantified using the 2^{-ddCt} method. A list of used primers can be found in supplemental table 1.

Statistical analysis

Patient data

Normally distributed variables were shown as mean with standard deviation, non-normally distributed variables as median with 25th–75th percentile, and categorical variables as numbers with percentages. Group differences were studied with t tests and one-way analysis of variance for normally distributed variables, Kruskal–Wallis and Mann–Whitney U tests for non-normally distributed continuous variables, and χ^2 tests for categorical variables. Multiple linear regression models were used to investigate the associations between GDF15 and the heart failure groups. Log-transformed biomarkers were used in the regression analyses. Multivariable survival analyses were performed using Cox regression models, correcting for the BIOSTAT-CHF risk model. The BIOSTAT risk model for predicting mortality included, age, blood urea nitrogen (BUN), N-terminal NT-proBNP, haemoglobin, and the use of a beta-blocker at time of inclusion. The BIOSTAT risk model for predicting mortality or heart failure hospitalization included age, NT-proBNP, haemoglobin, the use of a beta-blocker at time of inclusion, a heart failure hospitalization in year before inclusion, peripheral edema, systolic blood pressure, high-density lipoprotein cholesterol, and sodium.

In vivo and in vitro data

We used ESV as a clinical surrogate for heart failure as primary outcome measure to perform group size calculation. We powered, based on 2D echo imaging, for a difference of 0.4 mm ESV, which, with a power of 90%, alpha of 0.05, standard deviation of 0.29mm² and maximum mortality of 20%, culminates in 15 animals per group for TAC. Data are presented as mean±SD. Mixed models was used for repeated measurements (EDV, ESV and GLS), with a random intercept for each mouse and as fixed factors group and time

point. To determine whether the time course of the parameters was different for the groups, the interaction group*time point of measurement was also taken into the model. Heart weight/tibia length, WGA, Masson's trichrome, CD31 and qPCRs were analyzed with a student's T-test. Statistical analyses were performed using SPSS and GraphPad Prism 6 and $p \leq 0.05$ was considered statistically significant. All *in vitro* results are shown as mean \pm SD, representative data are shown in the figures.

Results

Patient characteristics

Baseline characteristics of 2300 patients included in BIOSTAT-CHF are reported in table 1, where heart failure patients were stratified into four quartiles ($n=575$ per group) based on GDF15 plasma levels (respectively 400-1707, 1709-2718, 2722-4563 and 4577-40000 pg/ml GDF15) (Table 1). Patients with increasing levels of GDF15 were significantly older, median age increased from 62.7 ± 11.9 to 72.0 ± 11.1 years ($p < 0.001$) with no differences in male to female ratio. Furthermore, increased levels of GDF15 positively correlates with diagnose of diabetes mellitus, chronic obstructive pulmonary disease (COPD), blood disorders, severe heart failure and multiple cardiovascular conditions. No differences were observed for hypertension, body mass index (BMI) and sex between the different groups of GDF15 levels.

Associations circulating levels of GDF15 with risk factors and clinical outcome in heart failure

Regression modeling was performed to analyze the relation between risk factors, heart failure and cardiac function with GDF15 levels. All risk factors represented in table 2, including age, sex, BMI, kidney function based on the estimated Glomerular Filtration Rate (eGFR) and diabetes were associated with continuous levels of GDF15 levels. However, the levels of GDF15 were not associated with heart failure symptoms according to the New York Heart Association (NYHA) functional classification or Left ventricular ejection fraction (LVEF) representing the cardiac function in patients.

Furthermore, GDF15 levels were not associated with patients with a prior ischemic event. To confirm previously described observations that higher levels of GDF15 were associated with adverse cardiovascular outcome in patients with heart failure of non-ischemic condition, we performed multivariable survival analyses using Cox regression models (Figure 1 and Table 3). After correcting for possible confounders with the BIOSTAT risk model for mortality (including age, blood urea nitrogen, NT-proBNP, haemoglobin and use of beta-blockers) higher levels of GDF15 associated with an increased all-cause mortality during 2-year follow-up (Figure 1a and Table 3, Hazard Ratio (HR) 1.26 (95% CI 1.16-1.37), $p < 0.001$). The associations between GDF15 and outcome were confirmed in the BIOSTAT-CHF validation cohort, where cox-regression analysis showed a strong association of GDF15 levels with all-cause mortality, HR 1.94 (95% CI 1.67-2.25), $p < 0.001$

Table 1. Baseline characteristics of patients categorized into GDF15 levels in BIostat CHF.

Risk factors	Q1 GDF15 400-1707 pg/ml n=575	Q2 GDF15 1709-2718 pg/ml n=575	Q3 GDF15 2722-4563 pg/ml n=575	Q4 GDF15 4577-40000 pg/ml n=575	p-value
Age (years), mean (SD)	62.7 (11.9)	69.3 (11.3)	71.4 (11.5)	72.0 (11.1)	<0.001
Women, n (%)	154 (27.2)	158 (27.6)	146 (25.6)	139 (24.4)	0.590
BMI (kg/m ²), mean (SD)	28.2 (5.4)	27.9 (5.2)	27.5 (5.6)	27.8 (5.8)	0.160
Smoking					
None	197 (34.8)	203 (35.4)	226 (39.6)	209 (36.9)	0.016
Past	283 (50.0)	268 (46.8)	268 (46.9)	297 (52.5)	
Current	86 (15.2)	102 (17.8)	77 (13.5)	60 (10.6)	
Diabetes mellitus, n (%)	104 (18.4)	173 (30.2)	197 (34.5)	262 (46.0)	<0.001
COPD, n (%)	63 (11.1)	105 (18.3)	122 (21.4)	105 (18.5)	<0.001
Hypertension, n (%)	324 (57.2)	366 (63.9)	363 (63.6)	364 (64.0)	0.050
eGFR (MDRD) (mL/min/1.73 m ²), median (IQR)	76.4 (62.4, 93.6)	65.8 (52.5, 79.8)	56.7 (44.6, 76.3)	48.6 (35.0, 63.6)	<0.001
Hepatomegaly, n (%)	51 (9.0)	69 (12.1)	85 (14.9)	119 (21.1)	<0.001
Anemia yes, n (%)	94 (18.9)	157 (30.0)	214 (40.7)	296 (55.2)	<0.001
Orthopnea, n (%)	127 (22.5)	175 (30.5)	228 (39.9)	258 (45.7)	<0.001
Clinical presentation					
LVEF (%), mean (SD)	29.9 (8.5)	31.7 (10.4)	31.9 (12.0)	30.5 (11.4)	0.007
HF classification based on LVEF, n (%)					
HFrEF	460 (87.5)	422 (81.0)	388 (76.1)	380 (79.3)	<0.001
HFmrEF	53 (10.1)	67 (12.9)	69 (13.5)	68 (14.2)	
HFpEF	13 (2.5)	32 (6.1)	53 (10.4)	31 (6.5)	
Ischemic etiology, n (%)	223 (40.2)	249 (44.5)	255 (45.4)	303 (53.9)	<0.001
NYHA prior to worsening HF, n (%)					
Class I	66 (11.7)	70 (12.2)	46 (8.1)	29 (5.1)	<0.001
Class II	300 (53.0)	258 (45.0)	259 (45.4)	240 (42.2)	
Class III	124 (21.9)	166 (29.0)	168 (29.4)	193 (33.9)	
Class IV	10 (1.8)	13 (2.3)	21 (3.7)	33 (5.8)	
Not assessed	66 (11.7)	66 (11.5)	77 (13.5)	74 (13.0)	
SBP (mmHg), mean (SD)	126.4 (20.8)	126.6 (23.1)	124.2 (22.0)	120.8 (21.2)	<0.001
DBP (mmHg), mean (SD)	77.4 (12.8)	76.4 (14.0)	74.2 (13.1)	71.6 (12.1)	<0.001
Heart rate (/min), mean (SD)	78.6 (19.5)	79.1 (19.2)	81.2 (19.3)	80.7 (20.2)	0.068
Peripheral edema, n (%)					
Not Present	280 (61.9)	213 (45.5)	164 (34.2)	109 (22.2)	<0.001
Ankle	114 (25.2)	149 (31.8)	166 (34.7)	124 (25.2)	
Below Knee	52 (11.5)	85 (18.2)	114 (23.8)	177 (36.0)	
Above Knee	6 (1.3)	21 (4.5)	35 (7.3)	82 (16.7)	

Table 1. Continued

Risk factors	Q1 GDF15 400-1707 pg/ml n=575	Q2 GDF15 1709-2718 pg/ml n=575	Q3 GDF15 2722-4563 pg/ml n=575	Q4 GDF15 4577-40000 pg/ml n=575	p-value
Elevated JVP, N (%)					
No	309 (78.2)	274 (69.5)	225 (55.7)	186 (46.4)	<0.001
Yes	66 (16.7)	102 (25.9)	157 (38.9)	185 (46.1)	
Uncertain	20 (5.1)	18 (4.6)	22 (5.4)	30 (7.5)	
Device therapy, n (%)					
None	460 (81.3)	451 (78.7)	432 (75.7)	376 (66.1)	<0.001
Pacemaker	23 (4.1)	38 (6.6)	48 (8.4)	55 (9.7)	
ICD	42 (7.4)	32 (5.6)	42 (7.4)	66 (11.6)	
Biventricular Pacer (CRT)	5 (0.9)	12 (2.1)	14 (2.5)	15 (2.6)	
Biventricular Pacer (CRT) and ICD	35 (6.2)	38 (6.6)	32 (5.6)	55 (9.7)	
Other	1 (0.2)	2 (0.3)	3 (0.5)	2 (0.4)	
Clinical history					
Atrial fibrillation, n (%)	193 (34.1)	248 (43.3)	273 (47.8)	311 (54.7)	<0.001
PAD, n (%)	33 (5.8)	63 (11.0)	69 (12.1)	81 (14.2)	<0.001
Stroke, n (%)	36 (6.4)	55 (9.6)	48 (8.4)	74 (13.0)	0.001
PCI, n (%)	99 (17.5)	136 (23.7)	134 (23.5)	136 (23.9)	0.023
CABG, n (%)	62 (11.0)	85 (14.8)	102 (17.9)	143 (25.1)	<0.001
Medication at inclusion					
Loop Diuretics (%)	563 (99.5)	572 (99.8)	568 (99.5)	566 (99.5)	0.750
ACE/ARB (%)	437 (77.2)	430 (75.0)	416 (72.9)	362 (63.6)	<0.001
Beta-blocker (%)	490 (86.6)	481 (83.9)	460 (80.6)	465 (81.7)	0.036
Blood parameters					
Hemoglobin (g/dL), mean (SD)	13.8 (1.7)	13.4 (1.8)	13.0 (1.9)	12.5 (2.0)	<0.001
Total cholesterol (mmol/L), median (IQR)	4.6 (4.0, 5.5)	4.3 (3.6, 5.3)	3.9 (3.2, 4.8)	3.5 (3.0, 4.2)	<0.001

This table represents the baseline characteristics of patients within BIostat-CHF based on their GDF15 level. Abbreviations: ACE; Angiotensin Converting Enzyme, ARB; Angiotensin-receptor blockers, PAD; Peripheral arterial Disease, PCI; Percutaneous Coronary Intervention, CABG; Coronary Artery Bypass Grafting, BMI; Body Mass Index, SBP; Systolic Blood Pressure, DBP; Diastolic Blood Pressure, LVEF; Left Ventricular Ejection Fraction, HFpEF; Heart Failure with preserved Ejection Fraction, HFrEF; Heart Failure with reduced Ejection Fraction, HFmrEF; Heart Failure with mid-range Ejection Fraction, ICD; Implantable cardioverter-defibrillator, COPD; Chronic Obstructive Pulmonary disease, NYHA; New York Heart Association, eGFR; estimated Glomerular Filtration Rate. Comparing quartiles, a p value <0.05 is considered statistically significant.

Table 2. Association of risk factors and hearth failure classification and with GDF15 levels.

Risk Factor	Beta	p-value
Age (years)	0.09	<0.001
Sex	-0.06	0.002
SBP	-0.06	0.001
Diabetes Mellitus	0.15	<0.001
Anemia	0.08	<0.001
BMI	0.05	0.009
eGFR (mL/min/1.73 m ²)	-0.21	<0.001
NT-proBNP	0.42	<0.001
Heart function		
LVEF (%)	0.022	0.279
NYHA classification		
I	Ref.	
II	0.03	0.418
III	0.06	0.071
IV	0.03	0.204

Table represents the multiple linear regression models used to investigate the associations between GDF15 and the cardiovascular risk factors and parameters of cardiac function. Log-transformed biomarkers were used in the regression analyses. Abbreviations, eGFR; estimated Glomerular Filtration Rate, BMI; Body Mass Index, SBP; Systolic Blood Pressure, NT-proBNP. A p-value <0.05 is considered statistically significant.

(Table 3). Next, we assessed if high levels of GDF15 also associated with a combined endpoint containing all-cause mortality combined with re-hospitalization for heart failure in both univariate and multivariate analysis (correcting for possible confounders with the BIOSTAT risk model including age, blood urea nitrogen, NT-proBNP, heamoglobin, use of beta-blocker, heart failure hospitalization in year before inclusion, peripheral edema, systolic blood pressure, high-density lipoprotein cholesterol, and sodium level) showed that the combined endpoint, of re-hospitalization and all-cause mortality, was more frequently observed in patients with increased GDF15 levels in a two-year follow-up period (Figure 1 and Table 3, HR 1.13 (95% CI 1.05-1.21) p<0.001). Again this was confirmed in the BIOSTAT-CHF validation cohort, where we found a strong association of GDF15 levels with all-cause mortality and re-hospitalization (HR 1.58 (95% CI 1.40-1.78) <0.001) after corrections for the appropriate BIOSTAT risk model (Table 3). Our data clearly show that high levels of GDF15 associate with worse outcome after two-years follow-up in patients with end stage heart failure of non-ischemic origin.

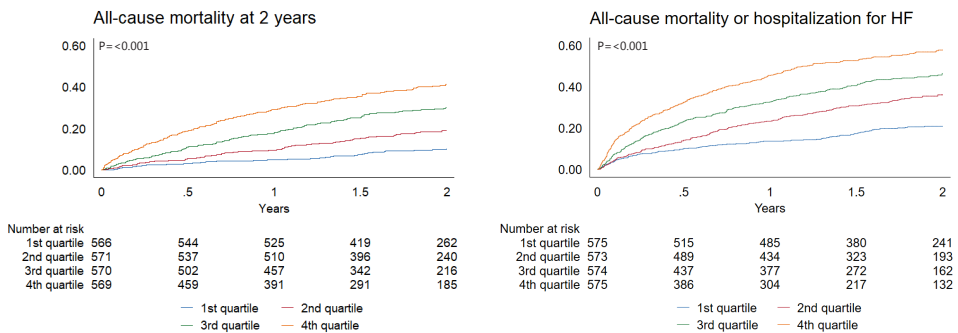


Figure 1. All-cause mortality and hospitalization for heart failure during 2-year follow-up.

Multivariable survival analyses were performed using Cox regression models, corrected for the BIOSTAT-CHF risk model. Patient quartiles are based on circulating levels of GDF15; 1st quartile: 400-1707 pg/ml, 2nd quartile: 1709-2718 pg/ml, 3rd quartile: 2722-4563 pg/ml, 4th quartile: 4577-40000 pg/ml. High levels of GDF15 are represented in the 4th quartile and show higher risk for mortality and heart failure hospitalization compared to patients in the 1st quartile in a 2-year follow-up period.

Table 3. BIOSTAT-CHF index and validation cohort, increased all-cause mortality and hospitalization after heart failure during 2 years follow-up.

	GDF15 (log-transformed)		
	HR	95%CI	p-value
Mortality (Index cohort)			
Univariate	1.68	(1.57-1.81)	<0.001
BIOSTAT risk model	1.26	(1.16-1.37)	<0.001
Mortality (Validation cohort)			
Univariate	2.85	(2.53-3.21)	<0.001
BIOSTAT risk model	1.94	(1.67-2.25)	<0.001
Mortality and/or HF-hospitalization (Index cohort)			
Univariate	1.51	(1.43-1.60)	<0.001
BIOSTAT risk model	1.13	(1.05-1.21)	<0.001
Mortality and/or HF-hospitalization (Validation cohort)			
Univariate	2.29	(2.07-2.52)	<0.001
BIOSTAT risk model	1.58	(1.40-1.78)	<0.001

Multivariable survival analyses in the BIOSTAT index and validation cohort, were performed using Cox regression model corrected for the BIOSTAT-CHF risk models. The BIOSTAT risk model for predicting mortality included, age, blood urea nitrogen (BUN), N-terminal NT-proBNP, haemoglobin, and the use of a beta-blocker at time of inclusion. The BIOSTAT risk model for predicting mortality or heart failure hospitalization included age, NT-proBNP, haemoglobin, the use of a beta-blocker at time of inclusion, a heart failure hospitalization in year before inclusion, peripheral edema, systolic blood pressure, high-density lipoprotein cholesterol, and sodium. A p-value <0.05 is considered statistically significant.

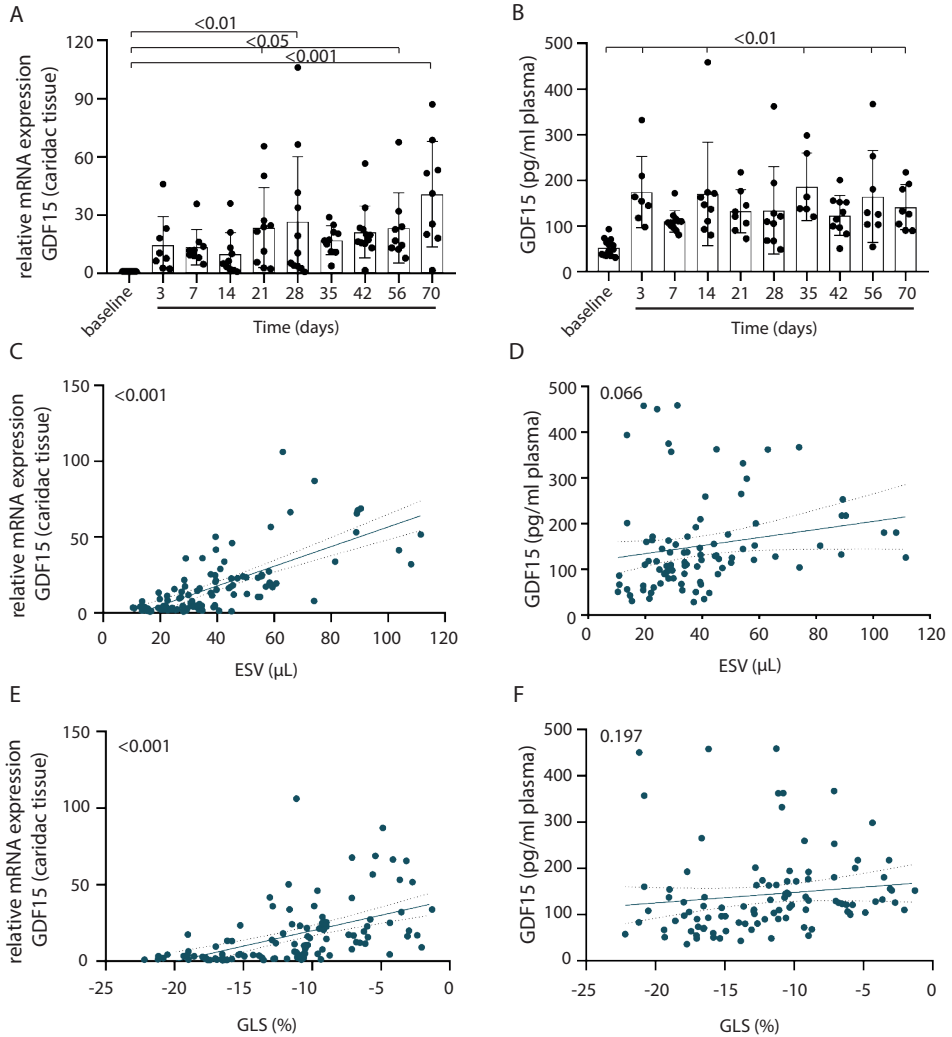


Figure 2. Circulating GDF15 levels increased with heart failure induced by pressure overload.

Upon induction of pressure overloaded heart failure, a deterioration of ESV (a) and GLS (b) are observed over time post-TAC. With reduced cardiac function, an increase in the HW/TL ratio(c) indicates an enlarged heart size indicative of structural cardiac remodeling. The GDF15 levels are higher upon heart failure (d), however do not increase progressively over time post-TAC. In contradiction to the relative expression of GDF15 in cardiac tissue which is progressively increased over time post-TAC (e). Mean \pm SD. Abbreviations, ESV; End Systolic Volume, GLS; Global Longitudinal Strain, HW/TL; Heart Weight / Tibia Length ratio. A p-value <0.05 is considered statistically significant.

Circulating GDF15 levels in pressure overloaded heart failure in mice

To establish if GDF15 levels, similar to our observation in patients, associate to heart failure progression we first set out to determine circulating levels and cardiac tissue expression of GDF15 in a murine non-ischemic heart failure model. During pressure overloaded heart failure post-TAC, qPCR analysis was used to assess the cardiac expression of GDF15 and results showed a progressive increase in expression of GDF15 over time (Figure 2a). Circulating levels of GDF15 measured in plasma increased already after 3 days of TAC and remained non progressively elevated over time post-TAC (Figure 2b). Increased levels at day 3 may be a response to the surgery itself. With deteriorating cardiac function over time determined by an increase in End Systolic Volume (ESV), the cardiac expression of GDF15 was increased as well ($p < 0.001$) (Figure 2c), including a trend towards circulating protein levels of GDF15 ($p = 0.066$) (Figure 2d). In line, cardiac expression of GDF15 correlated to cardiac stiffening measured by the GLS ($p < 0.001$) (Figure 2e), although no association was found between GLS and circulating GDF15 protein levels ($p = 0.197$) (Figure 2f). These results show that in the mouse, circulating GDF15 reflect presence of cardiac disease and cardiac GDF15 expression may point to a causal role for GDF15 in the underlying pathophysiological process of adverse cardiac remodeling.

Adverse cardiac remodeling is more severe in GDF15^{-/-} mice in response to cardiac pressure overload

To assess the contribution of GDF15 to heart failure and cardiac remodeling, GDF15^{-/-} mice and their WT littermates were subjected to pressure overload induced heart failure by means of transverse aortic constriction (TAC). Two GDF15^{-/-} mice and 1 WT mouse were excluded based on improper placement of the TAC (flow ratio < 5 , Supplemental figure 2). During the 42 days follow-up after TAC, $\approx 30\%$ (5 out of 16) of GDF15^{-/-} and $\approx 20\%$ (4 out of 18) WT mice died due to heart failure (Supplemental figure 2). GDF15^{-/-} mice showed a more severe adverse remodeling of the heart compared to WT littermates after one week of TAC, as seen by ESV ($41.4 \pm 10.6 \mu\text{l}$ vs. $31.2 \pm 5.7 \mu\text{l}$, $p = 0.031$) and by a decrease in cardiac deformation, reflected by GLS analyses ($-11.8 \pm 2.8\%$ vs. $-15.5 \pm 2.7\%$, $p < 0.001$) (Figure 3a,c) which progressively continued up to 42 days of follow-up. After 42 days, both EDV and ESV were significantly larger in GDF15^{-/-} mice compared to the WT littermates (EDV: $89.1 \pm 24.6 \mu\text{l}$ vs. $64.5 \pm 6.6 \mu\text{l}$, $p < 0.001$. ESV: $67.2 \pm 25.8 \mu\text{l}$ vs. $39.1 \pm 4.9 \mu\text{l}$, $p < 0.001$) (Figure 3a, b). Similarly, heart weight/tibia length ratios were more increased in GDF15^{-/-} mice compared to WT mice ($118.1 \pm 24.1 \text{ mg/cm}$ vs. $93.5 \pm 11.0 \text{ mg/cm}$, $p = 0.004$) (Figure 3d). In summary, we conclude that cardiac function is severely impaired in GDF15^{-/-} mice compared to WT littermates.

Structural changes in cardiac tissue GDF15^{-/-} mice post-TAC

To assess structural differences in cardiac remodeling, cardiomyocyte hypertrophy, vessel density and collagen content were evaluated in cardiac tissue. As expected, cardiomyocytes hypertrophy was increased upon TAC compared with sham operated

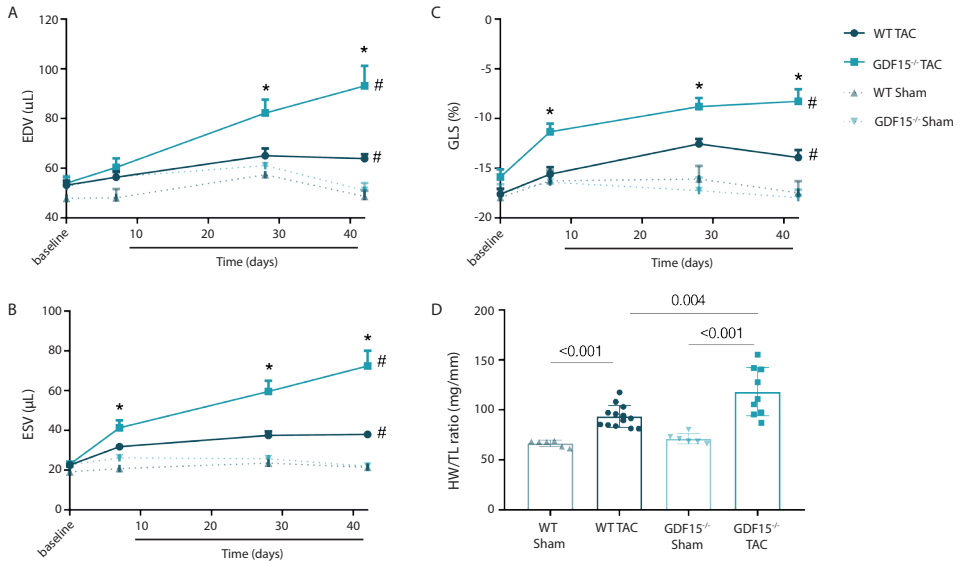


Figure 3. Adverse cardiac remodeling and function in GDF15^{-/-} mice.

Following TAC both ESV (a) end EDV (b) increases in WT mice. This increase is aggravated in GDF15^{-/-} mice. GLS is already affected in GDF15^{-/-} mice 1 week after TAC (c). Also, the increase in heart weight/ tibia length (HW/TL) ratio is more pronounced in GDF15^{-/-} mice compared to WT littermates (d). WT sham n=6, WT TAC n=13, GDF15^{-/-} sham n=6, GDF15^{-/-} TAC n=9. Mean±SD. *p <0.05 compared to baseline, #p<0.001 compared to Sham animals. Abbreviations, ESV; End Systolic Volume, EDV; End Diastolic Volume, GLS; Global longitudinal Strain. WT: Wild type. GDF15^{-/-}: GDF15 knock-out.

mice ($235.5 \pm 25.9 \mu\text{m}^2$ vs. $295.7 \pm 25.3 \mu\text{m}^2$ in WT Littermates ($p=0.001$) and $216.6 \pm 13.0 \mu\text{m}^2$ vs $291.5 \pm 30.3 \mu\text{m}^2$ in GDF15^{-/-} mice ($p<0.001$), with no apparent differences between sham mice ($235.5 \pm 25.9 \mu\text{m}^2$ in WT vs $216.6 \pm 13.0 \mu\text{m}^2$ in GDF15^{-/-}, $p=0.3$) or mice who underwent TAC surgery ($295.7 \pm 25.3 \mu\text{m}^2$ in WT vs $291.5 \pm 30.3 \mu\text{m}^2$ in GDF15^{-/-}, $p=1.0$)(Figure 4a, b). The number of micro vessels per cardiomyocyte was quantified using CD31 staining (Figure 4c). There was no increase in the number of micro vessels per cardiomyocyte after TAC, nor did we observe a difference between WT mice (1.3 ± 0.2 CD31⁺/nucleus vs. 1.4 ± 0.2 CD31⁺/nucleus, $p=0.1$) and GDF15^{-/-} mice (1.2 ± 0.2 CD31⁺/nucleus vs. 1.2 ± 0.1 CD31⁺/nucleus, $p=0.8$) (Figure 4b). It has been previously shown that cardiac interstitial fibrosis in mice increases upon TAC induction⁴⁰ and circulating GDF15 levels have been correlated with fibrosis levels in human heart failure patients⁴¹. Therefore, we determined collagen deposition by Trichrome staining (Figure 4e) and quantified this semi-quantitatively (Figure 4e). No difference in interstitial collagen content was observed between WT and GDF15^{-/-} mice (WT: 3.4 ± 1.0 vs. GDF15^{-/-}: 3.2 ± 0.9 , (arbitrary units, $p=0.6$)) (Figure 4e, f). Furthermore, we performed *in vitro* fibroblast activation assays in human cardiac fibroblasts to assess the effects of GDF15 in the production of Col1a1 (Figure 5). Ectopic TGF- β administration effectively induced the expression of Acta2 and Col1a1 ($p<0.001$), while BMP-9 administration induced only Acta2 expression.

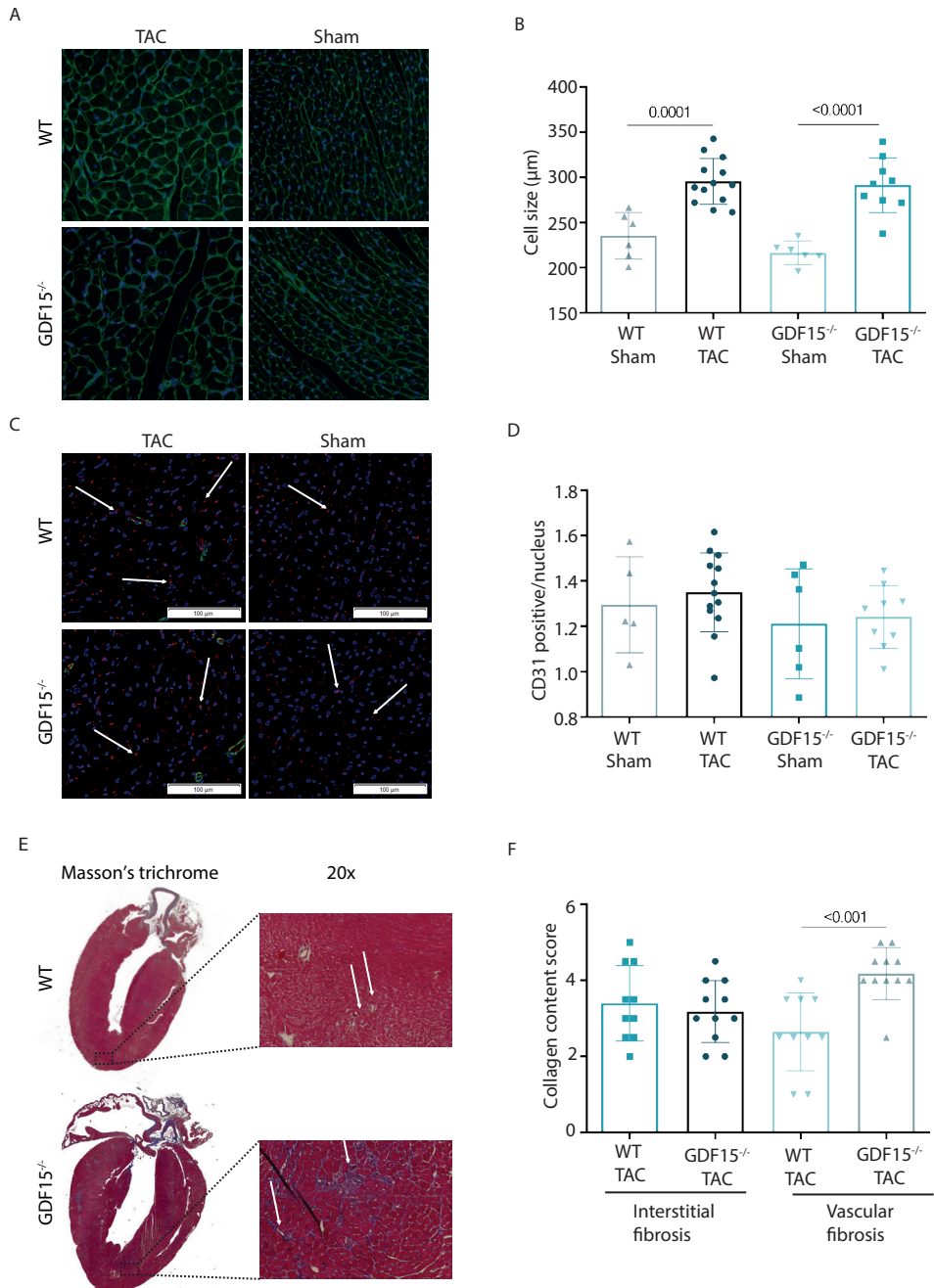


Figure 4. Hypertrophy, fibrosis and vasculature in cardiac remodeling.

Representative pictures of the WGA staining displaying cardiomyocyte cell size (a). Quantification of the cardiomyocyte cell size is in both WT and GDF15^{-/-} post-TAC compared to Sham animals. Post-TAC both WT and GDF15^{-/-} mice show an increase in cell size compared to the Sham mice (b) WT Sham n=6, WT TAC n=13, ▶▶▶

◀◀◀ GDF15^{-/-} Sham n=6, GDF15^{-/-} TAC n=9. To investigate the number of blood vessels per cardiomyocyte, a CD31 staining was performed (representative pictures in c). Quantification of the CD31 staining per nucleus showed no differences between the 4 groups of animals (d) WT Sham n=6, WT TAC n=13, GDF15^{-/-} Sham n=6, GDF15^{-/-} TAC n=9. To assess the amount of collagen content, cardiac tissue was stained with a Masson's trichrome (representative pictures in e). Quantification showed no differences in interstitial fibrosis but an increase in vascular fibrosis in the GDF15^{-/-} mice (f), WT TAC n=10, GDF15^{-/-} TAC n=11. Mean±SD. p<0.05 is considered significant.

Interestingly, exogenous addition of recombinant GDF15 had no effect on Acta2 and Col1a1 gene expression, alone or in combination with TGF-β3 or BMP-9. This suggests that increased amounts of interstitial collagen content are not under influence of GDF15. Strikingly, perivascular collagen content was significantly higher in GDF15^{-/-} mice compared to WT littermates (WT: 2.7 ± 1.0 vs. GDF15^{-/-}: 4.2 ± 0.7, p<0.001) (Figure 4e, f). Our results indicate that progressive heart failure and adverse cardiac remodeling may be correlated with microvascular fibrosis in GDF15 deficient mice. Therefore, we decided to investigate the role of GDF15 in endothelial cells.

Endothelial dysfunction in GDF15^{-/-} mice post-TAC

We previously shown that GDF15 expression in the murine heart is increased in response to cardiac injury. As endothelial dysfunction and more specific endothelial to mesenchymal transition (EndMT), has been associated with cardiac and perivascular fibrosis^{29,42,43}, we determined the degree of co-localization of endothelial and mesenchymal markers (defined as no, minor, moderate and major) indicative of EndMT in mice subjected to TAC (Figure 6). When comparing the hearts of GDF15^{-/-} mice and WT littermates, we observed a more frequent co-localization of endothelial CD31 (Platelet endothelial cell adhesion molecule-1, Pecam1) and mesenchymal α-SMA (α-smooth muscle actin) in microvessels within GDF15^{-/-} mice (Figure 6a). Assessing the presence of both markers, showed that no to minor co-localization was present in the WT mice, while minor to major amount of co-localization was observed in GDF15^{-/-} mice (Figure 6b). As the co-localization of CD31 and α-SMA is indicative for EndMT, these results suggest that GDF15 may protect cardiac endothelial cells to undergo EndMT in response to heart failure. In order to further support these results, we performed a qPCR analysis in heart bulk RNA to assess several endothelial and mesenchymal markers (i.e. endothelial Pecam1, CDH5, and mesenchymal FN1, ACTA2). However, we did not observe differences in expression of endothelial and mesenchymal markers between the WT and GDF15^{-/-} mice (Figure 6c).

GDF15 inhibits inflammation induced EndMT

In order to analyze the effect of GDF15 expression on EndMT in a cell autonomous manner, we generated primary human endothelial colony forming cells over-expressing GDF15 using a lentiviral vector. Even though we achieved high levels of GDF15 expression in these cells (Supplemental figure 3), we did not observe obvious morphological differences at baseline (Supplemental figure 3). Next, we induced EndMT in control or GDF15 over-expressing using either TNF-α or TGF-β3 both known to be able to induce EndMT (Figure 7). After 48 hours, the cells were fixed and immunofluorescent labeling

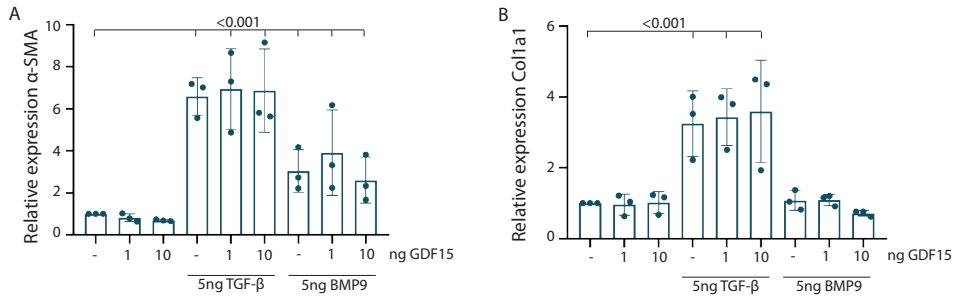


Figure 5. GDF15 does not affect inflammatory activation of hFCFs.

qPCR analysis on expression levels of α SMA (a) and Col1a1 (b) in hFCFs stimulated with GDF15 in combination with and without 5 ng TGF- β 3 or 5 ng BMP9. $n=3$ experiments (3 technical replicates each). Mean \pm SD. Abbreviations, BMP; Bone morphogenetic protein, Col1a1; Collagen 1a subunit 1, TGF- β ; Transforming growth factor- β , TNF; Tissue necrosis factor, α SMA; Smooth muscle actin α .

was performed to detect the expression and localization of the endothelial makers CD31 and VeCadherin, and the mesenchymal proteins Fibronectin and SM22a (Figure 7a). In addition, cell morphology was observed by phalloidin staining. As expected, in response to TNF- α , ECFCs acquired a spindle shape and downregulated the expression of Ve-Cadherin and CD31 from the cellular membrane, and increased the expression of SM22a. Noteworthy, ECFCs-GDF15 partially displayed a lower induction of SM22a and Fibronectin in response to TNF- α . Furthermore, we found less SM22a positive cells and a stronger Pecam1 expression upon TGF- β 3 stimulation in cells stably overexpressing GDF15. In addition, RNA was isolated and quantitative PCR analysis was performed in both control and GDF15 over-expressing cells stimulated for 48 hours. Our preliminary results confirmed that the endothelial gene markers CDH5 and PECAM1 were not downregulated by TNF α or TGF- β 3 in the presence of GDF15 (Figure 7b), whereas the induction of the fibroblast-like genes CDH2, ACTA2, FN1 was partially abrogated in pLV-GDF15 ECFCs. No differences could be observed in relative expression of mesenchymal markers TAGLN and Col1a1 between cells with or without GDF15 overexpression. These results indicate endothelial cells are less prone to undergo inflammation induced EndMT when high level of GDF15 are present.

Discussion

In end stage heart failure patients, high circulating GDF15 levels are associated with disease severity and worse outcome. However, whether these high levels are cause or consequence is still under debate. In a murine model of non-ischemic pressure overload induced heart failure, we showed that a reduced cardiac function is associated with increased circulating levels of GDF15. Furthermore, GDF15 expression in cardiac tissue was progressively increased with heart failure, indicating a possible causal role for GDF15

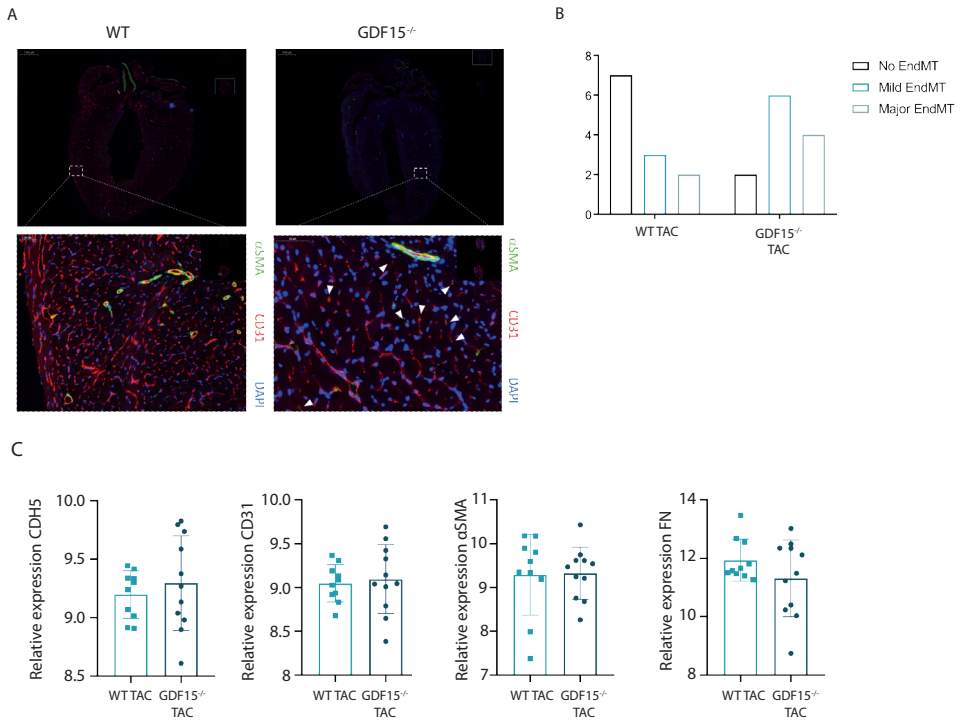


Figure 6. Co-localization of endothelial and mesenchymal markers.

Representative images of the CD31 (endothelial marker) and α SMA (mesenchymal marker) staining in both WT and GDF15^{-/-} mice (a). Semi-quantitative assessment of the co-localization of both CD31 and α SMA was more profound in GDF15^{-/-} indicative of EndMT (b). qPCR analysis on both endothelial (CDH5, CD31) and mesenchymal markers (α SMA, FN) showed no differences between GDF15^{-/-} and WT (c). n=12 per group. Mean \pm SD. Abbreviations: CDH5; Cadherin 5, CD31; Platelet endothelial cell adhesion molecule, α SMA; smooth muscle actin α , FN; fibronectin, EndMT; endothelial to mesenchymal transition.

in heart failure pathogenesis. Next, we subjected WT and GDF15^{-/-} mice to pressure-overload to induce the development of heart failure. We observed that GDF15^{-/-} mice responded heavily displaying an aggravated adverse cardiac remodeling. Although hypertrophy and interstitial fibrosis could not explain these functional differences, more perivascular fibrosis was present in GDF15^{-/-} mice, indicative of vascular dysfunction and possible EndMT. Furthermore, in GDF15^{-/-} mice, more co-localization of α SMA and PECAM was present, which further supports the occurrence of EndMT. This was substantiated by *in vitro* experiments showing that endothelial cells overexpressing GDF15 revealed that GDF15 may have a protective effect against inflammatory induced EndMT. We conclude, that the presence of GDF15 in cardiac tissue is needed to prevent adverse cardiac remodeling via inflammatory induced endothelial dysfunction.

Cardiomyocytes can become hypertrophic in response to pressure overload as induced in our TAC model⁴⁴. The role of GDF15 in these hypertrophic responses is under debate, as some studies have showed that GDF15 over-expression increases hypertrophy²², while

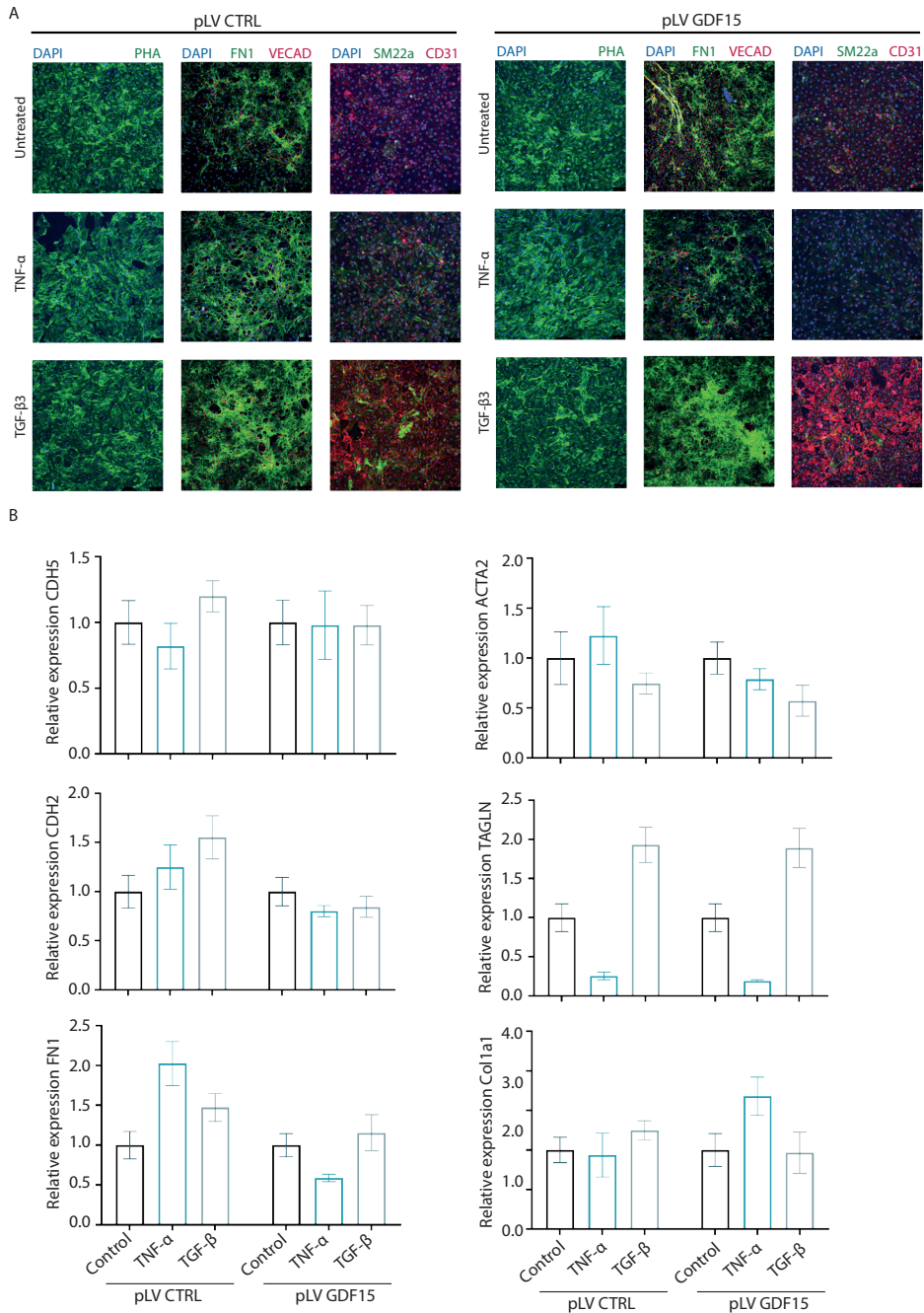


Figure 7. GDF15 overexpression inhibits inflammation induced EndMT. Endothelial cells with (PLV GDF15) and without (PLV control) GDF15 overexpression are subjected to treatments with either TNF-α, TGF-β3, or medium only (control) for 24h in complete medium. Immunohistochemistry for endothelial and mesenchymal markers after similar exposure to TNF-α and TGF-β3 (representative pictures ▶▶▶

◀◀◀ in a).qPCR analysis of endothelial markers i.e. CDH5 (Ve-cadherin) and PECAM (CD31) and mesenchymal markers i.e. CDH2 (N-cadherin), TAGLN (sm22 α), ACTA2 (α SMA), FN1 (Fibronectin-1), Col1a1 (Collagen 1 subunit a1) showed reduced EndMT in cells overexpressing GDF15 (b). Mean \pm SD. Abbreviations, TGF- β ; Transforming growth factor-beta, TNF- α ; Tissue necrosis factor-alpha.

others have reported an inhibitory hypertrophic response²⁴. Xu *et al* also studied GDF15 in a TAC model focusing on short term effects and did not observe a difference in cell size in the GDF15^{-/-} mice²⁵. In line, we found similar effects regarding the absence of GDF15 on cardiomyocyte cell size in our study.

Apart from hypertrophy, fibrosis is another major determinant of cardiac remodeling⁴⁵. Our results indicate that perivascular fibrosis is enhanced in GDF15^{-/-} mice. We could not quantify this with qPCR analysis as the relative expression of fibrosis markers is most likely dominated by expression related to interstitial fibrosis, combined with the modest differences in perivascular fibrosis between WT and GDF15^{-/-}. Though, it has been suggested that increased perivascular fibrosis in the microvasculature of the myocardium and thereby reduced micro coronary blood flow contributes to non-ischemic heart failure^{46,47}. However, the underlying pathophysiologic mechanism and contribution of vascular dysfunction to the progression of disease remains debated⁴⁶. The last decades more profound knowledge has shown that inflammation is an important determinant of endothelial and vascular dysfunction thereby aids to the onset and progression of non-ischemic heart failure^{48,49}. GDF15 is known to play a role in various endothelial driven processes. For example, GDF15 is known to induce angiogenesis⁵⁰ and secretion of GDF15 upon endothelial senescence is associated with enhanced proliferation and migration of endothelial cells, thereby preserving vascular function⁵¹. We explored the association between presence of GDF15 and endothelial dysfunction, as EndMT might be the underlying pathophysiological process for increased perivascular fibrosis²⁹. We found indications of increased EndMT in absence of GDF15 *in vivo*, while overexpression of GDF15 showed protection against EndMT *in vitro*. This finding is of great importance to understand the contribution of GDF15 to heart failure via EndMT. Future research should focus on the mechanism of GDF15 signaling in endothelial cells, and specifically EndMT validated in both *in vitro* and in patients. Our observation that GDF15 levels may directly reflect a specific pathological process of heart failure, being (micro)vascular dysfunction, has direct implications for the interpretation of GDF15 levels for diagnostic purposes.

Most research has focused on the role of GDF15 as a soluble protein, an external stimulus which resulted in the discovery of the Glial-derived neurotrophic factor receptor α -like (GFRAL) in the central nervous system and relating to the metabolic actions of GDF15⁵². Of interest, this receptor is not present on the cells in cardiac tissue but implicates the possibility for receptors aside receptors of the TGF- β family. Besides binding and signaling through a receptor, GDF15 can also locate to the nucleus and influence the transcriptional regulation of the SMAD pathway⁵³. GDF15 plays a role on Epithelial to Mesenchymal Transition in cancer metastasis⁵⁴, for example via SMAD signaling⁵³, however the specific

contribution and signaling of GDF15 in endothelial cells remains to be unraveled. So far, establishing the contribution of GDF15 to TGF- β / SMAD in endothelial cell signaling has been proven difficult, as GDF15 is closely related to the TGF- β family and the purity of GDF15 used in experimental settings is debated⁵⁵. Furthermore, as GDF15 is very pleiotropic, effects tend to differ between assays due to environmental aspects in culture conditions, cell types and diseases^{56,57}. We explored the effect of complete absence of GDF15, implying that both the nuclear transcriptional regulation function and the protein function of GDF15 are impaired. More specific analysis of conditional GDF15 knock-out and/ or knock-in mice would be beneficial to investigate i.e. the cell type specific effects of GDF15 and establish their contributions to cardiac remodeling. For example, more specific knock-out of GDF15 in endothelial cells to establish the contribution in heart failure.

From patient data we know that with disease severity the GDF15 levels are increased, which seems contradictory to our *in vivo* data observing more severe adverse remodeling in the absence of GDF15. It has recently been suggested that GDF15 is instrumental in maintenance of tissue tolerance against inflammation induced dysfunction³¹. Briefly, inflammation is inducing GDF15 production in various cells, which in turn promotes cellular survival in the setting of acute inflammation and potentially drives metabolic reprogramming³¹. This could explain the contradiction in our patient and mice data. GDF15 levels during cardiac stress might reflect vascular dysfunction, but also protect the vascular function needed for prevent tissue inflammation induced adverse cardiac remodeling. Unraveling the underlying signaling cascade in cardiac tissue inflammation is needed to understand the specific contribution of GDF15 as biomarker and potential intervention strategies. Comorbidities present in heart failure patients do contribute to the GDF15 levels, potential intervention might additionally target the comorbidities, thereby reducing the cardiovascular risk.

The endothelial cell has enormous potential as therapeutic target, however the heterogeneous properties of endothelial cells from different origin result in a large bench-to-bedside gap⁵⁸. Endothelial cell phenotypes, based on morphology, function, gene expression and antigen composition, vary between organs and vessel type, such as artery or venae. In addition, endothelial cells show substantial heterogeneity in function, i.e. permeability is differential across the vasculature^{58,59}. This heterogeneity is in part mediated by the tissue microenvironment *in vivo* and by the number of cell passages *in vitro*. Several studies have shown, that endothelial cells are capable of maintaining their site specific signatures in multiple passaged cells, however also suffer a loss of 50% of the specific signatures cultured *in vitro*^{60,61}. Our novel findings regarding the role of GDF15 on endothelial cell function is based on a single type of endothelial cells, the ECFCs, and these results should be validated in a tissue specific endothelial cell type, i.e. human cardiac microvascular endothelial cells. Furthermore, as cell culture will affect the endothelial cells signature and thereby function, the use of an endothelial lineage tracing model is essential in order to determine the origin and faith of endothelial cells vascular dysfunction.

Our data highlight the potential of GDF15 for future strategies to treat heart failure as we show an association with endothelial dysfunction. Though, elaborate research is needed to discover if we need to inhibit or stimulate GDF15 expression and if we should target intracellular or circulating GDF15. From the obesity field, we know that GDF15 is a candidate target for therapy via the GDF15/GFRAL axis⁶², furthermore others show that pharmacological GDF15 administration had a beneficial effect on food intake in mice⁶³. Similarly, we currently hypothesize and investigate if the reconstitution of GDF15 levels in GDF15^{-/-} mice exposed to TAC, will rescue the severe cardiac phenotype observed in the mice. We expect these experiments will contribute to our further understanding of the role for GDF15 in maintaining the vascular function and subsequent heart failure. Based on these experiments, future research should focus on the contribution of higher or lower levels of GDF15 in patients and their vascular function. Thereby it will guide us towards the development of intervention strategies, either based on inhibition or administration of GDF15 to preserve cardiac function upon remodeling.

Conclusion

In this study, we show GDF15^{-/-} mice with aggravated adverse remodeling following TAC due to endothelial dysfunction by increased EndMT. Although patients show increased levels of GDF15 with heart failure severity, total absence of GDF15^{-/-} is detrimental for the development of protective tissue tolerance. Further research will prove how GDF15 effects signaling cascades within EndMT and thereby perivascular fibrosis. Although our study suggests targeting of GDF15 or endothelial cells may be beneficial in heart failure, for both, targeting strategies remains challenging. In addition, the notion that GDF15 levels may directly reflect vascular dysfunction in patients is highly relevant as this may directly affect disease management in patients.

Financial interests

Financial support was provided by Roche diagnostics. And this study was supported by the Netherlands Cardiovascular Research Initiative: an initiative with support of the Dutch Heart Foundation (CVON2014-11 RECONNECT and 2013T084, Queen of Hearts).

Conflict of interests

None declared

Acknowledgements

We like to acknowledge Maïke Hulsbos and Julius de Poel for their contribution to the fibrosis analysis, and Kirsten Lodder for her valuable technical support.

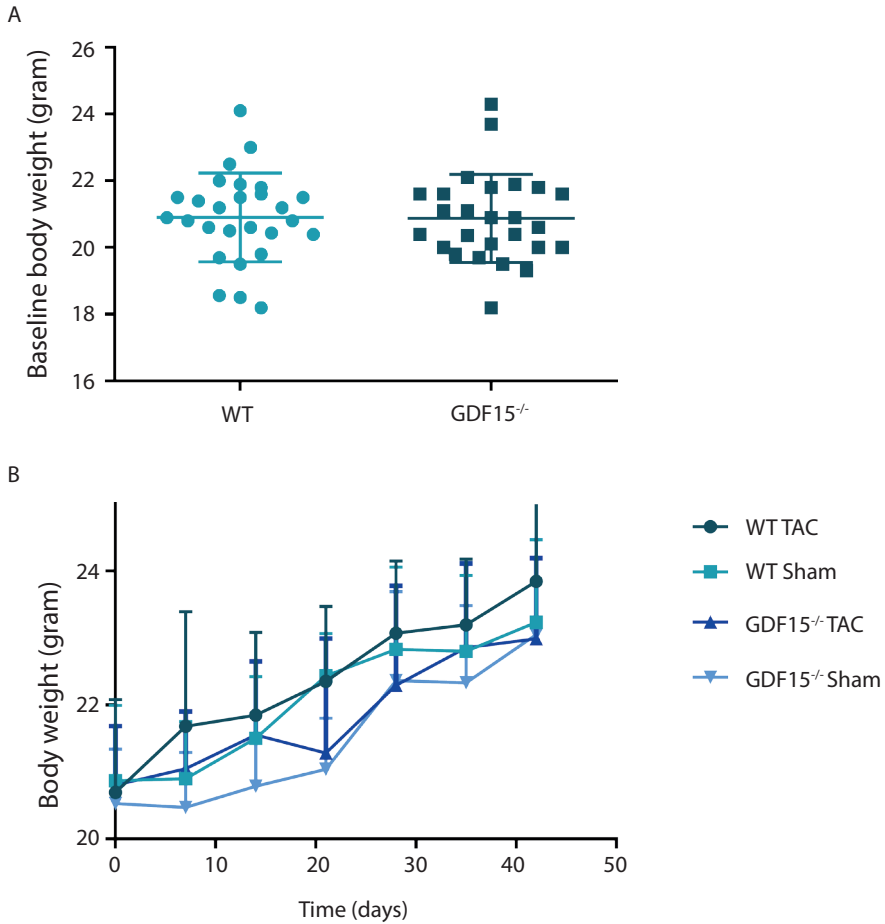
References

1. Bootcov, M. R. et al. MIC-1, a novel macrophage inhibitory cytokine, is a divergent member of the TGF-beta superfamily. *Proc. Natl. Acad. Sci. U. S. A.* **94**, 11514–9 (1997).
2. Goumans, M. J. & ten Dijke, P. TGF- β signaling in control of cardiovascular function. *Cold Spring Harb. Perspect. Biol.* **10**, (2018).
3. Morrell, N. W. et al. Targeting BMP signalling in cardiovascular disease and anaemia. *Nat. Rev. Cardiol.* **13**, 106–120 (2016).
4. Zhang, S. et al. Growth differentiation factor-15 predicts the prognoses of patients with acute coronary syndrome: a meta-analysis. *BMC Cardiovasc. Disord.* **16**, 1–7 (2016).
5. Wollert, K. C. et al. Prognostic Value of Growth-Differentiation Factor-15 in Patients With Non-ST-Elevation Acute Coronary Syndrome. *Circulation* **115**, 962–971 (2007).
6. Kempf, T. et al. Growth-differentiation factor-15 improves risk stratification in ST-segment elevation myocardial infarction. *Eur. Heart J.* **28**, 2858–2865 (2007).
7. Brown, D. A. et al. Concentration in plasma of macrophage inhibitory cytokine-1 and risk of cardiovascular events in women: a nested case-control study. *Lancet* **359**, 2159–63 (2002).
8. Lin, J.-F. et al. Growth-differentiation factor-15 and major cardiac events. *Am. J. Med. Sci.* **347**, 305–11 (2014).
9. Bonaca, M. P. et al. Growth Differentiation Factor-15 and Risk of Recurrent Events in Patients Stabilized After Acute Coronary Syndrome. *Arterioscler. Thromb. Vasc. Biol.* **31**, 203–210 (2011).
10. George, M., Jena, A., Srivatsan, V., Muthukumar, R. & Dhandapani, V. E. GDF 15--A Novel Biomarker in the Offing for Heart Failure. *Curr. Cardiol. Rev.* **12**, 37–46 (2016).
11. Mukherji, A., Ansari, U., Borggreffe, M., Akin, I. & Behnes, M. Clinically Relevant Biomarkers in Acute Heart Failure: An Update. *Curr. Pharm. Biotechnol.* **18**, 482–490 (2017).
12. Kempf, T. et al. Prognostic Utility of Growth Differentiation Factor-15 in Patients With Chronic Heart Failure. *J. Am. Coll. Cardiol.* **50**, 1054–1060 (2007).
13. Gaggin, H. K. & Januzzi, J. L. Biomarkers and diagnostics in heart failure. *Biochim. Biophys. Acta - Mol. Basis Dis.* **1832**, 2442–2450 (2013).
14. Li, J. et al. Additional Diagnostic Value of Growth Differentiation Factor-15 (GDF-15) to N-Terminal B-Type Natriuretic Peptide (NT-proBNP) in Patients with Different Stages of Heart Failure. *Med. Sci. Monit.* **24**, 4992–4999 (2018).
15. Wollert, K. C. & Kempf, T. Growth differentiation factor 15 in heart failure: An update. *Curr. Heart Fail. Rep.* (2012). doi:10.1007/s11897-012-0113-9
16. Anand, I. S. et al. Serial measurement of growth-differentiation factor-15 in heart failure: relation to disease severity and prognosis in the Valsartan Heart Failure Trial. *Circulation* **122**, 1387–95 (2010).
17. Chan, M. M. Y. et al. Growth differentiation factor 15 in heart failure with preserved vs. reduced ejection fraction. *Eur. J. Heart Fail.* **18**, 81–8 (2016).
18. Jankovic-Tomasevic, R. et al. Prognostic utility of biomarker growth differentiation factor-15 in patients with acute decompensated heart failure. *Acta Cardiol.* **71**, 587–595 (2016).
19. Stenemo, M. et al. Circulating proteins as predictors of incident heart failure in the elderly. *Eur. J. Heart Fail.* **20**, 55–62 (2018).
20. Kempf, T. et al. GDF-15 is an inhibitor of leukocyte integrin activation required for survival after myocardial infarction in mice. *Nat. Med.* **17**, 581–588 (2011).
21. Artz, A., Butz, S. & Vestweber, D. GDF-15 inhibits integrin activation and mouse neutrophil recruitment through the ALK-5/TGF- β RII heterodimer. *Blood* **128**, 529–541 (2016).
22. Heger, J. et al. Growth differentiation factor 15 acts anti-apoptotic and pro-hypertrophic in adult cardiomyocytes. *J. Cell. Physiol.* **224**, n/a-n/a (2010).
23. Kempf, T. et al. The Transforming Growth Factor- β Superfamily Member Growth-Differentiation Factor-15 Protects the Heart From Ischemia/Reperfusion Injury. *Circ. Res.* **98**, 351–360 (2006).
24. Xu, X. Y. et al. Growth differentiation factor (GDF)-15 blocks norepinephrine-induced myocardial hypertrophy via a novel pathway involving inhibition of epidermal growth factor receptor transactivation. *J. Biol. Chem.* (2014). doi:10.1074/jbc.M113.516278
25. Xu, J. et al. GDF15/MIC-1 Functions As a Protective and Antihypertrophic Factor Released From the Myocardium in Association With SMAD Protein Activation. *Circ. Res.* **98**, 342–350 (2006).
26. Giannitsi, S., Maria, B., Bechlioulis, A. & Naka, K. Endothelial dysfunction and heart failure: A review of the existing bibliography with emphasis on flow mediated dilation. *JRSM Cardiovasc. Dis.* **8**, 204800401984304 (2019).
27. Adela, R. & Banerjee, S. K. GDF-15 as a target and biomarker for diabetes and cardiovascular diseases: A translational prospective. *J. Diabetes Res.* (2015). doi:10.1155/2015/490842

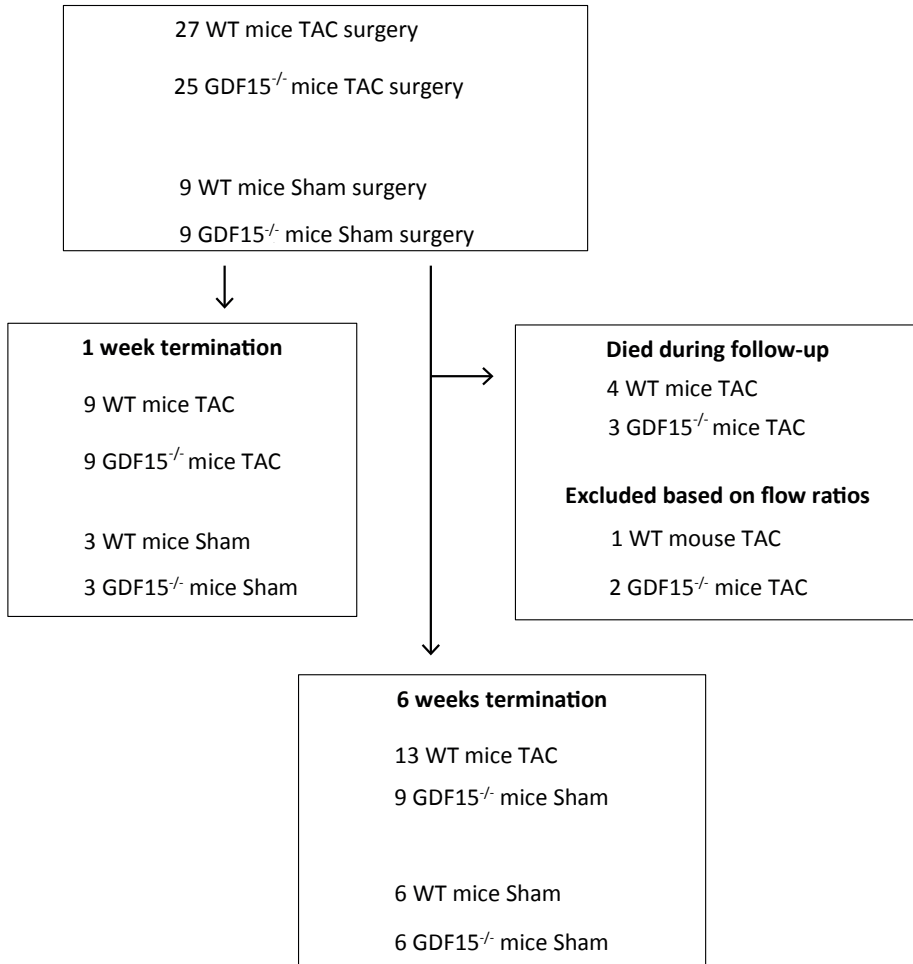
28. Sanchez-Duffhues, G., Garcia de Vinuesa, A. & Ten Dijke, P. Endothelial-to-mesenchymal transition in cardiovascular diseases: Developmental signaling pathways gone awry. *Dev. Dyn.* **247**, 492–508 (2018).
29. Zeisberg, E. M. et al. Endothelial-to-mesenchymal transition contributes to cardiac fibrosis. *Nat. Med.* **13**, 952–961 (2007).
30. Sánchez-Duffhues, G. et al. Inflammation induces endothelial-to-mesenchymal transition and promotes vascular calcification through downregulation of BMPR2. *J. Pathol.* **247**, 333–346 (2019).
31. Luan, H. H. et al. GDF15 Is an Inflammation-Induced Central Mediator of Tissue Tolerance. *Cell* **178**, 1231–1244 (2019).
32. Voors, A. A. et al. A systems BIOlogy Study to TAilored Treatment in Chronic Heart Failure: rationale, design, and baseline characteristics of BIOSTAT-CHF. *Eur. J. Heart Fail.* **18**, 716–726 (2016).
33. Voors, A. A. et al. A systems BIOlogy Study to TAilored Treatment in Chronic Heart Failure: rationale, design, and baseline characteristics of BIOSTAT-CHF. *Eur. J. Heart Fail.* **18**, 716–726 (2016).
34. The Jackson Laboratory. Available at: <https://www.jax.org/jax-mice-and-services>.
35. Fontes, M. S. C. et al. CTGF knockout does not affect cardiac hypertrophy and fibrosis formation upon chronic pressure overload. *J. Mol. Cell. Cardiol.* **88**, 82–90 (2015).
36. Roche-GDF15. Available at: https://pim-eservices.roche.com/eLD_SF/gb/en/Documents/GetDocument?documentId=f1b11d65-4888-e711-fbba-00215a9b3428.
37. Tasev, D., van Wijhe, M. H., Weijers, E. M., van Hinsbergh, V. W. M. & Koolwijk, P. Long-Term Expansion in Platelet Lysate Increases Growth of Peripheral Blood-Derived Endothelial-Colony Forming Cells and Their Growth Factor-Induced Sprouting Capacity. *PLoS One* **10**, e0129935 (2015).
38. Zhang, J. et al. LRP8 mediates Wnt/beta-catenin signaling and controls osteoblast differentiation. *J. Bone Miner. Res.* **27**, 2065–2074 (2012).
39. Gartner, T. C. L. B., Deddens, J. C. & Mol, E. A. Anti-fibrotic Effects of Cardiac Progenitor Cells in a 3D-Model of Human Cardiac Fibrosis. **6**, 1–11 (2019).
40. Xia, Y. et al. Characterization of the inflammatory and fibrotic response in a mouse model of cardiac pressure overload. *Histochem. Cell Biol.* **131**, 471–481 (2009).
41. Lok, S. I. et al. Circulating growth differentiation factor-15 correlates with myocardial fibrosis in patients with non-ischaemic dilated cardiomyopathy and decreases rapidly after left ventricular assist device support. *Eur. J. Heart Fail.* **14**, 1249–56 (2012).
42. Xu, X. et al. Endocardial fibroelastosis is caused by aberrant endothelial to mesenchymal transition. *Circ. Res.* **116**, 857–866 (2015).
43. Ghosh, A. K., Nagpal, V., Covington, J. W., Michaels, M. A. & Vaughan, D. E. Molecular basis of cardiac endothelial-to-mesenchymal transition (EndMT): differential expression of microRNAs during EndMT. *Cell. Signal.* **24**, 1031–1036 (2012).
44. el Azzouzi, H. et al. MEF2 transcriptional activity maintains mitochondrial adaptation in cardiac pressure overload. *Eur. J. Heart Fail.* **12**, 4–12 (2010).
45. Segura, A. M., Frazier, O. H. & Buja, L. M. Fibrosis and heart failure. *Heart Fail. Rev.* **19**, 173–85 (2014).
46. Dai, Z., Aoki, T., Fukumoto, Y. & Shimokawa, H. Coronary perivascular fibrosis is associated with impairment of coronary blood flow in patients with non-ischemic heart failure. *J. Cardiol.* (2012). doi:10.1016/j.jjcc.2012.06.009
47. Ytrehus, K., Hulot, J. S., Perrino, C., Schiattarella, G. G. & Madonna, R. Perivascular fibrosis and the microvasculature of the heart. Still hidden secrets of pathophysiology? *Vascular Pharmacology* (2018). doi:10.1016/j.vph.2018.04.007
48. Lu, X., Gong, J., Dennery, P. A. & Yao, H. Endothelial-to-mesenchymal transition: Pathogenesis and therapeutic targets for chronic pulmonary and vascular diseases. *Biochem. Pharmacol.* **168**, 100–107 (2019).
49. Paulus, W. J. & Tschöpe, C. A novel paradigm for heart failure with preserved ejection fraction: comorbidities drive myocardial dysfunction and remodeling through coronary microvascular endothelial inflammation. *J. Am. Coll. Cardiol.* **62**, 263–71 (2013).
50. Wang, S. et al. Growth differentiation factor 15 promotes blood vessel growth by stimulating cell cycle progression in repair of critical-sized calvarial defect. *Sci. Rep.* **7**, 9027 (2017).
51. Ha, G. et al. GDF15 secreted by senescent endothelial cells improves vascular progenitor cell functions. *PLoS One* **14**, e0216602 (2019).
52. Emmerson, P. J. et al. The metabolic effects of GDF15 are mediated by the orphan receptor GFRAL. *Nat. Med.* **1–9** (2017). doi:10.1038/nm.4393
53. Min, K.-W. et al. NAG-1/GDF15 accumulates in the nucleus and modulates transcriptional regulation of the Smad pathway. *Oncogene* **35**, 377–388 (2015).
54. Li, C. et al. GDF15 promotes EMT and metastasis in colorectal cancer. *Oncotarget* (2016). doi:10.18632/oncotarget.6205
55. Olsen, O. E., Skjærvik, A., Størdal, B. F., Sundan, A. & Holien, T. TGF- β contamination of purified recombinant GDF15. *PLoS One* **12**, e0187349 (2017).

56. Breit, S. N. et al. The TGF- β superfamily cytokine, MIC-1/GDF15: A pleiotropic cytokine with roles in inflammation, cancer and metabolism. *Growth Factors* **29**, 187–195 (2011).
57. Murielle, M. & Batra, S. K. Divergent molecular mechanisms underlying the pleiotropic functions of macrophage inhibitory cytokine-1 in cancer. *Journal of Cellular Physiology* **224**, 626–635 (2010).
58. Aird, W. C. Endothelial cell heterogeneity. *Cold Spring Harb. Perspect. Med.* **2**, a006429 (2012).
59. Conway, E. M. & Carmeliet, P. The diversity of endothelial cells: a challenge for therapeutic angiogenesis. *Genome Biol.* **5**, 207 (2004).
60. Lacorre, D.-A. et al. Plasticity of endothelial cells: rapid dedifferentiation of freshly isolated high endothelial venule endothelial cells outside the lymphoid tissue microenvironment. *Blood* **103**, 4164–4172 (2004).
61. Chi, J.-T. et al. Endothelial cell diversity revealed by global expression profiling. *Proc. Natl. Acad. Sci. U. S. A.* **100**, 10623–10628 (2003).
62. Cheung, C. L., Tan, K. C. B., Au, P. C. M., Li, G. H. Y. & Cheung, B. M. Y. Evaluation of GDF15 as a therapeutic target of cardiometabolic diseases in human: A Mendelian randomization study. *EBioMedicine* **41**, 85–90 (2019).
63. Patel, S. et al. GDF15 Provides an Endocrine Signal of Nutritional Stress in Mice and Humans. *Cell Metab.* **29**, 707–718 (2019).

Supplemental

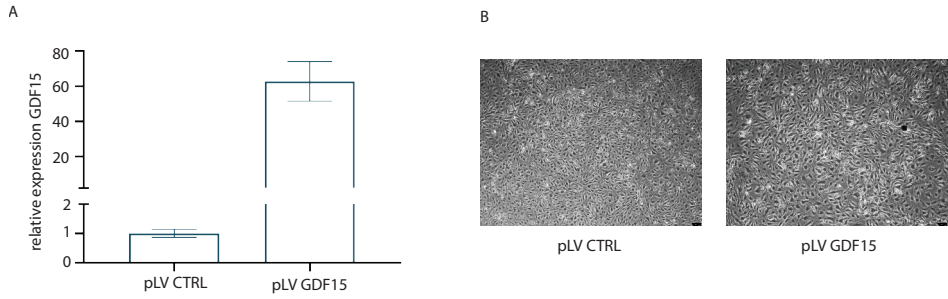
**Supplemental figure 1. Mice weight at baseline and over time post-surgery.**

At baseline, no differences in body weight of GDF15^{-/-} and their WT littermates could be observed (a) n=27 WT, n=26 GDF15^{-/-}. Over time post-TAC or Sham surgery, no differences in weight gain or loss could be observed between the GDF15^{-/-} mice and the WT littermates (b) WT TAC n=13, WT Sham n=6, GDF15^{-/-} TAC n=9, GDF15^{-/-} Sham n=6.



Supplemental figure 2. Flow chart of GDF15^{-/-} mice experiments.

Flow chart of mice experiments showing mice included at baseline, mice sacrificed after 1 week and 6 weeks and mice lost during follow-up or excluded based on flow ratios.



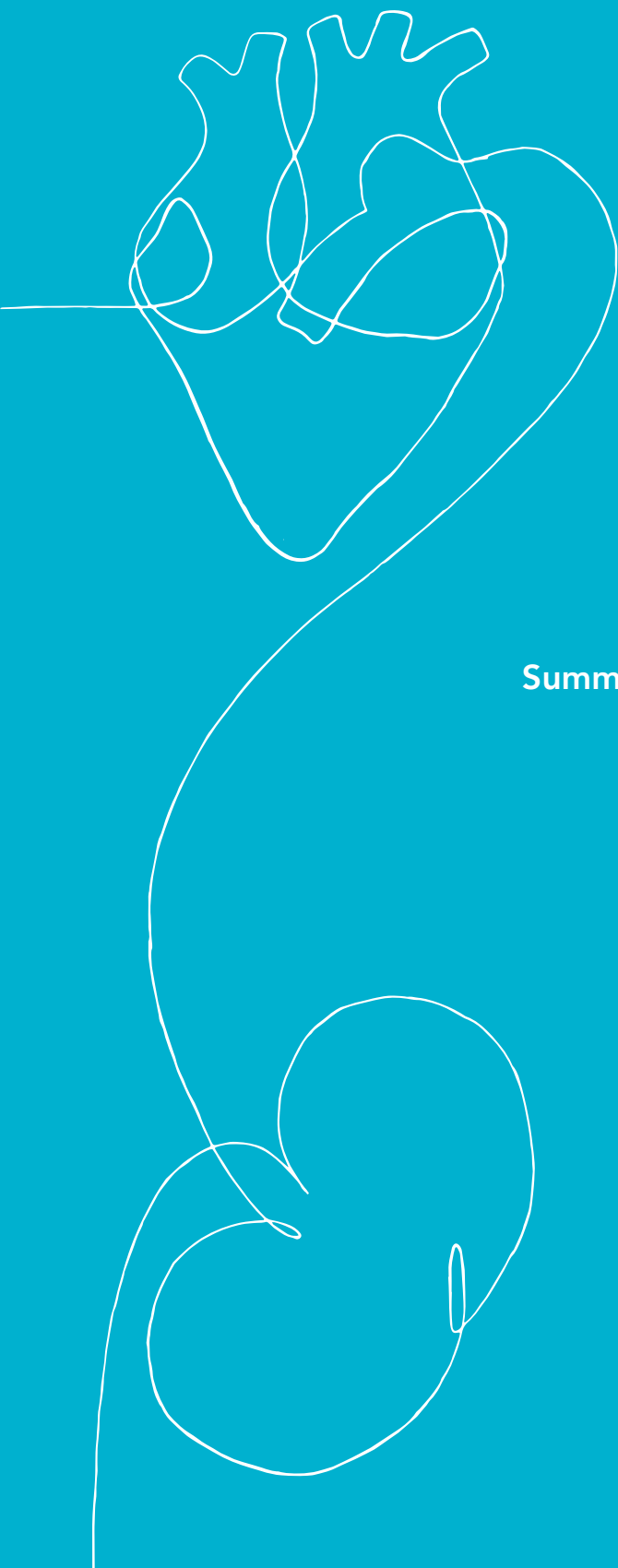
Supplemental figure 3. Human endothelial colony forming cells over-expressing GDF15.

High levels of GDF15 expression in human endothelial colony forming cells over-expressing GDF15 generated using a lentiviral vector (a), with no obvious morphological differences at baseline (b). Mean \pm SD.

Supplemental table 1. Primers and antibodies.

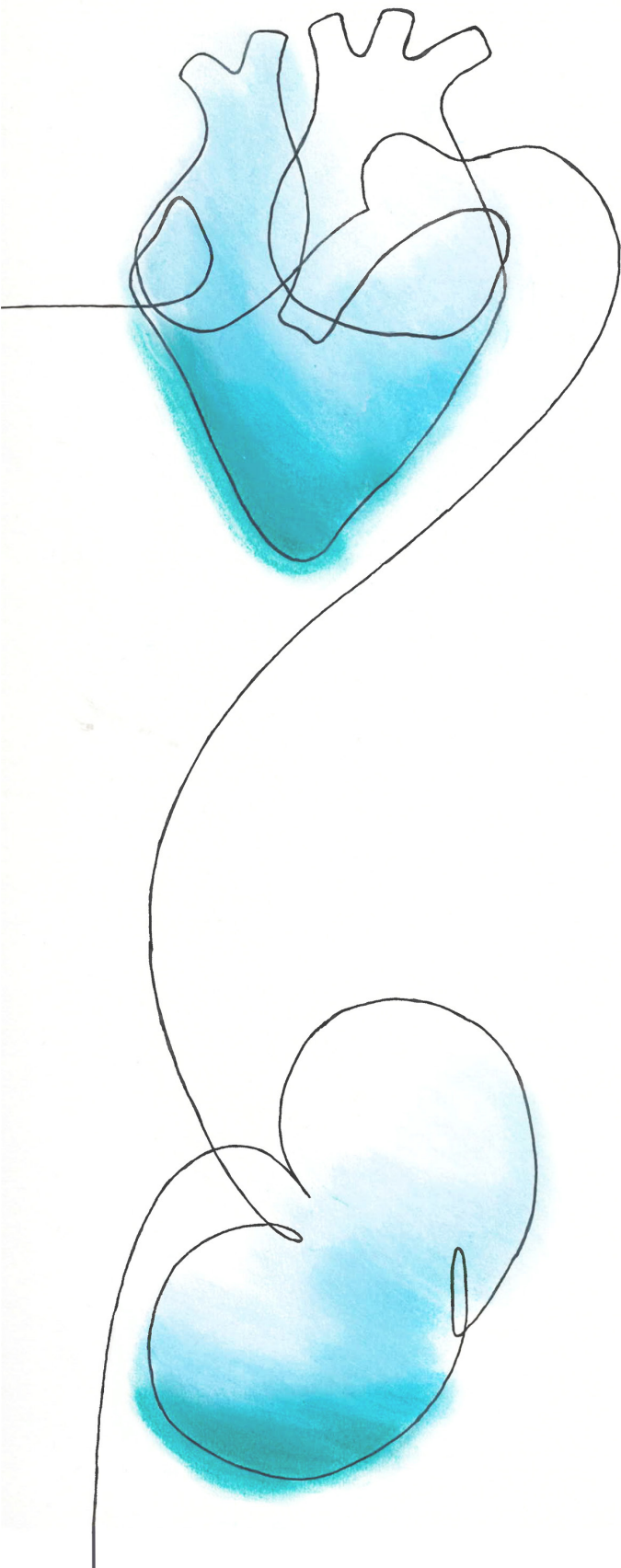
Gene	Species	Forward primer (5'-3')	Reverse primer (5'-3')
Pecam-1	Human	ATCGGTTGTTCAATGCGTCC	CCTTCAGGATTGGTACATGACA
Cdh5	Human	TCGTTGCGCTCTTCGTGAC	CAGCCCCGAAAACAGGTAG
Fn1	Human	CGTCATAGTGGAGGCACTGA	CAGACATTTCGTTCCCACTCA
Cdh2	Human	CAGACCGACCCAAAACAGCAAC	GCAGCAACAGTAAGGACAAACATC
Gapdh	Human	GCACCGTCAAGGCTGAGAAC	TGGTGAAGACGCCAGTGGGA
Col1a1	Human	CAGCCGCTTCACCTACAGC	TTTGTATTCAATCACTGTCTTGCC
Tagln	Human	CATCCTGTCTGTCCGAACCC	GACTGAGAGGGTGGGTTTCC
Pecam-1	Mouse	CTCCAACAGAGCCAGCAGTA	GACCACTCCAATGACAACCA
Acta2	Mouse	AGCGTGAGATTGTCCGTGACAT	GCGTTCGTTTCCAATGGTGA
Gapdh	Mouse	TGGCAAAGTGGAGATTGTTGCC	AAGATGGTGATGGGCTTCCCG
Cdh5	Mouse	AGCGCAGCATCGGGTACT	TCGGAAGAATTGGCCTCTGT
Fn1	Mouse	AGGCAGAAAACAGGTCTCGATT	TGAATGAGTTGGCGGTGATATC

Antibody	Species	Dilution	Provider	Reference
Cdh5	Rabbit	1:100	Cell Signaling	#2158
PECAM-1	Goat	1:100	Santa Cruz	Sc-1506
SM22 α	Rabbit	1:400	Abcam	ab14106
Fn	Mouse	1:400	Sigma-Aldrich	F7387



PART IV

Summary and general discussion



8

General summary and discussion

Cardiovascular disease is the leading cause of death and accounts for more than 31% of global mortality rates¹. Presence of multiple co-morbidities, such as kidney failure and diabetes interfere with current standard disease management of heart failure². Heart failure is clinically characterized by fatigue, dyspnea and left ventricular function (LVF). Based on the LVF, heart failure is classified in either heart failure with reduced ejection fraction (HFrEF), defined as a left ventricular ejection fraction (LVEF) below 40%, or heart failure with preserved ejection fraction (HFpEF), with a LVEF of $\geq 50\%$ ^{3,4}. More recently, a patient population of heart failure with mild reduced ejection fraction (HFmrEF) has been defined with an LVEF between 40 and 49%⁵. Current treatment for heart failure is based on a combination of pharmaceutical interventions to relieve heart failure symptoms and reduce cardiac stress, as a curative treatment is not yet found. Most of these medications have clinically proven beneficial effect in HFrEF patients^{2,6}, but lack effectivity in HFpEF patients. It is important to accurately identify HFpEF patients in existing and new clinical trials, to evaluate the potential benefit of treatments in this specific population. In this regard, there is an urgent need for improved diagnostics and prognostic biomarkers for the classification of HFpEF patients. This development is only possible based on a thorough understanding of the underlying pathophysiological mechanisms in chronic non-ischemic heart failure, which may result in the identification of novel targets for therapeutical intervention. In this thesis we focus on the effects of renal dysfunction, vascular inflammation, biological sex and endothelial (dys)function on the development and progression of chronic heart failure with emphasize on vascular dysfunction. Thereby, we address possible mechanisms involved with vascular inflammation in heart failure and suggest cytokine GDF15 as potential new therapeutic target and added biomarker value on top of existing markers.

Inflammation in the cardiorenal axis

How inflammation contributes to cardiovascular disease is a continuous topic of research, mainly based on two aspects, local and systemic inflammation⁷. Both, local inflammation induced by tissue injury and systemic inflammation related to comorbidities (i.e., kidney failure) play a pathogenic role in cardiovascular diseases. Several cardiovascular diseases, i.e. atherosclerosis and heart failure are known to be strongly driven by inflammation, but this also accounts for cardiovascular comorbidities like chronic kidney disease (CKD) and diabetes. The interplay between cardiovascular and comorbidity driven inflammation on the progression of cardiovascular disease has been underappreciated for many years. Therefore, in **chapter 3** we hypothesized that inflammation could be a primary mechanism of CKD driving disease progression of atherosclerosis. We investigated the influence of kidney dysfunction and inflammation on plaque stability in human carotid plaques obtained by carotid endarterectomy. In this study we confirmed an association between impaired kidney function and an unstable plaque phenotype and poor outcome during follow up. Local immune responses are known to activate inflammatory cells to release cytokines and proteases that inhibit the formation of and degrade the atheroma fibrous cap, thus increasing plaque vulnerability⁸. However, surprisingly, associations of

decreased kidney function with inflammatory histological plaque features were absent or inconsistent. No supportive evidence for a role of inflammation was found to associate with a decreased kidney function in our atherosclerotic patient population that could support the conceptual thought that a systemic vascular inflammatory response explains the increased cardiovascular event rate in atherosclerotic patients suffering from CKD. However, it is debated if the selected patient population is the best cohort to study these associations. For instance, in this cohort we executed a retrospective assessment of kidney function based on creatinine levels and severely impaired glomerular filtration rates was prevalent among a relative low number of patients. In order to better assess pathophysiological associations between kidney function and vascular inflammation, it would be of interest to optimally phenotype disease populations. Therefore it is critical to develop novel inclusion criteria which clearly establish the presence of comorbidities. For instance, kidney dysfunction should be established by blood and urinary markers, i.e. urine albumin levels in order to classify cardiovascular patients following the CKD guidelines⁹. For many years, patients with comorbidities were excluded from participating in study cohorts and clinical trials, because comorbidities are interfering with both disease and the effect of treatment¹⁰. Consequently, this leaves a gap in today's knowledge of the complex interplay of comorbidities in cardiovascular diseases. Since it is clearly established and appreciated that the interplay between the heart and the kidney acts as an important mediator in the cardiorenal syndrome (CRS)^{11,12}, it has become crucial to obtain well defined specific cardiorenal cohorts to improve disease knowledge.

The cardio-renal axis in the TAC model

We need animal models to further explore the pathophysiological mechanisms underlying the onset and progression of organ failure in CRS. The transverse aortic constriction (TAC) mouse model is commonly used surrogate to study heart failure induced by pressure overload, which is relevant for the characterization of cardiac remodeling in chronic heart failure. Although Renin-Angiotensin System (RAS) stimulation by CKD has been documented to exacerbate heart failure progression after TAC^{13,14}, little information is available on the deterioration of kidney function in this model. Therefore, in **chapter 4** we assessed the possible contribution of renal dysfunction to heart failure progression by evaluating the kidney function in the TAC model. With progressive heart failure as seen by reduced stroke volume, we observed elevated levels of renin, indicative of RAS activation, without any signs of kidney injury. A large variety of bidirectional pathway interactions between heart and kidney, like hemodynamic, humoral, metabolic and cell mediated communication are known to stimulate disease progression^{11,15}. Despite the severe cardiac dysfunction we observe in our mice, one may argue that our model may lack characteristics of a proper CRS model, as no indications are present for kidney failure. Further studies are needed to gain more insights into these interactions of the cardiorenal axis in a variety of animal models^{16,17}. To overcome the current limitations of the existing models¹⁶⁻¹⁸, such as the lack of multiple comorbidities and the absence of low grade systemic inflammation, new animal models to investigate cardiorenal syndrome are

currently being developed¹⁹⁻²¹. Still, caution should be taken with overinterpretation of experimental outcomes, as these models remain only representative of a subpopulation of CRS patients²⁰. Nevertheless, these complex models may contribute to research into CRS and eventually disease management.

Inflammation and GDF15 in cardiac remodeling

Cardiac remodeling can be induced by various cardiomyopathies, comorbidities and/or inflammatory responses. The initiating event in cardiac remodeling is likely different in HFpEF compared to HFrEF, nonetheless both will result in adverse cardiac remodeling. In HFpEF, left ventricular hypertrophy and sex-specific cardiac remodeling is associated with adverse cardiovascular outcome. Although sex differences are observed in cardiac remodeling^{22,23}, the underlying mechanisms are largely unknown. In **chapter 5**, we assessed the effect of biological sex on cardiac remodeling and function within an extensive longitudinal TAC mice study. We found striking differences in cardiac remodeling phenotypes between the sexes, where male mice primarily show eccentric remodeling and female mice display concentric remodeling post-TAC. Although sex differences in cardiac remodeling were observed, both males and females showed a similar deteriorating in cardiac function. Furthermore, no differences in cardiomyocyte hypertrophy or interstitial collagen content were found. Analysis of a set of 92 circulating proteins revealed potential sex specific pathways underlying the difference in cardiac remodeling between males and females. In males, we identified pathways mainly associated with regulation of cellular and organ homeostasis, likely reflecting the severe outward remodeling we observed in these male hearts. Interestingly, in females we found pathways that were associated to vascular dysfunction, more specific endothelial dysfunction induced by inflammation. In line, histological analysis revealed increased perivascular fibrosis in female hearts. These results are in line with the reduced vascular function and endothelial dysfunction postulated to play a role in chronic heart failure, specifically in women²⁴. We expect that these results will encourage the future study of cellular pathways and pathophysiological mechanisms contributing to disease initiation and progression, which remain crucial for understanding the disease process. Furthermore, it will aid to identification of novel (sex-specific) biomarkers and potential therapeutic targets.

Growth differentiation factor 15 (GDF15), a TGF- β superfamily member is involved in various processes, including inflammation²⁵. Furthermore, GDF15 is a strong prognostic marker in heart failure, but its biological function in cardiac remodeling is poorly understood^{26,27}. In **chapter 6** we introduced GDF15 as a causal player in adverse cardiac remodeling, with pleiotropic effects on cardiac cell types. Recently, Roche Diagnostics has developed a diagnostic GDF15 tool in the first step towards a clinical biomarker approach²⁸. However, as the contribution of GDF15 to the pathophysiological mechanisms of heart failure remains unknown, specific implications for disease management upon elevated GDF15 levels have not been identified. Therefore, in **chapter 7** we focus on the causal role of GDF15 in progressive heart failure and cardiac remodeling. In

absence of GDF15, mice show extreme adverse cardiac remodeling and loss of cardiac function upon pressure overload heart failure compared to wildtype mice. Although GDF15^{-/-} mice did not exhibit enhanced hypertrophy, fibrosis and inflammation (*data not shown*), which are major determinants of cardiac remodeling, regional assessment of vascular morphology revealed an increase in perivascular fibrosis and endothelial to mesenchymal transition (EndMT). *In vitro* experiments revealed a mediating effect of GDF15, preventing inflammation induced EndMT. We conclude that the increase in GDF15 levels in patients might reflect the poor state of vascular function of patients with adverse cardiac remodeling.

Cardiac dysfunction in the individual heart failure patient might be driven by different processes i.e. hypertrophy, fibrosis, inflammation and endothelial dysfunction²⁹. The presence of different and often multiple combinations of comorbidities in heart failure patients, makes it a very heterogeneous patient population where circulating levels of biomarkers are needed to identify these underlying processes. At this moment, only biomarkers indicative of cardiac injury, such as natriuretic peptide and troponins, are used for heart failure diagnostics in the clinic^{2,30}. However, they have limited value about processes associated with heart failure progression. A demand for non-cardiac specific markers like endothelial dysfunction (including EndMT) and vascular inflammation are needed to provide added prognostic value, thus improving patient care²⁹. Although GDF15 is prognostic in heart failure, it is also associated with many other diseases (severity and mortality) such as cancer and kidney dysfunction³¹⁻³³, therefore interpretation of GDF15 levels merit careful consideration. For example, in the UCORBIO biobank where patients with all indications for a coronary angiography are enrolled, we observed that the presence of renal dysfunction, based on blood creatinine levels, is associated with an increase in GDF15 levels (Figure 1, *unpublished data*). On top of this we still observed an association between increasing GDF15 levels and reduced LVEF (Figure 1, *unpublished data*). Therefore, we postulate that GDF15 could be of added value to the management of heart failure patients alongside the established cardiac biomarkers. However, while considering possible existing comorbidities (i.e., kidney disease) to influence its systemic levels. We emphasize that in-depth research on the causal relation of biomarkers to disease specific mechanisms and comorbidities is an unmet need that is required to validate the utility of such biomarkers. Biomarkers able to address underlying disease processes in patients, are expected to guide clinicians in optimal treatment of disease. Future research on the pathophysiological mechanisms by which GDF15 may mediate vascular dysfunction is crucial before GDF15 can be implemented as biomarker in standard care for treatment responsiveness in management of i.e. vascular inflammation.

The challenges and difficulties on route to improved clinical care

Although thorough investigation into the utility of several novel biomarkers has been performed^{29,30,33}, inflammation related biomarkers in heart failure have not met the expectations which could be explained by the fact that they represent a systemic pathological condition and are not heart failure specific²⁹. Different comorbidities have

been associated with systemic low grade inflammation in chronic heart failure patients³⁴, for example chronic increased circulating levels of tumor necrosis factor (TNF)- α in diabetics and hypertensive patients^{35,36}. During the last decade, multiple studies have tried to block key players in ameliorate low-grade inflammation with targeting studies. For example, in chronic heart failure patients, TNF- α levels were targeted with antibodies^{37,38}. However, these therapeutics suffer from systemic side effects which has not inspired the development of novel anti-inflammatory treatments in the field of heart failure. The sub stratification of patient populations in these trials could be debated. Especially in HFpEF patients suffering from suboptimal treatment, systemic levels of increased low-grade inflammation are hypothesized to drive disease progression via vascular inflammation³⁴. If targeting vascular inflammation is the new strategy for HFpEF patients, as it is suggested to drive disease, a clear definition of the patient subpopulations would most likely benefit the study outcomes. This clear definition should include a thorough assessment of both cardiac function and comorbidities, such as kidney dysfunction and diabetes. Furthermore systemic effects of organ failure, with accurate assessment of state of systemic induced vascular inflammation would be needed to classify patient disease severity. However, even more challenges occur when we would consider GDF15 as possible target for treatment. For example, in **chapter 7** we show that in absence of GDF15 cardiac function deteriorates much faster, resulting in a more severe heart failure phenotype, while seemingly contradictory in heart failure patients high levels of GDF15 are associated with worse outcome. The mouse data suggests that GDF15 is beneficial to the heart, which raises the question whether in patients high levels of GDF15 does associate with a beneficial heart function. We expect that circulating levels of GDF15 directly reflects the disease state of the heart in heart failure patients. As other TGF- β family

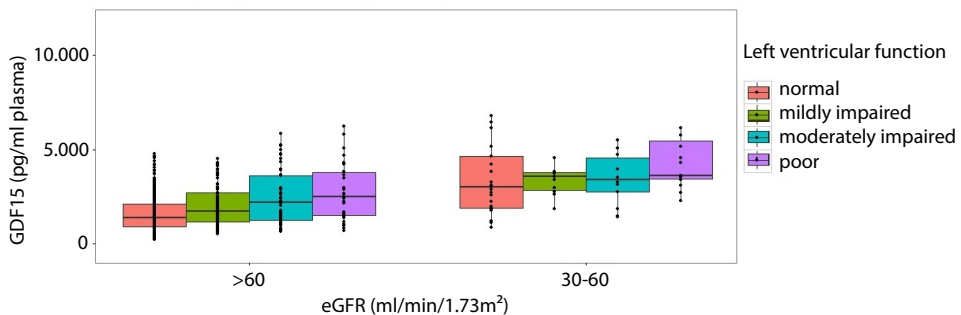


Figure 1. GDF15 levels in patients with possible coronary artery disease.

Circulating GDF15 levels increase with worse kidney function (based on the estimate Glomerular Filtration Rate, eGFR) and reduced cardiac function (based on the Left Ventricular Function, LVF). An eGFR >60 ml/min/1.73m² is considered a normal renal function, whereas an eGFR <60 is considered renal dysfunction whereas we excluded patients with an eGFR <30 which are considered patients with severe renal failure and therefore renal clearance might interfere with renal dysfunction. GDF15 levels are measured with a Magnetic Luminex Assay (human premixed multi-analyte kit, LXSAMH, R&D Systems, Inc. Minneapolis, USA), LVF based on echocardiography was subtracted from the patients clinical data, the eGFR is calculated based on the plasma creatinine levels measured at inclusion. n = respectively from left to right 383, 121, 51, 38, 25, 11, 14, and 15 patients per group.

members, GDF15 is produced as a non-mature pro-GDF15 peptide, which undergoes proteolytic cleavage to mature³⁹. Even though it has been shown that such step is required for TGF- β to become biologically active, it remains elusive whether this is true for GDF15. In that case it would be very interesting to assess the ratio between active and inactive GDF15 in patients and associate this to disease severity. Although various pathophysiological processes including apoptosis and hypertrophy^{40,41} are suggested to be affected by GDF15, the exact role of this protein in adverse remodeling has to be clarified.

It is crucial to gain more insight in the specific signaling effects of GDF15 (intracellular and extracellular) within cardiac tissue, studying which cell types express and respond to GDF15 in order to establish which GDF15 mediated responses contribute to protective effects in HFpEF. So far, unraveling the exact signaling pathways and cellular responses to GDF15 in different cell types has been proven difficult⁴². The levels of GDF15 are known to influence by an inflammatory environment⁴³. We found that exogenous addition of GDF15 alone, in absence of a secondary inflammatory trigger, does not affect the expression of endothelial-specific markers (Chapter 7). This is consistent with previous data suggesting that GDF15 may mediate inflammation⁴³ and therefore, in endothelial cells, may only be functional under a pro-inflammatory environment. Furthermore, endothelial heterogeneity interferes with experimental outcomes as each tissue specific endothelial cell harbors its own characteristics upon inflammatory activation, i.e. differences in ICAM and VCAM expression^{44,45}. However, in combination with other growth factors well known to modulate the response of vascular tissues, such as TGF- β , Bone morphogenetic proteins (BMPs) and the inflammatory cytokine TNF- α , over-expression of GDF15 was able to prevent EndMT and modulate TGF- β and BMP-induced downstream signaling. Assessing cleave variants might be highly relevant, as the ratio between cleave variants has proven to be prognostic for worse outcome in prostate cancer patients⁴⁶. The difference in bioactivity of GDF15 cleave variants⁴⁷ might be resulting in different experimental outcomes when assessing signaling cascades of GDF15. Besides bioactivity, the circulating levels of GDF15 can be altered by genetic variation (SNPs) in the GDF15 gene⁴⁸. Combined, these parameters suggest the interpretation of circulating GDF15 levels in patients should be re-evaluated and the possible cell mediating effects *in vitro* assays should unravel the complex interplay between GDF15 form and signaling cascades.

The identification of a GDF15 receptor in cardiac cells will definitely favor the development of therapeutic approaches to modulate its activity. Recently, a GDF15 receptor was identified in neurons, the GDNF family receptor α -like (GFRAL) receptor, which upon targeting yielded beneficial potential treatment for obesity^{49,50}. The GFRAL receptor is not present in the heart. However, targeting obesity could be beneficial for comorbidity treatment in heart failure patients. Receptors are interesting druggable targets as they are easily accessible for pharmacological compounds. For heart failure, this will remain complex due to the lack of known cardiac or endothelial receptors for GDF15. Therefore,

identifying a specific cardiac receptor for GDF15 is crucial, and might be the only way to turn GDF15 into a valid therapeutic target for HFpEF.

Endothelial to mesenchymal transition as novel mechanism of disease in heart failure

Endothelial cells have a remarkable cell plasticity. This is exemplified during embryonic development, where endothelial cells undergo fate transition into other cell types like hematopoietic or cardiac mesenchymal cells. This transition is needed during the formation of a functional cardiovascular system. While still poorly understood, many studies have addressed the possible contribution of endothelial to mesenchymal cell transition (EndMT) during disease onset and progression⁵¹⁻⁵⁶. EndMT is a complex biological process in which endothelial cells lose their endothelial characteristics transitioning towards a mesenchymal phenotype⁵⁷. Among other stimuli, EndMT is induced by inflammatory responses, causing endothelial dysfunction and increasing the pool of multipotent mesenchymal cells, and contributes to the onset and development of pathological states, including tissue fibrosis, pulmonary arterial hypertension, and atherosclerosis^{53,58}. In **chapter 5** and **chapter 7**, we found indications of EndMT contributing to vascular dysfunction and thereby adverse cardiac remodeling in mice. As EndMT may be a reaction to endothelial injury and is suggested to be of pathological significance for vascular repair, EndMT could become an underlying cause for vascular maladaptation and disease progression^{58,59}. EndMT can be induced by inflammation, mechanical stress and hypoxia, which results in vascular dysfunction^{60,61}. These three factors take place in atherosclerosis^{62,63}. Although the signaling pathways of inflammation-induced EndMT have been identified, unraveling the specific role of this phenotype switching in vascular dysfunction remains a challenge. Traditionally, EndMT is identified based on mutual expression of both endothelial and mesenchymal markers by means of immunohistochemistry or western blot, and gene expression profile. However, as EndMT is a dynamic and reversible transition process and cells lose their endothelial cell expression and will be seen as mesenchymal cells, it can be detected only in a narrow time window^{53,56}. Endothelial lineage tracing studies provide the unique opportunity to confirm the *in vivo* contribution of EndMT to cardiac remodeling and are crucial to understand the extent of EndMT mediated vascular remodeling. Inhibiting EndMT is suggested as a novel strategy in the battle against cardiovascular diseases⁵³, although current approaches are not specific for EndMT and target mechanisms common to wound healing. For example, small molecule inhibitors of TGF- β receptors have shown to be able to block EndMT⁶⁴. Others have shown that a peptide based drug therapy targeting protein phosphatase 2A signaling, was able to preserve endothelial function by inhibiting EndMT and thereby improve the recovery of renal fibrosis in a murine model of obstructive nephropathy⁶⁵. Although these are all preliminary results obtained in experimental models, it clearly indicates a promising future for therapy targeting of EndMT in heart failure.

Endothelial cells as therapeutic target

Endothelial cells display a remarkable potential for therapeutic targeting, as the endothelial layer is in close contact to the blood circulation, thereby easily accessible to systemically delivered agents⁶⁶. Furthermore, they are important in various pathophysiological processes i.e. permeability, and are of importance during vascular inflammation. However, so far the specific affinity of therapeutics to endothelial cells is often limited⁶⁶. Furthermore, the functional role of endothelial cells in various biological processes, like inflammation, tissue perfusion and thrombosis⁶⁶ make their targeting more relevant but also complex. For example, inducing endothelial apoptosis in cancer models can cause tumor regression⁶⁷, although this might cause endothelial dysfunction in healthy organs. This exemplifies the need for safe therapeutic interventions with improved tissue specificity and affinity for organ specific endothelial cells. For example, vascular targeting using nanocarriers with a selection of endothelial cell specific epitopes may refine targeting to specific endothelial lineages⁶⁸.

Some attempts have been made in unraveling the contribution of cardiovascular risk factors to vascular dysfunction. In atherosclerosis, the inflammatory response induces changes in DNA methylation in endothelial cells, thereby altering endothelial gene expression and function, which may contribute to disease progression^{69,70}. Furthermore, risk factors (i.e., smoking) has shown to specifically alter DNA methylation in atherosclerotic

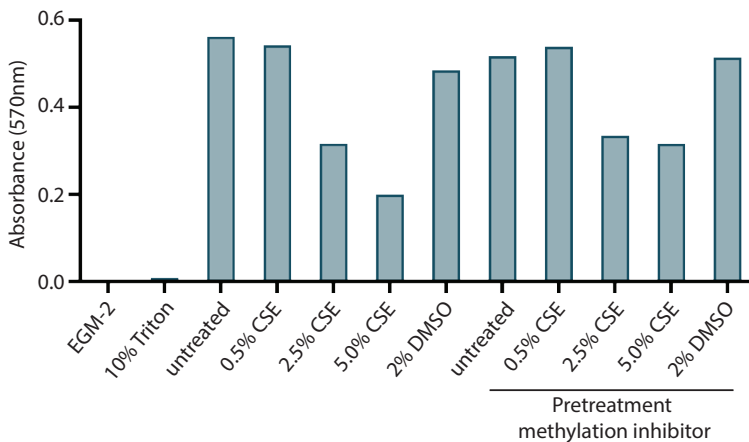


Figure 2. Endothelial cell viability post cigarette smoke extract exposure.

Endothelial cell viability is measured with a cell viability assay (AlamarBlue reagent, AlamarBlue reagent, Thermo Fisher) after exposure to 0.5, 2.5 and 5% of cigarette smoke extract (CSE), with or without 48h pretreatment with a methylation inhibitor (1 μ M 5-aza-2-deoxycytidine, A3656, Sigma Aldrich). Cigarette smoke extract was prepared by collecting the main stream of 1 research graded, unfiltered cigarette (University of Kentucky) bubbled through 25ml of EGM-2 medium. The assay yields a fluorescent signal that colorimetric changes upon cell viability. We included 2 negative controls, EGM-2 without cells to assess interference of medium with the viability assay read out, and cells treated with 10% triton to reduce cell viability. Both show a low absorbance level indicating no cell viability. Untreated endothelial cells as positive control are considered optimal viable, as shown to have a high absorbance level. With increasing levels of CSE cell viability is reduced, though pretreatment seems to prevent the reduced cell viability.

lesions and thereby contribute to worsen disease prognosis⁷¹. We have found that human endothelial cells acutely exposed to cigarette smoke extract show a reduced cell viability (Figure 2, *unpublished data*). However, pre-treatment of cells with a methylation inhibitor (5-aza-2-deoxycytidine) showed protection against loss of cell viability due to smoke extract (Figure 2, *unpublished data*). This shows potential for pharmacological inhibition of endothelial DNA methylation to prevent adverse endothelial dysfunction induced by risk factors. Modulating the activity of epigenetic enzymes of endothelial cells have been suggested as novel potential strategy to enhance vascular repair⁷².

Conclusion

In order to improve HFpEF patient care with novel diagnostics and therapeutics, we have emphasized the importance to gain insights into disease mechanisms. This should include a thorough assessment of the intermediate effects of comorbidities and risk factors, such as CKD, that are often present in the heterogeneous heart failure patient population. The potential of GDF15 as diagnostic biomarker for vascular function, and future therapeutic target is still under investigation. With future research to understand the mechanism of action of GDF15, it might become a clinically relevant tool in disease management or treatment. Research should then focus on the identification of the pathophysiological role of current highly potential biomarkers to eventually benefit heart failure disease management.

References

1. World Health Organization (WHO). Cardiovascular diseases (CVDs). *Lancet Global Health* [https://www.who.int/en/news-room/fact-sheets/detail/cardiovascular-diseases-\(cvds\)](https://www.who.int/en/news-room/fact-sheets/detail/cardiovascular-diseases-(cvds)) (2017).
2. Ponikowski, P. et al. 2016 ESC Guidelines for the Diagnosis and Treatment of Acute and Chronic Heart Failure. *Rev. Española Cardiol.* **69**, 1167 (2016).
3. Shah, K. S. et al. Heart Failure With Preserved, Borderline, and Reduced Ejection Fraction: 5-Year Outcomes. *J. Am. Coll. Cardiol.* **70**, 2476–2486 (2017).
4. Gorter, T. M. et al. Right heart dysfunction and failure in heart failure with preserved ejection fraction: mechanisms and management. Position statement on behalf of the Heart Failure Association of the European Society of Cardiology. *Eur. J. Heart Fail.* **20**, 16–37 (2018).
5. Lam, C. S. P. & Solomon, S. D. The middle child in heart failure: heart failure with mid-range ejection fraction (40–50%). *Eur. J. Heart Fail.* **16**, 1049–1055 (2014).
6. Voors, A. A. et al. A systems BIOlogy Study to TAilored Treatment in Chronic Heart Failure: rationale, design, and baseline characteristics of BIOSTAT-CHF. *Eur. J. Heart Fail.* **18**, 716–726 (2016).
7. Katsiari CG, Bogdanos DP, S. L. Inflammation and cardiovascular disease. *World J Transl Med* **8**, 1–8 (2019).
8. Hansson, G. K., Libby, P. & Tabas, I. Inflammation and plaque vulnerability. *J. Intern. Med.* **278**, 483–493 (2015).
9. Gansevoort, R. T. et al. Chronic kidney disease and cardiovascular risk: Epidemiology, mechanisms, and prevention. *Lancet* **382**, 339–352 (2013).
10. Duma, N. et al. Characterization of Comorbidities Limiting the Recruitment of Patients in Early Phase Clinical Trials. *Oncologist* **24**, 96–102 (2019).
11. Gnanaraj, J. & Radhakrishnan, J. Cardio-renal syndrome. *F1000Research* **5**, 1–10 (2016).
12. Ronco, C. Cardiorenal Syndromes: Definition and Classification. *Contrib. Nephrol.* **164**, 33–38 (2010).
13. Li, Z. et al. Hydrogen Sulfide Attenuates Renin Angiotensin and Aldosterone Pathological Signaling to Preserve Kidney Function and Improve Exercise Tolerance in Heart Failure. *JACC. Basic to Transl. Sci.* **3**, 796–809 (2018).
14. Rockman, H. A., Wachhorst, S. P., Mao, L. & Ross, J. ANG II receptor blockade prevents ventricular hypertrophy and ANF gene expression with pressure overload in mice. *Am. J. Physiol. - Hear. Circ. Physiol.* **266**, 35–36 (1994).
15. Liu, S. Heart-kidney interactions: mechanistic insights from animal models. *Am. J. Physiol. Renal Physiol.* **316**, 974–985 (2019).
16. Szymanski, M. K., de Boer, R. A., Navis, G. J., van Gilst, W. H. & Hillege, H. L. Animal models of cardiorenal syndrome: a review. *Heart Fail. Rev.* **17**, 411–20 (2012).
17. Hewitson, T. D., Holt, S. G. & Smith, E. R. Animal Models to Study Links between Cardiovascular Disease and Renal Failure and Their Relevance to Human Pathology. *Front. Immunol.* **6**, 465 (2015).
18. Valero-Muñoz, M., Backman, W. & Sam, F. Murine Models of Heart Failure With Preserved Ejection Fraction: A “Fishing Expedition”. *JACC Basic to Transl. Sci.* **2**, 770–789 (2017).
19. Matsushita, K. et al. The acute kidney injury to chronic kidney disease transition in a mouse model of acute cardiorenal syndrome emphasizes the role of inflammation. *Kidney Int.* In press (2019).
20. Sharp, T. E., Lefer, D. J. & Houser, S. R. Cardiometabolic Heart Failure and HFpEF: Still Chasing Unicorns. *JACC Basic to Transl. Sci.* **4**, 422–424 (2019).
21. Sorop, O. et al. Multiple common comorbidities produce left ventricular diastolic dysfunction associated with coronary microvascular dysfunction, oxidative stress, and myocardial stiffening. *Cardiovasc. Res.* **114**, 954–964 (2018).
22. DeLeon-Pennell, K. Y. & Lindsey, M. L. Somewhere over the sex differences rainbow of myocardial infarction remodeling: hormones, chromosomes, inflammasome, oh my. *Expert Rev. Proteomics* **16**, 1–8 (2019).
23. Kostkiewicz, M., Tracz, W., Olszowska, M., Podolec, P. & Drop, D. Left ventricular geometry and function in patients with aortic stenosis: gender differences. *Int. J. Cardiol.* **71**, 57–61 (1999).
24. Paulus, W. J. & Tschöpe, C. A novel paradigm for heart failure with preserved ejection fraction: comorbidities drive myocardial dysfunction and remodeling through coronary microvascular endothelial inflammation. *J. Am. Coll. Cardiol.* **62**, 263–71 (2013).
25. Wang, C. Obesity, inflammation, and lung injury (OILI): The good. *Mediators Inflamm.* 978463 (2014).
26. Wollert, K. C. & Kempf, T. Growth differentiation factor 15 in heart failure: An update. *Curr. Heart Fail. Rep.* **9**, 337–345 (2012).
27. Kempf, T. & Wollert, K. C. Growth differentiation factor-15: A new biomarker in cardiovascular disease. *Herz* **34**, 594–599 (2009).
28. Wollert, K. C. et al. An Automated Assay for Growth Differentiation Factor 15. *J. Appl. Lab. Med.* **1**, 510–521 (2017).

29. Piek, A., Du, W., de Boer, R. A. & Silljé, H. H. W. Novel heart failure biomarkers: why do we fail to exploit their potential? *Crit. Rev. Clin. Lab. Sci.* **55**, 246–263 (2018).
30. Gaggin, H. K. & Januzzi, J. L. Biomarkers and diagnostics in heart failure. *Biochim. Biophys. Acta - Mol. Basis Dis.* **1832**, 2442–2450 (2013).
31. Corre, J., Hébraud, B. & Bourin, P. Concise review: growth differentiation factor 15 in pathology: a clinical role? *Stem Cells Transl. Med.* **2**, 946–52 (2013).
32. Li, C. et al. GDF15 promotes EMT and metastasis in colorectal cancer. *Oncotarget* (2016) doi:10.18632/oncotarget.6205.
33. Minamisawa, M. et al. Comparison of Inflammatory Biomarkers in Outpatients With Prior Myocardial Infarction. *Int. Heart J.* (2016) doi:10.1536/ihj.15-197.
34. van der Wal, H. H., van Deursen, V. M., van der Meer, P. & Voors, A. A. *Comorbidities in Heart Failure. Handbook of experimental pharmacology* vol. 243 (2017).
35. Boulogne, M. et al. Inflammation versus mechanical stretch biomarkers over time in acutely decompensated heart failure with reduced ejection fraction. *Int. J. Cardiol.* (2017) doi:10.1016/j.ijcard.2016.10.038.
36. Elouey, A. K., Alameddine, R. Y., Osta, B. A. & Awad, D. M. Correlations between serum inflammatory markers and comorbidities in patients with end-stage renal disease. *J. Taibah Univ. Med. Sci.* (2019) doi:10.1016/J.JTUMED.2019.10.003.
37. Chung, E. S., Packer, M., Lo, K. H., Fasanmade, A. A. & Willerson, J. T. Randomized, double-blind, placebo-controlled, pilot trial of infliximab, a chimeric monoclonal antibody to tumor necrosis factor-alpha, in patients with moderate-to-severe heart failure: results of the anti-TNF Therapy Against Congestive Heart Failure. *Circulation* **107**, 3133–3140 (2003).
38. Anker, S. D. & Coats, A. J. S. How to RECOVER from RENAISSANCE? The significance of the results of RECOVER, RENAISSANCE, RENEWAL and ATTACH. *Int. J. Cardiol.* **86**, 123–130 (2002).
39. Min, K.-W. et al. NAG-1/GDF15 accumulates in the nucleus and modulates transcriptional regulation of the Smad pathway. *Oncogene* **35**, 377–388 (2015).
40. Heger, J. et al. Growth differentiation factor 15 acts anti-apoptotic and pro-hypertrophic in adult cardiomyocytes. *J. Cell. Physiol.* **224**, 120–126 (2010).
41. Xu, J. et al. GDF15/MIC-1 Functions As a Protective and Antihypertrophic Factor Released From the Myocardium in Association With SMAD Protein Activation. *Circ. Res.* **98**, 342–350 (2006).
42. Olsen, O. E., Skjærvi, A., Stordal, B. F., Sundan, A. & Holien, T. TGF- β contamination of purified recombinant GDF15. *PLoS One* **12**, e0187349 (2017).
43. Luan, H. H. et al. GDF15 Is an Inflammation-Induced Central Mediator of Tissue Tolerance. *Cell* **178**, 1231–1244 (2019).
44. Scott, D. W., Vallejo, M. O. & Patel, R. P. Heterogenic endothelial responses to inflammation: role for differential N-glycosylation and vascular bed of origin. *J. Am. Heart Assoc.* **2**, e000263 (2013).
45. Garlanda, C. & Dejana, E. Heterogeneity of endothelial cells. Specific markers. *Arterioscler. Thromb. Vasc. Biol.* **17**, 1193–1202 (1997).
46. Bauskin, A. R. et al. The Propeptide Mediates Formation of Stromal Stores of PROMIC-1: Role in Determining Prostate Cancer Outcome. *Cancer Res.* **65**, 2330–2336 (2005).
47. Bauskin, A. R. et al. The propeptide of macrophage inhibitory cytokine (MIC-1), a TGF-beta superfamily member, acts as a quality control determinant for correctly folded MIC-1. *EMBO J.* **19**, 2212–2220 (2000).
48. Wang, J. et al. The H6D genetic variation of GDF15 is associated with genesis, progress and prognosis in colorectal cancer. *Pathol. Res. Pract.* **211**, 845–850 (2015).
49. Yang, L. et al. GFRAL is the receptor for GDF15 and is required for the anti-obesity effects of the ligand. *Nat. Med.* **23**, 1158–1166 (2017).
50. Mullican, S. E. & Rangwala, S. M. Uniting GDF15 and GFRAL: Therapeutic Opportunities in Obesity and Beyond. *Trends Endocrinol. Metab.* **29**, 560–570 (2018).
51. Yao, Y. et al. A role for the endothelium in vascular calcification. *Circ. Res.* **113**, 495–504 (2013).
52. Wermuth, P. J., Carney, K. R., Mendoza, F. A., Piera-Velazquez, S. & Jimenez, S. A. Endothelial cell-specific activation of transforming growth factor- β signaling in mice induces cutaneous, visceral, and microvascular fibrosis. *Lab. Invest.* **97**, 806–818 (2017).
53. Li, Y., Lui, K. O. & Zhou, B. Reassessing endothelial-to-mesenchymal transition in cardiovascular diseases. *Nat. Rev. Cardiol.* **15**, 445–456 (2018).
54. Rieder, F. et al. Inflammation-induced endothelial-to-mesenchymal transition: A novel mechanism of intestinal fibrosis. *Am. J. Pathol.* **179**, 2660–2673 (2011).
55. Piera-Velazquez, S., Mendoza, F. A. & Jimenez, S. A. Endothelial to Mesenchymal Transition (EndoMT) in the Pathogenesis of Human Fibrotic Diseases. *J. Clin. Med.* **5**, 45 (2016).
56. Lu, X., Gong, J., Dennery, P. A. & Yao, H. Endothelial-to-mesenchymal transition: Pathogenesis and therapeutic targets for chronic pulmonary and vascular diseases. *Biochem. Pharmacol.* **168**, 100–107 (2019).
57. Yoshimatsu, Y. & Watabe, T. Roles of TGF β Signals in Endothelial-Mesenchymal Transition during Cardiac Fibrosis. *Int. J. Inflamm.* **2011**, 1–8 (2011).

58. Zeisberg, E. M. et al. Endothelial-to-mesenchymal transition contributes to cardiac fibrosis. *Nat. Med.* **13**, 952–961 (2007).
59. Van Meeteren, L. A. & Ten Dijke, P. Regulation of endothelial cell plasticity by TGF- β . *Cell Tissue Res.* **347**, 177–186 (2012).
60. Sánchez-Duffhues, G. et al. Inflammation induces endothelial-to-mesenchymal transition and promotes vascular calcification through downregulation of BMPR2. *J. Pathol.* **247**, 333–346 (2019).
61. Lerman, A. & Zeiher, A. M. Endothelial function: Cardiac events. *Circulation* **111**, 363–368 (2005).
62. Vitiello, L. et al. Microvascular inflammation in atherosclerosis. *IJC Metab. Endocr.* **3**, 1–7 (2014).
63. Libby, P., Ridker, P. M. & Maseri, A. Inflammation and atherosclerosis. *Circulation* **105**, 1135–1143 (2002).
64. Ghosh, A. K., Nagpal, V., Covington, J. W., Michaels, M. A. & Vaughan, D. E. Molecular basis of cardiac endothelial-to-mesenchymal transition (EndMT): differential expression of microRNAs during EndMT. *Cell. Signal.* **24**, 1031–1036 (2012).
65. Deng, Y. et al. Blocking protein phosphatase 2A signaling prevents endothelial-to-mesenchymal transition and renal fibrosis: a peptide-based drug therapy. *Sci. Rep.* **6**, 19821 (2016).
66. Kiseleva, R. Y. et al. Targeting therapeutics to endothelium: are we there yet? *Drug Deliv. Transl. Res.* **8**, 883–902 (2018).
67. Brooks, P. C. et al. Integrin $\alpha v\beta 3$ antagonists promote tumor regression by inducing apoptosis of angiogenic blood vessels. *Cell* **79**, 1157–1164 (1994).
68. Howard, M. et al. Vascular targeting of nanocarriers: perplexing aspects of the seemingly straightforward paradigm. *ACS Nano* **8**, 4100–4132 (2014).
69. Tabaei, S. & Tabaei, S. S. DNA methylation abnormalities in atherosclerosis. *Artif. Cells, Nanomedicine, Biotechnol.* **47**, 2031–2041 (2019).
70. Dunn, J. et al. Flow-dependent epigenetic DNA methylation regulates endothelial gene expression and atherosclerosis. *J. Clin. Invest.* **124**, 3187–3199 (2014).
71. Siemelink, M. A. et al. Smoking is Associated to DNA Methylation in Atherosclerotic Carotid Lesions. *Circ. Genomic Precis. Med.* **11**, e002030 (2018).
72. Fraineau, S., Palii, C. G., Allan, D. S. & Brand, M. Epigenetic regulation of endothelial-cell-mediated vascular repair. *FEBS J.* **282**, 1605–1629 (2015).



APPENDICES

Nederlandse samenvatting

Dankwoord

List of publications

Curriculum Vitae

Nederlandse samenvatting

Cardiovasculaire ziekten zijn wereldwijd doodsoorzaak nummer 1 en jaarlijks verantwoordelijk voor 31% van het totale aantal sterftegevallen. Met name in westerse landen neemt het aantal patiënten met cardiovasculaire ziekte toe door een verhoogde aanwezigheid van diabetes, hypertensie en obesitas in een snel vergrijzende populatie. Onder cardiovasculaire ziekten vallen onder andere atherosclerose (slagaderverkalking) en hartfalen. Zowel atherosclerose als acuut hartfalen veroorzaakt door een hartinfarct zijn tegenwoordig goed en snel te behandelen met daarbij een grote overlevingskans voor de patiënt. Het gevolg is een groeiende populatie van chronisch hartfalenpatiënten waarbij de functie van het hart en daarmee de pompkracht ervan langzaam achteruit gaat. Tot op heden bestaat er geen behandeling voor chronisch hartfalen.

Symptomen van hartfalen zijn vermoeidheid en kortademigheid, zowel tijdens beweging als in rust. Bij hartfalen spreken we over een verminderde hartfunctie. Door de verminderde pompkracht wordt er minder bloed rondgepompt, hetgeen dit heet ook wel een verminderde ejectiefractie van het hart wordt genoemd. Er zijn verschillende subtypes hartfalen bekend, waarbij onderscheid wordt gemaakt tussen patiënten met een verminderde ejectiefractie en patiënten met behoud van de ejectiefractie maar die wel de symptomen van hartfalen hebben. Patiënten met chronisch hartfalen worden behandeld met medicatie die de symptomen bestrijdt, maar niet in staat is om de hartfunctie te herstellen. Deze medicatie is helaas niet effectief in het verlichten van de klachten van hartfalenpatiënten met behoud van ejectiefractie. Dit suggereert dat er niet alleen klinisch een verschil in de hartfalenpopulatie aanwezig is maar ook een onderliggend biologisch verschil. Er is meer onderzoek nodig om kennis te vergaren over de onderliggende biologie, die kan bijdragen aan de ontwikkeling van een behandeling die wel werkzaam is in deze patiëntengroep.

Daarbij is het allereerst van belang dat we de patiënten met behoud van ejectiefractie vroegtijdig kunnen identificeren. Patiënten met behoud van ejectiefractie zijn vaak een lange periode asymptomatisch en hebben vaker (niet-)cardiovasculaire nevenaandoeningen (comorbiditeiten). Onder comorbiditeiten vallen onder andere hypertensie (een hoge bloeddruk), diabetes en nierfalen. Deze comorbiditeiten zijn verantwoordelijk voor een chronische ontsteking (inflammatie) van de bloedvaten. Door de comorbiditeiten zijn patiënten vaak niet meegenomen in patiëntstudies, omdat ze zorgen voor te veel diversiteit binnen de hartfalenpopulatie en daardoor de resultaten van de studie beïnvloeden. Door deze aanpak missen we nog veel informatie over deze groep patiënten. In dit proefschrift hebben we onderzoek gedaan naar de effecten van nierfalen en een chronische inflammatie op de functie van bloedvatjes in het hart. Daarbij belichten we specifieke biologische mechanismen die een rol spelen bij vasculaire inflammatie en suggereren we dat het eiwit GDF15 mogelijk een nieuw diagnostisch of therapeutisch doeleiwit kan zijn.

Het endotheel is een bedekkende cellaag aan de binnenkant van de bloedvaten die een belangrijke rol speelt in de bloedstolling en het transport van voedingsstoffen naar de organen. In **hoofdstuk 2** beschrijven we het moleculaire signaalproces genaamd endotheel-mesenchymale overgang (EndMT), waarbij de plasticiteit van endotheelcellen een rol speelt in de ontwikkeling van cardiovasculaire aandoeningen. Verschillende oorzaken, waaronder inflammatie, kunnen EndMT induceren wat een belangrijke rol speelt bij verschillende processen zoals bij het vormen van littekenweefsel maar ook bij het uitzaaien van kanker. Wij benadrukken dat EndMT ook een belangrijke rol speelt in de progressie en vorming van instabiele plaques, een plaatselijke verdikking in de vaatwand bij patiënten met atherosclerose. Een instabiele plaque kan leiden tot ernstige gevolgen zoals verstopping van het bloedvat of bloedstolsels met verminderde bloedtoevoer naar organen zoals het hart. Daarom heeft EndMT veel potentieel voor doelgerichte therapie in de toekomst ter voorkoming van instabiele plaques.

Hoe inflammatie bijdraagt aan cardiovasculaire ziekten blijft een continue onderwerp van discussie. Zowel lokale inflammatie door schade aan weefsel als systemische inflammatie veroorzaakt door comorbiditeiten, bijvoorbeeld nierfalen, spelen een rol in de onderliggende pathologie van cardiovasculaire ziekten. Naar de invloed van de combinatie van atherosclerose en comorbiditeit gedreven inflammatie op de ontwikkeling van cardiovasculaire ziekten is zeer weinig onderzoek gedaan. In **hoofdstuk 3** hebben wij gekeken naar de aanwezigheid van inflammatie door nierfalen in patiënten met atherosclerose en het effect daarvan op de progressie van de ziekte. Daarbij hebben we gekeken naar de samenstelling van plaques uit de patiënten en deze beoordeeld op stabiliteit. We bevestigen de aanwezigheid van een instabiele plaque in patiënten met een slechte nierfunctie, hetgeen op den duur een nadelig effect heeft op de gezondheid van de patiënt. De invloed van inflammatie op deze associatie kon niet worden vastgesteld, dit ten gevolge van de gekozen patiëntenpopulatie. Mogelijk waren de gegevens over de nierfunctie van deze patiënten niet optimaal omdat de patiënten eerst gezien worden bij de cardioloog en dan pas naar de nefroloog gaan. Het is belangrijk dat we voor toekomstig onderzoek meer aandacht besteden aan deze criteria, bijvoorbeeld door het verkrijgen van een compleet beeld van de patiënt zoals bloed- en urinemarkers voor het bepalen van de nierfunctie. Door het gebrek aan patiënten met comorbiditeiten zoals nierfalen in studiepopulaties is er een hiaat in de huidige kennis omtrent het interfereren van de nieren op de hartfunctie. Voordat we hartpatiënten met nierfalen, kortom patiënten met een cardio-renaal syndroom, kunnen behandelen zullen we meer informatie moeten verzamelen over deze specifieke patiëntenpopulatie.

Voor het beter begrijpen van ziektes zijn diermodellen noodzakelijk om te onderzoeken wat de biologische processen achter een ziekte zijn. Het transversale aorta constrictie (TAC) model wordt veel gebruikt in onderzoek naar de functie en structurele verschillen van het hart tijdens chronisch hartfalen. Het renine angiotensine systeem (RAS) speelt een rol bij de bloeddruk regulatie. Nierfalen en hartfalen zijn door het RAS aan elkaar

verbonden, waardoor nierfalen een negatief effect kan hebben op de progressie van hartfalen. Toch is er weinig bekend over eventuele nierschade en de nierfunctie in het TAC model. In **hoofdstuk 4** hebben we gekeken naar de nieren in dit diemodel, waarbij we een toename zagen van renine, onderdeel van het RAS systeem. Met progressie van hartfalen zagen we een stijging in renineniveaus zonder enige structurele schade aan de nier. Dit geeft aan dat de nieren wel een verminderde doorbloeding waarnemen ten gevolge van het hartfalen maar hier nog geen ernstige gevolgen van ondervinden. Deze resultaten moeten wel voorzichtig geïnterpreteerd worden, de muis is immers niet één op één te vergelijken met een patiënt die aan het cardio-renaal syndroom lijdt. In de patiënt met cardio-renaal syndroom zijn meerdere complexe interacties in de cardio-renale as aanwezig die we nog niet optimaal kunnen nabootsen in een diemodel. Daarom zullen er in de toekomst complexere modellen nodig zijn zodat meer onderzoek kan worden gedaan naar het cardio-renaal syndroom, voordat eventuele behandelingen ontwikkeld kunnen worden.

Bij hartfalen gaat het hart compenseren met structurele aanpassingen, ook wel remodeleren genoemd, om zijn pompkracht en functie te behouden. Het remodeleren van het hart kan geïnduceerd worden door verschillende oorzaken en zal in een gevorderd stadium zorgen voor zeer ernstig hartfalen. Uit onderzoek is gebleken dat onder patiënten met hartfalen, het geslacht een rol speelt in het type remodeleren van het hart en daarbij ook zal resulteren in een ander verloop van het hartfalen. Bij vrouwelijke patiënten wordt vaak een verdikte hartwand gevonden, terwijl bij mannelijke patiënten vaker een dunne en uitgerekte hartwand wordt gevonden. Het is echter onduidelijk welke onderliggende mechanismen hieraan ten grondslag liggen. In **hoofdstuk 5** volgen we de hartremodelering en -functie in zowel mannelijke als vrouwelijke muizen na TAC. De resultaten na TAC zijn bijzonder duidelijk: waar de mannelijke muizen een vergroot hart laten zien met een zeer dunne hartwand, laten de vrouwelijke muizen een verdikt hart zien wat in totale grootte niet extreem is toegenomen. Ondanks het verschil in remodeleren na TAC zien we geen verschillen in de hartfunctie, zowel mannelijke als vrouwelijke muizen laten met de tijd een verslechtering zien. Door middel van eiwitanalyses in het bloed hebben we signaalroutes gevonden die het verschil zouden kunnen verklaren. Met name bij de vrouwelijke muizen vonden we een interessante relatie tussen de ernst van hartremodelering met een verminderde vasculaire functie en een specifiek EndMT. Tegelijkertijd vonden we een toename van bindweefselvorming (litteken) rond de bloedvaatjes in het hart, hetgeen een reeds beschreven effect van EndMT is. Deze prille bevindingen zijn van belang voor het begrijpen van hartfalen in vrouwelijke patiënten en de identificatie van nieuwe geslachts-specifieke markers waarmee we patiënten kunnen diagnosticeren en uiteindelijk behandelen. Zeker voor vrouwen met hartfalen is dit van belang, door minder symptomen zijn ze vaak moeilijker te diagnosticeren.

Groei en differentiatiefactor 15 (GDF15) is een signaal-eiwit betrokken bij inflammatie. Het is een sterke voorspellende marker voor hartfalen, maar de biologische functie in

het hartremodeleren is tot dusver onbekend. In **hoofdstuk 6** introduceren we GDF15 als belangrijke speler in het proces achter hartremodelering en benadrukken we de vele verschillende effecten van GDF15 op de celtypen in het hart. Ondanks dat we GDF15 kunnen meten in het bloed, weten we nog niet goed wat de bijdrage van GDF15 is aan hartfalen. Daarom focussen we ons in **hoofdstuk 7** op de rol van GDF15 in ernstig hartfalen en hartremodelering. Patiënten met hartfalen hebben een verhoogd niveau van GDF15, daarom zijn we gaan kijken naar muizen zonder GDF15. In vergelijking met gezonde muizen, blijkt in afwezigheid van GDF15 ernstiger hartfalen na TAC aanwezig te zijn. Daarnaast hebben muizen zonder GDF15 een toename in vasculaire bindweefselvorming en EndMT. Zoals is bevestigd met celkweek- experimenten, blijkt GDF15 in staat te zijn om te voorkomen dat de endotheelcellen EndMT ondergaan. Hieruit concluderen we dat een toename van GDF15 in het bloed van patiënten een reflectie is van de vasculaire functie van patiënten tijdens het negatief remodeleren van het hart. Er is op dit moment een grote behoefte aan markers zoals GDF15 die niet alleen kunnen bijdragen aan het diagnosticeren maar ook indicaties geven over het onderliggend mechanisme dat zorgt voor het ontstaan of de voortgang van hartfalen. Dit is met name van belang bij het optimaal behandelen van de hartfalenpatiënt. Door meer kennis over het mechanisme kan met een simpele GDF15-meting een nauwkeurigere beslissing over de behandeling worden genomen. Voor het zover is, blijft het cruciaal dat er meer onderzoek nodig is naar de rol van GDF15 in het onderliggende mechanisme en de vasculaire disfunctie voordat GDF15 als standaardmarker geïmplementeerd kan worden in de huidige diagnostiek.

Ondanks dat er de laatste jaren veel onderzoek is geweest naar het remmen van systemische ontstekingen in patiënten met hartfalen, hebben deze therapieën nooit de kliniek bereikt door de vele bijwerkingen. Dit heeft met name te maken met de eerder genoemde hartfalenpopulatie waarbij veel verschillende oorzaken van een verhoogd level van systemische ontsteking aanwezig zijn, zoals diabetes en nierfalen. Daarnaast hebben ontstekingseiwitten zoals GDF15 verschillende effecten op een heleboel cellen. Het zomaar remmen of stimuleren van deze signaal eiwitten heeft grote en soms negatieve gevolgen op heel veel cellen en organen. Daarom moeten we onderzoeken hoe en waar GDF15 aangrijpt op de hartcellen of op de vaatwand. Momenteel is dat nog niet duidelijk. Doelgericht inspelen op het aangrijpingspunt van GDF15 op hart- en vaatcellen heeft meer therapeutische mogelijkheden dan globaal remmen van GDF15 in het lichaam. Deze aanpak kan in de toekomst zorgen voor een specifieke aanpak van het aangrijpingspunt van GDF15 op endotheelcellen. Meerdere studies richten zich op de mogelijkheid tot het behandelen van de endotheelcel. Zowel in hoofdstuk 5 als 7 laten we zien dat het disfunctioneren van het endotheel door middel van EndMT bijdraagt aan de vasculaire disfunctie en daarbij hartfalen. Ondanks de brede kennis over EndMT zijn er tot op heden geen behandelingen ontwikkeld door de complexiteit van het proces. Toch hebben endotheelcellen veel potentie, aangezien de endotheelcellaag in nauw contact staat met de bloedcirculatie en daardoor gemakkelijk te bereiken is voor medicijnen. Dit blijft een complex proces, waardoor breed georiënteerd onderzoek nodig is, van

patiëntstudies tot aan cellweken in het laboratorium, om een antwoord te vinden op de vraag naar verbeterde behandelingen bij patiënten met hartfalen.

Met dit proefschrift is benadrukt hoe belangrijk het is dat we goed begrijpen wat het mechanisme is achter de ziekte. Dit houdt in dat we met name de interfererende effecten van comorbiditeiten zoals nierfalen moeten bestuderen in de aanwezigheid van de zeer diverse hartfalenpopulaties. Daarnaast hebben we laten zien dat GDF15 een grote potentie heeft als marker en mogelijke behandeling van hartfalen, toch is hier nog veel onderzoek nodig. We laten zien dat GDF15 waarschijnlijk de grootste bijdrage kan leveren als marker voor de algemene gezondheidsstatus van de patiënt. Uiteindelijk hopen we dat met dit onderzoek een bijdrage geleverd kan worden aan het begrijpen van hartfalen en dat het in de toekomst voor de patiënt resulteert in een betere behandeling.

Dankwoord

De afgelopen jaren heb ik met veel plezier en enthousiasme gewerkt aan het onderzoek gebundeld in dit proefschrift. Maar dit kon ik niet alleen, dit proefschrift zou er niet zijn zonder hulp van collega's en de nodige afleiding door vrienden en familie. Een aantal mensen wil ik hierbij in het bijzonder bedanken.

Prof. dr. Pasterkamp, beste **Gerard**, alweer bijna 7 jaar geleden was jij in een bachelor cursus de begeleider van onze groepsopdracht. Je vroeg naar onze toekomst plannen en toen ik aangaf het onderwijs in te willen, was je het daar duidelijk niet mee eens. Wat ben ik blij dat ik je toen een mail heb gestuurd met de vraag waarom dat toch was. Nu 7 jaar en een PhD later ben ik je dankbaar voor alle mogelijkheden en leerzame adviezen die je me hebt gegeven, over zowel onderzoek als niet werk gerelateerde onderwerpen. Fijn dat ik me de komende twee jaar onder jouw supervisie verder mag ontwikkelen. Dankjewel!

Dr. de Jager, beste **Saskia**, vanaf het moment dat ik wist dat ik een PhD binnen Reconnect mocht gaan doen was ik erg blij dat ik dit onder jou begeleiding mocht uitvoeren. Het eerste jaar zat vol met onverwachte wisselingen, het was fijn om steun aan je te hebben en daardoor toch mijn weg te vinden in zowel het UMCU als het LUMC. Dit proefschrift was er absoluut niet geweest zonder jouw motivatie, kennis en gedrevenheid om iedereen te overtuigen van GDF15. Met het GDF15 project in Virginia blijven we nog samen verder werken aan ons favoriete maar frustrerende eiwit. Dank voor alles!

Prof. dr. Marie-Jose Goumans, beste **Marie-José**, wat ontzettend fijn dat ik bij jou terecht kon voor constant advies en het uitvoeren van verschillende endotheel experimenten. Jouw hulp heeft mijn PhD gemaakt tot een ontzettende leerzame tijd en veel nieuwe lab ervaring. Ik voelde me ontzettend welkom in je groep en ben dan ook met veel plezier dagenlang op en neer gereisd naar Leiden. Ik hoop dat we ook in de toekomst kunnen blijven samenwerken, bedankt voor alles!

Dr. Gonzalo Sanchez, dear **Gonzalo**, you are a very busy and dedicated scientist, your knowledge on the TGF- β pathway and molecular biology is amazing. Thank you for helping me with many things, you have taught me a lot. It took me some time to completely get your sense of humor, but now it makes me laugh every time, just what we sometimes need to cope with frustrating experiments. Thank you for everything!

Leden van de leescommissie, prof. dr. **D.P.V. de Kleijn**, prof. dr. **M. L. Bots**, prof. dr. **R. Goldschmeding**, prof. dr. **P.H.A. Quax** en prof. dr. **H. van Goor**, bedankt voor het zitting nemen in mijn beoordelingscommissie en het kritisch lezen van mijn proefschrift.

Reconnect, beste **Dirk** en **Marianne** en andere consortium leden, dank voor jullie kritische blik op mijn projecten tijdens de vele meetings. De Summer schools waren niet alleen zeer nuttig en leerzaam maar zorgden ook in korte tijd voor een fijn netwerk. Daarnaast wil ik jullie ook allemaal en zeker de PhD's bedanken voor de gezelligheid!

Experimentele cardiologie, **Hester** dankjewel dat ik altijd langs kon komen voor advies en feedback op epidemiologische vragen of je visie op de wetenschap. **Joost**, dank dat ik ondanks alle veranderingen op het cardio lab kon blijven werken en deels kon aansluiten bij je groep. **Suzanne, Imo, Alain, Klaus, Zhiyong, Pieter, Elise, Peter-Paul, Lena, Aisha, Jonne**, dank voor jullie hulp, feedback en gezelligheid. **Saskia** (Haitjema), bij jou mocht ik mijn eerste stage lopen, dank voor deze ervaring en het mogen lenen van je schattige auto! **Jelte**, bedankt voor de ontzettend gezellige borrels en leuke gesprekken! **Ian**, we hebben van elkaar kunnen leren, dank voor een fijne samenwerking! **Dennie**, dank voor je hulp tijdens maar ook zeker na mijn stage. **Tom**, dank voor de goede gesprekken waardoor we vaak niet meer op de tijd letten. Ik hoop dat we onze koffiepauzes blijven voortzetten. Veel succes bij de thoraxchirurgie! **Gideon**, je mag een paar weken na mij promoveren, veel succes in de kliniek. **Robin**, wat ben je gedreven, slim en een goede wetenschapper. Je hebt me vaak geholpen met feedback, analyses in R maar we hadden ook gewoon goede inhoudelijke discussies. Ik vond het ontzettend gezellig om met jou op het lab te zitten, dankjewel voor deze fijne tijd. En ik weet zeker, waar je ook terecht komt het gaat helemaal goed komen met je carrière! **Tim**, we kennen elkaar al van de bachelor en je was even mijn collega. Ik ben blij dat ik af en toe met jou kan sparren en reflecteren, dankjewel! **Judith**, jou moet ik nog even extra bedanken want zonder jouw werk aan GDF15 was ik niet zo ver gekomen. Ik ben blij dat ik met je mocht samenwerken en veel van je geleerd heb, en dat je nog steeds bereid bent om mee te denken of feedback te geven. **Simon**, ik blijf langs lopen voor een gezellig praatje, succes met je PhD! **Marieke** zonder jou waren er niet zoveel leuke borrels, ik heb nu al zin in Budapest! **Sophie** en **Klaske** altijd gezellig om even bij jullie te buurten in de toren! **Lotte**, dank voor de gezelligheid tijdens onze mini vakantie in Washington. **Michelle, Juntao, Margarida, Clemencé, Renee, Marijn, Casper, Sandra** good luck with finishing your PhDs!

Beste **Maïke**, wat hebben we veel samengewerkt de afgelopen jaren, bijna constant draaide er wel een of andere muisstudie die grotendeels in dit boekje zitten. Je bent onmisbaar en ik vind het erg leuk dat we nog een tijdje doorgaan om alle muisstudies mooi af te ronden. Dankjewel voor alle hulp en de gezelligheid!

Beste **Petra**, ook jij verdient een extra dankjewel, je hebt me ontzettend veel geholpen met allerlei kleuringen en niet te min al het doorvoeren van de stroom aan muismateriaal. Fijn dat ik altijd bij je terecht kon om even te kletsen, een kopje thee en het juiste advies. Dank voor alles!

En natuurlijk alle (ex-)analisten die zorgen voor een goed draaiend lab. **Arjan**, lichte paniek toen je besloot de experimentele cardiologie te verlaten. Maar ook nu weet ik je nog te vinden als het nodig is, dank dat ik altijd binnen mocht lopen voor hulp en advies! **Esther, Hemse, Corina, Daniek, Danny, Mark, Nanique, Anouska, Joëlle**, en **Noortje**, allen dank voor de hulp en ook zeker de gezelligheid! **Naomi**, zeker in de laatste drukke maanden ben je van onschatbare waarde geweest in het oppakken van dingen die voor mij teveel waren, dankjewel!

De biotechnici van proefdier groot, **Evelyn, Joyce, Marlijn** en **Martijn**. Alle dank voor de hulp als ik vastliep in de planning of als ik iets nodig had uit voorraad of vriezer. Maar ook de gezelligheid op borrels en koffie pauzes.

Beste **Ineke, Joukje** en **Ingrid**, allen ontzettend bedankt voor de hulp met allerlei verschillende vragen. Wat fijn dat jullie ons door het logge systeem van het UMC helpen en hard werken om overall een antwoord voor te vinden. Dank voor alle ondersteuning!

Beste studenten, **Eva, Maïke, Tim** en **Julius**. Stuk voor stuk hebben jullie bijgedragen aan mijn boekje zoals ook te zien is in de auteurslijsten van de hoofdstukken. Ik vond het ontzettend leuk om jullie te begeleiden en te zien hoe jullie groeide en zelfstandig werden op het lab. **Maïke, Tim** en **Julius**, dank voor alle hulp, support en geduld tijdens het afronden van mijn boekje!

Lieve kamergenootjes, **John**, leuk om te zien dat je op je plek zit bij onderwijs! **Danielle**, je hebt je krachtig door je PhD geslagen, succes met je verdere carrière. **Lianne**, ook al was je er maar een jaar je was een gezellige toevoeging aan onze kamer, fijn dat je een leuke plek hebt gevonden bij Genmab. **Evelyne**, je bent een harde werker met een hart voor je projecten, je houdt alles draaiend ook al is dat met je grote varkensstudies niet altijd makkelijk. Leuk om te zien hoe je de afgelopen jaren bent gegroeid. Houd vol, je bent er bijna! **Nazma**, elke kamer heeft een iemand nodig die van aanpakken weet, maar ook door heeft wanneer iemand even een luisterend oor nodig heeft, dankjewel!

CVCB groep, beste **Esther, Annemarie, Vera, Babu, Tom, Tiago, Anke, Kirsten**, en **Tessa**. Als een soort adoptie PhD werd ik met periodes door jullie opgevangen, ik heb me altijd ontzettend welkom gevoeld. Ik vind het jammer dat ik vaak niet meer de tijd vind om naar Leiden te reizen om even bij te kletsen. Dankjulliewel voor alle praktische hulp, tips en adviezen over projecten en carrières, taarten bakken, borrels en lunches. Tot snel!

LKCH research, beste allemaal, ondanks dat ik officieel bij de LKCH hoor ben ik maar slecht geïntegreerd in het lab. Desalniettemin hebben jullie me nog regelmatig uit de brand geholpen met voorraadjes, adviezen of een kritische blik op mijn projecten. Met

name **Arnold**, dank voor al je hulp met van alles en nog wat de afgelopen jaren. Ook wil ik jullie allen bedanken voor de gezellige borrels!

Nefrologie, dankjulliewel voor alle hulp bij vragen en experimenten betreffende de nieren. **Jaap**, dankjewel voor het delen van je enorme hoeveelheid kennis, het was ontzettend leerzaam om met je samen te werken! **Krista** en **Melanie**, bedankt voor alle praktische hulp. **Paul**, ik leerde je kennen op de winterschool van de Nierstichting, altijd gezellig om even langs te lopen en bij te kletsen over zowel onderzoek als niet werk gerelateerde dingen. Veel succes met het laatste jaar van je PhD!

Eureka buddy's, **Birgit** en **Floor**, hebben jullie je zwarte boekje inmiddels al geopend? Het was een pittige cursus maar wat fijn om er met jullie nuchterheid en gezelligheid door heen te komen. **Floor**, het maakt niet uit waar ik zit, ik vind je wel voor een koffie, kritische feedback en een dosis nuchtere humor. Ik ben ontzettend blij dat je me af en toe hielp te ontsnappen aan het schrijven en de frustraties tijdens het afronden van mijn boekje. Beide, heel veel succes met het afronden jullie PhD's!

Lieve **Emma**, samen als eerste een plekje uitgezocht in onze kamer op het lab, samen koffie zetten, de dag starten en af en toe even bijkomen. Zonder jou was de kamer voor mij niet meer hetzelfde, maar ben blij dat je snel een leuke baan hebt gevonden. Ik vind het heerlijk om een wijntje met je te drinken, samen te koken (maar eigenlijk vooral te eten) en om samen met **Danny** wat af te spreken, dat gaan we volhouden! Je hebt mijn PhD tijd een ontzettend fijne tijd gemaakt, dankjewel.

Lieve vrienden, lieve **Elsa** en **Lotte**, we kennen elkaar al heel lang en hebben veel gedeeld. Ondanks dat we na de middelbare school allemaal een andere kant op zijn gevlogen, blijft 5 mei in Wageningen elk jaar een vaste prik. Jullie zijn er altijd voor me en kan ik bij jullie even alles loslaten, dankjulliewel! Lieve **Thijs**, we spreken elkaar te weinig sinds je bent verhuisd naar Zürich, maar zodra ik je weer zie is het als vanouds. Ik wil je bedanken voor alle gezelligheid maar ook fijne gesprekken als we elkaar weer is zien. Heel veel succes met je PhD, tot snel!

Lieve Patricia, lieve **Pat**, toen je aan het begin van onze PhD ook mijn buurvrouw werd bleken we al snel bleken we een verassend goede klik te hebben. We hebben ontzettend veel gedeeld, ik blij dat ik met jou samen mocht promoveren, wijntjes en cappuccino's drinken, uithuilen en bijpraten, koken en eten, op vakanties en eindeloos veel dagjes weg. Maar wat hebben we samen ook hard gewerkt, ik vergeet niet snel dat we huilend en lachend tegelijk hebben zitten pipeteren in de flowkast om 3 uur s 'nachts. En kijk naar onze mooie boekjes die we met drie weken verschil mogen verdedigen. Ik ben ontzettend trots op je, je proefschrift, je nieuwe baan en de mooie toekomst die voor je ligt. Je niet meer op werk zien is wel even wennen, maar je bent nog altijd dichtbij als het nodig is, lieve vriendin dankjewel voor alles! Lieve **Roel**, mijn vaste padelmaatje! Ook

al snapt Pat je humor niet altijd, stiekem moet ik er altijd hard om lachen. Dank voor je geduld om te luisteren naar gezeur over het doen van onderzoek en alle gezelligheid en ontspanning bij etentjes. Dankjewel!

Lieve paranimf, lieve **Julie**. Ik leerde je kennen toen je nog analist was op het lab en je mij onder je hoede kreeg als studentje. Je hebt me alle basis geleerd die ik nodig had om me te redden op het lab. Wat konden we goed samenwerken, compleet parallel cellen isoleren en het ene protocol na het andere, helemaal op elkaar ingespeeld. Maar we hebben ook ontzettend veel gelachen, gekletst en gedeeld tijdens de uren in de flowkast, deze constante stroom aan gekwetter was wel is tot irritatie van menig ander op het lab. Toen je besloot een carrière switch te maken is het ons gelukt om contact te houden en spreken we nog zeer regelmatig af om bij te kletsen ondanks dat je inmiddels samen met Rayner een fijn gezin hebt met twee lieve kleine meiden. Je bent een ontzettend lieve en waardevolle vriendin, bij jou kan ik echt voor alles terecht. Ik ben ontzettend blij dat je naast me staat tijdens mijn verdediging!

Dear paranimf, my dear **Cinzia**, with a bunch of internationals we shared two amazing years in Utrecht, trips to Gent and breweries, many dinners, borrels, Dutch pancakes and nights out in Tivoli. I am so happy that we stayed in touch after you left for a PhD in Basel, and even more proud that a few months ago you finished all your hard work and graduated. I love to come to Basel as I feel always welcome with you and Carlos. But I also love the times when you visit Utrecht, like you never went away. You are a strong woman with a loving and caring heart, I am very happy to have you as my friend as you are always there for me. Though you might not understand a word of Dutch, thank you for standing next to me at my defense, it means a lot to me!

Familie van de Weg, **Peter, Wilma, Emiel, Petra** en **Lars**, dank dat jullie me zo welkom laten voelen in jullie gezin. Ondanks dat het soms lastig uitleggen is welk eiwit ik nu weer aan het bestuderen ben, hebben jullie altijd interesse getoond. Dankjewel!

Lieve familie, **Piotr, Klaudia, Marcin** en **Patryk**, jullie zijn een bijzonder stel broertjes en zusje, het is nooit saai thuis en jullie blijven me verbazen met jullie talenten! Ondanks dat ik niet elk weekend meer naar Wageningen kom, vind ik het fijn om te zien en horen hoe goed het met jullie gaat. Het schrijven van mijn boekje is nu af, tijd voor een feestje!

Lieve **Papa** en **Mama**, zonder jullie was ik nooit zover gekomen. Ik heb me ondanks sommige tegenslagen altijd gesteund gevoeld en weet dat ik altijd bij jullie terecht kan. Jullie hebben me de vrijheid gegeven om zelf mijn keuzes te maken, dat heeft me veel geleerd en gebracht waar ik ben vandaag. Ik ben ontzettend trots op jullie, jullie hebben geen makkelijke route gekozen maar hebben me binnen een bijzonder gezin alle kansen en veel liefde gegeven. Dank jullie wel voor alles, een hele dikke kus!

Lieve **Sander**, wie had 7 jaar geleden gedacht dat jij de laatste zou zijn die ik in mijn boekje zou bedanken. Je was in het begin best een beetje geïrriteerd door die kortharige stuiterbal van een student die maar bleef praten. Maar 4 jaar later, ondanks dat we in vele opzichten twee extreme tegenpolen zijn, konden we ook niet meer zonder elkaar. Het afgelopen jaar is een enorme rollercoaster geweest zowel op als naast het werk, maar ik weet nu zeker dat ik samen met jou alles aan kan. Binnenkort verhuizen we naar ons huisje en deze zomer word je mijn man, ik ben blij dat ik met jou mijn leven mag delen. Ik hou van je.

List of publications

Published

M. Wesseling, I.D. van Koeverden, G.W. van Lammeren, S.W. van der Laan, S. Haitjema, J.P.M. de Vries, H.M. den Ruijter, S.C.A. de Jager, I. Hoefler, P. Blankestijn, M. Verhaar, D.P.V. de Kleijn, G.J. de Borst, G. Pasterkamp. *Impaired kidney function is associated with intraplaque hemorrhage in patients undergoing carotid endarterectomy*. *Atherosclerosis*, 2017.

J.A.L. Meeuwssen, **M. Wesseling**, I.E. Hoefler, S.C.A. de Jager. *Prognostic value of circulating inflammatory cells in patients with stable and acute coronary artery disease*. *Frontiers in cardiovascular medicine*, 2017.

M. Wesseling, T. R. Sakkers, S. C.A. de Jager, G. Pasterkamp, M.J. Goumans. *The morphological and molecular mechanisms of epithelial/endothelial-to-mesenchymal transition and its involvement in atherosclerosis*. *Vascular pharmacology*, 2018.

M.A. Siemelink, S.W. van der Laan, S. Haitjema, I.D. Koeverden, J. Schaap, **M. Wesseling**, S.C.A. de Jager, M. Mokry, M. van Iterson, K.F. Dekkers, R. Luijk, H.F. Asl, T. Michoel, J.L.M. Björkegren, E. Aavik, S. Ylä-Herttuala, G.J. de Borst, F.W. Asselbergs, H. el Azzouzi, H.M. den Ruijter, B.T. Heijmans, G. Pasterkamp. *Smoking is associated to DNA methylation in atherosclerotic carotid Lesions*. *Circulation: Genomic and precision medicine*, 2018.

Accepted

M. Wesseling, J.H.C. de Poel, S.C.A. de Jager. *GDF15 in adverse cardiac remodelling: from biomarker to causal player*. *ESC Heart failure*.

Submitted

M. Wesseling, E. Mulder, M.A.D. Brans, M. Bulthuis, G. Pasterkamp, M.C. Verhaar, H. van Goor, J.A. Joles, S.C.A. de Jager. *High renin expression in the absence of kidney injury in the murine trans aortic constriction model*. *American journal of physiology, renal physiology*.

In preparation

M. Wesseling, M. Hulsbos, M. A.D. Brans, R.J.G. Hartman, P. van de Kraak, H.M. den Ruijter, G. Pasterkamp, M.J. Goumans, S.C.A. de Jager. *Sex-specific cardiac remodelling in mice undergoing transverse aortic constriction.*

M. Wesseling, G. Sanchez-Duffhues, J.J. de Haan, J. Tromp, T.C.L. Bracco Gartner, L. Bosch, M.A.D. Brans, S.J. Lee, J.P.G. Sluijter, G. Pasterkamp, A.A. Voors, M.J. Goumans, S.C.A. de Jager. *GDF15 as a marker and mediator of vascular dysfunction in heart failure of non-ischemic origin.*

Curriculum vitae

Marian Wesseling was born on 16 May 1991 in Wageningen, The Netherlands. After finishing high school at 'Het Pantarijn' in Wageningen, she continued her studies at Utrecht University. There, she completed her bachelor Biomedical Sciences, followed by the master Biology of Disease with a specific cardiovascular track. During her master internship at the Experimental Cardiology department, she became enthusiastic about cardiovascular research. In extension of her internships, she started her PhD at the Laboratory for Experimental Cardiology under the supervision of Prof. dr. Gerard Pasterkamp and dr. Saskia de Jager. As part of the RECONNECT consortium, she partly performed her research at the Leiden University, at the Cell Chemistry Biology department under supervision of Prof. dr. Marie-José Goumans and dr. Gonzalo Sanchez-Duffhues. Her research focused on the role of vascular inflammation and endothelial dysfunction in microvascular disease in cardio-renal syndrome. She will proceed a career in science as a postdoc in the research group of Prof. Gerard Pasterkamp. In 2019, she was awarded a Junior Investigator Grant from the PlaQOmics LeDucq foundation to partly perform her research as postdoc in collaboration with the lab of Prof. Gary Owens at the University of Virginia, USA.



